

**Lipid biomarker proxies:
Calibration and application at the southern Italian shelf
(Central Mediterranean)**

Dissertation
Zur Erlangung des Doktorgrades
der Naturwissenschaften
- Dr. rer. nat. -

Am Fachbereich Geowissenschaften
der Universität Bremen

Vorgelegt von

Arne Leider

Bremen
13. Februar 2012

1. Gutachter: Prof. Dr. Kai-Uwe Hinrichs
2. Gutachter: Prof. Dr. Gesine Mollenhauer

*Data is not information,
Information is not knowledge,
Knowledge is not understanding,
Understanding is not wisdom.
(Clifford Stoll)*

PREFACE

The studies presented in this thesis took place in the framework of the ‘Multidisciplinary study Of Continental/ocean Climate dynamics using High-resolution records from the eastern mediterranean’ (MOCCHA) project of the European Scientific Foundation (ESF) EuroMARC Programme through national funding by the Deutsche Forschungsgemeinschaft. Additional support has been provided by the Bremen International Graduate School for Marine Sciences (GLOMAR) and by the European Research Council (ERC) project ‘Deep subsurface Archaea: carbon cycle, life strategies, and role in sedimentary ecosystems’ (DARCLIFE). The thesis was prepared in the Organic Geochemistry group of Prof. Dr. Kai-Uwe Hinrichs affiliated at the University of Bremen.

This thesis provides a better understanding of lipid-derived proxies and their control mechanisms in a shelf setting for future high-resolution paleoenvironmental reconstructions. **CHAPTER I** emphasizes on the importance of having accurate proxy records for the reconstruction of past climate conditions. It gives an overview about lipid biomarkers as paleoceanographic proxies to reconstruct Sea Surface Temperatures (SSTs) and the hydrological cycle in order to provide a basis for the studies in **CHAPTERS II-IV**. The recent environmental characteristics of the study area, the Adriatic Sea and Gulf of Taranto, are described, as well as previous high-resolution climate studies on the last two millennia. It closes with the main objectives and outline of this thesis, followed by a short description of the study material and methodology. Finally, a summary of specific contributions to publications are given. **CHAPTERS II** (published in *Earth and Planetary Science Letters*) and **III** (submitted to *Geochimica et Cosmochimica Acta*) focus on calibration studies of lipid-derived proxies using marine surface sediments from the southern Italian shelf and complementary terrestrial surface sediments from a N-S transect in eastern Italy. **CHAPTER IV** (draft in preparation for submission to *Paleoceanography*) deals with a multiple inorganic and organic proxy approach for the high-resolution reconstruction of environmental conditions during the last 500 year. The thesis closes with the major findings of the studies and perspectives for future investigations.

TABLE OF CONTENTS

PREFACE

ABSTRACT

Thesis Abstract.....	I
Zusammenfassung.....	III

CHAPTER I

INTRODUCTION

I.1. Reconstructing the history of global climate.....	2
I.1.1. Biomarkers as molecular proxies and their application.....	3
I.2. The study area - The southern Italian shelf.....	16
I.2.1. Oceanographic setting of the Adriatic Sea and Gulf of Taranto.....	16
I.2.2. High resolution studies at the Gulf of Taranto – A retrospective.....	20
I.3. Main objectives and thesis outline.....	23
I.4. Methodological approach.....	25
I.4.1. Study material.....	25
I.4.2. Overview lipid biomarker analyses.....	25
I.5. Contributions to publications.....	27
I.6. References.....	29

CHAPTER II

CORE TOP CALIBRATION OF THE LIPID-BASED $U^{K'}_{37}$ AND TEX_{86} TEMPERATURE PROXIES ON THE SOUTHERN ITALIAN SHELF (SW ADRIATIC SEA, GULF OF TARANTO)

II.1. Abstract.....	52
II.2. Introduction.....	52
II.3. Study area.....	55
II.4. Material and Methods.....	58
II.5. Results.....	63
II.6. Discussion.....	66
II.7. Conclusions.....	72
II.8. Acknowledgements.....	73
II.9. References.....	74
II.A1. Appendix.....	85
II.S1. Supplementary material (Electronic Annex).....	86

CHAPTER III

DISTRIBUTION AND STABLE ISOTOPES OF PLANT WAX DERIVED *N*-ALKANES IN MARINE SURFACE SEDIMENTS ALONG A SE ITALIAN TRANSECT AND THEIR POTENTIAL TO RECONSTRUCT THE WATER BALANCE

III.1. Abstract.....	90
----------------------	----

TABLE OF CONTENTS

III.2. Introduction	90
III.3. Study area	93
III.4. Material and Methods	95
III.5. Results	99
III.6. Discussion	104
III.7. Conclusions	111
III.8. Acknowledgements	112
III.9. References	112
III.EA1. Supplementary data	122
CHAPTER IV	
MULTIPROXY ENVIRONMENTAL RECONSTRUCTIONS: WHAT DO SST PROXIES REALLY TELL US (A HIGH-RESOLUTION COMPARISON OF $U^{K'}_{37}$, TEX^H_{86} AND FORAMINIFERAL BASED $\delta^{18}O$ DURING THE LAST 500 YEARS IN THE GULF OF TARANTO)	
IV.1. Abstract	128
IV.2. Introduction	128
IV.3. SST Proxies and their biases	130
IV.4. Study area	132
IV.5. Material and Methods	135
IV.6. Results	140
IV.7. Discussion	146
IV.8. Conclusion	158
IV.9. Acknowledgements	159
IV.10. References	160
IV.S1. Supplementary material (Electronical Annex)	176
CHAPTER V CONCLUSIONS AND OUTLOOK	
V.1. Conclusions	186
V.2. Outlook – future perspectives	188
V.2.1. Future work on the recent setting	189
V.2.2. Future work on sediment cores	189
V.3. References	189
DANKSAGUNG	193
APPENDIX	195
Published manuscript I	196
Manuscript II	198
<u>ERKLÄRUNG GEMÄß § 6 ABS. 5</u>	201

THESIS ABSTRACT

Accurate and reliable proxy records with a sufficient temporal resolution are required for the interpretation of past climate variability beyond the period, where instrumental data become available. Hence, various proxies have been developed on the basis of lipid biomarkers and are applied commonly in paleoceanography for the reconstruction of sea surface temperatures (SSTs), salinity, vegetation changes or terrestrial organic matter (OM) input. Additionally, shelf systems, which are characterized by high sedimentation rates and contributions from marine and terrestrial OM are well-suited for generating high quality environmental records. However, these settings are highly dynamic and the quality of the proxy records depends even more on a careful calibration of the transfer functions used to translate the sedimentary lipid signals to the local environment.

This thesis aims at such a calibration for the SW Adriatic Sea and Gulf of Taranto (S Italy) to provide a better understanding of lipid-derived proxies and their control mechanisms for future high-resolution paleoenvironmental reconstructions.

The first study examines and calibrates the lipid-based temperature proxies $U^{K'}_{37}$ (alkenone-derived from haptophyte algae) and TEX_{86} (Glycerol dialkyl glycerol tetraether from planktonic archaea) in marine surface sediments from the southern Italian shelf and relate these to ambient SSTs and other environmental data. The $U^{K'}_{37}$ -based temperatures in surface sediments reflect winter/spring SSTs in line with the maximum haptophyte production during the colder season. The TEX_{86} -based temperatures for the nearshore sites also reflect winter SSTs, but show an increase with distance to coast, where they correspond to summer SSTs. The comparison to additional lipid and environmental data suggest a shoreward increase of the impact of seasonal and spatial variability in nutrients and control of planktonic archaeal abundance by primary productivity, particle loading in surface waters and/or overprint by a cold-biased terrestrial TEX_{86} signal. As such the offshore TEX_{86} values seem to reflect a true summer signal to the effect that offshore $U^{K'}_{37}$ and TEX_{86} provide information on the annual temperature amplitude.

In the second study the stable hydrogen and carbon isotope composition and distribution of plant wax derived *n*-alkanes in terrestrial, coastal and offshore surface sediments along a N-S transect in east Italy are used to decipher their potential for further hydrological reconstructions. The *n*-alkanes from the terrestrial and coastal samples show a southward increase of δD of 40‰ VSMOW and an increase in the *n*-alkane average chain length, which is in agreement with the generally southward increasing δD of precipitation and mean annual

air temperature, respectively. However, the D enrichment of plant waxes is much larger than that of precipitation, which is attributed to an additional effect of increased leaf water transpiration and/or soil water evaporation in S Italy. Differences in the $\delta^{13}\text{C}$ - δD relation of plant waxes between the northern Po and Apennine river systems and that in south Italian sediments reveal that plant waxes in the Gulf of Taranto derive from regional southern Italian sources. This study provides a calibration of δD of plant waxes and a solid basis to apply the δD of plant waxes as a proxy for past changes in the precipitation-evaporation balance.

The third study applies the new findings from the SST core top calibration for a reconstruction of SSTs and coastal environmental changes on a sub-decadal resolution covering the last 500 years from sediments in the Gulf of Taranto. It includes the SST proxies $\text{U}^{\text{K}'}_{37}$, the recently proposed $\text{TEX}^{\text{H}}_{86}$ as well as the $\delta^{18}\text{O}$ and $\delta^{13}\text{C}$ of planktic and benthic foraminifera (*Globigerinoides ruber* (white and pink) and *Uvigerina mediterranea*). The changes in SSTs reconstructed from $\delta^{18}\text{O}$ of *G. ruber* (white), $\text{TEX}^{\text{H}}_{86}$ and $\text{U}^{\text{K}'}_{37}$ exceed the variability observed in other local and global Northern Hemisphere temperature reconstructions. The $\text{U}^{\text{K}'}_{37}$ reflects temperatures when atmospheric circulation leads to nutrient supply by vertical mixing and runoff that induce haptophyte growth. $\text{TEX}^{\text{H}}_{86}$ -based temperatures are higher than the $\text{U}^{\text{K}'}_{37}$ -based SSTs and reflect summer conditions. The co-variation between both SST records suggests a common environmental mechanism during the last 500 years. SSTs reconstructed from the $\delta^{18}\text{O}$ of *G. ruber* (white) record summer conditions and are in good agreement to summer temperature reconstructions from the European Alps. Moreover, the $\delta^{18}\text{O}$ and $\delta^{13}\text{C}$ of *G. ruber* (white) and *U. mediterranea* are influenced by changes in salinity and food availability related to variations of the major circulation patterns in the Gulf of Taranto. Changes in circulation are also indicated by a negative correlation between SSTs based on $\text{TEX}^{\text{H}}_{86}$ and $\delta^{18}\text{O}$ of *G. ruber* (white). The foraminifera and biomarker records indicate a steady increase in eutrophication and terrestrial input during the last 200 years. This is attributed to an increasing human impact on the region. This thesis reveals the complexity of factors influencing proxies in shelf areas and thus improves the knowledge on lipid-based proxies in these systems.

ZUSAMMENFASSUNG

Zur Interpretation der Variabilität vergangener Klimabedingungen, vor Beginn der instrumentalen Aufzeichnungen, werden präzise und zuverlässige Proxies sowie Datensätze mit hinreichender zeitlicher Auflösung benötigt. Hierbei wurden Lipid Biomarker basierte Proxies entwickelt, welche in der Paläozeanographie zur Rekonstruktion von Oberflächenwassertemperaturen (SSTs; von engl.: sea surface temperature), der Salinität, Vegetationsänderungen oder dem Eintrag terrestrischem organischem Materials (OM) genutzt werden. Darüber hinaus besitzen Schelf Systeme, charakterisiert durch hohe Sedimentationsraten und Eintrag von marinem und terrestrischem OM, die Möglichkeit zur Erstellung zeitlich hoch-auflösende Datensätze. Allerdings, sind diese Systeme hoch-dynamisch und die Qualität der Proxy Datensätze ist demnach noch stärker von einer sorgfältigen Kalibrierung des sedimentären Lipid Signals gegen die lokalen Umweltbedingungen abhängig.

Diese Arbeit umfasst eine solche Kalibrierung für die süd-westliche Adria und den Golf von Taranto (Süd-Italien) zur Vermittlung eines besseren Verständnisses von Lipid-basierten Proxies und ihrer Kontroll-Mechanismen für die zukünftige hoch-auflösende Rekonstruktion von Umweltänderungen.

Die erste Studie dient zur Untersuchung und Kalibrierung der Lipid-basierten Temperatur Proxies $U^{K'}_{37}$ (basierend auf Alkenonen produziert durch Haptophyten) and TEX_{86} (basierend auf GDGTs produziert durch planktische Archaeen), beruhend auf marinen Oberflächensedimenten des südlichen italienischen Schelfgebietes. Zusätzlich werden SSTs der Umgebung und weitere Umweltdaten für einen Vergleich hinzugezogen. Die $U^{K'}_{37}$ -basierten Temperaturen weisen auf SSTs hin, die während des Winters/Frühlings zu finden sind, was mit der Hauptblütephase der Haptophyten während der kälteren Jahreszeit übereinstimmt. Die TEX_{86} -basierten Temperaturen in den küstennahen Proben spiegeln ebenfalls Winter SSTs wider, zeigen allerdings einen Anstieg mit zunehmender Entfernung von der Küste. In den offenen marinen Bereichen repräsentieren sie SSTs die während des Sommers vorkommen. Dieses Muster kann durch saisonale und räumliche Unterschiede im Nährstoffangebot, des Einflusses der Primärproduktion, der Schwebstofffracht im Oberflächenwasser und/oder einer Überprägung durch terrestrische GDGTs erklärt werden. In diesem Fall eröffnet die Kombination von $U^{K'}_{37}$ und TEX_{86} tiefere Einblicke in die jährliche Temperaturamplitude.

In der zweiten Studie wird die stabile Wasserstoff- und Kohlenstoffsignatur sowie die Verteilung von langkettigen *n*-Alkanen (welche von Pflanzenwachsen stammen) in Sedimenten aus terrestrischen und küstennahen Bereichen entlang eines Nord-Süd Transekts in Italien und dem Schelfgebiet herangezogen, um das Potential für die Rekonstruktion des hydrologischen Kreislaufs aufzudecken. Die *n*-Alkane entlang des Nord-Süd Transekts zeigen eine D-Anreicherung von 40‰ VSMOW sowie einen Trend zu längerkettigen Homologen, erkennbar durch einen Anstieg der ACL (durchschnittliche Kettenlänge, von engl.: average chain length). Generell stimmen diese Trends mit dem Anstieg im δD des Niederschlags und der jährlichen mittleren Lufttemperatur überein. Allerdings, ist die D-Anreicherung der Pflanzenwachse wesentlich höher als die des Niederschlags, welches auf eine stärkere Transpiration des Blattwassers und/oder Evaporation des Bodenwassers in Süditalien schließen lässt. Unterschiede im $\delta^{13}C$ - δD Muster zwischen den Flusssystemen des Po, der Apenninen und marinen Sedimenten zeigen den lokalen Ursprung von Pflanzenwachsen im Golf von Taranto. Daher dient diese Kalibrierung als Basis für die Anwendung des δD in Pflanzenwachsen als Proxy für Veränderungen in der Bilanz zwischen Niederschlag und Evaporation.

Die dritte Studie greift die Schlussfolgerungen der SST Kalibrierung auf, um die Veränderungen der SSTs und küstennahen Umweltbedingungen für die letzten 500 Jahre mit einer zeitlichen Auflösung von <10 Jahren im Golf von Taranto zu rekonstruieren. Diese Anwendung umfasst die SST Proxies $U^{K'}_{37}$, den kürzlich entwickelten TEX^H_{86} sowie die stabile Sauerstoff ($\delta^{18}O$) - und Kohlenstoffisotopie ($\delta^{13}C$) von planktischen und benthischen Foraminiferen (*Globigerinoides ruber* (*white* und *pink*) und *Uvigerina mediterranea*). Die Variationen der rekonstruierten SSTs übersteigt die anderer lokaler und globaler Temperaturrekonstruktionen der nördlichen Hemisphäre. Variationen in SSTs basierend auf dem $U^{K'}_{37}$ Index werden durch Änderungen in der atmosphärischen Zirkulation verursacht, die Nährstoffeintrag durch Umwälzung der Wassersäule sowie Flusseinträge beeinflusst. TEX^H_{86} -basierte Temperaturen sind höher als $U^{K'}_{37}$ -basierte SST und spiegeln Sommerbedingungen wider. Simultane Veränderungen in beiden Datensätzen lassen auf einen gemeinsamen Mechanismus während der letzten 500 Jahr schließen. SSTs basierend auf $\delta^{18}O$ von *G. ruber* (*white*) zeigen ebenfalls Sommerbedingungen und stimmen mit rekonstruierten Sommer-Temperaturen der Europäischen Alpen überein. Darüber hinaus, werden $\delta^{18}O$ und $\delta^{13}C$ von *G. ruber* (*white*) und *U. mediterranea* durch Veränderungen in der Salinität und dem Nährstoffangebot beeinflusst, welche durch Änderungen in der Zirkulation der Wassermassen gesteuert werden. Diese Veränderungen im Zirkulationsmuster werden ebenfalls durch eine

negative Korrelation zwischen SSTs aus $\text{TEX}_{86}^{\text{H}}$ und $\delta^{18}\text{O}$ von *G. ruber (white)* aufgezeigt. Des Weiteren weisen die Foraminiferen- und Biomarker-basierten Datensätze auf einen stetigen Anstieg des Nährstoff- als auch terrestrischen Eintrags während der letzten 200 Jahre hin, der durch einen verstärkten anthropogenen Einfluss verursacht wird.

Die Dissertation zeigt auf, dass die komplexen Einflüsse auf Proxies in Schelfgebieten nur durch regionale Kalibrierungen erfasst werden können um diese für die Rekonstruktion von Klima- und Umweltbedingungen zu nutzen. Darüber hinaus trägt sie zu einem besseren Verständnis von Lipid-basierten Proxies in diesen Systemen bei.

CHAPTER I

Introduction

I.1. RECONSTRUCTING THE HISTORY OF GLOBAL CLIMATE

Sea Surface Temperatures (SSTs) and the hydrological cycle play a major role for the heat storage and transfer between the oceans and atmosphere, which interact via complex feedback loops within the climate system of the Earth (Rahmstorf, 1995; Henshaw et al., 2000; Pierrehumbert, 2002; Stephens et al., 2004; IPCC, 2007; Bates et al., 2008). For example, air temperatures influence SSTs and ocean circulation redistributes this heat before it is released to the atmosphere, while ocean currents are related to atmospheric wind patterns (e.g., Rahmstorf, 2002). Additionally, higher SSTs increase the vapor pressure difference between the sea surface and the ambient atmosphere, resulting in higher evaporation rates. This leads to an enhanced hydrological cycle due to increasing precipitation and continental runoff (IPCC, 2007). Simultaneously, water vapor acts as the most important greenhouse gas (e.g., Chahine, 1992). This amplifies the effect of other greenhouse gases, like carbon dioxide and methane, influencing water circulation and availability with all its consequences on the environment and society (e.g., Rind et al., 1992). Consequently, knowledge of past SSTs and changes in the hydrological cycle in response to anthropogenic influences and natural climate variability is essential for the assessment of the current warming trend and for the general understanding of ocean and atmosphere dynamics and their links with global climate (e.g., Kucera et al., 2009).

The best way to determine past changes are instrumental records (e.g., Oldfield and Thompson, 2004). Relatively widespread instrumental data of Northern Hemisphere (NH) temperatures date back to the mid-1850s and measurements of the ocean and upper atmosphere are largely confined to the last 50 years (e.g., Jones et al., 1999). However, time series of measured environmental parameters are often temporal inhomogeneous and spatially too inconsistent to capture short-term processes, rare events and non-analogue situations (e.g., Sachs et al., 1977, Versteegh et al, 2005). Therefore, instrumental records fail to encompass the complete picture of climatic variability (Jones et al., 2001). In contrast, historical records can reach back several thousands of years but may not be continuous and capture only extreme events. Beyond the instrumental and documentary data, climate and environmental reconstructions rely on proxy records. In general, a proxy is a natural environmental recorder, which is interpreted, using physical and biophysical principles, to represent some combination of climate-related variations back in time (IPPC, 2007). Proxies in paleoclimatology can derive from natural archives, such as ice cores, boreholes, terrestrial biological sources (tree rings, pollen, insects), corals, speleothems, lake and marine sediments (e.g., Oldfield and

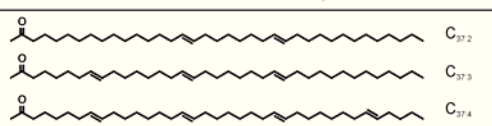
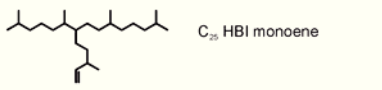
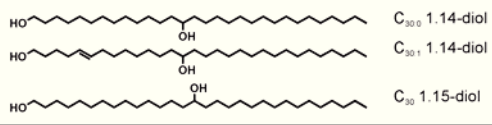
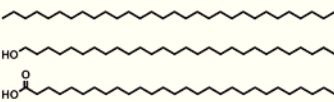
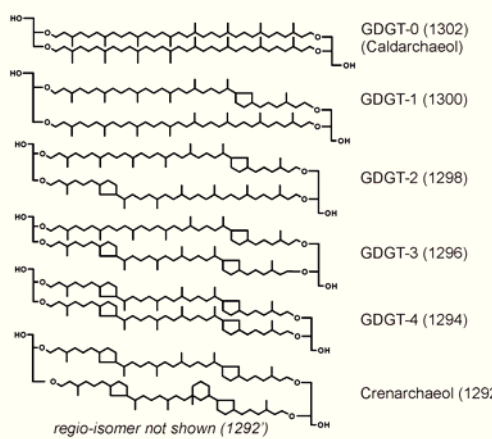
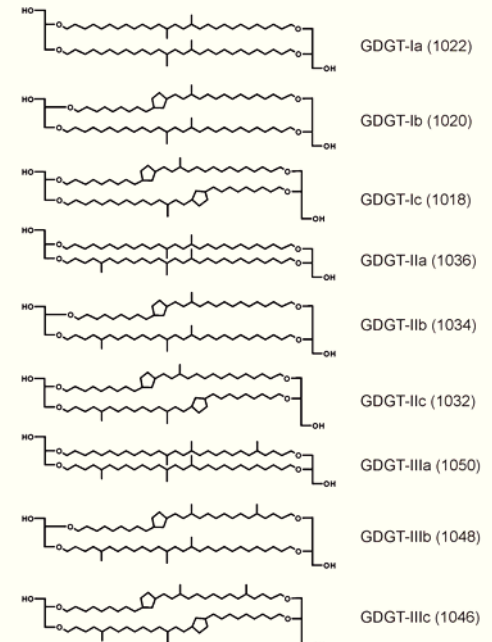
Thompson, 2004). The usefulness of an archive depends on its spatial coverage, the period to which it pertains and its ability to resolve events accurately in time (Bradley et al., 1985). The proxy application itself depends on the physical parameter that is under review. Accurate proxy records are essential to improve our knowledge about climate variability as those can be used to test and verify climate models. However, exact proxies require calibrations to the physical parameters and recent climate records before they can be applied to the past (e.g., Hecht et al., 1979; Kucera et al., 2009).

I.1.1. Biomarkers as molecular proxies and their application

Biomarkers are complex organic compounds (primarily lipids) consisting of carbon and hydrogen, and other elements, which can be attributed to formerly living organisms and contribute to the organic matter (OM) found in the marine and terrestrial environment. They can also be defined as molecular fossils as these molecules are preserved in sediments, rocks and crude oil (e.g., Eglinton et al., 1964, Peters et al., 2005; Gaines et al., 2009). In the marine realm lipid biomarkers can be initially produced by organisms from the aquatic (e.g., alkenones produced by haptophytes, highly branched isoprenoids synthesized by diatoms, hopanoids produced by bacteria) (e.g., Volkman et al., 1998) or the terrestrial environment (e.g., long chain *n*-alkyl lipids derived from plant-waxes of higher plants, phenolic monomers of lignin, from woody and non-woody tissue of higher plants or pentacyclic triterpenoids) (e.g., Pancost and Boot, 2004) (Table I.1).

Their usefulness largely depends on their resistance against early degradation processes during transport, sedimentation and after burial into the sediments (e.g., Rosell-Mélé, 2007). The transport of biomarkers may also differ, as they are deposited with the remains of the original organisms, digested remains or adsorbed to mineral particles. Allochthonous biomarkers can be transported by winds and/or rivers to the ocean and might derive from pre-aged and -altered OM. After deposition, biomarkers can be laterally and vertically transported by sediment erosion and re-deposition through e.g., bottom water currents or tidal movements (e.g., Rosell-Mélé, 2007 and references therein). In high sedimentation settings lateral advection may introduce large age differences between biomarkers and other sediment constituents like foraminifera (Ohkouchi et al., 2002; Mollenhauer et al., 2003; Smittenberg et al., 2004; Mollenhauer et al., 2007; 2008). Conversely, in low sedimentation settings the association of biomarkers and microfossils to particles of different sizes may result in differences between paleo records due to the extent of bioturbation (Bard, 2001).

Table I.1. Selected biomarkers used for paleoceanographic proxies (see Table I.2), their structure and biological origin. Numbers in parentheses refer to the m/z value of the $(M+H)^+$ ions of GDGTs (AOM: Anaerobic Oxidation of Methane)

Molecule	Structure/Example	Source organisms	Reference
1 Alkenones C_{37} - C_{39}		Haptophytes	Volkman et al. (1980) Marlowe et al. (1984)
2 Highly branched isoprenoids (HBIs)		Diatoms	Volkman et al. (1994) Belt et al. (1996)
3 <i>n</i>-alkyl diols		Planktonic algae: Diatoms (<i>Proboscia spp.</i>) Eustigmatophytes	Volkman et al. (1992) review in Versteegh et al. (1997) Volkman et al. (1999) Sinninghe Damsté et al. (2003) Rampen et al. (2007)
4 <i>n</i>-alkyl lipids <i>n</i> -alkanes ($\geq C_{25}$, odd numbered) <i>n</i> -alkanols ($\geq C_{24}$, even numbered) <i>n</i> -fatty acids ($\geq C_{24}$, even numbered)		Leaf waxes of higher land plants	Eglinton and Hamilton (1963) Eglinton and Hamilton (1967)
5 Isoprenoid Glycerol dialkyl glycerol tetraethers (GDGTs)		GDGT-0 to -4: mesophilic AOM and methanogenic Euryarchaeota thermophilic Euryarchaeota mesophilic and thermophilic Crenarchaeota Crenarchaeol: mesophilic and thermophilic Crenarchaeota not found in Euryarchaeota	Tornabene and Langworthy (1979) Koga et al. (1993) De Long et al. (1998) Pancost et al. (2001) Uda et al. (2001) Aloisi et al. (2002) Gattinger et al. (2002) Bouloubassi et al. (2006) de la Torre et al. (2008) Schouten et al. (2008) Sinninghe Damsté et al. (2002) de la Torre et al. (2008) Schouten et al. (2008)
6 Branched Glycerol dialkyl glycerol tetraethers (GDGTs)		presumably anaerobic soil bacteria	Sinninghe Damsté et al. (2000) Weijers et al. (2006a) Sinninghe Damsté et al. (2011)

Therefore, the most valuable biomarkers are taxonomically specific, i.e., they can be related to a certain group of organisms, carry a signal from the environment in which they were synthesized, show only small changes in their chemical structure from precursor molecules and are resistant against diagenesis and catagenesis (e.g., Killips and Killips, 2005). Lipid biomarker structures, abundances, ratios and their stable isotope compositions provide widespread insights about present and past environments including food and energy sources of microbial organisms, ecology of source organisms, processes during transport of OM to the ocean, degradation and fate of OM or the evolution of life on Earth (e.g., Meyers, 1997; Bianchi and Canuel, 2011). Hence, several lipid biomarker proxies (quantitative and qualitative) have been developed in paleoceanography to reconstruct e.g., SST, salinity, upwelling intensity, soil input, changes in vegetation and precipitation patterns (e.g., Eglinton and Eglinton, 2008) (Table I.2).

The following section is focused on the analyses of SSTs based on marine biomarkers and the interaction between the terrestrial and marine environment using terrestrial biomarkers and their stable isotopic composition as these are the two main research topics of this thesis:

1.1.1.1. Reconstruction of Sea Surface Temperature (SST)

In paleoceanography a number of SST proxies have been developed. Commonly used methods include faunal assemblages, the stable oxygen isotopes ($\delta^{18}\text{O}$) and elemental composition (Mg/Ca) of planktonic foraminifera (e.g., CLIMAP, 1976; Nürnberg et al., 1996; Elderfield and Gansen, 2000; Barker et al., 2005; Kucera et al., 2005; Waelbrock et al., 2005), the $\delta^{18}\text{O}$ and Sr/Ca composition in corals (e.g., Beck et al., 1992; Gagan et al., 2000) and chemistry of organic constituents produced in surface waters (e.g., Schouten et al., 2000; Herbert, 2006 and references therein) (Fig. I.1.). The advantage to conventional approaches is that lipid biomarker SST proxies are not directly controlled by the chemistry of sea water and do not rely on hard parts of organisms and thus can provide information on SSTs when calcareous microfossils are absent. Additionally, they occur over wide areas of the ocean and are not restricted to specific settings like e.g., corals. However, all these proxies are based on the response of an organism or assemblage to temperature and related environmental changes. Consequently, the SST estimates may differ as the various proxy carriers each have their particular seasonal distribution, depth habitat, and preservation potential.

Chapter I

Table I.2 Main summary of paleoceanographic proxies based on lipid biomarkers (see numbering in Table I.1 for molecules, structures and origin). Numbers in TEX₈₆ equations correspond to the m/z value of the (M+H)⁺ ions of GDGTs

Proxy	Parameter	Rationale	Equation/Determination	Calibration	Error	Range	References	Basis / Application	Biases/ Uncertainties					
U ₃₇ ^K	Sea Surface Temperature (SST)	Unsaturation degree of long-chain ketones (alkenones) (1)	$U_{37}^K = \frac{[C_{37:2}]}{[C_{37:2}] + [C_{37:3}]}$	SST = (U ₃₇ ^K - 0.044) / 0.033	1.5 °C	0-29 °C	Brassel et al. (1986) Prahl and Wakeham (1987)	global core tops	a) uncertainty about species composition					
				SST = 29.876 x U ₃₇ ^K - 1.334	1.1 °C	-1-29 °C	Conte et al. (2006)		global core tops	b) seasonality and depth habitat of species				
				SST = (U ₃₇ ^K - 0.093) / 0.03	-	0-28 °C	Rosell-Mélé et al. (1995)		NE Atlantic Ocean	c) preferential degradation of C _{37:3}				
				SST = (U ₃₇ ^K - 0.092) / 0.031	-	26.7-28.2 °C	Pelejero and Grimalt (1997)		S China Sea	d) influence of nutrient input and light availability				
				SST = (U ₃₇ ^K - 0.084) / 0.031	-	0-30 °C	Sonzogni et al. (1997)		various regions					
TEX ₈₆	Sea Surface Temperature (SST)	TetraEther index of isoprenoidal GDGTs with 86 carbons (5)	$TEX_{86} = \frac{[1298] + [1296] + [1292']}{[1300] + [1298] + [1296] + [1292']}$ $TEX_{86}' = \frac{[1298] + [1296] + [1292']}{[1300] + [1298] + [1292']}$ $TEX_{86}^H = \log(TEX_{86})$ $TEX_{86}^L = \log\left(\frac{[1298]}{[1300] + [1298] + [1296]}\right)$	SST = (TEX ₈₆ - 0.28) / 0.015	2.0 °C	0-30 °C	Schouten et al. (2002)	global core tops, regional calibrations for polar, tropical regions	a) seasonality and depth habitat of species					
				SST = (TEX ₈₆ + 0.016) / 0.027	-	22-36 °C	Schouten et al. (2003)			b) uncertainty about species				
				SST = (TEX ₈₆ + 0.20) / 0.016	-	-	Slujs et al. (2006)			c) riverine terrestrial GDGT input may bias TEX ₈₆				
								SST = 50.475 - 6.332 x (1/TEX ₈₆)	-	-2-29 °C	Liu et al. (2009)	Red Sea	d) sedimentary sources of GDGTs	
								SST = (TEX ₈₆ + 0.09) / 0.035	-	25-28 °C	Trommer et al. (2009)			
								SST = -10.78 + 56.2 x TEX ₈₆	1.7 °C	5-30 °C	Kim et al. (2008)		global core tops	
								SST = 68.4 x TEX ₈₆ ^H + 38.6	2.5 °C	5-30 °C	Kim et al. (2010)			
				SST = 67.5 x TEX ₈₆ ^L + 46.9	4.0 °C	-3-30 °C	Kim et al. (2010)							
Diol (Isomer) Index	Sea Surface Temperature (SST)	Chain length of long-chain diols (3)	$1.14 - DI = \frac{[C_{30:1} + C_{30:0} - diols]}{[all\ 1.14 - diols]}$ $1.14 - DI = \frac{[C_{30:0} - diol]}{[C_{28:0} + C_{30:1} - diols]}$ <i>DI based on 1.13- and 1.15-diols</i>	SST = (1.14-DI - 0.275) / 0.018	-	16-26 °C	Rampen et al. (2009; 2011)	Arabian Sea based on water column	a) unknown Diol sources					
				SST = (1.14DI + 0.013) / 0.028					SE Atlantic Ocean based on surface sediments	b) no SST relation on global scale				
							<i>in progress</i>			-	Rampen et al. (unpubl.)	<i>global core top calibration in progress</i>		
%C _{37:4}	Sea Surface Salinity	Relative abundance of C _{37:4} alkenone (1)	$\%C_{37:4} = \frac{[C_{37:4}]}{[C_{37:2}] + [C_{37:3}] + [C_{37:4}]}$	S = (%C _{37:4} x 146.9(±10.6)) / 4.1(±0.3) S = (%C _{37:4} - 1691) / 48.1 S = (%C _{37:4} - 397.6) / 11.7	-	31-35 psu 34-36 psu 30-33 psu	Rosell-Melé et al. (2002) Sicre et al. (2002) Harada et al. (2003)	North Atlantic Ocean and Nordic Seas based on suspended particulate matter and surface sediments	a) restricted to individual basins b) effect of other environmental factors unclear c) covariation of SST and salinity					
δD _{alkenones}	Sea Surface Salinity	Salinity effect on fractionation (1)	$\delta D = \left(\frac{\delta D_{sample}}{\delta D_{standard}} - 1 \right) \times 1000 \text{ (VSMOW)}$	δD _{C37:2} = 0.724 x δD _{water} - 226		0-600‰ VSMOW	Englebrecht and Sachs (2005)	Haptophyte cultures	a) effect of diagenetic H exchange					
				<i>G. oceanica:</i> δD _{alkenones} = 2.9 x δD _{water} - 242		-5 - +16‰ VSMOW	Schouten et al. (2006)	Tropical Pacific and N Atlantic Ocean	b) different fractionation factors between species					
				<i>E. huxleyi:</i> δD _{alkenones} = 2.6 x δD _{water} - 215			van der Meer et al. (2007) Pahnke et al. (2007)	E Mediterranean Sea E tropical Pacific Ocean	c) growth rate dependency					

Proxy	Parameter	Rationale	Equation/Determination	Calibration	Error	Range	References	Basis/ Application	Biases/ Uncertainties
$\delta^{13}\text{C}_{\text{alkenones}}$	$p\text{CO}_2(\text{aq})$	Utilization of dissolved inorganic carbon (1)	$\delta^{13}\text{C} = \left(\frac{\delta^{13}\text{C}_{\text{sample}}}{\delta^{13}\text{C}_{\text{standard}}} - 1 \right) \times 1000 \text{ (VPDB)}$	$\epsilon_p = 25.3 - 182 \left(\frac{\mu}{c} \right) \left(\frac{V}{S} \right)$ ϵ_p : isotopic fractionation photosynthesis μ : specific growth rate (μ/day) c : CO_2 concentration ($\mu\text{mol}/\text{kg}$) V/S : cell volume:surface area (μm) Popp et al. (1998)			Jasper and Hayes (1990) Freeman and Hayes (1992) Benthien et al. (2002) Pagani et al. (2002)	particulate matter of surface waters S Atlantic Ocean core tops Paleogene sediments	a) physiological factors (size, cell geometry) b) nutrient supply affecting growth rate
IP ₂₅	Sea Ice coverage	Abundance of C ₂₅ HBI monoene (2)	-	only qualitative	-	-	Belt et al. (2007)	applied to Arctic Ocean sediments and sediment traps	a) other sources
Diol Index	Upwelling intensity	Chain length of long-chain diols (3)	$\frac{[C_{28} + C_{30} \cdot 1.14 - \text{diol}]}{[C_{28} + C_{30} \cdot 1.14 - \text{diol}] + [C_{30} \cdot 1.15 - \text{diol}]}$	only qualitative	-	-	Rampen et al.(2007; 2008)	Arabian Sea based on water column	a) other sources
$\delta^{13}\text{C}_{n\text{-alkyl lipids}}$	Vegetation changes	Fractionation in plants depends on fixation pathway (4)	Endmember modelling to estimate C ₄ plant contribution (f_{C_4}): $f_{C_4} = \left(\frac{\delta^{13}\text{C}_{n\text{-alkyl lipid}} - \delta^{13}\text{C}_{C_3}}{\delta^{13}\text{C}_{C_4} - \delta^{13}\text{C}_{C_3}} \right) \times 100\%$	Regional calibration needed for the end-member of source regions Reference values from the literature $\delta^{13}\text{C}_{C_3}$: -36‰ VPDB $\delta^{13}\text{C}_{C_4}$: -21.5‰ VPDB (e.g., Rieley et al., 1993; Collister et al., 1994)			Bird et al. (1995) Yamada and Ishiwatari (1999) Huang et al. (2000) Freeman and Colarusso (2001) Schefuß et al. (2003a)	global core tops and sediment cores	a) source regions b) ancient sources c) transport pathway d) effects during transport
$\delta\text{D}_{n\text{-alkyl lipids}}$	Terrestrial hydrological cycle	Records δD of source water which varies with temperature, evaporation and precipitation (4)	$\delta\text{D} = \left(\frac{\delta\text{D}_{\text{sample}}}{\delta\text{D}_{\text{standard}}} - 1 \right) \times 1000 \text{ (VSMOW)}$	The reconstruction of the δD of precipitation requires known fractionation factor between the lipid and water ($\epsilon_{\text{lipid-water}}$). Various calibrations based on plant leaves and lake sediments are provided for different climatic settings on regional and global scale.			Sachse et al. (2004) Chikaraishi et al. (2003), Chikaraishi and Naraoka (2007) Smith and Freeman (2006) Liu and Yang (2008) Feakins and Sessions (2010) Polissar and Freeman (2010)	N-S Europe Japan and Thailand US Great Plains global compilation S California N-S America	a) soil water evaporation b) plant types influencing fractionation c) physiological differences
BIT	Soil OM input	Branched vs. isoprenoid GDGT ratio (6) and (5)	$\text{BIT} = \frac{[Ia] + [IIa] + [IIIa]}{[Ia] + [IIa] + [IIIa] + [1292]}$	BIT=0: no soil OM input BIT=1: dominant soil OM input			Hopmans et al. (2004)	based on surface sediments in open oceans, estuaries, lakes and soils	a) varying contribution of crenarchaeol
MBT	Air Temperature (MAT)	Methylation index of branched GDGTs (6)	$\text{MBT} = \frac{[Ia] + [Ib] + [Ic]}{[all \text{ branched GDGTs}]}$	MAT = (MBT - 0.122 - 0.187 x CBT) / 0.020		-2.9-27 °C	Weijers et al. (2007)	based on soil samples, applied to soils and estuaries	b) preferential degradation c) in situ production of branched GDGTs (e.g., lakes)
CBT	Soil pH	Cyclisation ratio of branched GDGTs (6)	$\text{CBT} = -\log \left(\frac{[Ib] + [IIb]}{[Ia] + [IIa]} \right)$	soil pH = (3.33 - CBT) / 0.38		pH 3.3-8.2			

The Unsaturation index based on alkenones ($U^{K'}_{37}$). The $U^{K'}_{37}$ index is the most widespread used lipid-derived SST proxy and it is based on long chain di- and triunsaturated ketones with 37 carbon atoms (alkenones) (Table I.2). These are produced by a limited species of haptophyte algae e.g., *Emiliana huxleyi* and *Gephyrocapsa oceanica* (Volkman et al., 1980; Marlowe et al., 1984; Volkman et al., 1995; Conte et al., 1998), which dwell in the surface waters of the ocean (Fig. I.1.). The $U^{K'}_{37}$ index is defined as the ratio of the diunsaturated alkenone ($C_{37:2}$) relative to the sum of di- and triunsaturated alkenones ($C_{37:3}$). It is based on the fact that the relative proportion of $C_{37:3}$ increases with decreasing ambient temperature which was observed in cultures, field measurements and sediments (Brassel, 1986; Prahl and Wakeham, 1987). Global surveys on core tops confirmed this relationship resulting in the development of calibration functions of $U^{K'}_{37}$ to mean annual SSTs (e.g., Müller et al., 1998; Conte et al., 2006). Regional calibrations try to account for deviations from this relation, which have been attributed to differences in depth of maximum alkenone production (Ternois et al., 1997; Bentaleb et al., 1999; Ohkouchi et al., 1999; Conte et al., 2001; Prahl et al., 2005) or seasonal blooming of haptophytes (Bentaleb et al., 1999; Sikes and Volkman, 1993; Sikes et al., 1997; Volkman et al., 2000; Prahl et al., 2001; Popp et al., 2006 and references therein) Additionally, $U^{K'}_{37}$ may be affected by lateral transport of alkenones from remote regions in settings influenced by strong currents as suggested from the deviation of alkenone-based SSTs to the overlying water column (Benthien and Müller, 2000) and large age offsets to complementary planktonic sources determined by radiocarbon dating (Ohkouchi et al., 2002; Mollenhauer et al., 2003; Sachs and Anderson, 2003; Mollenhauer et al., 2007; 2008). Further discrepancies between $U^{K'}_{37}$ and SSTs may be introduced by selective degradation of $C_{37:3}$ (causing warmer SST estimates) (Sun and Wakeham, 1994; Hoefs et al., 1998; Gong and Hollander, 1999; Rontani et al., 2006; Kim et al., 2009b; Rontani et al., 2009) and influences of light and nutrients (Epstein et al., 1998; Versteegh et al., 2001; Prahl et al., 2003). Nonetheless, the $U^{K'}_{37}$ paleothermometer has been successfully applied for millennial scale SST reconstructions since the Late Pleistocene, in high-resolution studies covering the Holocene and in combination with other SST proxies (see review in Herbert et al., 2006).

The Tetraether index based on Glycerol Dialkyl Glycerol Tetraethers (TEX_{86}). The second temperature proxy is the TEX_{86} index (TetraEther indeX of tetraethers consisting of 86 carbon atoms), which is based on isoprenoid Glycerol Dialkyl Glycerol Tetraethers (GDGTs)

occurring ubiquitously in marine and lacustrine sediments and soils (Schouten et al., 2002; Powers et al., 2004) (Table I.2). GDGTs have been identified in various types of archaea (Table I.1 and references therein). In the oceans non-hyperthermophilic planktonic archaea are likely the dominant source of sedimentary isoprenoid GDGTs as they represent a major group of prokaryotes (Schouten et al., 2000; Karner et al., 2001; Schouten et al., 2002). Initially, an increase in cyclisation of GDGTs with increasing temperature has been observed in cultures of extremophilic archaeons (Gliozzi et al., 1983; Uda et al., 2001), which has been extended to marine crenarchaeota by mesocosm experiments (Wuchter et al., 2004). Accordingly, the TEX₈₆ index is based on changes in the cyclisation pattern of pentacyclic rings in isoprenoid GDGTs as a response to temperature. Temperatures based on TEX₈₆ are supposed to reflect annual mean temperatures of the upper mixed layer and a first calibration of the TEX₈₆ index to annual mean SSTs on global core tops has been published by Schouten et al. (2002). Although, planktonic archaea do not depend on light, studies on particulate organic matter confirmed that the TEX₈₆ signal derives from the upper 100 m of the water column due to grazing and the more effective transport by packaging in larger particles (Wakeham et al., 2003; Wuchter et al., 2005; Huguet et al., 2006). More recently, new calibrations have been developed, which are based on larger datasets as well as modifications of the original TEX₈₆ definition, which are more suitable for the application in specific regions (Sluijs et al., 2006; Kim et al., 2008; Liu et al., 2009; Trommer et al., 2009; Kim et al., 2010) (Table I.2).

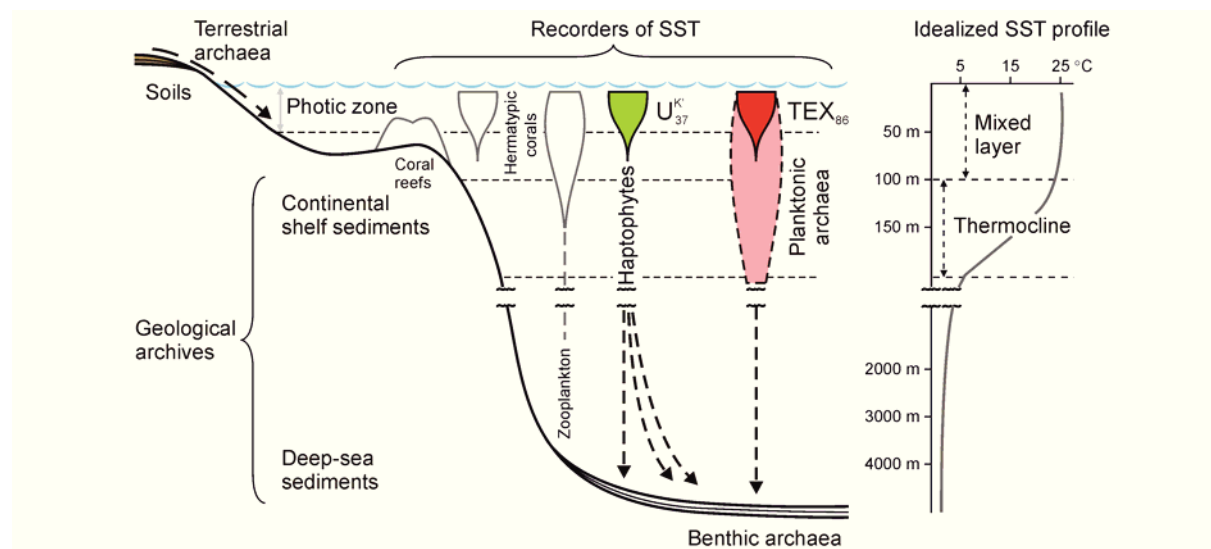


Figure I.1. Idealized scheme showing the main SST signal carriers, their habitat and the occurrence of geological archives of SST. Hermatypic corals and phytoplankton, such as haptophytes (U^{K}_{37}) grow only in the photic zone, which normally overlaps with the mixed layer. Some zooplankton species live below the photic zone and record thermocline temperatures rather than SST. The TEX₈₆-signal reflects SSTs from planktonic archaea, while GDGTs may be contributed by sedimentary and terrestrial sources (adapted from Kucera, 2009).

Almost 10 years after the first calibration, the TEX₈₆ index represents an established tool for the reconstruction of SSTs in recent environments using suspended particulate matter and core tops (e.g., Huguet et al., 2007; Lee et al., 2008) and has been applied for the characterization of extreme events like Oceanic Anoxic Events during the Cretaceous (e.g., Schouten et al., 2003; Bornemann et al., 2008; Mutterlose et al., 2010) or the Paleocene-Eocene Thermal Maximum (PETM) (e.g., Sluijs et al., 2007). Likewise, this also has led to the discovery of potential uncertainties, requiring further investigations. GDGT contributions from marine crenarchaeota residing in subsurface waters (e.g., Huguet et al., 2007; Lee et al., 2008), pelagic euryarchaeota (Turich et al., 2007), active archaea in continental shelf and deep sea sediments (Lipp et al., 2008; Lipp and Hinrichs, 2009; Liu et al., 2011) as well as the supply of terrestrial-derived GDGTs (Weijers et al., 2006a) may bias the TEX₈₆ temperature signal. Age offsets between crenarchaeol, solely produced by crenarchaeota, and the crenarchaeol regioisomer also suggest different origins of GDGTs (Shah et al., 2008). Additionally, the abundance of crenarchaeota may differ during the year, between regions and might be influenced by the seasonal cycle of the phytoplankton (e.g., Schouten et al., 2002; Wuchter et al., 2005; Herfort et al., 2006; 2007). The effects of changing redox conditions on the TEX₈₆ are minor (Sinninghe Damsté et al., 2002a; Schouten et al., 2004; Huguet et al., 2009; Kim et al., 2009b). Long-distance lateral transport of isoprenoid GDGTs seems to be less important than for alkenones, which are preferentially preserved, as inferred from relatively younger ¹⁴C ages of crenarchaeol compared to alkenones (e.g., Mollenhauer et al., 2007; 2008; Kim et al., 2009a). Therefore, TEX₈₆-based temperatures are suggested to derive from local source areas.

1.1.1.2. Interaction between terrestrial and marine environment

Terrestrial biomarkers carried by rivers and winds to the ocean are common in marine sediments and can be used to develop records of past continental vegetation, from which climatic change can be inferred (e.g., Pancost and Boot, 2004 and references therein). Although, not as diagnostic as pollen records, the terrestrial biomarkers can constitute a significant amount in sediments, especially in coastal regions with high fluvial input or in the open ocean, where aeolian supply exceeds that of pelagic inputs. While certain terrestrial lipid biomarkers are linked to specific origins, the determination of the dominant transport mechanisms and source areas can be difficult (Eglinton and Eglinton, 2008 and references therein). Supplementary information can be obtained by using e.g., the stable carbon isotope composition of plant-wax derived *n*-alkanes as an indicator of relative C₃ vs. C₄ inputs.

Additionally, their stable hydrogen isotope composition is used as a proxy for reconstructions of the hydrological cycle.

Plant-wax derived long chain n-alkanes. Homologues of long chain *n*-alkyl lipids are typically found in terrestrial and marine sediments (e.g., Cranwell, 1973; Poynter et al., 1989; Bird et al., 1995; Huang et al., 2000; Freeman and Colarusso, 2001; Huang et al., 2002) as well as in dust (e.g., Simoneit et al., 1977; Gagosian et al., 1981; Schefuß et al., 2003a) (Table I.1.). They derive from the protective epicuticular waxes on the leaf surfaces of higher land plants (Eglinton and Hamilton, 1963; 1967) and are relatively resistant to degradation (Cranwell, 1981). They are ablated by winds and rain and are carried long distances by winds or are delivered directly by rivers with plant detrital material and soils to the ocean (e.g., Eglinton and Eglinton, 2008).

Plant-wax derived *n*-alkanes have a typical carbon chain-length between C_{25} and C_{35} and show a strong predominance of odd-carbon homologues over even-carbon homologues (the most dominant representatives being the C_{27} , C_{29} , C_{31} and C_{33}) (Eglinton and Hamilton, 1967). The magnitude of this odd-over-even predominance, expressed by the Carbon Preference Index (CPI) (Bray and Evans, 1961), is used to distinguish between plant (CPI>4 in plants and sediments) and petroleum (lower CPI) sources (e.g., Cranwell, 1981). Their carbon number distribution can be characterized by the Average Chain Length (ACL), which can vary among plants but also within plant species (e.g., Poynter et al., 1989; Poynter and Eglinton, 1990). Additionally, changes in the environment and vegetation may play an important role as shifts to higher homologues occur with increasing temperatures and aridity at the source regions (e.g., Gagosian and Peltzer, 1986; Hinrichs et al., 1998; Schefuß et al., 2003a) as well as increasing C_4 plant contributions (e.g., Eglinton and Eglinton, 2008 and references therein). Though, biosynthesis of longer chain homologues in response to higher ambient temperature is thought to prevent water loss during respiration and to maintain the hardness of the waxes, the predominant controlling factor maintains poorly understood (e.g., Kozłowski and Pallardy, 1997; Kawamura et al., 2003).

Compound-specific stable carbon isotopes on plant-waxes. Carbon occurs in nature as a mixture of the stable isotopes ^{12}C (98.9%) and ^{13}C (1.1%) (Killops and Killops, 2005). Changes in the isotopic composition are expressed by the $\delta^{13}\text{C}$ notation in ‰ relative to the Vienna Pee Dee Belemnite (VPDB) standard (Table I.II). In general, carbon of biological origin is relatively enriched in ^{12}C , which depends upon several factors, such as the $\delta^{13}\text{C}$ of

the primary carbon source, isotopic effects during carbon assimilation by a particular organism as well as metabolic and biosynthetic processes and cellular carbon budgets (Hayes 1993).

The photosynthetic fixation of atmospheric CO₂ by plants is associated with a discrimination against ¹³C. A significant isotopic difference in plant tissue and plant-waxes ($\delta^{13}\text{C}_{\text{plant-wax}}$) is observed between plants utilizing the C₃ (Calvin–Benson) and C₄ (Hatch–Slack) carbon assimilation mechanism (O’Leary, 1981; Fry and Sherr, 1984). On average, this varies between -36‰ (C₃ plants) and -21‰ (C₄ plants) (for the *n*-C₃₁ alkane, Rieley et al., 1993; Collister et al., 1994) and is commonly used in the sedimentary record to reconstruct the continental vegetation in the source areas and the relative C₃ vs. C₄ plant contribution to the ocean (Bird et al., 1995; Huang et al., 2000; Schefuß et al., 2003a) (Table I.II).

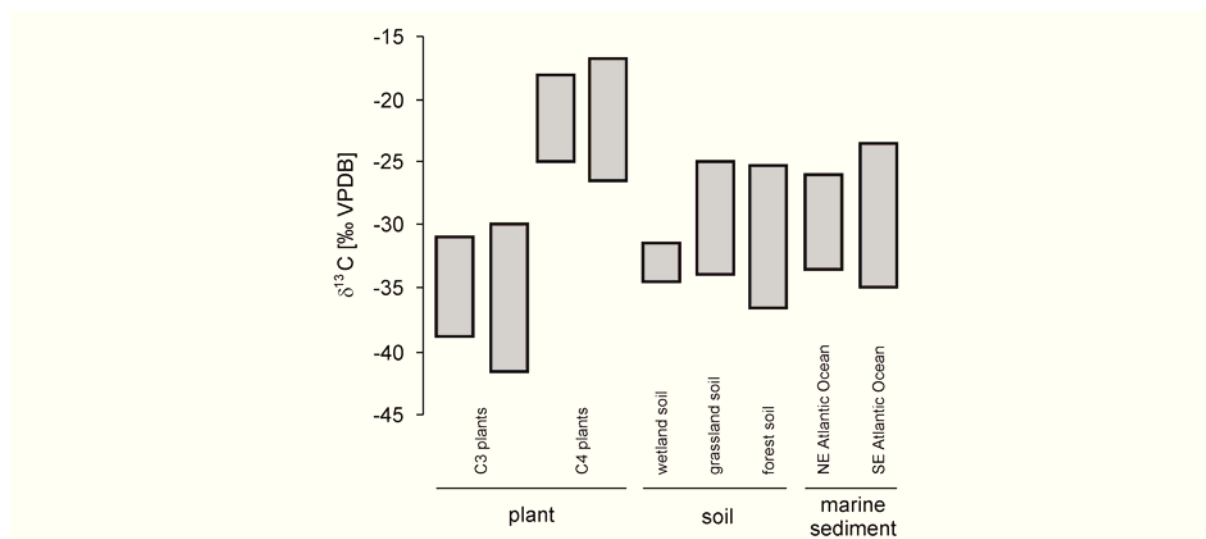


Figure I.2. Plot showing the distribution and range of $\delta^{13}\text{C}$ in plant-wax derived *n*-alkanes found in plants, soils and marine sediments (values are reported for the *n*-C₃₁ alkane; except for NE Atlantic Ocean sediments, where the *n*-C₂₉ alkane has been used) (data adapted from Bi et al., 2005; Chikaraishi & Naraoka, 2003; Collister, 1994; Huang et al., 2000; Krull et al., 2006; Rieley et al., 1993; Schefuß et al., 2004; Seki et al., 2010; Rao et al., 2009).

Accordingly, it is suggested that higher temperatures, aridity and low *p*CO₂ favor C₄ type ecosystems over C₃ plants due to their ability to internally concentrate CO₂ before carbon fixation. This allows them to decrease their stomatal conductance, increasing water use efficiency (Ehleringer et al., 1997). As the vegetation itself depends on climatic parameters, like aridity, temperature, atmospheric *p*CO₂ and insolation, the use of the $\delta^{13}\text{C}$ of plant-waxes allows e.g., to reconstruct the main mechanisms controlling continental humidity (Schefuß et al., 2003b; Castañeda et al., 2009; Niedermeyer et al., 2010; Collins et al., 2011).

Compound-specific stable hydrogen isotopes. The stable isotopes of hydrogen are represented by ^1H (99.984%) and ^2H or D (deuterium) (0.016%) (e.g., Jouzel, 2003). Changes in the stable isotopic hydrogen composition are based on the D/H ratio, which is expressed by the δD notation in ‰ relative to the Vienna Standard Mean Ocean Water (VSMOW) standard (Gonfiantini et al., 1978; Hoefs et al., 2009) (Table I.II).

The stable isotopic composition of water (δD and $\delta^{18}\text{O}$) within the hydrological cycle changes as a function of evaporation (leading to D-enrichment) and precipitation (D-depleted relative to seawater), which provide a recognizable signature showing a range of 250‰ (e.g., modern δD of precipitation in the tropics: 0‰; high latitudes: <-150‰; deserts: +100‰) (Dansgaard, 1964; Gonfiantini et al., 1986; Gat, 1996; Mook and Rozanski, 2000) (Fig. I.3a). Therefore, the δD signal preserved in groundwater lakes, fluid inclusions in speleothems, ice core records and cellulose of tree rings has been examined early as a tool for climate reconstructions (e.g., Epstein, 1976; Harmon et al., 1979; Rozanski, 1985; Jouzel et al., 1997). Technical advances in isotope-ratio mass spectrometry opened a new analytical window for paleoclimatologists by the possibility in analyzing the δD on a compound-specific basis (e.g., see review in Sessions, 2006). Consequently, the δD of individual organic compounds is being increasingly used to reconstruct the δD of environmental water in various

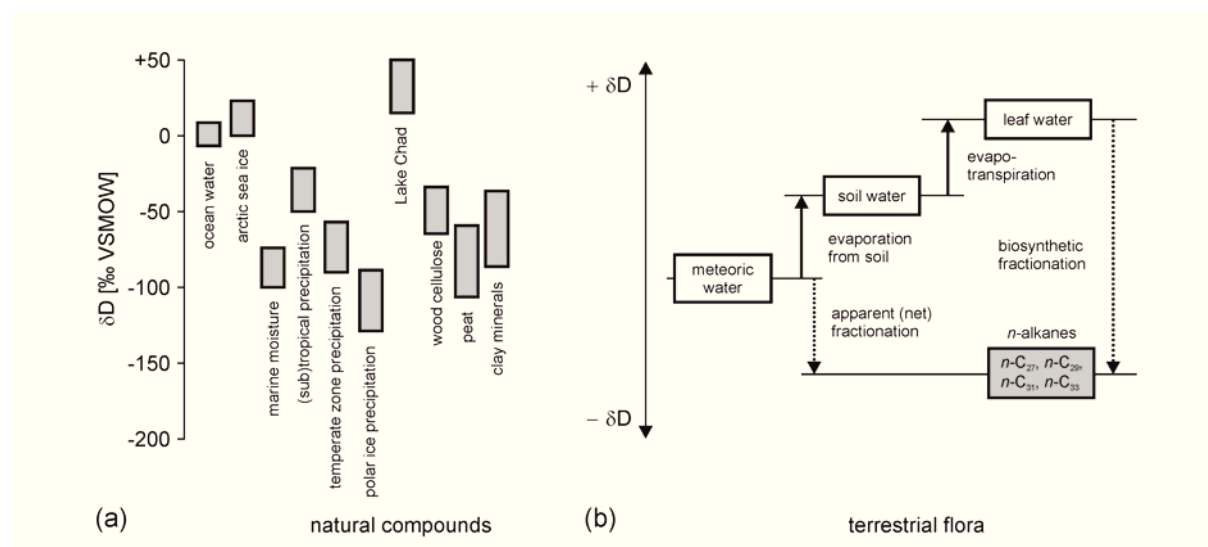


Figure I.3 (a) Variations of δD in selected compartments within the hydrological cycle (adapted from Mook and Rozanski, 2000); (b) Schematics of the isotopic relationships between source water and plant-wax derived n -alkanes. Soil water evaporation and evapotranspiration lead to a D-enrichment in the leaf water reflected in the δD of n -alkanes (not to scale) (adapted from Sachse et al., 2004).

compartments of the water cycle, and hence, climate variability in the past (e.g., Xie et al., 2000; Andersen et al., 2001; Sauer et al., 2001; Huang et al., 2002; Schefuß et al., 2005; Tierney et al., 2008; Niedermeyer et al., 2010).

The δD of plant wax-derived *n*-alkanes ($\delta D_{\text{plant-wax}}$) in leaves, sediments and soils has been shown to reflect the δD of precipitation and recent environmental conditions in different climates demonstrating their potential for reconstructing hydrological change (Sachse et al., 2004; 2006; Smith & Freeman, 2006; Rao et al., 2009) (Table I.II). However, the δD of the environmental water may be modified by soil evaporation as well as evapotranspiration from leaves, both leading to a D-enrichment in plant waxes relative to precipitation (Sachse et al., 2004; 2006; Smith & Freeman, 2006; Hou et al., 2007; 2008; Feakins and Sessions, 2010) (Fig. I.3b). Additionally, the influence of relative humidity and vegetation characteristics (photosynthetic pathway, plant physiology) on the $\delta D_{\text{plant-wax}}$ is poorly understood and is the focus of ongoing research (e.g., Chikaraishi & Naraoka, 2003; Bi et al., 2005; Liu and Huang, 2005; Krull et al., 2006; Smith & Freeman, 2006; Hou et al., 2007; McInerney et al., 2011).

Branched vs. Isoprenoid Tetraether (BIT) index. The Branched vs. Isoprenoid Tetraether (BIT) index is defined by the ratio between branched GDGTs, presumably derived from anaerobic bacteria living in soils and peats, and crenarchaeol, synthesized by marine crenarchaeota, respectively (Sinninghe Damsté et al., 2000; Hopmans et al., 2004; Weijers et al., 2006a; Liu et al., 2010; Sinninghe Damsté et al., 2011) (Table I.1. and I.2.). The BIT index is used as a proxy for fluvial soil OM input to coastal marine sediments and can range between 0 (no soil OM input) and 1 (high soil OM input) (Hopmans et al., 2004; Herfort et al., 2006; Kim et al., 2006; Weijers et al., 2006b; Walsh et al., 2008; Rueda et al., 2009). BIT index values are highest in terrestrial settings (soils, lakes and rivers) and tend to decrease rapidly from shelf areas to the open ocean (Hopmans et al., 2004) (Fig. I.4.). In lakes, in situ production in the water column and sediments may contribute to the branched GDGT pool (e.g., Bechtel et al., 2010; Blaga et al., 2009, 2010). In near-coastal areas discrepancies are observed between the BIT index and other terrestrial OM proxies (e.g., $\delta^{13}\text{C}$ of TOC, phenol monomers of lignin), which have been attributed to a lack of soils at the source regions, association to different grain size fractions affecting transport and a primarily control by the abundance of crenarchaeol compared to branched GDGTs (Walsh et al., 2008; Schmidt et al., 2010; Smith et al., 2010).

Additionally, the BIT index is used to determine a terrestrial bias on the TEX_{86} , due to the potential contribution of terrestrial-derived isoprenoid GDGTs, as indicated by a simultaneous

increase in BIT index and TEX_{86} values (Weijers et al., 2006b). Though, care has to be taken as preferential preservation of branched GDGTs seems to occur more effectively compared to isoprenoid GDGTs (Huguet et al., 2008, 2009). Applications of the BIT index in sediment cores (and in combination with other proxies) allowed the qualitative (e.g., Ménot et al., 2006; Sluijs et al., 2006) and quantitative (Weijers et al., 2009) reconstruction of riverine soil OM input in past environments related to hydrological changes on land. More recently, the use of branched GDGTs has been further extended by exploiting their degree of methylation and cyclisation (MBT and CBT indices) to reconstruct soil pH and mean annual air temperatures (Weijers et al., 2007a, b, c; Peterse et al., 2009; Rueda et al., 2009; Peterse et al., 2010) (Table I.II).

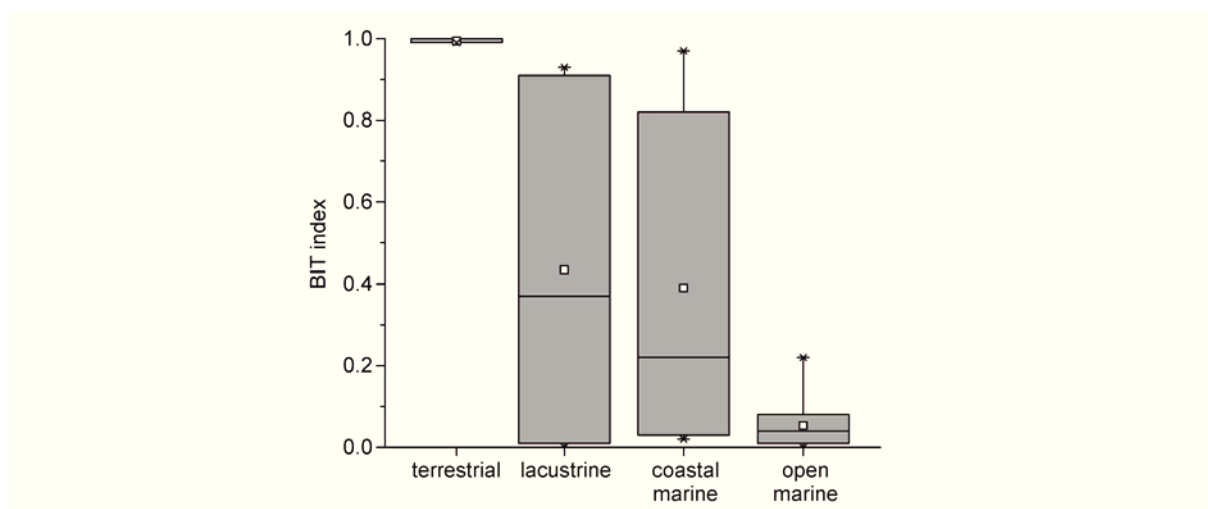


Figure I.4. Box and whiskers plots of BIT index values measured on Holocene sediments from a range of environments reported by Hopmans et al. (2004); bars represent 90%, 75%, 50% (median), 25% and 10% percentiles, stars: maximum/minimum values, squares: means) (adapted from Trommer et al., 2009).

I.2. THE STUDY AREA - THE SOUTHERN ITALIAN SHELF

Shelf areas play an important role in the accumulation and redistribution of OM from terrestrial and marine sources but are complex due to their highly dynamic character (e.g., Meybeck, 1982; Hedges and Keil, 1995; Hedges et al., 1997; Goñi et al., 2000; Schmidt et al., 2010). An enhanced marine productivity due to nutrient supply from the continent or upwelling (Wollast, 1998), supply of terrestrial OM and shallow water depths promote high sedimentation rates. This may provide continuous marine high resolution climate records with sufficient time resolution to detect high-frequency variations in paleo-climate. Additionally, the vicinity to the continental margins makes them even more attractive as changes in the marine environment can be set alongside evidence for changes on land. However, the high complexity of continental margins require the study of regions, where local factors influencing environmental conditions are well constrained (e.g., morphology, current system, nutrient supply, marine productivity, river runoff, vegetation).

I.2.1. Oceanographic setting of the Adriatic Sea and Gulf of Taranto

The Adriatic Sea is a mid latitude, narrow epicontinental basin (ca. 200x800 km) connected to the Central Mediterranean Sea in the south via the Strait of Otranto (Fig. I.5.). The Gulf of Taranto, located in the northern Ionian Sea is connected to the southern Adriatic through the Cape St. Maria di Leuca (e.g., Rossi et al., 1983). The Adriatic Sea plays an important role in the freshwater, OM and nutrient supply to the Mediterranean Sea, mostly through contributions from the Po River, Alpine and Apennine rivers, which are distributed along the north-western Adriatic coast (Degobbis and Gilmartin, 1990; Raicich, 1996; Civitarese et al., 1998; Pettine et al., 1998). It is characterized by a microtidal regime and dominated by thermohaline currents (Artegiani et al., 1997b; Poulain, 2001; Gačić et al., 2002). The surface circulation is characterized by a cyclonic movement, driven by buoyancy effects and wind patterns with seasonal variability (Malanotte Rizzoli and Bergamasco, 1983; Orlic et al., 1992; Artegiani et al., 1997a).

Discharge from the Po and Apennine rivers shows maxima during autumn and late spring, associated with increased rainfall and snowmelt, respectively (e.g., Cattaneo, 2003). This generates the cold, nutrient-rich and less saline coastal Western Adriatic Current (WAC) characterized as Adriatic Surface Water (ASW) (Fig. I.5a). The ASW flows southwards along the Italian eastern margin through the Strait of Otranto into the Gulf of Taranto where it mixes

with oligotrophic Ionian Sea water masses (Malanotte Rizzoli and Bergamasco, 1983; Zavatarelli and Pinardi, 2003).

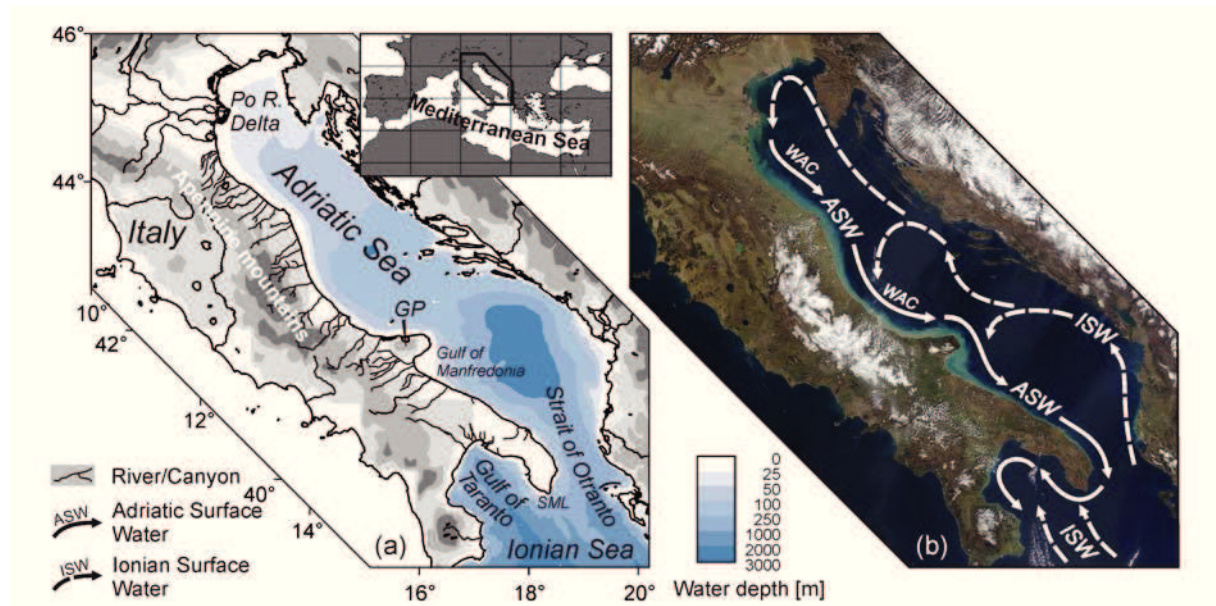


Figure I.5. Map showing Italy, the Adriatic Sea and Gulf of Taranto. (a) Distribution of the main river systems along the eastern coast and bathymetry of the Adriatic Sea and Gulf of Taranto (GP: Gargano Promontory, SML: Cape St. Maria di Leuca) (adapted from Cattaneo, 2003). (b) True color MODIS image from the TERRA satellite showing the southward moving Western Adriatic Current (WAC) during March 25, 2003 (<http://visibleearth.nasa.gov/>); Arrows indicate the general surface circulation (adapted from Poulain, 2001).

The southern Adriatic Sea open waters show oligotrophic characteristics comparable to the Ionian Sea and nutrient supply to the euphotic zone depends strongly on vertical stratification and mixing processes (Viličić et al., 1989). Here, the WAC system plays a crucial role for the nutrient supply and drives primary production (PP) of the Adriatic Sea. As a consequence, higher pigment concentrations can be observed in satellite images along the Italian coastal zone into the Gulf of Taranto (e.g., Morović, 2002; Focardi et al., 2009; Zonneveld et al., 2009) (Fig. I.6.a-d). For the southern Italian shelf remote sensing shows a negative correlation between seasonal SSTs to chlorophyll-*a* indicating that main PP occurs during the colder season (Zonneveld et al., 2009). Additionally, maxima in PP in surface waters of the middle Adriatic Sea are observed during autumn and spring due to increased runoff (Totti et al., 2000). Intrusion of the Ionian Surface Water (ISW) is restricted to the eastern coast of the Adriatic Sea, balancing the outflow of the ASW. Nutrient-rich and high-salinity intermediate waters, with a core at 200 m, form the Levantine Intermediate Water (LIW). The Levantine Intermediate Water invades the southern Adriatic Sea during winter at the western Adriatic shelf, where it mixes with the Adriatic Surface Water, affecting the phytoplankton community (Caroppo et al., 2001).

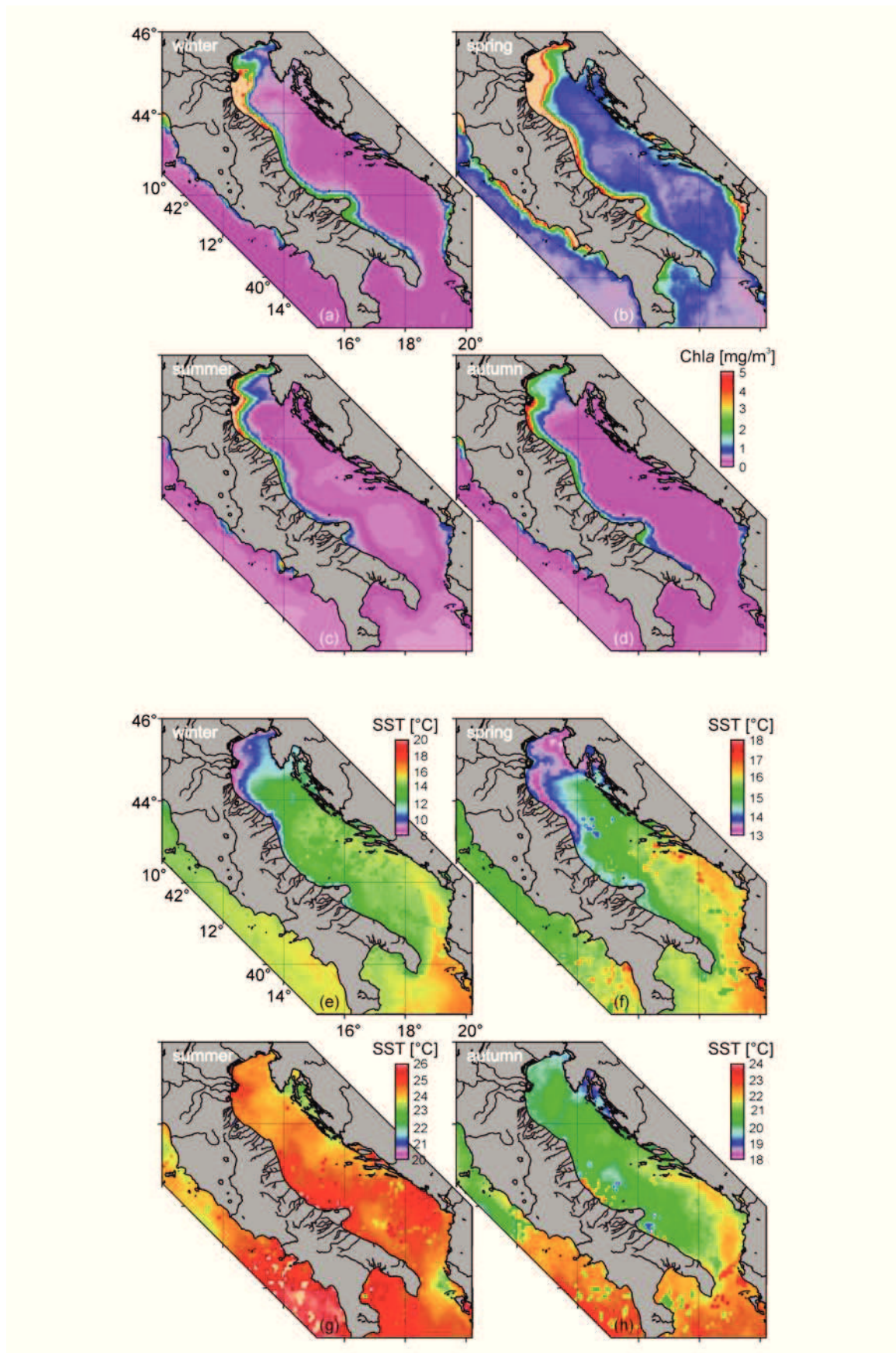


Figure I.6. Seasonal variations of (a-d) chlorophyll-*a* and (e-g) SSTs in the Adriatic Sea and Gulf of Taranto during 2003/2004 from OBPG MODIS-Aqua satellite products (winter: Dec-Jan-Feb, spring: Mar-Apr-May, summer: Jun-Jul-Aug, autumn: Sep-Oct-Nov). Analyses were produced with the Giovanni online data system, developed and maintained by the NASA GES (Acker and Leptoukh, 2007).

In general, SSTs vary between 13 °C in winter and 26 °C in summer (Zavatarelli et al., 1998; Caroppo et al., 1999; Socal et al., 1999; Caroppo et al., 2001; Boldrin et al., 2002; Zonneveld et al., 2009) (Fig. I.6.e-h). The upper water column is well mixed during winter and spring while a thermocline starts to develop at 50–70 m water depth in March leading to open-ocean stratification during summer. This controls nutrient distribution, which is additionally influenced by river input and resuspension due to vertical mixing during winter. As a result, nutrient concentrations in the surface waters decrease from NW to SE (e.g., Civitarese et al., 1998). This seasonality in nutrients and other water column characteristics affects the phytoplankton community structure (Socal et al., 1999; Boldrin et al., 2002).

The sedimentation, accumulation and transport processes of clastic sediments as well as OM have been extensively studied within the northern and central Adriatic Sea, whereby little is known about the southern Adriatic shelf and the Gulf of Taranto (Fig. I.7.). The main fluvial sediment source regions for the Adriatic basin are the Po River and the eastern Apennine rivers north of the Gargano promontory, which in total deliver $\sim 51.7 \times 10^6$ t/yr of mean suspended load (Milliman and Syvitski, 1992; Milligan and Cattaneo, 2007) (Fig. I.7a). In contrast, the sediment load of the rivers south of the Gargano promontory is as low as 1.5×10^6 t/yr (Cattaneo et al., 2003). While 60% of the Po River sediment load is stored in its prodelta, along-shore transport of fine sediments is very effective (1-2 orders greater than transport in the cross shelf direction) following the general current circulation ($\sim 35\%$ of riverine supply) (Correggiari et al., 2001; Frignani et al., 2005; Milligan and Cattaneo, 2007). Sediment transport events in the western Adriatic Sea occur predominantly during the winter months and are linked to wind events (Fain et al., 2007; Milligan and Cattaneo, 2007). The sediment supply and resuspension results in hydrodynamic sorting along the coast in belts, in line with the modern sedimentation on continental shelves: coastal sands, mud, and shelf relict sand farther offshore (Frignani et al., 2005). In the deepest southern Adriatic Sea, besides the NS-oriented fluxes, cross-shelf turbidity currents carry clay sediments from the Apulian shelf into the bathyal basin (Tomadin, 2000). Approximately $\sim 10\%$ of the annual river input escapes the western continental shelf to the southern Adriatic Sea/Mediterranean Sea (Frignani et al., 2005).

In the Po prodelta, the content and distribution patterns of OC are primarily related to the high in situ primary production and the high discharge of the Po River (Fig. I.7b). On the western Adriatic continental shelf highest TOC values are found in the mud fraction indicating that the dispersion of fine material drives the surficial OC distribution (Tesi et al., 2006).

Tesi et al. (2007) examined the sources, transport and deposition of OM along a N-S transect using the distribution of $\delta^{13}\text{C}$ of TOC, C:N ratios and phenol monomers from lignin. They showed that land-derived nutrients promote phytoplankton growth and that terrestrial material travels southward suspended within the WAC. In surface sediments soil-derived OM represents the largest fraction (~50-94%), while contributions of riverine-estuarine phytoplankton decrease and marine phytoplankton increase with distance from the Po River.

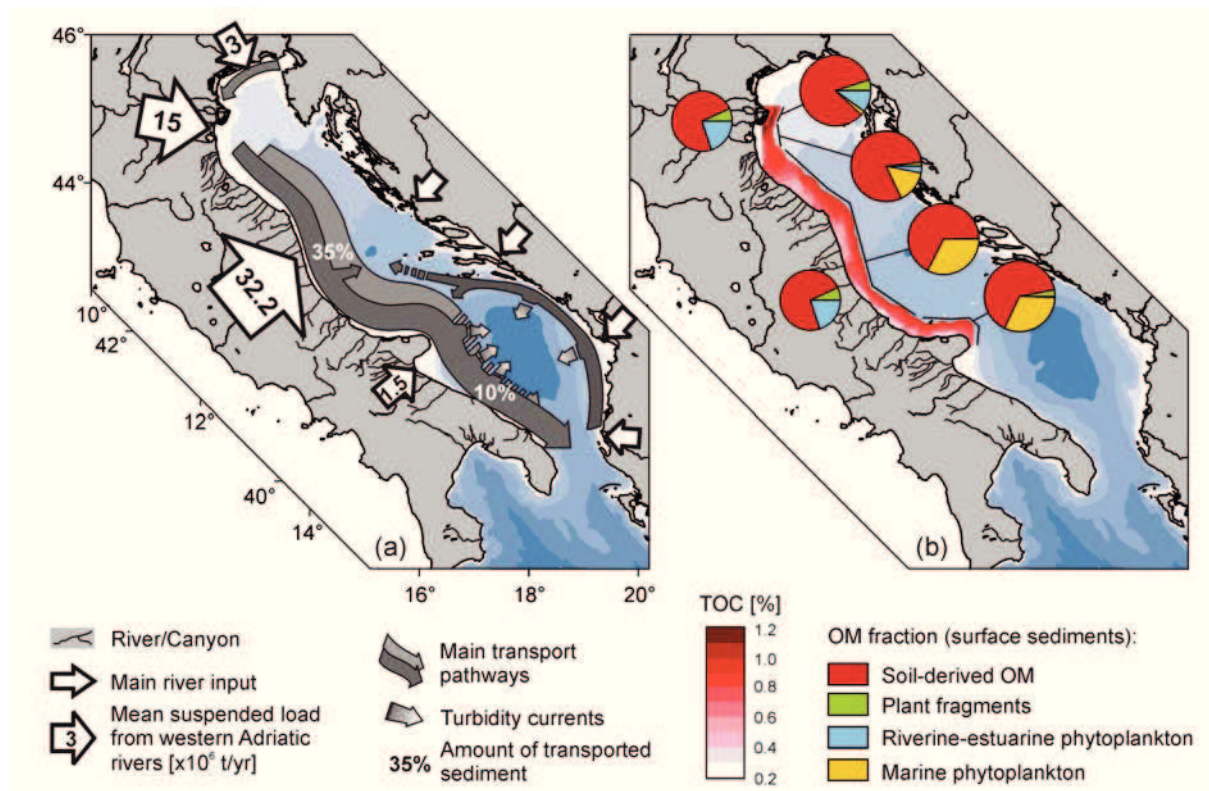


Figure I.7. Map of the Adriatic Sea and Gulf of Taranto. (a) Estimates of mean suspended sediment load supplied by western Adriatic rivers (adapted from Cattaneo, 2003), main transport pathways (adapted from Tomadin, 2000) and estimates for the transported sediments relative to the total river supply (adapted from Frignani et al., 2005). (b) TOC distribution and contributions of soil-derived OC, plant fragments, estuarine/riverine phytoplankton and marine phytoplankton in surficial sediments along the Adriatic shelf (adapted from Tesi et al., 2006; 2007).

I.2.2. High resolution studies at the Gulf of Taranto – A retrospective

The Gulf of Taranto has been in the attention of paleoenvironmental research for more than 30 years. Investigations mainly focused on the relation between climate and solar forcing covering the last two millennia.

The first shallow water core (GT14; 39°45'55"N/17°53'30"E; 166 m water depth) was collected from the Gallipoli shelf located at the E Gulf of Taranto in 1979 and the upper 20 cm was radiometrical dated using ²¹⁰Pb analyses (T_{1/2}=22.3 years) and ¹³⁷Cs (T_{1/2}=30.2 years) (Cini Castagnoli et al., 1990; Bonino et al., 1993; Taricco et al., 2009). The exposure of the Gulf of Taranto downwind of the south Italian volcanoes, allowed the identification of

several ash layers based on sharp clinopyroxene peaks, which were related to the historical eruptions of e.g., Pompei (79 AD), Pollena (472 AD), Ischia (1301 AD), Monte Nuovo (1538 AD). The comparison of carbonate profiles and clinopyroxene peaks enabled the cross correlation to other cores (GT89/3, 39°45'53''N/17°53'33''E; 178 m water depth; GT90/3, 39°45'53''N/17°53'33''E; 174 m water depth; GT91-1, 39°59'23''N/ 17°45'25''E; 250 m water depth) and suggested a uniform and constant sedimentation rate of 0.0646 ± 0.0007 cm/yr (1 cm per 15.5 years) on the Gallipoli shelf from at least 79 AD allowing investigations on temporal high resolution of less than 4 years (Cini Castagnoli et al., 1990; 1992; Bonino et al., 1993).

First high-resolution analyses of thermoluminescence (Cini Castagnoli et al., 1990; 1997) and the $\delta^{13}\text{C}$ and $\delta^{18}\text{O}$ of the planktic foraminifera *Globigerinoides ruber* (Cini Castagnoli et al., 1999a; b; 2000; 2002; 2005) revealed decadal to centennial variations suggesting a strong solar forcing during the past two millennia. The good agreement of the $\delta^{13}\text{C}$ of *G. ruber* with historical records of rainy days and aurorae numbers was interpreted as solar induced modulation of cloud coverage affecting illumination (Cini Castagnoli et al., 1999b; Cini Castagnoli et al., 2002). A global character of this solar imprint has been suggested from similar centennial $\delta^{13}\text{C}$ oscillations observed in a Japanese cedar tree (Cini Castagnoli et al., 2005). For the $\delta^{18}\text{O}$ of *G. ruber* an anti-correlation has been identified to the sunspot number record from 1700 to 1900, suggesting that higher solar activity operates via increased temperatures and evaporation resulting in lower $\delta^{18}\text{O}$ values (Cini Castagnoli et al., 1999a; b). A composite SST reconstruction based on the $U^{K'}_{37}$ index, covering the period from 1305 to 1979, showed that SSTs reflect a seasonal signal of haptophyte production occurring during the cooler part of the year (Versteegh et al., 2007). Moreover, the authors suggested that wind induced mixing is important for the variations in timing and magnitude of alkenone production. The study also showed a centennial solar forcing imprint through the agreement between alkenone-based SSTs and atmospheric $\Delta^{14}\text{C}$.

Taricco et al. (2009) extended the investigations on the $\delta^{18}\text{O}$ record of *G. ruber* to the last two millennia using advanced spectral methods. The $\delta^{18}\text{O}$ variations have been correlated to known climate oscillations, such as the Medieval Optimum (MO) (9th-13th century) (e.g., Hughes and Diaz, 1994) and the Little Ice Age (LIA) (15th-19th century) (e.g., Bradley and Jones, 1993). The authors suggested that long-term trends in the $\delta^{18}\text{O}$, as well as the alkenone-based SSTs from Versteegh et al. (2007), are temperature driven. Additionally, they interpreted high $\delta^{18}\text{O}$ values around 0 AD as a low temperature signal, which generally disagrees with the relative warmth and dryness of the Roman Classical Period (RCP) in the

Mediterranean region (~2000 years BP) (e.g., Reale and Dirmeyer, 2000; Schilman et al., 2001).

I.3. MAIN OBJECTIVES AND THESIS OUTLINE

Given the suitability of the Gulf of Taranto for high resolution studies on past climate variability, there is a lack of knowledge about how the recent environment influences the paleoenvironmental proxies.

The main objective of this thesis is to calibrate lipid biomarkers and their proxies along the southern Italian shelf against today's environmental conditions to improve the understanding for future high resolution paleoenvironmental reconstructions. This approach aims at the characterization of SSTs and the hydrological cycle based on surface sediments of marine and terrestrial origin (**CHAPTER II-III**). Subsequently, the new findings are applied in a case study for the reconstruction of SSTs and environmental changes using multiple proxies on a high resolution core spanning the last 500 years in the Gulf of Taranto (**CHAPTER IV**). Furthermore, this thesis addresses the following specific questions:

- (1) What is/affects the distribution of SSTs based on the $U^{K'}_{37}$ and TEX_{86} indices along the southern Italian shelf and to what extent can those be related to environmental conditions?**

Recorders of SSTs exhibit different responses to environmental changes according to different ecologies and live strategies of the source organisms. This may bias the preserved SST signal. Previous downcore studies in the Gulf of Taranto revealed that SSTs based on alkenones show a cold seasonal imprint but it is unknown if this reflects today's conditions over a broader area.

- (2a) Can we characterize the supply of terrestrial lipid biomarkers to the Adriatic shelf by the Western Adriatic Coastal Current (WAC)?**

Shelf areas play an important role in the accumulation and transport of allochthonous and autochthonous OM. The Po River and Apennine rivers located in North and Central Italy are suggested to be the major sources of terrestrial OM to the Adriatic Sea. Additionally, the WAC plays an important role in the transport and resuspension along the coast to the southern Adriatic Sea.

(2b) Do plant-waxes in terrestrial sediments reflect environmental and climatic conditions on land?

In general, the distribution, $\delta^{13}\text{C}$ and δD of plant waxes vary in response to multiple factors (e.g., temperature, aridity, vegetation). Italy provides strong environmental and climatic gradients e.g., mean annual air temperature and precipitation, influencing the hydrological cycle and suggesting that plant-waxes hold different signatures from their source regions.

(3) What is the provenance of sedimentary plant-waxes in marine sediments and how does this influence the interpretation of the $\delta\text{D}_{\text{plant-wax}}$ as a hydrological proxy?

Beside different transport pathways via rivers and winds, source regions can contain different climatic and vegetation signatures affecting the signal preserved in marine sediments. Knowing the source regions is essential to assess if local or regional climate signals can be reconstructed. The identification of these sources preserved in marine sediments requires supplementary information from the terrestrial environment.

(4) What are the factors controlling variations in different SST proxies during the last 500 years in the Gulf of Taranto?

Decadal to centennial climate variations during the last 500 years are mostly available from terrestrial settings (e.g., tree rings). In contrast, little is known about rapid changes in the marine environment due to the paucity of high-resolution records that are based on multiple proxies. Previous core top calibrations set the basis for an application of inorganic and organic SST proxies in the Gulf of Taranto.

These questions have been addressed in three first-author manuscripts, which are presented in **CHAPTER II-IV**. **CHAPTER II** deals with a calibration study of the lipid-derived temperature proxies U^{K}_{37} and TEX_{86} based on a grid of core tops along the southern Italian shelf. It focuses directly on question **(1)** and is related to question **(2a)** by the application of the BIT index. Different distribution patterns were examined in relation to environmental as well as other lipid data and linked to seasonal productivity maxima and water column characteristics. **CHAPTER III** provides insight in the distribution of plant-wax derived *n*-alkanes in marine and terrestrial surface sediments using their chain length distribution, $\delta^{13}\text{C}$ and δD to target questions **(2a)**, **(2b)** and **(3)**. The comparison to the recent climate gradients

on land suggests that the δD of plant waxes can be used to reconstruct the hydrological cycle taking into account potential source areas. In **CHAPTER IV** variations in SSTs and environmental changes were investigated during the last 500 years in the Gulf of Taranto based on the comparison of multiple proxies using the lipid-derived temperature proxies $U^{K'}_{37}$ and TEX_{86} and stable isotopes of benthic and planktic foraminifera. This chapter aims to answer the question (4). The multiproxy approach suggests that the different ecologies of the source organisms influence SST estimates and that SST variations provide information on circulation changes.

I.4. METHODOLOGICAL APPROACH

I.4.1. Study Material

Lipid biomarkers were analyzed in marine and terrestrial surface sediments as well as a multicore (see **CHAPTER II-IV** for sample locations). Marine surface sediments (GeoB10701 to -49) and the multicore (GeoB10709-4 MUC) were retrieved during RV POSEIDON cruise P339 'CAPPUCCINO' in June 2006 along the SE Italian shelf (Zonneveld and et al., 2008). Surface sediments represent the top 2 cm of multicores from 48 stations collected from the southern Adriatic Sea, Strait of Otranto, Cape St. Maria di Leuca and Gulf of Taranto. The material was stored in petri dishes and frozen to $-20\text{ }^{\circ}\text{C}$ directly upon collection and kept at this temperature until geochemical processing. Core GeoB10709-4 was collected directly from the Gulf of Taranto and stored at $-20\text{ }^{\circ}\text{C}$. Prior sampling, GeoB10709-4 was stored at $4\text{ }^{\circ}\text{C}$ for two days. High resolution sampling took place in the MARUM core depository by cutting the complete core in 2.5 mm slices. The material was stored in glass vials at $-20\text{ }^{\circ}\text{C}$ until geochemical processing.

Terrestrial samples (M1-M30) were taken during a land survey in October 2009 along a NE-SE transect in Italy. These samples represent the upper 1 cm of sediments collected from freshwater environments (rivers and lakes) and near-coastal settings. The material was stored in glass vials directly upon collection and stayed at $-20\text{ }^{\circ}\text{C}$.

I.4.2. Overview lipid biomarker analyses

The following contains a brief overview of methods used for lipid biomarker analyses in the studies. Freeze-dried samples were extracted using an Accelerated Solvent Extracor (ASE) system (Dionex) suitable for a high sample flow. The total lipid extracts underwent

purification following conventional organic geochemical lab procedures resulting in lipid biomarker fractions of different polarities. For apolar biomarkers like alkenones and long chain *n*-alkanes gas chromatography coupled to a mass spectrometer (GC-MS) or flame ionization detector (GC-FID) was used for identification and quantification, respectively. Analyses of the more polar isoprenoid and branched GDGTs required the use of high performance liquid chromatography-atmospheric chemical ionization-mass spectrometry (HPLC-APCI-MS) using selected ion monitoring (SIM) and integration of the protonated ions (M+H)⁺ (e.g., Hopmans et al., 2000; Schouten et al., 2007; Schouten et al., 2009). Biomarker contents were determined by adding internal standards before extraction and were normalized to dry weight sediment and/or TOC.

The compound-specific stable carbon and hydrogen isotope composition was determined on long chain *n*-alkanes using gas chromatograph-isotope ratio mass spectrometry (GC-IRMS) (e.g., Freeman et al., 1990; Hilkert et al., 1999; Sessions, 2006). Co-eluting compounds visible in several samples were separated using urea adduction, a purification technique for the separation of straight chain compounds from non-straight chain compounds. More detailed information on instrumentation parameters during analyses can be found in the corresponding studies in **CHAPTER II -IV**.

I.5. CONTRIBUTIONS TO PUBLICATIONS

This thesis includes the complete versions of three manuscripts as first-author publications (**CHAPTER II-IV**). **CHAPTER II** includes an already published manuscript and **CHAPTER III** is accepted by an international journal considering major revisions. **CHAPTER IV** includes a first draft of a manuscript. Additionally, two co-authorship manuscripts are presented as abstracts in **APPENDIX**: Published manuscript I and Manuscript II.

Chapter II – published manuscript

Core top calibration of the lipid-based $U^{K'}_{37}$ and TEX_{86} temperature proxies on the southern Italian shelf (SW Adriatic Sea, Gulf of Taranto)

Arne Leider, Kai-Uwe Hinrichs, Gesine Mollenhauer and Gerard J.M. Versteegh

Extraction of sediments, lipid fraction purification and analysis were performed by Arne Leider. Gesine Mollenhauer provided analytical facilities and assistance during GDGT analysis. Arne Leider and Gerard J.M. Versteegh wrote the manuscript jointly with input from all co-authors. Published in *Earth and Planetary Science Letters*, vol. 300, issues 1-2, page 112-124, doi:10.1016/j.epsl.2010.09.042, © 2010 Elsevier Ltd.

Chapter III – full manuscript

Distribution and stable isotopes of plant wax derived *n*-alkanes in marine surface sediments along a SE Italian transect and their potential to reconstruct the water balance

Arne Leider, Kai-Uwe Hinrichs, Enno Schefuß and Gerard J.M. Versteegh

Extraction of sediments, lipid fraction purification, analysis on *n*-alkanes and compound specific $\delta^{13}C$ and δD were performed by Arne Leider. Arne Leider and Gerard J.M. Versteegh wrote the manuscript jointly with input from all co-authors. The manuscript has been accepted by *Geochimica et Cosmochimica Acta* considering major revisions in October 2011. This version includes the revised manuscript based on the reviewers' comments.

Chapter IV – full manuscript

Multiproxy environmental reconstructions: What do SST proxies really tell us (a high-resolution comparison of $U^{K'}_{37}$, TEX^H_{86} and foraminiferal based $\delta^{18}O$ during the last 500 years in the Gulf of Taranto)

Anna-Lena Grauel, Arne Leider, Marie-Louise S. Goudeau, Inigo Müller, Stefano M. Bernasconi, Kai-Uwe Hinrichs, Gert de Lange and Gerard J.M. Versteegh

Anna-Lena Grauel and Arne Leider are listed both as first author and contributed equally to this study. Foraminifera sampling and analysis on $\delta^{18}\text{O}$ and $\delta^{13}\text{C}$ were performed by Anna-Lena Grauel with assistance from Inigo Müller. Core sampling, extraction of sediments for lipid biomarkers, purification and analysis were done by Arne Leider. Marie-Louise S. Goudeau provided analysis on Total Organic Carbon (TOC) content. Anna-Lena Grauel and Arne Leider wrote the manuscript jointly with input from all co-authors. The manuscript is in the form of a draft for submission to *Paleoceanography*.

APPENDIX: Published manuscript I – abstract

Identification of polar lipid precursors of the ubiquitous branched GDGT orphan lipids in a peat bog in Northern Germany

Xiaolei Liu, Arne Leider, Aimee Gillespie, Jens Gröger, Gerard J.M. Versteegh and Kai-Uwe Hinrichs

Xiaolei Liu and Kai-Uwe Hinrichs designed the project. Sampling of the peat bog was done by Xiaolei Liu, Arne Leider, Aimee Gillespie, Jens Gröger and Gerard J.M. Versteegh. Jens Gröger provided the coring system and performed geochemical field analysis. Aimee Gillespie helped with sample extraction and analysis during her summer student project. Lipid identification was done by Xiaolei Liu. Co-supervision of Aimee Gillespie was provided by Xiaolei Liu and Arne Leider. Xiaolei Liu and Kai-Uwe Hinrichs wrote the manuscript jointly with input from all co-authors. Published in *Organic Geochemistry*, vol. 41, issue 7, page 653-660, doi:10.1016/j.orggeochem.2010.04.004, © 2010 Elsevier Ltd.

APPENDIX: Manuscript II – abstract

Environmental changes observed by high-resolution XRF core scanning in Holocene (0-16 ka cal. BP) sediments from the Gulf of Taranto, Central Mediterranean

Marie-Louise S. Goudeau & Anna-Lena Grauel, Chiara Tessarolo, Arne Leider, Liang Chen, Stefano M. Bernasconi, Gerard J.M. Versteegh, Karin A.F. Zonneveld and Gert J. De Lange

Marie-Louise S. Goudeau and Anna-Lena Grauel designed the study, prepared and measured most of the samples, analyzed and interpreted the results. Chiara Tessarolo conducted the geoaoustic data, provided input to the analyses and wrote and drafted the geoaoustic parts of the manuscript. Arne Leider, Liang Chen, Karin A.F. Zonneveld and Gerard J.M. Versteegh prepared and measured the cores for the ITRAX XRF core scans. Stefano M. Bernasconi and

Gert J. de Lange assisted in designing this study and interpreting of the data. Marie-Louise S. Goudeau and Anna-Lena Grauel wrote the manuscript jointly with input from all co-authors. The manuscript has been submitted to *Geochemistry, Geophysics, Geosystems* in January 2012.

I.6. REFERENCES

- Acker, J.G. and Leptoukh, G., 2007. Online Analysis Enhances Use of NASA Earth Science Data. *Eos*, 88, 14-17.
- Aloisi, G., Bouloubassi, I., Heijs, S.K., Pancost, R.D., Pierre, C., Sinninghe Damsté, J.S., Gottschal, J.C., Forney, L.J., Rouchy, J.-M., 2002. CH₄-consuming microorganisms and the formation of carbonate crusts at cold seeps. *Earth Planet. Sci. Lett.* 203, 195-203.
- Andersen, N., Paul, H.A., Bernasconi, S.M., McKenzie, J.A., Behrens, A., Schaeffer, P., Albrecht, P., 2001. Large and rapid climate variability during the Messinian salinity crisis: Evidence from deuterium concentrations of individual biomarkers. *Geology* 29, 799-802.
- Artegiani, A., Paschini, E., Russo, A., Bregant, D., Raicich, F., Pinardi, N., 1997. The Adriatic Sea general circulation. Part I: Air-sea interactions and water mass structure. *J. Phys. Oceanogr.* 27, 1492-1514.
- Artegiani, A., Paschini, E., Russo, A., Bregant, D., Raicich, F., Pinardi, N., 1997b. The Adriatic Sea general circulation. Part II: baroclinic circulation structure. *J. Phys. Oceanogr.* 27, 1515-1532.
- Bard, E., 2001. Paleoceanographic Implications of the Difference in Deep-Sea Sediment Mixing Between Large and Fine Particles. *Paleoceanography* 16, 235-239. doi: 10.1029/2000pa000537.
- Barker, S., Cacho, I., Benway, H., Tachikawa, K., 2005. Planktonic foraminiferal Mg/Ca as a proxy for past oceanic temperatures: a methodological overview and data compilation for the Last Glacial Maximum. *Quat. Sci. Rev.* 24, 821-834.
- Bates, B., Kundzewicz, Z., Wu, S., Palutikof, J., 2008. Climate change and water. technical paper of the intergovernmental panel on climate change. IPCC Secretariat, Geneva, pp 210.
- Bechtel, A., Smittenberg, R.H., Bernasconi, S.M., Schubert, C.J., 2010. Distribution of branched and isoprenoid tetraether lipids in an oligotrophic and a eutrophic Swiss lake: Insights into sources and GDGT-based proxies. *Org. Geochem.* 41, 822-832.
- Beck, J.W., Edwards, R.L., Ito, E., Taylor, F.W., Recy, J., Rougerie, F., Joannot, P., Henin, C., 1992. Sea-Surface Temperature from Coral Skeletal Strontium/Calcium Ratios. *Science* 257, 644-647.

- Belt, S.T., Cooke, D.A., Robert, J.-M., Rowland, S., 1996. Structural characterisation of widespread polyunsaturated isoprenoid biomarkers: A C₂₅ triene, tetraene and pentaene from the diatom *Haslea ostrearia simonsen*. *Tetrahedron Lett.* 37, 4755-4758.
- Belt, S.T., Massé, G., Rowland, S.J., Poulin, M., Michel, C., LeBlanc, B., 2007. A novel chemical fossil of palaeo sea ice: IP25. *Org. Geochem.* 38, 16-27.
- Bentaleb, I., Grimalt, J.O., Vidussi, F., Marty, J.C., Martin, V., Denis, M., Hatté, C., Fontugne, M., 1999. The C₃₇ alkenone record of seawater temperature during seasonal thermocline stratification. *Mar. Chem.* 64, 301-313.
- Benthien, A., Müller, P.J., 2000. Anomalously low alkenone temperatures caused by lateral particle and sediment transport in the Malvinas Current region, western Argentine Basin. *Deep-Sea Res. I* 47, 2369-2393.
- Benthien, A., Andersen, N., Schulte, S., Müller, P.J., Schneider, R.R., Wefer, G., 2002. Carbon isotopic composition of the C_{37:2} alkenone in core top sediments of the South Atlantic Ocean: Effects of CO₂ and nutrient concentrations. *Global Biogeochem. Cycles* 16, 1012. doi:10.1029/2001gb001433
- Blaga, C., Reichart, G.-J., Heiri, O., Sinninghe Damsté, J.S., 2009. Tetraether membrane lipid distributions in water-column particulate matter and sediments: a study of 47 European lakes along a north-south transect. *J. Paleolimn.* 41, 523-540.
- Blaga, C.I., Reichart, G.J., Schouten, S., Lotter, A.F., Werne, J.P., Kosten, S., Mazzeo, N., Lacerot, G., Sinninghe Damsté, J.S., 2010. Branched glycerol dialkyl glycerol tetraethers in lake sediments: Can they be used as temperature and pH proxies? *Org. Geochem.* 41, 1225-123.
- Bi, X., Sheng, G., Liu, X., Li, C., and Fu, J., 2005. Molecular and carbon and hydrogen isotopic composition of *n*-alkanes in plant leaf waxes. *Org. Geochem.* 36, 1405-1417.
- Bianchi, T.S., Canuel, E.A., 2011. *Chemical Biomarkers in Aquatic Ecosystems*. Princeton University Press.
- Bird, M.I., Summons, R.E., Gagan, M.K., Roksandic, Z., Dowling, L., Head, J., Keith Fifield, L., Cresswell, R.G., Johnson, D.P., 1995. Terrestrial vegetation change inferred from *n*-alkane $\delta^{13}\text{C}$ analysis in the marine environment. *Geochim. Cosmochim. Acta* 59, 2853-2857
- Boldrin, A., Miserocchi, S., Rabitti, S., Turchetto, M.M., Balboni, V., Socal, G., 2002. Particulate matter in the southern Adriatic and Ionian Sea: characterisation and downward fluxes. *J. Mar. Syst.* 33-34, 389-410.
- Bonino, G., Cini Castagnoli, G., Callegari, E., Zhu, G.-M., 1993. Radiometric and tephroanalysis dating of recent Ionian Sea cores. *Il Nuovo Cimento C*, 16, 155-162.
- Bornemann, A., Norris, R.D., Friedrich, O., Beckmann, B., Schouten, S., Sinninghe Damstée, J.S., Vogel, J., Hofmann, P., Wagner, T., 2008. Isotopic Evidence for Glaciation During the Cretaceous Supergreenhouse. *Science* 319, 189-192.

- Bouloubassi, I., Aloisi, G., Pancost, R.D., Hopmans, E., Pierre, C., Sinninghe Damsté, J.S., 2006. Archaeal and bacterial lipids in authigenic carbonate crusts from eastern Mediterranean mud volcanoes. *Org. Geochem.* 37, 484-500.
- Bradley, R.S., Jones, P.D., 1993. 'Little Ice Age' summer temperature variations: their nature and relevance to recent global warming trends. *The Holocene* 3, 367-376.
- Brassell, S.C., Brereton, R.G., Eglinton, G., Grimalt, J., Liebezeit, G., Marlowe, I.T., Pflaumann, U., Sarnthein, M., 1986. Palaeoclimatic signals recognized by chemometric treatment of molecular stratigraphic data. *Org. Geochem.* 10, 649-660.
- Bray, E.E., Evans, E.D., 1961. Distribution of *n*-paraffins as a clue to recognition of source beds. *Geochim. Cosmochim. Acta* 22, 2-15.
- Caroppo, C., Fiocca, A., Sammarco, P., Magazzu, G., 1999. Seasonal variations of nutrients and phytoplankton in the coastal SW Adriatic Sea (1995–1997). *Bot. Mar.* 42, 389-400.
- Caroppo, C., Congestri, R., Bruno, M., 2001. Dynamics of *Dinophysis sensu lato* species (Dinophyceae) in a coastal Mediterranean environment (Adriatic Sea). *Cont. Shelf Res.* 21, 1839-1854.
- Castañeda, I.S., Schefuß, E., Pätzold, J., Sinninghe Damsté, J.S., Weldeab, S., Schouten, S., 2010. Millennial-scale sea surface temperature changes in the eastern Mediterranean (Nile River Delta region) over the last 27,000 years. *Paleoceanography* 25, PA1208.
- Cattaneo, A., Correggiari, A., Langone, L., Trincardi, F., 2003. The late-Holocene Gargano subaqueous delta, Adriatic shelf: Sediment pathways and supply fluctuations. *Mar. Geol.* 193, 61-91.
- Chahine, M.T., 1992. The hydrological cycle and its influence on climate. *Nature* 359, 373-380.
- Chikaraishi, Y., Naraoka, H., 2003. Compound-specific δD - $\delta^{13}C$ analyses of *n*-alkanes extracted from terrestrial and aquatic plants. *Phytochemistry* 63, 361-371.
- Chikaraishi, Y., Naraoka, H., 2007. $\delta^{13}C$ and δD relationships among three *n*-alkyl compound classes (*n*-alkanoic acid, *n*-alkane and *n*-alkanol) of terrestrial higher plants. *Org. Geochem.* 38, 198-215.
- Cini Castagnoli, G., Bonino, G., Provenzale, A., Serio, M., 1990. On the presence of regular periodicities in the thermoluminescence profile of a recent sea sediment core. *Phil. Trans. R. Soc. Lond.* 330, 481-486.
- Cini Castagnoli, G., Bonino, G., Provenzale, A., Serio, M., Callegari, E., 1992a. The $CaCO_3$ profiles of deep and shallow Mediterranean sea cores as indicators of past solar-terrestrial relationships. *Nuovo Cimento Soc. Ital. Fis. C* 15, 547-563.
- Cini Castagnoli, G., Bonino, G., Della Monica, P., Taricco, C., 1997. Record of thermoluminescence in sea sediments in the last millennia. *Nuovo Cimento Soc. Ital. Fis. C* 20, 1-8.

- Cini Castagnoli, G., Bernasconi, S.M., Bonino, G., Della Monica, P., Taricco, C., 1999a. 700 year record of the 11 year solar cycle by planktonic foraminifera of a shallow water Mediterranean core. *Adv. Space Res.* 24, 233-236.
- Cini Castagnoli, G., Bonino, G., Della Monica, P., Taricco, C., Bernasconi, S.M., 1999b. Solar activity in the last millennium recorded in the $\delta^{18}\text{O}$ profile of planktonic foraminifera of a shallow water Ionian Sea core. *Sol. Phys.* 188, 191-202.
- Cini Castagnoli, G., Bonino, G., Taricco, C., Bernasconi, S.M., 2000. The 11 year solar cycle and the modern Increase in the $\delta^{13}\text{C}$ of planktonic foraminifera of a shallow water Mediterranean Sea Core (590-1979). In: *Proc. 1st Solar & Space Weather Euroconference. 'The solar cycle and terrestrial climate', Solar and space weather. Santa Cruz de Tenerife. Tenerife. Spain., ESA SP-463, 481-484.*
- Cini Castagnoli, G., Bonino, G., Taricco, C., Bernasconi, S.M., 2002. Solar radiation variability in the last 1400 years recorded in the carbon isotope ratio of a mediterranean sea core. *Adv. Space Res.* 29, 1989-1994.
- Cini Castagnoli, G., Taricco, C., Alessio, S., 2005. Isotopic record in a marine shallow-water core: Imprint of solar centennial cycles in the past 2 millennia. *Adv. Space Res.* 35, 504-508.
- Civitarese, G., Gačić, M., Vetrano, A., Boldrin, A., Bregant, D., Rabitti, S., Souvermezoglou, E., 1998. Biogeochemical fluxes through the Strait of Otranto (Eastern Mediterranean). *Cont. Shelf Res.* 18, 773-789.
- CLIMAP, 1976. The Surface of the Ice-Age Earth. *Science* 191, 1131-1137.
- Collins, J.A., Schefuß, E., Heslop, D., Mulitza, S., Prange, M., Zabel, M., Tjallingii, R., Dokken, T.M., Huang, E., Mackensen, A., Schulz, M., Tian, J., Zariess, M., Wefer, G., 2010. Interhemispheric symmetry of the tropical African rainbelt over the past 23,000 years. *Nature Geoscience.* 4, 42-45.
- Collister, J.W., Rieley, G., Stern, B., Eglinton, G., Fry, B., 1994. Compound-specific d^{13}C analyses of leaf lipids from plants with differing carbon dioxide metabolisms. *Org. Geochem.* 21, 619-627.
- Conte, M.H., Thompson, A., Lesley, D., Harris, R.P., 1998. Genetic and physiological influences on the alkenone/alkenoate versus growth temperature relationship in *Emiliana huxleyi* and *Gephyrocapsa oceanica*. *Geochim. Cosmochim. Acta* 62, 51-68.
- Conte, M.H., Weber, J.C., King, L.L., Wakeham, S.G., 2001. The alkenone temperature signal in western North Atlantic surface waters. *Geochim. Cosmochim. Acta* 65, 4275-4287.
- Conte, M.H., Sicre, M.-A., Rühlemann, C., Weber, J.C., Schulte, S., Schulz-Bull, D., Blanz, T., 2006. Global temperature calibration of the alkenone unsaturation index ($U^{K'}_{37}$) in surface waters and comparison with surface sediments. *Geochim. Geophys. Geosyst.* 7, Q02005, doi: 10.1029/2005GC001054.
- Correggiari, A., Trincardi, F., Langone, L., Roveri, M., 2001. Styles of Failure in Late Holocene Highstand Prodelta Wedges on the Adriatic Shelf. *J. Sed. Res.* 71, 218-236.

- Cranwell, P. A., 1973. Chain-length distribution of n-alkanes from lake sediments in relation to post-glacial environmental change. *Freshwater Biol.* 3, 259-265.
- Cranwell, P.A., 1981. Diagenesis of free and bound lipids in terrestrial detritus deposited in a lacustrine sediment. *Org. Geochem.* 3, 79-8
- Degobbis, D., Gilmartin, M., 1990. Nitrogen, phosphorus, and biogenic silicon budgets for the northern Adriatic Sea. *Oceanol. acta* 13, 31-45.
- De La Torre, J.R., Walker, C.B., Ingalls, A.E., Könneke, M., Stahl, D.A., 2008. Cultivation of a thermophilic ammonia oxidizing archaeon synthesizing crenarchaeol. *Environ. Microbiol.* 10, 810-818.
- De Long, E.F., 2006. Archaeal mysteries of the deep revealed. *PNAS* 103, 6417-6418.
- Elderfield, H., Ganssen, G., 2000. Past temperature and $\delta^{18}\text{O}$ of surface ocean waters inferred from foraminiferal Mg/Ca ratios. *Nature*, 405, 442-445.
- Eglinton, G. and Hamilton, R. J., 1963. The distribution of alkanes. In: *Chemical plant taxonomy* (Ed. Swain, T.). Academic Press. pp. 187-217.
- Eglinton, G. and Hamilton, R. J., 1967. Leaf Epicuticular Waxes. *Science* 156, 1322-1335.
- Eglinton, T. I. and Eglinton, G., 2008. Molecular proxies for paleoclimatology. *Earth Planet. Sci. Lett.* 275, 1-16.
- Ehleringer, J.R., Cerling, T.E., Helliker, B.R., 1997. C_4 photosynthesis, atmospheric CO_2 , and climate. *Oecologia* 112, 285-299.
- Englebrecht, A.C., Sachs, J.P., 2005. Determination of sediment provenance at drift sites using hydrogen isotopes and unsaturation ratios in alkenones. *Geochim. Cosmochim. Acta* 69, 4253-4265.
- Epstein, S., Yapp, C.J., Hall, J.H., 1976. The determination of the D/H ratio of non-exchangeable hydrogen in cellulose extracted from aquatic and land plants. *Earth Planet. Sci. Lett.* 30, 241-251.
- Epstein, B.L., D'Hondt, S., Quinn, J.G., Zhang, J., Hargraves, P.E., 1998. An effect of dissolved nutrient concentrations on alkenone-based temperature estimates. *Paleoceanography* 13, 122-126, PA03358.
- Fain, A.M.V., Ogston, A.S., Sternberg, R.W., 2007. Sediment transport event analysis on the western Adriatic continental shelf. *Cont. Shelf Res.* 27, 431-451.
- Feakins, S. J. and Sessions, A. L., 2010. Controls on the D/H ratios of plant leaf waxes in an arid ecosystem. *Geochim. Cosmochim. Acta* 74, 2128-2141.
- Freeman, K.H., Hayes, J.M., Trendel, J.-M., Albrecht, P., 1990. Evidence from carbon isotope measurements for diverse origins of sedimentary hydrocarbons. *Nature* 343, 254-256.
- Freeman, K.H., Hayes, J., 1992. Fractionation of carbon isotopes by phytoplankton and estimates of ancient CO_2 levels. *Global Biogeochem. Cycles* 6, 185-198.
- Freeman, K.H., Colarusso, L.A., 2001. Molecular and isotopic records of C_4 grassland expansion in the late miocene. *Geochim. Cosmochim. Acta* 65, 1439-1454.

- Frignani, M., Langone, L., Ravaioli, M., Sorgente, D., Alvisi, F., Albertazzi, S., 2005. Fine-sediment mass balance in the western Adriatic continental shelf over a century time scale. *Mar. Geol.* 222-223, 113-133.
- Fry, B., Sherr, E.B., 1984. $\delta^{13}\text{C}$ measurements as indicators of carbon flow on marine and freshwater ecosystems. *Contrib. Mar. Sci.* 27, 13-47.
- Focardi, S., Specchiulli, A., Spagnoli, F., Fiesoletti, F., Rossi, C., 2009. A combined approach to investigate the biochemistry and hydrography of a shallow bay in the South Adriatic Sea: the Gulf of Manfredonia (Italy). *Environ. Monit. Assess.*, 153, 209-220.
- Gacic, M., Civitarese, G., Miserocchi, S., Cardin, V., Crise, A., Mauri, E., 2002. The open-ocean convection in the Southern Adriatic: a controlling mechanism of the spring phytoplankton bloom. *Cont. Shelf Res.* 22, 1897-1908.
- Gagan, M.K., Ayliffe, L.K., Beck, J.W., Cole, J.E., Druffel, E.R.M., Dunbar, R.B., Schrag, D.P., 2000. New views of tropical paleoclimates from corals. *Quat. Sci. Rev.* 19, 45-64.
- Gagosian, R. B., Peltzer, E. T., and Zafiriou, O. C., 1981. Atmospheric transport of continentally derived lipids to the tropical North Pacific. *Nature* 291, 312-314.
- Gagosian, R. B. and Peltzer, E. T., 1986. The importance of atmospheric input of terrestrial organic material to deep sea sediments. *Org. Geochem.* 10, 661-669.
- Gaines, S.M., Eglinton, G., Rullkötter, J., 2009. *Echoes of life: what fossil molecules reveal about earth history.* Oxford University Press, USA.
- Gat, J.R., 1996. Oxygen and hydrogen isotopes in the hydrologic cycle. *Annual Rev. Earth Planet. Sci.* 24, 225-262.
- Gattinger, A., Schloter, M., Munch, J.C., 2002. Phospholipid etherlipid and phospholipid fatty acid fingerprints in selected euryarchaeotal monocultures for taxonomic profiling1. *FEMS Microbiol. Lett.* 213, 133-139
- Gliozzi, A., Paoli, G., De Rosa, M., Gambacorta, A., 1983. Effect of isoprenoid cyclization on the transition temperature of lipids in thermophilic archaebacteria. *Biochim. Biophys. Acta - Biomembranes* 735, 234-242
- Gonfiantini, R., 1986. Environmental isotopes in lake studies. *Handbook of environmental isotope geochemistry* 2, 113-168.
- Gonfiantini, R., 1978. Standards for stable isotope measurements in natural compounds. *Nature* 271, 534-536
- Gong, C., Hollander, D.J., 1999. Evidence for differential degradation of alkenones under contrasting bottom water oxygen conditions: implication for paleotemperature reconstruction. *Geochim. Cosmochim. Acta* 63, 405-411.
- Goñi, M.A., Yunker, M.B., Macdonald, R.W., Eglinton, T.I., 2000. Distribution and sources of organic biomarkers in arctic sediments from the Mackenzie River and Beaufort Shelf. *Mar. Chem.* 71, 23-51.

- Harada, N., Shin, K.H., Murata, A., Uchida, M., Nakatani, T., 2003. Characteristics of alkenones synthesized by a bloom of *emiliana huxleyi* in the Bering Sea. *Geochim. Cosmochim. Acta* 67, 1507-1519.
- Harmon, R.S., Schwarcz, H.P., O'Neil, J.R., 1979. D/H ratios in speleothem fluid inclusions: A guide to variations in the isotopic composition of meteoric precipitation? *Earth Planet. Sci. Lett.* 42, 254-266.
- Hayes, J.M., 1993. Factors controlling ^{13}C contents of sedimentary organic compounds: Principles and evidence. *Mar. Geol.* 113, 111-125.
- Hecht, A.D., Barry, R., Fritts, H., Imbrie, J., Kutzbach, J., Mitchell, J.M., Savin, S.M., 1979. Paleoclimatic research: Status and opportunities. *Quat. Res.* 12, 6-17.
- Hedges, J.I., Keil, R.G., 1995. Sedimentary organic matter preservation: an assessment and speculative synthesis. *Mar. Chem.* 49, 81-115.
- Hedges, J.I., Keil, R.G., Benner, R., 1997. What happens to terrestrial organic matter in the ocean? *Org. Geochem.* 27, 195-212.
- Henshaw, P.C., Charlson, R.J., Burges, S.J., 2000. 6 Water and the hydrosphere. In: *Earth System Science – From Biochemical Cycles to Global Change* (eds. Jacobson, M.C., Charlson Henning Rodhe, R.J., Orians, H.O.), *Int. Geophys.*. Academic Press, pp. 109-131.
- Herbert, T.D., Heinrich, D.H., Karl, K.T., 2003. Alkenone Paleotemperature Determinations. In: *Treatise on Geochemistry*, pp. 391-432. Pergamon, Oxford.
- Herfort, L., Schouten, S., Boon, J.P., Sinninghe Damsté, J.S., 2006. Application of the TEX₈₆ temperature proxy to the southern North Sea. *Org. Geochem.* 37, 1715-1726.
- Herfort, L., Schouten, S., Abbas, B., Veldhuis, M.J.W., Coolen, M.J.L., Wuchter, C., Boon, J.P., Herndl, G.J., Sinninghe Damsté, J.S., 2007. Variations in spatial and temporal distribution of Archaea in the North Sea in relation to environmental variables. *FEMS Microbiol. Ecol.* 62, 242-257.
- Hilkert, A.W., Douthitt, C.B., Schlüter, H.J., Brand, W.A., 1999. Isotope ratio monitoring gas chromatography/Mass spectrometry of D/H by high temperature conversion isotope ratio mass spectrometry. *Rapid Commun. Mass Spectrom* 13, 1226-1230.
- Hinrichs, K.-U., Rinna, J., and Rullkötter, J., 1998. Late Quaternary paleoenvironmental conditions indicated by marine and terrestrial molecular biomarkers in sediments from the Santa Barbara basin. In: *Proceedings of the Fourteenth Annual Pacific Climate (PACLIM) Workshop, April 6–9, 1997* (eds. Wilson, R.C. & Tharp, V.L.), *Interagency Ecological Program, Technical Report 57*, California Department of Water Resources. pp. 125–133.
- Hoefs, M.J.L., Versteegh, G.J.M., C. Rijpstra, W.I., de Leeuw, J.W., Sinninghe Damsté, J.S., 1998. Postdepositional Oxidative Degradation of Alkenones: Implications for the Measurement of Palaeo Sea Surface Temperatures. *Paleoceanography* 13, 42-49.
- Hoefs, J., 2009. *Stable isotope geochemistry*. Springer Verlag.

- Hopmans, E.C., Schouten, S., Pancost, R.D., van der Meer, M.T.J., Sinninghe Damsté, J.S., 2000. Analysis of intact tetraether lipids in archaeal cell material and sediments by high performance liquid chromatography/atmospheric pressure chemical ionization mass spectrometry. *Rap. Commun. Mass. Spectrom.* 14, 585-589.
- Hopmans, E.C., Weijers, J.W.H., Schefuß, E., Herfort, L., Sinninghe Damsté, J.S., Schouten, S., 2004. A novel proxy for terrestrial organic matter in sediments based on branched and isoprenoid tetraether lipids. *Earth Planet. Sci. Lett.* 224, 107-116.
- Hou, J., D'Andrea, W. J., MacDonald, D., and Huang, Y., 2007. Hydrogen isotopic variability in leaf waxes among terrestrial and aquatic plants around Blood Pond, Massachusetts (USA). *Org. Geochem.* 38, 977-984.
- Huang, Y., Dupont, L., Sarnthein, M., Hayes, J.M., Eglinton, G., 2000. Mapping of C₄ plant input from North West Africa into North East Atlantic sediments. *Geochim. Cosmochim. Acta* 64, 3505-3513.
- Huang, Y., Shuman, B., Wang, Y., and Webb, T., 2002. Hydrogen isotope ratios of palmitic acid in lacustrine sediments record late Quaternary climate variations. *Geology* 30, 1103-1106.
- Hughes, M.K., Diaz, H.F., 1994. Was there a 'medieval warm period', and if so, where and when? *Clim. Change* 26, 109-142.
- Huguet, C., Kim, J.-H., Sinninghe Damsté, J.S., Schouten, S., 2006. Reconstruction of sea surface temperature variations in the Arabian Sea over the last 23 kyr using organic proxies (TEX₈₆ and U^{K'}₃₇). *Paleoceanography* 21, PA3003.
- Huguet, C., Schimmelmann, A., Thunell, R., Lourens, L.J., Sinninghe Damsté, J.S., Schouten, S., 2007. A study of the TEX₈₆ paleothermometer in the water column and sediments of the Santa Barbara Basin. *California. Paleoceanography* 22, PA3203.
- Huguet, C., de Lange, G.J., Gustafsson, Ö., Middelburg, J.J., Sinninghe Damsté, J.S., Schouten, S., 2008. Selective preservation of soil organic matter in oxidized marine sediments (Madeira Abyssal Plain). *Geochim. Cosmochim. Acta* 72, 6061-6068.
- Huguet, C., Kim, J.-H., de Lange, G.J., Sinninghe Damsté, J.S., Schouten, S., 2009. Effects of long term oxic degradation on the , TEX₈₆ and BIT organic proxies. *Org. Geochem.* 40, 1188-1194.
- IPCC, 2007. *Climate Change 2007: The physical science basis. Contribution of working group I to the fourth assessment report of the intergovernmental panel on climate change* (eds. Solomon, S., Qin, D., Manning, M., Chen, Z., Marquis, M., Averyt, K. B., Tignor, M., and Miller, H. L.) New York: Cambridge University Press.
- Jasper, J.P., Hayes, J.M., 1990. A carbon isotope record of CO₂ levels during the late Quaternary. *Nature* 347, 462-464.
- Jones, P.D., New, M., Parker, D.E., Martin, S., Rigor, I.G., 1999. Surface air temperature and its changes over the past 150 years. *Rev. Geophys.* 37, 173-199.
- Jones, P.D., Osborn, T.J., Briffa, K.R., 2001. The Evolution of Climate Over the Last Millennium. *Science* 292, 662-667.

- Jouzel, J., Alley, R.B., Cuffey, K., Dansgaard, W., Grootes, P., Hoffmann, G., Johnsen, S.J., Koster, R., Peel, D., Shuman, C., 1997. Validity of the temperature reconstruction from water isotopes in ice cores. *J. Geophys. Res.* 102, 26-26.
- Jouzel, J., 2003. Water Stable Isotopes: Atmospheric Composition and Applications in Polar Ice Core Studies. In: *Treatise on Geochemistry, Volume 4* (eds. Keeling, R.F., Holland, H.D and Turekian K.K.). Elsevier. pp. 213-239
- Karner, M.B., DeLong, E.F., Karl, D.M., 2001. Archaeal dominance in the mesopelagic zone of the Pacific Ocean. *Nature* 409, 507-510.
- Kawamura, K., Ishimura, Y., and Yamazaki, K., 2003. Four years' observations of terrestrial lipid class compounds in marine aerosols from the western North Pacific. *Global Biogeochem. Cycles* 17, 1003.doi:10.1029/2001gb001810.
- Killops, S. D., Killops, V. J. (2005). *Introduction to Organic Geochemistry*, 2nd ed., Blackwell Publishing, Malden, Mass.
- Kim, J.-H., Schouten, S., Buscail, R., Ludwig, W., Bonnin, J., Sinninghe Damsté, J.S., Bourrin, F., 2006. Origin and distribution of terrestrial organic matter in the NW Mediterranean (Gulf of Lions): Exploring the newly developed BIT index. *Geochim. Geophys. Geosyst.* 7, Q11017, doi: 10.1029/2006GC001306.
- Kim, J.-H., Schouten, S., Hopmans, E.C., Donner, B., Sinninghe Damsté, J.S., 2008. Global sediment core-top calibration of the TEX₈₆ paleothermometer in the ocean. *Geochim. Cosmochim. Acta* 72, 1154-1173.
- Kim, J.-H., Crosta, X., Michel, E., Schouten, S., Duprat, J., Sinninghe Damsté, J.S., 2009a. Impact of lateral transport on organic proxies in the Southern Ocean. *Quat. Res.* 71, 246-250.
- Kim, J.-H., Hugué, C., Zonneveld, K.A.F., Versteegh, G.J.M., Roeder, W., Sinninghe Damsté, J.S., Schouten, S., 2009b. An experimental field study to test the stability of lipids used for the TEX₈₆ and palaeothermometers. *Geochim. Cosmochim. Acta* 73, 2888-2898.
- Kim J.-H., van der Meer, J., Schouten, S., Helmke, P., Willmott, V., Sangiorgi, F., Koç, N., Hopmans, E.C., Sinninghe Damsté, J.S., 2010. New indices and calibrations derived from the distribution of crenarchaeal isoprenoid tetraether lipids: Implications for past sea surface temperature reconstructions. *Geochim. Cosmochim. Acta* 74, 4639-4654.
- Koga, Y., Nishihara, M., Morii, H., Akagawa-Matsushita, M., 1993. Ether polar lipids of methanogenic bacteria: structures, comparative aspects, and biosyntheses. *Microbiol. Mol. Biol. Rev.* 57, 164-182.
- Könneke, M., Bernhard, A.E., De la Torre, J.R., Walker, C.B., Waterbury, J.B., Stahl, D.A., 2005. Isolation of an autotrophic ammonia-oxidizing marine archaeon. *Nature* 437, 543-546.
- Kozlowski, T. T. and Pallardy, S. G., 1997. *Growth control in woody plants*. Academic Press, San Diego, California, USA.

- Krull, E., Sachse, D., Mügler, I., Thiele, A., and Gleixner, G., 2006. Compound-specific $\delta^{13}\text{C}$ and $\delta^2\text{H}$ analyses of plant and soil organic matter: A preliminary assessment of the effects of vegetation change on ecosystem hydrology. *Soil Biol. Biochem.* 38, 3211-3221.
- Kucera, M., Weinelt, M., Kiefer, T., Pflaumann, U., Hayes, A., Weinelt, M., Chen, M.-T., Mix, A.C., Barrows, T.T., Cortijo, E., Duprat, J., Juggins, S., Waelbroeck, C., 2005. Reconstruction of sea-surface temperatures from assemblages of planktonic foraminifera: multi-technique approach based on geographically constrained calibration data sets and its application to glacial Atlantic and Pacific Oceans. *Quat. Sci. Rev.* 24, 951-998.
- Kucera, M., John, H.S., Karl, K.T., Steve, A.T., 2009. Determination of Past Sea Surface Temperatures, *Encyclopedia of Ocean Sciences*. Academic Press, Oxford, pp. 98-113.
- Lee, K.E., Kim, J.-H., Wilke, I., Helmke, P., Schouten, S., 2008. A study of the alkenone, TEX₈₆, and planktonic foraminifera in the Benguela upwelling system: Implications for past sea surface temperature estimates. *Geochem., Geophys., Geosyst.* 9, Q10019, doi: 10.1029/2008GC002056.
- Lipp, J.S., Hinrichs, K.-U., 2009. Structural diversity and fate of intact polar lipids in marine sediments. *Geochim. Cosmochim. Acta* 73, 6816-6833.
- Lipp, J.S., Morono, Y., Inagaki, F., Hinrichs, K.-U., 2008. Significant contribution of Archaea to extant biomass in marine subsurface sediments. *Nature*, 454, 991-994.
- Liu, W. and Huang, Y., 2005. Compound specific D/H ratios and molecular distributions of higher plant leaf waxes as novel paleoenvironmental indicators in the Chinese Loess Plateau. *Org. Geochem.* 36, 851-860.
- Liu, W. and Yang, H., 2008. Multiple controls for the variability of hydrogen isotopic compositions in higher plant *n*-alkanes from modern ecosystems. *Global Change Biol.* 14, 2166-2177.
- Liu, X.-L., Leider, A., Gillespie, A., Gröger, J., Versteegh, G.J.M., Hinrichs, K.-U., 2010. Identification of polar lipid precursors of the ubiquitous branched GDGT orphan lipids in a peat bog in Northern Germany. *Org. Geochem.* 41, 653-660.
- Liu, Z., Pagani, M., Zinniker, D., DeConto, R., Huber, M., Brinkhuis, H., Shah, S.R., Leckie, R.M., Pearson, A., 2009. Global Cooling During the Eocene-Oligocene Climate Transition. *Science* 323, 1187-1190
- Liu, X., Lipp, J.S., Hinrichs, K.-U., 2011. Distribution of intact and core GDGTs in marine sediments. *Org. Geochem.* 42, 368-375.
- Malanotte Rizzoli, P.M., Bergamasco, A., 1983. The Dynamics of the coastal region of the northern Adriatic Sea. *J. Phys. Oceanogr.* 13, 1105-1130.
- Marlowe, I.T., Green, J.C., Neal, A.C., Brassell, S.C., Eglinton, G., Course, P.A., 1984. Long chain(*n*-C₃₇-C₃₉) alkenones in the Prymnesiophyceae, distribution of alkenones and other lipids and their taxonomic significance. *Brit. Phycolog. J.* 19, 203-216.

- McInerney, F. A., Helliker, B. R., and Freeman, K. H., 2011. Hydrogen isotope ratios of leaf wax n-alkanes in grasses are insensitive to transpiration. *Geochim. Cosmochim. Acta* 75, 541-554.
- Ménot, G., Bard, E., Rostek, F., Weijers, J.W.H., Hopmans, E.C., Schouten, S., Damsté, J.S.S., 2006. Early Reactivation of European Rivers During the Last Deglaciation. *Science* 313, 1623-1625.
- Meybeck, M., 1982. Carbon, nitrogen, and phosphorus transport by world rivers. *Am. J. Sci.* 282, 401-450.
- Meyers, P.A., 1997. Organic geochemical proxies of paleoceanographic, paleolimnologic, and paleoclimatic processes. *Org. Geochem.* 27, 213-250
- Milligan, T.G., Cattaneo, A., 2007. Sediment dynamics in the western Adriatic Sea: From transport to stratigraphy. *Cont. Shelf Res.* 27, 287-295.
- Milliman, J.D., Syvitski, J.P.M., 1992. Geomorphic/Tectonic Control of Sediment Discharge to the Ocean: The Importance of Small Mountainous Rivers. *J. Geol.* 100, 525-544.
- Mollenhauer, G., Eglinton, T.I., Ohkouchi, N., Schneider, R.R., Müller, P.J., Grootes, P.M., Rullkötter, J., 2003. Asynchronous alkenone and foraminifera records from the Benguela Upwelling System. *Geochim. Cosmochim. Acta* 67, 2157-2171.
- Mollenhauer, G., Inthorn, M., Vogt, T., Zabel, M., Sinninghe Damsté, J.S., Eglinton, T.I., 2007. Aging of marine organic matter during cross-shelf lateral transport in the Benguela upwelling system revealed by compound-specific radiocarbon dating. *Geochem., Geophys., Geosyst.* 8, Q09004, doi:10.1029/2007GC001603.
- Mollenhauer, G., Eglinton, T.I., Hopmans, E.C., Sinninghe Damsté, J.S., 2008. A radiocarbon-based assessment of the preservation characteristics of crenarchaeol and alkenones from continental margin sediments. *Org. Geochem.* 39, 1039-1045.
- Mook, W., Rozanski, K., 2000. Environmental isotopes in the hydrological cycle. IAEA Publish.
- Morović, M., 2002. Seasonal and interannual variations in pigments in the Adriatic Sea. *J. Earth Syst. Sci.* 111, 215-225.
- Müller, P.J., Kirst, G., Ruhland, G., von Storch, I., Rosell-Melé, A., 1998. Calibration of the alkenone paleotemperature index U^{K}_{37} based on core-tops from the eastern South Atlantic and the global ocean (60°N-60°S). *Geochim. Cosmochim. Acta* 62, 1757-1772.
- Mutterlose, J., Malkoc, M., Schouten, S., Sinninghe Damsté, J.S., Forster, A., 2010. TEX86 and stable $\delta^{18}O$ paleothermometry of early Cretaceous sediments: Implications for belemnite ecology and paleotemperature proxy application. *Earth Planet. Sci. Lett.* 298, 286-298.
- Niedermeyer, E. M., Schefuß, E., Sessions, A. L., Mulitza, S., Mollenhauer, G., Schulz, M., and Wefer, G., 2010. Orbital- and millennial-scale changes in the hydrologic cycle and vegetation in the western African Sahel: insights from individual plant wax δD and $\delta^{13}C$. *Quat. Sci. Rev.* 29, 2996-3005.

- Nürnberg, D., Bijma, J., Hemleben, C., 1996. Assessing the reliability of magnesium in foraminiferal calcite as a proxy for water mass temperatures. *Geochim. Cosmochim. Acta* 60, 803-814.
- Ohkouchi, N., Kawamura, K., Kawahata, H., Okada, H., 1999. Depth ranges of alkenone production in the central Pacific Ocean. *Global Biogeochem. Cycles* 13, 695-704.
- Ohkouchi, N., Eglinton, T.I., Keigwin, L.D., Hayes, J.M., 2002. Spatial and temporal offsets between proxy records in a sediment drift. *Science* 298, 1224-1227.
- Oldfield, F., Thompson, R., 2004. Archives and Proxies along the PEP III Transect. In: *Past Climate Variability through Europe and Africa* (eds. Battarbee, R.W., Gasse, F., Stickley, C.E.). Springer Netherlands, pp. 7-29.
- O'Leary, M.H., 1981. Carbon isotope fractionation in plants. *Phytochemistry* 20, 553-567.
- Orlić, M., Gačić, M., La Violette, P.E., 1992. The currents and circulation of the Adriatic Sea. *Oceanolog. Acta* 15, 109-124.
- Pagani, M., 2002. The alkenone-CO₂ proxy and ancient atmospheric carbon dioxide. *Phil. Trans. R. Soc. London A* 360, 609-632.
- Pahnke, K., Sachs, J.P., Keigwin, L., Timmermann, A., Xie, S.-P., 2007. Eastern tropical Pacific hydrologic changes during the past 27,000 years from D/H ratios in alkenones. *Paleoceanography* 22, PA4214. doi:10.1029/2007PA001468.
- Pancost, R.D., Hopmans, E.C., Sinninghe Damsté, J.S., 2001. Archaeal lipids in Mediterranean cold seeps: molecular proxies for anaerobic methane oxidation. *Geochim. Cosmochim. Acta* 65, 1611-1627.
- Pancost, R.D., Boot, C.S., 2004. The palaeoclimatic utility of terrestrial biomarkers in marine sediments. *Mar. Chem.* 92, 239-261.
- Pelejero, C., Grimalt, J.O., 1997. The correlation between the UK37 index and sea surface temperatures in the warm boundary: The South China Sea. *Geochim. Cosmochim. Acta* 61, 4789-4797.
- Peters, K.E., Walters, C.C., Moldowan, J.M., 2005. *The biomarker guide: Biomarkers and isotopes in the environment and human history*, Volume 1. Cambridge University Press.
- Peterse, F., Kim, J.-H., Schouten, S., Kristensen, D.K., Koç, N., Sinninghe Damsté, J.S., 2009. Constraints on the application of the MBT/CBT palaeothermometer at high latitude environments (Svalbard, Norway). *Org. Geochem.* 40, 692-699.
- Peterse, F., Hopmans, E.C., Schouten, S., Mets, A., Rijpstra, W.I.C., Sinninghe Damsté, J.S., 2011. Identification and distribution of intact polar branched tetraether lipids in peat and soil. *Org. Geochem.* 42, 1007-1015.
- Pettine, M., Patrolecco, L., Camusso, M., Crescenzo, S., 1998. Transport of Carbon and Nitrogen to the Northern Adriatic Sea by the Po River. *Estuar. Coast. Shelf Sci.* 46, 127-142.

- Pierrehumbert, R.T., 2002. The hydrologic cycle in deep-time climate problems. *Nature* 419, 191-198.
- Polissar, P.J., Freeman, K.H., 2010. Effects of aridity and vegetation on plant-wax δD in modern lake sediments. *Geochim. Cosmochim. Acta* 74, 5785-5797
- Popp, B.N., Laws, E.A., Bidigare, R.R., Dore, J.E., Hanson, K.L., Wakeham, S.G., 1998. Effect of Phytoplankton Cell Geometry on Carbon Isotopic Fractionation. *Geochim. Cosmochim. Acta* 62, 69-77.
- Popp, B.N., Prah, F.G., Wallsgrove, R.J., Tanimoto, J., 2006. Seasonal patterns of alkenone production in the subtropical oligotrophic North Pacific. *Paleoceanography* 21, PA1004.
- Poulain, P.-M., 2001. Adriatic Sea surface circulation as derived from drifter data between 1990 and 1999. *J. Mar. Syst.* 29, 3-32.
- Poynter, J. G., Farrimond, P., Robinson, N., and Eglinton, G., 1989. Aeolian-derived higher plant lipids in the marine sedimentary record: Links with palaeoclimate. In: *Palaeoclimatology and Palaeometeorology: Modern and Past Patterns of Global Atmosphere Transport* (eds. Leinen, M. & Sarnthein, M.). Kluwer. pp. 435-462.
- Poynter, J. and Eglinton, G., 1990. Molecular composition of three sediments from hole 717C: the Bengal Fan. *Proc. ODP Sci. Results* 116, 155-161.
- Powers, L.A., Werne, J.P., Johnson, T.C., Hopmans, E.C., Sinninghe Damsté, J.S., Schouten, S., 2004. Crenarchaeotal membrane lipids in lake sediments: A new paleotemperature proxy for continental paleoclimate reconstruction? *Geology* 32, 613-616.
- Prah, F.G., Wakeham, S.G., 1987. Calibration of unsaturation patterns in long-chain ketone compositions for palaeotemperature assessment. *Nature* 330, 367-369.
- Prah, F.G., Pilskalns, C.H., Sparrow, M.A., 2001. Seasonal record for alkenones in sedimentary particles from the Gulf of Maine. *Deep-Sea Res. I* 48, 515-528.
- Prah, F.G., Wolfe, G.V., Sparrow, M.A., 2003. Physiological impacts on alkenone paleothermometry. *Paleoceanography* 18, PA1025.
- Prah, F.G., Popp, B.N., Karl, D.M., Sparrow, M.A., 2005. Ecology and biogeochemistry of alkenone production at Station ALOHA. *Deep-Sea Res. I* 52, 699-719.
- Rahmstorf, S., 1995. Bifurcations of the Atlantic thermohaline circulation in response to changes in the hydrological cycle. *Nature* 378, 145-149.
- Rahmstorf, S., 2002. Ocean circulation and climate during the past 120,000 years. *Nature* 419, 207-214.
- Raicich, F., 1996. On the fresh balance of the Adriatic Sea. *J. Mar. Syst.* 9, 305-319.
- Rampen, S.W., Schouten, S., Wakeham, S.G., Sinninghe Damsté, J.S., 2007. Seasonal and spatial variation in the sources and fluxes of long chain diols and mid-chain hydroxy methyl alkanoates in the Arabian Sea. *Org. Geochem.* 38, 165-179.
- Rampen, S.W., Schouten, S., Schefuß, E., Sinninghe Damsté, J.S., 2009. Impact of temperature on long chain diol and mid-chain hydroxy methyl alkanoate composition

- in Proboscia diatoms: Results from culture and field studies. *Org. Geochem.* 40, 1124-1131.
- Rampen, S.W., Schouten, S., Sinninghe Damsté, J.S., 2011. Occurrence of long chain 1,14-diols in *Apedinella* radians. *Org. Geochem.* 42, 572-574.
- Rao, Z., Zhu, Z., Jia, G., Henderson, A. C. G., Xue, Q., and Wang, S., 2009. Compound specific δD values of long chain *n*-alkanes derived from terrestrial higher plants are indicative of the δD of meteoric waters: Evidence from surface soils in eastern China. *Org. Geochem.* 40, 922-930.
- Reale, O., Dirmeyer, P., 2000. Modeling the effects of vegetation on Mediterranean climate during the Roman Classical Period: Part I: Climate history and model sensitivity. *Global and Planet. Change* 25, 163-184.
- Rieley, G., Collister, J.W., Stern, B., Eglinton, G., 1993. Gas chromatography/isotope ratio mass spectrometry of leaf wax *n*-alkanes from plants of differing carbon dioxide metabolisms. *Rapid Commun. Mass Spectrom* 7, 488-491.
- Rind, D., Rosenzweig, C., Goldberg, R., 1992. Modelling the hydrological cycle in assessments of climate change. *Nature* 358, 119-122.
- Rontani, J.-F., Marty, J.-C., Miquel, J.-C., Volkman, J.K., 2006. Free radical oxidation (autoxidation) of alkenones and other microalgal lipids in seawater. *Org. Geochem.* 37, 354-368.
- Rontani, J.F., Zabeti, N., Wakeham, S.G., 2009. The fate of marine lipids: Biotic vs. abiotic degradation of particulate sterols and alkenones in the Northwestern Mediterranean Sea. *Mar. Chem.* 113, 9-18.
- Rosell-Mélé, A., Carter, J.F., Parry, A.T., Eglinton, G., 1995. Determination of the $U^{K'}_{37}$ index in geological samples. *Anal. Chem.* 67, 1283-1289.
- Rosell-Mélé, A., Jansen, E., Weinelt, M., 2002. Appraisal of a molecular approach to infer variations in surface ocean freshwater inputs into the North Atlantic during the last glacial. *Global and Planet. Change* 34, 143-152.
- Rosell-Mélé, A., McClymont, E.L., Claude, H.-M., Anne De, V., 2007. Chapter Eleven Biomarkers as Paleoceanographic Proxies, *Developments in Marine Geology*. Elsevier, pp. 441-490.
- Rossi, S., Auroux, C., Mascle, J., 1983. The Gulf of Taranto (Southern Italy): Seismic stratigraphy and shallow structure. *Mar. Geol.* 51, 327-346.
- Rozanski, K., 1985. Deuterium and oxygen-18 in European groundwaters - Links to atmospheric circulation in the past. *Chem. Geol.* 52, 349-363.
- Rueda, G., Rosell-Melé, A., Escala, M., Gyllencreutz, R., Backman, J., 2009. Comparison of instrumental and GDGT-based estimates of sea surface and air temperatures from the Skagerrak. *Org. Geochem.* 40, 287-291.
- Sachs, H.M., Webb III, T., Clark, D., 1977. Paleocological transfer functions. *Annual Rev. Earth Planet. Sci.* 5, 159.

- Sachs, J.P., Anderson, R.F., 2003. Fidelity of alkenone paleotemperatures in southern Cape Basin sediment drifts. *Paleoceanography* 18, 1082
- Sachse, D., Radke, J., and Gleixner, G., 2004. Hydrogen isotope ratios of recent lacustrine sedimentary *n*-alkanes record modern climate variability. *Geochim. Cosmochim. Acta* 68, 4877-4889.
- Sachse, D., Radke, J., and Gleixner, G., 2006. δD values of individual *n*-alkanes from terrestrial plants along a climatic gradient - Implications for the sedimentary biomarker record. *Org. Geochem.* 37, 469-483.
- Sauer, P. E., Eglinton, T. I., Hayes, J. M., Schimmelmann, A., and Sessions, A. L., 2001. Compound-specific D/H ratios of lipid biomarkers from sediments as a proxy for environmental and climatic conditions. *Geochim. Cosmochim. Acta* 65, 213-222.
- Schefuß, E., Ratmeyer, V., Stuut, J.-B.W., Jansen, J.H.F., Sinninghe Damsté, J.S., 2003a. Carbon isotope analyses of *n*-alkanes in dust from the lower atmosphere over the central eastern Atlantic. *Geochim. Cosmochim. Acta* 67, 1757-1767.
- Schefuß, E., Schouten, S., Jansen, J.H.F., Sinninghe Damsté, J.S., 2003b. African vegetation controlled by tropical sea surface temperatures in the mid-Pleistocene period. *Nature* 422, 418-421.
- Schefuß, E., Versteegh, G.J.M., Jansen, J.H.F., Sinninghe Damsté, J.S., 2004. Lipid biomarkers as major source and preservation indicators in SE Atlantic surface sediments. *Deep-Sea Res. I* 51, 1199-1228.
- Schefuß, E., Schouten, S., and Schneider, R. R. (2005) Climatic controls on central African hydrology during the past 20,000 years. *Nature* 437, 1003-1006.
- Schlitzer, R., 2010. Ocean Data View, <http://odw.awi.de> (version 4.3.2).
- Schilman, B., Bar-Matthews, M., Almogi-Labin, A., Luz, B., 2001. Global climate instability reflected by Eastern Mediterranean marine records during the late Holocene. *Palaeogeogr., Palaeoclimatol., Palaeoecol.* 176, 157-176.
- Schmidt, F., Hinrichs, K.-U., Elvert, M., 2010. Sources, transport, and partitioning of organic matter at a highly dynamic continental margin. *Mar. Chem.* 118, 37-55.
- Schouten, S., Hopmans, E.C., Pancost, R.D., Sinninghe Damsté, J.S., 2000. Widespread occurrence of structurally diverse tetraether membrane lipids: evidence for the ubiquitous presence of low-temperature relatives of hyperthermophiles. *Proc. Natl. Acad. Sci. USA* 97, 14421-14426.
- Schouten, S., Hopmans, E.C., Schefuss, E., Sinninghe Damsté, J.S., 2002. Distributional variations in marine crenarchaeotal membrane lipids: a new tool for reconstructing ancient sea water temperatures? *Earth Planet. Sci. Lett.* 204, 265-274.
- Schouten, S., Hopmans, E.C., Forster, A., van Breugel, Y., Kuypers, M.M.M., Sinninghe Damsté, J.S., 2003. Extremely high sea-surface temperatures at low latitudes during the middle Cretaceous as revealed by archaeal membrane lipids. *Geology* 31, 1069-1072.

- Schouten, S., Hopmans, E.C., Sinninghe Damsté, J.S., 2004. The effect of maturity and depositional redox conditions on archaeal tetraether lipid palaeothermometry. *Org. Geochem.* 35, 567-571.
- Schouten, S., Ossebaar, J., Schreiber, K., Kienhuis, M.V.M., Langer, G., Benthien, A., Bijma, J., 2006. The effect of temperature, salinity and growth rate on the stable hydrogen isotopic composition of long chain alkenones produced by *Emiliania huxleyi* and *Gephyrocapsa oceanica*. *Biogeosciences* 3, 113-119.
- Schouten, S., Huguet, C., Hopmans, E.C., Kienhuis, M.V.M., Sinninghe Damsté, J.S., 2007a. Analytical methodology for TEX₈₆ paleothermometry by High-Performance Liquid Chromatography/Atmospheric Pressure Chemical Ionization-Mass Spectrometry. *Anal. Chem.* 79, 2940-2944.
- Schouten, S., Hopmans, E.C., Baas, M., Boumann, H., Standfest, S., Könneke, M., Stahl, D.A., Sinninghe Damsté, J.S., 2008. Intact Membrane Lipids of “*Candidatus Nitrosopumilus maritimus*,” a Cultivated Representative of the Cosmopolitan Mesophilic Group I Crenarchaeota. *Appl. and Environm. Microbiol.* 74, 2433-2440.
- Schouten, S., Hopmans, E.C., van der Meer, J., Mets, A., Bard, E., Bianchi, T.S., Diefendorf, A., Escala, M., Freeman, K.H., Furukawa, Y., Huguet, C., Ingalls, A., Ménot-Combes, G., Nederbragt, A.J., Oba, M., Pearson, A., Pearson, E.J., Rosell-Melé, A., Schaeffer, P., Shah, S.R., Shanahan, T.M., Smith, R.W., Smittenberg, R., Talbot, H.M., Uchida, M., Van Mooy, B.A.S., Yamamoto, M., Zhang, Z., Sinninghe Damsté, J.S., 2009. An interlaboratory study of TEX₈₆ and BIT analysis using high-performance liquid chromatography-mass spectrometry. *Geochem. Geophys. Geosyst.* 10, Q03012, doi: 10.1029/2008GC002221.
- Seki, O., Nakatsuka, T., Shibata, H., Kawamura, K., 2010. A compound-specific n-alkane d13C and dD approach for assessing source and delivery processes of terrestrial organic matter within a forested watershed in northern Japan. *Geochim. Cosmochim. Acta* 74, 599-613.
- Sessions, A.L., 2006. Isotope-ratio detection for gas chromatography. *J. Sep. Sci.* 29, 1946-1961.
- Shah, S.R., Mollenhauer, G., Ohkouchi, N., Eglinton, T.I., Pearson, A., 2008. Origins of archaeal tetraether lipids in sediments: Insights from radiocarbon analysis. *Geochim. Cosmochim. Acta* 72, 4577-4594.
- Sicre, M.-A., Bard, E., Ezat, U., Rostek, F., 2002. Alkenone distributions in the North Atlantic and Nordic sea surface waters. *Geochem. Geophys. Geosyst.* 3, 1013, doi:10.1029/2001GC000159, 2002.
- Sikes, E.L., Volkman, J.K., 1993. Calibration of alkenone unsaturation ratios (Uk'37) for paleotemperature estimation in cold polar waters. *Geochimica et Cosmochimica Acta* 57, 1883-1889.
- Sikes, E.L., Volkman, J.K., Robertson, L.G., Pichon, J.-J., 1997. Alkenones and alkenes in surface waters and sediments of the Southern Ocean: Implications for

- paleotemperature estimation in polar regions. *Geochim. Cosmochim. Acta* 61, 1495-1505.
- Simoneit, B.R.T., 1977. Organic matter in eolian dusts over the Atlantic Ocean. *Mar. Chem.* 5, 443-464
- Sinninghe Damste, J.S., Hopmans, E.C., Pancost, R.D., Schouten, S., Geenevasen, J.A.J., 2000. Newly discovered non-isoprenoid glycerol dialkyl glycerol tetraether lipids in sediments. *Chem. Comm.* 17, 1683-1684
- Sinninghe Damsté, J.S., Rijpstra, W.I.C., Reichart, G.-J., 2002a. The influence of oxic degradation on the sedimentary biomarker record II. Evidence from Arabian Sea sediments. *Geochim. Cosmochim. Acta* 66, 2737-2754.
- Sinninghe Damsté, J.S., Schouten, S., Hopmans, E.C., van Duin, A.C.T., Geenevasen, J.A.J., 2002b. Crenarchaeol: the characteristic core glycerol dibiphytanyl glycerol tetraether membrane lipid of cosmopolitan pelagic crenarchaeota. *J. Lipid Res.* 43, 1641-1651.
- Sinninghe Damsté, J.S., Rampen, S., Irene, W., Rijpstra, C., Abbas, B., Muyzer, G., Schouten, S., 2003. A diatomaceous origin for long-chain diols and mid-chain hydroxy methyl alkanates widely occurring in quaternary marine sediments: indicators for high-nutrient conditions. *Geochim. Cosmochim. Acta* 67, 1339-1348.
- Sinninghe Damsté, J.S., Rijpstra, W.I.C., Hopmans, E.C., Weijers, J.W.H., Foesel, B.U., Overmann, J., Dedysch, S.N., 2011. 13,16-Dimethyl octacosanedioic acid (iso-diabolic acid): A common membrane-spanning lipid of Acidobacteria subdivisions 1 and 3. *Appl. Environ. Microbiol.* 77, 4147-4154.
- Sluijs, A., Schouten, S., Pagani, M., Woltering, M., Brinkhuis, H., Sinninghe Damsté, J.S., Dickens, G.R., Huber, M., Reichart, G.-J., Stein, R., Matthiessen, J., Lourens, L.J., Pedentchouk, N., Backman, J., Moran, K., the Expedition, S., 2006. Subtropical Arctic Ocean temperatures during the Palaeocene/Eocene thermal maximum. *Nature* 441, 610-613.
- Sluijs, A., Brinkhuis, H., Schouten, S., Bohaty, S.M., John, C.M., Zachos, J.C., Reichart, G.-J., Sinninghe Damste, J.S., Crouch, E.M., Dickens, G.R., 2007. Environmental precursors to rapid light carbon injection at the Palaeocene/Eocene boundary. *Nature* 450, 1218-1221.
- Socal, G., Boldrin, A., Bianchi, F., Civitarese, G., De Lazzari, A., Rabitti, S., Totti, C., Turchetto, M.M., 1999. Nutrient, particulate matter and phytoplankton variability in the photic layer of the Otranto strait. *J. Mar. Syst.* 20, 381-398.
- Smith, R.W., Bianchi, T.S., Savage, C., 2010. Comparison of lignin phenols and branched/isoprenoid tetraethers (BIT index) as indices of terrestrial organic matter in Doubtful Sound, Fiordland, New Zealand. *Org. Geochem.* 41, 281-290.
- Smith, F. A. and Freeman, K. H., 2006. Influence of physiology and climate on δD of leaf wax *n*-alkanes from C₃ and C₄ grasses. *Geochim. Cosmochim. Acta* 70, 1172-1187.
- Smittenberg, R.H., Hopmans, E.C., Schouten, S., Hayes, J.M., Eglinton, T.I., Sinninghe Damsté, J.S., 2004. Compound-specific radiocarbon dating of the varved Holocene

- sedimentary record of Saanich Inlet, Canada. *Paleoceanography* 19, PA2012.doi: 10.1029/2003pa000927.
- Sonzogni, C., Bard, E., Rostek, F., Lafont, R., Rosell-Mele, A., Eglinton, G., 1997. Core-top calibration of the alkenone index vs sea surface temperature in the Indian Ocean. *Deep-Sea Res. II*: 44, 1445-1460.
- Stephens, G.L., Webster, P.J., Johnson, R.H., Engelen, R., L'Ecuyer, T., 2004. Observational evidence for the mutual regulation of the tropical hydrological cycle and tropical sea surface temperatures. *J. climatol.* 17, 2213-2224.
- Sun, M.Y., Wakeham, S.G., 1994. Molecular evidence for degradation and preservation of organic matter in the anoxic Black Sea basin. *Geochim. Cosmochim Acta* 58, 3395-3406.
- Taricco, C., Ghil, M., Vivaldo, G., 2009. Two millennia of climate variability in the Central Mediterranean. *Clim. Past* 5, 171-181.
- Ternois, Y., Sicre, M.A., Boireau, A., Conte, M.H., Eglinton, G., 1997. Evaluation of long-chain alkenones as paleo-temperature indicators in the Mediterranean Sea. *Deep-Sea Res. I* 44, 271-286.
- Tesi, T., Miserocchi, S., Langone, L., Boni, L., Guerrini, F., 2006. Sources, Fate and Distribution of Organic Matter on the Western Adriatic Continental Shelf, Italy. *Water, Air, & Soil Poll.*, 593-603.
- Tesi, T., Miserocchi, S., Goñi, M.A., Langone, L., Boldrin, A., Turchetto, M., 2007. Organic matter origin and distribution in suspended particulate materials and surficial sediments from the western Adriatic Sea (Italy). *Estuar. Coast. Shelf Sci.* 73, 431-446.
- Tierney, J. E., Russell, J. E., Huang, Y., Sinninghe Damsté, J. S., Hopmans, E. C., and Cohen, A. S., 2008. Northern Hemisphere Controls on Tropical Southeast African Climate During the Past 60,000 Years. *Science*. 322, 252-255.
- Tomadin, L., 2000. Sedimentary fluxes and different dispersion mechanisms of the clay sediments in the Adriatic Basin. *Rendiconti Lincei* 11, 161-174.
- Tornabene, T., Langworthy, T., 1979. Diphytanyl and dibiphytanyl glycerol ether lipids of methanogenic archaeobacteria. *Science* 203, 51-53
- Totti, C., Civitarese, G., Acri, F., Barletta, D., Candelari, G., Paschini, E., Solazzi, A., 2000. Seasonal variability of phytoplankton populations in the middle Adriatic sub-basin. *J. Plankton Res.* 22, 1735-1756.
- Trommer, G., Siccha, M., van der Meer, M.T.J., Schouten, S., Sinninghe Damsté, J.S., Schulz, H., Hemleben, C., Kucera, M., 2009. Distribution of Crenarchaeota tetraether membrane lipids in surface sediments from the Red Sea. *Org. Geochem.* 40, 724-731.
- Turich, C., Freeman, K.H., Bruns, M.A., Conte, M., Jones, A.D., Wakeham, S.G., 2007. Lipids of marine archaea: Patterns and provenance in the water-column and sediments. *Geochim. Cosmochim. Acta* 71, 3272-3291.

- Uda, I., Sugai, A., Itoh, Y.H., Itoh, T., 2004. Variation in molecular species of core lipids from the order thermoplasmatales strains depends on the growth temperature. *J. Oleo Sci.* 53, 399-404.
- van der Meer, M.T.J., Baas, M., Rijpstra, W.I.C., Marino, G., Rohling, E.J., Sinninghe Damsté, J.S., Schouten, S., 2007. Hydrogen isotopic compositions of long-chain alkenones record freshwater flooding of the Eastern Mediterranean at the onset of sapropel deposition. *Earth Planet. Sci. Lett.* 262, 594-600.
- Versteegh, G.J.M., Bosch, H.J., De Leeuw, J.W., 1997. Potential palaeoenvironmental information of C₂₄ to C₃₆ mid-chain diols, keto-ols and mid-chain hydroxy fatty acids; a critical review. *Org. Geochem.* 27, 1-13.
- Versteegh, G.J.M., Riegman, R., de Leeuw, J.W., Jansen, J.H.F., 2001. U^K₃₇ values for *Isochrysis galbana* as a function of culture temperature, light intensity and nutrient concentrations. *Org. Geochem.* 32, 785-794.
- Versteegh, G.J.M., 2005. Solar Forcing of Climate. 2: Evidence from the Past. *Space Sci. Rev.* 120, 243-286.
- Versteegh, G.J.M., de Leeuw, J.W., Taricco, C., Romero, A., 2007. Temperature and productivity influences on U^K₃₇ and their possible relation to solar forcing of the Mediterranean winter. *Geochem., Geophys., Geosyst.* 8, Q09005, doi: 10.1029/2006GC001543
- Viličić, D., Vučak, Z., Škrivanić, A., Gržetić, Z., 1989. Phytoplankton blooms in the oligotrophic open south Adriatic waters. *Mar. Chem.* 28, 89-107.
- Volkman, J.K., Eglinton, G., Corner, E.D.S., Forsberg, T.E.V., 1980. Long-chain alkenes and alkenones in the marine coccolithophorid *Emiliana huxleyi*. *Phytochemistry* 19, 2619-2622.
- Volkman, J.K., Barrett, S.M., Dunstan, G.A., Jeffrey, S.W., 1992. C₃₀ - C₃₂ alkyl diols and unsaturated alcohols in microalgae of the class Eustigmatophyceae. *Org. Geochem.* 18, 131-138.
- Volkman, J.K., Barrett, S.M., Dunstan, G.A., 1994. C₂₅ and C₃₀ highly branched isoprenoid alkenes in laboratory cultures of two marine diatoms. *Org. Geochem.* 21, 407-414.
- Volkman, J.K., Barrett, S.M., Blackburn, S.I., Sikes, E.L., 1995. Alkenones in *Gephyrocapsa oceanica*: Implications for studies of paleoclimate. *Geochim. Cosmochim. Acta* 59, 513-520.
- Volkman, J.K., Barrett, S.M., Blackburn, S.I., Mansour, M.P., Sikes, E.L., Gelin, F., 1998. Microalgal biomarkers: a review of recent research developments. *Organic Geochemistry* 29, 1163-1179.
- Volkman, J.K., Barrett, S.M., Blackburn, S.I., 1999. Eustigmatophyte microalgae are potential sources of C₂₉ sterols, C₂₂-C₂₈ *n*-alcohols and C₂₈-C₃₂ *n*-alkyl diols in freshwater environments. *Org. Geochem.* 30, 307-318.

- Volkman, J.K., 2000. Ecological and environmental factors affecting alkenone distributions in seawater and sediments. *Geochem. Geophys. Geosyst.* 1, 2000GC000061, doi: 10.1029/2000gc000061.
- Waelbroeck, C., Mulitza, S., Spero, H., Dokken, T., Kiefer, T., Cortijo, E., 2005. A global compilation of late Holocene planktonic foraminiferal ^{18}O : relationship between surface water temperature and ^{18}O . *Quat. Sci. Rev.* 24, 853-868.
- Walsh, E.M., Ingalls, A.E., Keil, R.G., 2008. Sources and transport of terrestrial organic matter in Vancouver Island fjords and the Vancouver-Washington Margin: A multiproxy approach using $\delta^{13}\text{C}_{\text{org}}$, lignin phenols, and the ether lipid BIT index. *Limnol. Oceanogr.* 53, 1054-1063.
- Wakeham, S.G., Lewis, C.M., Hopmans, E.C., Schouten, S., Sinninghe Damsté, J.S., 2003. Archaea mediate anaerobic oxidation of methane in deep euxinic waters of the Black Sea. *Geochim. Cosmochim. Acta* 67, 1359-1374.
- Weijers, J.W.H., Schouten, S., Hopmans, E.C., Geenevasen, J., A.J., David, O.R.P., Coleman, J.M., D., P.R., Sinninghe Damsté, J.S., 2006a. Membrane lipids of mesophilic anaerobic bacteria thriving in peats have typical archaeal traits. *Environ. Microbiol.* 8, 648-657.
- Weijers, J.W.H., Schouten, S., Spaargaren, O.C., Sinninghe Damsté, J.S., 2006b. Occurrence and distribution of tetraether membrane lipids in soils: Implications for the use of the TEX_{86} proxy and the BIT index. *Org. Geochem.* 37, 1680-1693.
- Weijers, J.W.H., Schouten, S., van den Donker, J.C., Hopmans, E.C., Sinninghe Damsté, J.S., 2007a. Environmental controls on bacterial tetraether membrane lipid distribution in soils. *Geochim. Cosmochim Acta* 71, 703-713.
- Weijers, J.W.H., Schefuß, E., Schouten, S., Sinninghe Damsté, J.S., 2007b. Coupled Thermal and Hydrological Evolution of Tropical Africa over the Last Deglaciation. *Science* 315, 1701-1704.
- Weijers, J.W.H., Schouten, S., Sluijs, A., Brinkhuis, H., Sinninghe Damsté, J.S., 2007c. Warm arctic continents during the Palaeocene-Eocene thermal maximum. *Earth Planet. Sci. Lett.* 261, 230-238.
- Weijers, J.W.H., Schouten, S., Schefuß, E., Schneider, R.R., Sinninghe Damsté, J.S., 2009. Disentangling marine, soil and plant organic carbon contributions to continental margin sediments: A multi-proxy approach in a 20,000 year sediment record from the Congo deep-sea fan. *Geochim. Cosmochim Acta* 73, 119-132.
- Wollast, R., 1998. Evaluation and comparison of the global carbon cycle in the coastal zone and in the open ocean. *The sea* 10, 213-252.
- Wuchter, C., Schouten, S., Coolen, M.J.L., Sinninghe Damsté, J.S., 2004. Temperature-dependent variation in the distribution of tetraether membrane lipids of marine Crenarchaeota: implications for TEX_{86} paleothermometry. *Paleoceanography* 19, 1537-1546.

- Wuchter, C., Schouten, S., Wakeham, S.G., Sinninghe Damsté, J.S., 2005. Temporal and spatial variation in tetraether membrane lipids of marine crenarchaeota in particulate organic matter: Implications for TEX₈₆ paleothermometry. *Paleoceanography* 20, PA3013. Doi: 10.1029/2004PA001110.
- Wuchter, C., Schouten, S., Wakeham, S.G., Sinninghe Damsté, J.S., 2006. Archaeal tetraether membrane lipid fluxes in the northeastern Pacific and the Arabian Sea: Implications for TEX₈₆ paleothermometry. *Paleoceanography* 21, PA4208. Doi: 10.1029/2006pa001279.
- Xie, S., Yao, T., Kang, S., Xu, B., Duan, K., Thompson, L.G., 2000. Geochemical analyses of a Himalayan snowpit profile: implications for atmospheric pollution and climate. *Org. Geochem.* 31, 15-23.
- Yamada, K., Ishiwatari, R., 1999. Carbon isotopic compositions of long-chain n-alkanes in the Japan Sea sediments: implications for paleoenvironmental changes over the past 85 kyr. *Org. Geochem.* 30, 367-377.
- Zavatarelli, M., Pinardi, N., 2003. The Adriatic Sea modelling system: a nested approach. *Ann. Geophys.* 21, 345-364.
- Zavatarelli, M., Raicich, F., Bregant, D., Russo, A., Artegiani, A., 1998. Climatological biogeochemical characteristics of the Adriatic Sea. *J. Mar. Syst.* 18, 227-263.
- Zonneveld, K.A.F., and cruise participants, 2008. Report and preliminary results of R/V POSEIDON Cruise P339, Piräus - Messina, 16 June - 2 July 2006. *Berichte, Fachbereich Geowissenschaften, Universität Bremen* 268, 61.
- Zonneveld, K.A.F., Chen, L., Möbius, J., Mahmoud, M.S., 2009. Environmental significance of dinoflagellate cysts from the proximal part of the Po-river discharge plume (off southern Italy, Eastern Mediterranean). *J. Sea Res.* 62, 189-213.

CHAPTER II

Core top calibration of the lipid-based $U^{K'}_{37}$ and TEX_{86} temperature proxies on the southern Italian shelf (SW Adriatic Sea, Gulf of Taranto)

Arne Leider^{a,*}, Kai-Uwe Hinrichs^a, Gesine Mollenhauer^{a,b},
and Gerard J.M. Versteegh^a

Published in *Earth and Planetary Science Letters*
vol. 300, issues 1-2, page 112-124, doi:10.1016/j.epsl.2010.09.042
© 2010 Elsevier Ltd.

^a MARUM Center for Marine Environmental Sciences & Dept. of Geosciences, University of Bremen, D-28334 Bremen, Germany

^b Alfred Wegener Institute for Polar and Marine Research, D-27570 Bremerhaven, Germany

* corresponding authors,

E-mail addresses: AL: arneleider@uni-bremen.de; GJMV: versteegh@uni-bremen.de

Phone: +49 421 218 65742 (AL)

Fax: +49 421 218 65715

Keywords

Mediterranean climate; Southern Adriatic Sea; Gulf of Taranto; SST; surface sediments; $U^{K'}_{37}$; TEX_{86} ; BIT; alkenones; GDGTs

II.1. ABSTRACT

The Mediterranean Sea is at the transition between temperate and tropical air masses and as such of importance for studying climate change. The Gulf of Taranto and adjacent SW Adriatic Sea are at the heart of this region. Their sediments are excellently suited for generating high quality environmental records for the last millennia with a sub-decadal resolution. The quality of these records is dependent on a careful calibration of the transfer functions used to translate the sedimentary lipid signals to the local environment. Here, we examine and calibrate the $U^{K'}_{37}$ and TEX_{86} lipid-based temperature proxies in 48 surface sediments and relate these to ambient sea surface temperatures and other environmental data. The $U^{K'}_{37}$ -based temperatures in surface sediments reflect winter/spring sea surface temperatures in agreement with other studies demonstrating maximum haptophyte production during the colder season. The TEX_{86} -based temperatures for the nearshore sites also reflect winter sea surface temperatures. However, at the most offshore sites, they correspond to summer sea surface temperatures. Additional lipid and environmental data including the distribution of the BIT index and remote-sensed chlorophyll-*a* suggest a shoreward increase of the impact of seasonal and spatial variability in nutrients and control of planktonic archaeal abundance by primary productivity, particle loading in surface waters and/or overprint by a cold-biased terrestrial TEX_{86} signal. As such the offshore TEX_{86} values seem to reflect a true summer signal to the effect that offshore $U^{K'}_{37}$ and TEX_{86} reconstruct winter and summer temperature, respectively, and hence provide information on the annual temperature amplitude.

II.2. INTRODUCTION

A valid and powerful method to better understand short-term environmental and climate change is to study the past. The interactions between atmosphere and ocean are complex so deciphering them requires quantitative and reliable proxies for key environmental parameters such as temperature, air pressure, sea level and the precipitation-evaporation budget. This is also valid for the Mediterranean climate, which is especially sensitive to climate change due to its location between the subtropical high-pressure belt and mid-latitude westerlies (e.g., Trigo et al., 1999; Xoplaki et al., 2003, 2004).

As Sea Surface Temperature (SST) is an important factor in the Earth's climate, its reconstruction is essential for an understanding of past climate change. The commonly used

geochemical temperature proxies include $\delta^{18}O$ and Mg/Ca ratios of planktonic foraminifera (Erez & Luz, 1983; Nürnberg et al., 1996; Elderfield & Ganssen, 2000), the $U^{K'}_{37}$ from alkenones synthesized by haptophytes (Prah1 & Wakeham, 1987) and the TEX_{86} based on archaeal isoprenoidal tetraether lipids (Schouten et al., 2002; Kim et al., 2008).

The $U^{K'}_{37}$ exploits the observation that the abundance of the diunsaturated C_{37} methyl alkenone, relative to the total of di- and triunsaturated C_{37} methyl alkenones in surface waters and algal cultures increases with increasing water temperature. These alkenones are produced by a small group of haptophyte algae thriving in the mixed layer: the coccolithophore *Emiliana huxleyi* and related species (Volkman et al., 1980; Marlowe et al., 1984; Brassell et al., 1986; Prah1 & Wakeham, 1987; Conte et al., 1998). Global calibrations of marine core-top $U^{K'}_{37}$ values with mean annual SSTs show a consistent linear relationship with an uncertainty of 1.1°C (Müller et al., 1998; Conte et al., 2006). This led to the establishment of the $U^{K'}_{37}$ index as a reliable paleoceanographic tool to estimate SSTs in a variety of oceanic settings (Herbert et al., 2003 and references therein; Haug et al., 2005; Sachs & Anderson, 2005).

Nevertheless, some studies reveal clear discrepancies between the $U^{K'}_{37}$ signal in sediments and annual mean SST (e.g., Volkman, 2000). Factors suggested to cause these discrepancies include preferential degradation of the triunsaturated alkenone (Sun & Wakeham, 1994; Gong & Hollander, 1999; Hoefs et al., 2002; Rontani et al., 2006, 2009; Kim et al., 2009b), influence of nutrients and light (Epstein et al., 1998; Versteegh et al., 2001; Prah1 et al., 2003), input of alkenones from remote regions (Benthien & Müller, 2000; Goñi et al., 2001; Ohkouchi et al., 2002; Mollenhauer et al., 2007), differences in species composition (Volkman et al., 1995; Conte et al., 1998), production at greater depths within the euphotic zone (Ternois et al., 1997; Bentaleb et al., 1999; Prah1 et al., 2005) or strong blooming of haptophytes in periods with water temperatures that are significantly different from the annual mean (Sikes et al., 1997; Bentaleb et al., 1999; Prah1 et al., 2001 and references therein; Popp et al., 2006; Versteegh et al., 2007). In spite of these deviations from the global calibration the utility of site-specific calibrations between environment and $U^{K'}_{37}$ is contentious.

The TEX_{86} temperature proxy is based on archaeal glycerol dialkyl glycerol tetraethers (GDGT), which are abundant in marine sediments (Schouten et al., 2000, 2002). The biological sources are non-hyperthermophilic cren- and euryarchaeota, a major group of prokaryotes in today's oceans and lakes (Karner et al., 2001; Powers et al., 2004). The relative distribution of these isoprenoidal GDGTs varies with growth temperature and (similar to the $U^{K'}_{37}$) linear regressions of core-top TEX_{86} values to SST enable the use of the TEX_{86} as a temperature proxy (Schouten et al., 2002, 2007a; Wuchter et al., 2005; Kim et al., 2008,

2010). The TEX_{86} is considered to reflect annual mean temperatures of the upper mixed layer (Schouten et al., 2002; Kim et al., 2008). Although, the TEX_{86} is increasingly used for reconstructing ancient SSTs, a number of issues remain unresolved (Huguet et al., 2006; Pearson et al., 2007). It appears that the TEX_{86} can be biased due to additional production of GDGTs below the mixed layer (Pearson et al., 2001; Huguet et al., 2007; Lee et al., 2008), by seasonality in crenarchaeotal growth (Schouten et al., 2002; Herfort et al., 2006; Huguet et al., 2006, 2007; Menzel et al., 2006; Wuchter et al., 2006) and by the ecology of planktonic cren- and euryarchaeota due to their presence in different water depths of the ocean and the theoretical possibility of GDGT synthesis by marine euryarchaeota (Wuchter et al., 2005; DeLong, 2006, Turich et al., 2007). Additionally, archaea living in sediments of continental margins and the deep-sea may contribute to the GDGT pool and thus influence the TEX_{86} value (Sorensen & Teske, 2006; Lipp et al., 2008; Shah et al., 2008; Lipp & Hinrichs, 2009). In coastal settings, fluvial input of terrestrial isoprenoidal GDGTs may bias the TEX_{86} (Herfort et al., 2006). Fortunately, this latter bias can be determined by using the Branched and Isoprenoid Tetraether (BIT) index (Hopmans et al., 2004), a ratio between the abundance of branched GDGTs (presumably derived from anaerobic soil bacteria) and crenarchaeol indicating the relative importance of terrestrial organic matter input (Herfort et al., 2006; Kim et al., 2006, Weijers et al., 2006a; Weijers et al., 2006b).

Diagenetic overprints of the TEX_{86} due to changing redox conditions seem to be less important than for other biomarkers (Sinninghe Damsté et al., 2002a; Schouten et al., 2004; Kim et al., 2009b). However, selective degradation during resuspension, transport and re-deposition may be significant in some cases and has to be considered for the reliable application of the TEX_{86} as a SST proxy (Mollenhauer et al., 2007; Kim et al., 2009a). Considering these factors, careful assessment of site-specific relations between $U^{K'}_{37}$ values, TEX_{86} and SST is vital to arrive at reliable SST reconstructions.

At the Gallipoli shelf (Gulf of Taranto, southern Italy) the influence of the mid-latitude westerlies, represented by the seasonal modes of the Northern Atlantic Oscillation (NAO), have a significant effect on the region causing for example maxima in precipitation during winter and arrival of Atlantic storm tracks in southern Italy (e.g., Hurrell and Van Loon, 1997; Xoplaki et al., 2004). Sediments at the shelf are suitable for high resolution environmental reconstruction (e.g., Cini Castagnoli et al., 1999b; Versteegh et al., 2007) (Fig. II.1.). Shallow-water cores revealed the unique potential for high-resolution down-core studies of the past two centuries based on radiometric dating and tephroanalysis (Cini Castagnoli et al., 1990; Bonino et al., 1993). Furthermore, carbonate contents (Cini Castagnoli et al., 1992a,

1992b), thermoluminescence (Cini Castagnoli et al., 1997) and the stable carbon and oxygen isotope compositions of the planktonic foraminifer *G. ruber* show significant decadal to centennial components, assumed to be related to solar forcing (Cini Castagnoli et al., 1999, 2000, 2002, 2005). An alkenone-based SST reconstruction covering 1305 A.D. to 1979 A.D. proposed that $U^{K'}_{37}$ reflects mainly SST of the cooler part of the year. In the same study an imprint was observed of centennial-scale SST variations consistent with the record of atmospheric $\Delta^{14}C$, a proxy for solar energy variability, suggesting a solar forcing mechanism (Versteegh et al., 2007).

Given the suitability of the Gallipoli region for high-resolution climate reconstruction, we carefully calibrated lipid-derived SST proxies in comparison to the most recent environmental conditions over a broader area covering the Italian shelf within the southern Adriatic Sea and Gulf of Taranto, taking into consideration the preservation, transport and other control mechanisms related to these signals.

II.3. STUDY AREA

The Adriatic Sea is a narrow semi-enclosed sub-basin of the northeastern Mediterranean Sea which is elongated in NW-SE direction (ca. 200x800 km) (Cattaneo et al., 2003) (Fig. II.1.). Morphologically its northern part is characterized by shallow and gently sloping shelf (Artegiani et al., 1997a). The southern Adriatic Sea is flanked by a steep slope and narrow shelf, except south of the Gargano Promontory, where the shelf broadens to about 70-80 km and the Strait of Otranto where the Adriatic Sea is separated from the Ionian Sea (Artegiani et al., 1997a; Cattaneo et al., 2003; Zavatarelli & Pinardi, 2003).

The circulation of the Adriatic Sea is known to be cyclonic with seasonal variability (Rizzoli & Bergamasco, 1983; Orlić et al., 1992; Artigiani et al., 1997b; Poulain, 2001). There are three main forcing factors affecting the circulation: a) river run-off causing heat loss and low-salinity water gain; b) atmospheric forcing responsible for dense water formation and seasonal differences in circulation; c) exchange via the Strait of Otranto balancing the water budget by intrusion of warm and salty waters from the Ionian Sea (Artegiani et al., 1997a; Cattaneo et al., 2003; Zavatarelli & Pinardi, 2003; Milligan & Cattaneo, 2007).

The northern Po-river system and Apennine rivers located north of the Gargano Promontory play the major role in freshwater supply for the western Adriatic Sea by contributing more than 70% of the total runoff, whereas in the south-western Adriatic Sea rivers are nearly absent (Raicich, 1996). On a seasonal scale increased river runoff is observed in late autumn

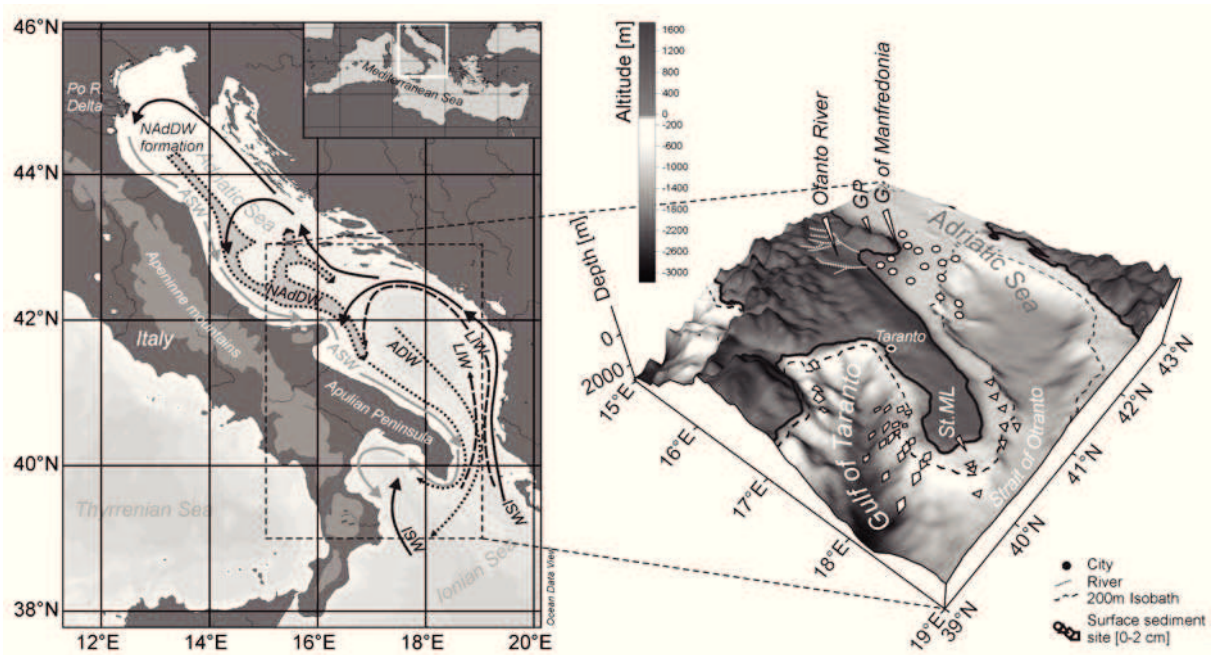


Figure II.1. Map of the Adriatic and Ionian Sea indicating the study area and general circulation pattern (ISW: Ionian Surface Water, ASW: Adriatic Surface Water, LIW: Levantine Intermediate Water, NAdDW: Northern Adriatic Deep Water; ADW: Adriatic Deep Water; redrawn from Artegiani et al., 1997b, Poulain et al., 2001, Vilibić et al., 2004). Right zoom in 3D-map showing the locations of the surface sediment analyzed in this study (GP: Gargano Promontory; G. of Manfredonia: Gulf of Manfredonia; St.ML: Cape Santa Maria di Leuca). Samples were grouped in accordance to their spatial distribution within the southern Adriatic Sea (circles: GP and G. of Manfredonia, triangles: Strait of Otranto) and Gulf of Taranto (diamonds: E Gulf of Taranto, squares: W Gulf of Taranto).

and late spring corresponding to precipitation maxima and snow melting (Cattaneo et al., 2003). This creates the coastal buoyancy-driven Western Adriatic Current (WAC) characterized as Adriatic Surface Water (ASW), which is confined to a narrow coastal strip flowing southwards along the Italian eastern margin through the Strait of Otranto into the Gulf of Taranto where it mixes with Ionian Sea water masses. Its intensity and extension can also be tracked by the development of a thermal front showing low temperatures of Adriatic Surface Water trapped in the western Adriatic coast (e.g., Morović et al., 2006).

The southern Adriatic open waters show oligotrophic characteristics comparable to the Ionian Sea and nutrient supply to the euphotic zone depends strongly on vertical stratification and mixing processes (Viličić et al., 1989). Here, the Western Adriatic Current system plays a crucial role for nutrient supply and drives primary production (PP) of the Adriatic Sea. As a consequence, higher pigment concentrations can be observed in satellite images along the Italian coastal zone (Morović, 2002), the Strait of Otranto, around the Apulian Peninsula into the Gulf of Taranto (e.g. Focardi et al., 2009; Zonneveld et al., 2009). For this region remote-sensing shows a negative correlation between seasonal SSTs to chlorophyll-*a*, whereas SSTs and salinity are positively correlated, indicating that main PP takes place during the colder season and demonstrating the influence of freshwater input and associated heat loss

(Zonneveld et al., 2009). Additionally, highest phytoplankton densities in the surface layer of the water column are observed in spring and autumn at the western shelf in the middle Adriatic sub-basin as a consequence of intensified continental water input (Totti et al., 2000). Intrusion of Ionian Surface Water (ISW) is restricted to the eastern coast of the Adriatic Sea, balancing the outflow of Adriatic Surface Water. Advection of nutrient-rich Mediterranean waters into the southern Adriatic Sea is also an important productivity factor (Marasović et al., 1995). Nutrient-rich and high-salinity intermediate waters, with a core at 200 m, form the Levantine Intermediate Water (LIW). The Levantine Intermediate Water invades the southern Adriatic Sea during winter at the western Adriatic shelf, where it mixes with Adriatic Surface Water, affecting the phytoplankton community (Caroppo et al., 2001).

Deep-water formation takes place in the northern Adriatic Sea. Here, Northern Adriatic deep Dense Water (NAdDW) occupies the northern shelf, promoted by surface cooling due to wind outbreaks during winter (e.g. Vilibić et al., 2005). Additionally, Adriatic Deep Water (ADW) is formed in the southern Adriatic Sea basin. The two deep waters spread into the Ionian Sea. In the Gulf of Taranto, where the width of the shelf rapidly decreases, dense coastal water is released to depth and transformed by intrusion and mixing with ambient water (Kourafalou, 2001; Sellschopp & Alvaréz, 2003; Hainbucher et al., 2006; Bignami et al., 2007).

SSTs from satellite and limited available in-situ measurements in the research area vary between 13 °C in winter and 26 °C in summer and show a good agreement (Zavatarelli et al., 1998; Caroppo et al., 1999, 2001; Socal et al., 1999; Boldrin et al., 2002; Zonneveld et al., 2009). Lower SSTs of 13-15 °C during winter and spring are especially observed at the near-coastal locations in the Gulf of Manfredonia due to the influence of the Western Adriatic Current and freshwater input of the adjacent Ofanto river draining into the gulf.

In the region the upper water column is well mixed during winter and spring while a thermocline starts to develop at 50-70 m water depth in March leading to open-ocean stratification during summer. This controls nutrient distribution, which is additionally influenced by river input and resuspension due to vertical mixing during winter. As a result, nutrient concentrations in the surface waters decrease from NW to SE (e.g., Civitarese et al., 1998). This seasonality in nutrients and other water column characteristics affects the phytoplankton community structure (Boldrin et al., 2002; Socal et al., 1999).

II.4. MATERIAL AND METHODS

II.4.1. Surface sediment samples

The sediments analyzed represent the top 2 cm of multicores from 48 stations obtained from the southern Adriatic Sea, Strait of Otranto, Cape St. Maria di Leuca and Gulf of Taranto. They have been collected during P339 POSEIDON cruise 'CAPPUCCINO' in June 2006 (Fig. II.1., Table II.1) (Zonneveld et al., 2009). The material was frozen to -20 °C directly upon collection and stayed at this temperature until geochemical processing. ^{210}Pb ages imply high sedimentation rates along the Italian shelf (compilation in Zonneveld et al., 2009). Given the high sedimentation rates and sampling strategy, samples represent a record of very recent sedimentation between 2 and 29 years.

II.4.2. Lipid Extraction

For GDGT and alkenone analyses, 5-15 g of freeze dried and homogenized sediment were extracted using an accelerated solvent extractor (ASE 200, DIONEX) with a mixture of dichloromethane (DCM):methanol (MeOH) 9:1 (v/v, three cycles of 5 min each) at 100 °C and 7.6×10^6 Pa. Before extraction known amounts of *n*-hexatriacontane, 2-nonadecanone, *n*-nonadecanol and *n*-nonadecanoic acid were added as internal standards. The obtained total lipid extracts (TLE) were combined and dried using a Turbovap LV (Zymark Corp.) at 35 °C under a nitrogen stream. The dried TLEs were re-dissolved in DCM and subdivided into two aliquots for further purification.

II.4.3. Alkenone analysis and SST assessment

For alkenone analysis alkenoates were removed by base hydrolysis of the TLE fraction following the procedure described by Elvert et al. (2003). The resulting fraction was separated in DCM-soluble asphaltenes and *n*-hexane-soluble maltenes. The maltenes were desulfurized with activated copper powder and separated by solid phase extraction (Supelco LC-NH₂ glass cartridges; 500 mg sorbent). Four fractions of increasing polarity (hydrocarbons, ketones, alcohols, and fatty acids) were obtained by elution with 4 ml *n*-hexane, 6 ml *n*-hexane:DCM 3:1 (v/v), 7 ml DCM:acetone 9:1 (v/v), and 8 ml 2% formic acid in DCM (v/v). The ketone fraction was dissolved in 100 µl *n*-hexane prior to capillary gas chromatography (GC).

Gas chromatography was performed by using a Trace GC Gas Chromatograph (ThermoQuest) equipped with a 30 m DB-5MS fused silica capillary column (0.32 mm ID, 0.25 µm film thickness) and a flame ionization detector (FID), He as carrier gas with a flow

rate of 1 ml/min. The GC temperature program for alkenones used was: injection at 60 °C, 1 min isothermal; from 60 °C to 150 °C at 15 °C/min; from 150 °C to 310 °C at 4 °C/min; 28 min isothermal with a total oven run-time of 75 min. Peak identification of di- and triunsaturated C_{37} alkenones ($C_{37:2}$ and $C_{37:3}$) was based on retention time and comparison with parallel GC-MS runs. All samples were analyzed in duplicate and quantification was by peak integration and by assuming the same response factor as the internal standard (2-nonadecanone). Concentrations of di- and triunsaturated C_{37} alkenones are given as sum in ng/g dw (dry weight) sediment.

The $U^{K'}_{37}$ was calculated using the definition of Prahl & Wakeham (1987) and converted into SSTs by applying the sediment core top transfer function of Conte et al. (2006). Analytical precision of duplicate runs was better than $\pm 0.007 U^{K'}_{37}$ units (± 0.02 °C).

II.4.4 GDGT analysis and SST assessment

For GDGT analysis, TLE aliquots were separated by alumina oxide column chromatography (activated Al_2O_3 , basic, ~150 mesh, 58 Å, Type 5016A, Sigma Aldrich) into an apolar and polar fraction using *n*-hexane:DCM 9:1 (v/v) and DCM:MeOH 1:1 (v/v), respectively. The polar fraction was dried under a stream of nitrogen, weighed and dissolved ultrasonically in *n*-hexane:isopropanol 99:1 (v/v) with a concentration of 2 mg/ml (Schouten et al., 2009). The polar fraction containing the GDGTs was filtered using a 0.45 µm pore size PTFE filter prior to analysis as described by Hopmans et al. (2000, 2004).

Analyses were performed by high performance liquid chromatography/atmospheric pressure chemical ionization-mass spectrometry (HPLC/APCI-MS) using an Agilent 1200 series HPLC coupled to an HP 6120 MSD equipped with automatic injector and HP Chemstation software. 20 µl aliquots were injected on to an Alltech Prevail Cyano column (2.1x150 mm, 3 µm; Grace) maintained at 30 °C. GDGTs were eluted using the following gradient with solvent A (*n*-hexane) and solvent B (5% isopropanol in *n*-hexane): 80% A:20% B for 5 min, linear gradient to 36% B in 45 min. Flow rate was 0.2 ml/min. After each analysis the column was cleaned by back-flush of *n*-hexane:isopropanol 90:10 (v/v) at 0.2 ml/min for 8 min.

Conditions for APCI-MS were as follows: nebulizer pressure 4.1×10^5 Pa, vaporizer temperature 450 °C, drying gas (N_2) flow 5 l/min and temperature 350 °C, capillary voltage -4 kV, corona 4 µA. For isoprenoidal and non-isoprenoidal GDGTs peak integration of their $[M+H]^+$ ions (m/z 1302, 1300, 1298, 1296, 1292, 1022, 1036, 1050) detected in selective ion monitoring (SIM) mode was used (dwell time=76 ms) (Schouten et al., 2007a). The TEX_{86} ratio was calculated according to Schouten et al. (2002). For temperature conversion we used

the calibration with annual mean SST using marine sediment core tops after Kim et al. (2008). Additionally, we provide GDGT based temperatures using the recently published calibration from Kim et al. (2010) in the supplementary material (S1).

To examine the potential influence of terrestrial archaeal GDGTs we applied the BIT index (Hopmans et al., 2004). Selected samples were analyzed in duplicate and analytical precision was determined by replicate injections of laboratory internal reference material with known TEX₈₆ and BIT values. Mean deviation from reference samples was -0.01 TEX₈₆ units and mean standard deviation of duplicate samples was ± 0.013 (± 0.72 °C). Deviation of duplicate BIT values was better than 0.01 units. Concentrations of GDGTs were not determined.

II.4.5. TOC and Environmental data

Total Organic Carbon (TOC) values of the surface sediments were obtained from parallel multicores taken together with our samples and range between 0.17 and 0.96% (Zonneveld et al., 2009). Seasonal chlorophyll-*a* (Chl-*a*) and SST data were derived from compiled SeaWiFS satellite data for 2002-2006 A.D. Data were extracted from the OBPG MODIS-Aqua Monthly Global 9-km database (<http://reason.gsfc.nasa.gov/OPS/Giovanni/ocean.aqua.shtml>) on a 0.1 °-grid resolution. Seasonal sea surface salinity (SSS) data were retrieved from the MEDATLAS bottle database (<http://odv.awi.de/data/ocean/medatlasii.html>) spanning the last 20 years on a 0.2 °-grid resolution. Data based on the NOAA World Ocean Data Atlas 2005 on a 0.25 °-grid resolution were used for: summer-SSS (sites GeoB 10714 and GeoB 10715), autumn-SSS (GeoB 10731, 10732 and 10733), winter-SSS (GeoB 10748 and 10749) and mean annual SSTs (MA SST) and annual salinity data. Seasons were defined as follows: Winter: December – February (DJF), Spring: March – May (MAM), Summer: June – August (JJA), Autumn: September – November (SON)) (Zonneveld et al., 2009).

II.4.6 Correlation analysis, cluster analysis and contour plots

Correlation analysis was performed to interpret the relation between the biomarker and environmental data sets. The software XLStat version 7.5.2[®] was used to create a cross correlation table giving a Pearson correlation coefficient *r*, for significant ($p < 0.05$) and highly significant correlations ($p < 0.0001$). Cluster analysis was performed on abundances of GDGT-0 to GDGT-4' using the software PAST (PAleontological STatistics) version 1.96[®] (Hammer et al., 2001) using euclidian distances and ward linkage. Contour plots were generated with Ocean Data View (ODV) version 4.3.2[®] (Schlitzer, 2010) using a DIVA gridding algorithm (25 per mil x/y length-scale).

Table I.1 Station data and results of alkenones and GDGT analysis for core top sediments (Part 1/2)

Sample [GeoB]	Lat [°N]	Lon [°E]	Water Depth [m]	U ^{K'} ₃₇	SST _{UK'37} ^a [°C]	TEX ₈₆	SST _{TEX86} ^b [°C]	BIT index	Conc alkenones [µg/g dw]	TOC [%]	SST satellite [°C] ^c					Chl <i>a</i> [mg/dm ³] ^c				SSS [psu] ^c				
											an	sp	su	au	wi	sp	su	au	wi	an	sp	su	au	wi
10701	40.000	17.467	1186	0.601	16.61	0.63	24.70	0.03	194	0.79	18.64	17.40	25.57	21.50	14.49	0.30	0.15	0.22	0.26	38.21	38.58	38.43	38.47	37.96
10702	40.000	17.586	911	0.575	15.86	n.d.	n.d.	0.03	311	0.81	18.62	17.50	25.43	21.41	14.47	0.30	0.16	0.24	0.29	38.20	38.54	38.43	38.46	37.94
10703	40.000	17.742	277	0.578	15.93	0.60	22.86	0.04	502	0.96	18.62	17.70	25.32	21.34	14.21	0.35	0.17	0.25	0.34	38.20	38.52	38.31	38.50	38.46
10704	40.000	17.833	219	0.564	15.52	0.50	17.25	0.06	109	0.92	18.61	17.80	25.26	21.30	14.03	0.35	0.18	0.26	0.37	38.18	38.37	38.31	38.54	38.46
10705	39.853	17.913	128	0.572	15.74	0.49	16.76	0.06	175	0.94	18.67	17.90	25.16	21.14	14.19	0.32	0.18	0.27	0.32	38.18	38.36	38.31	38.52	38.35
10706	39.825	17.833	218	0.561	15.44	n.d.	n.d.	n.d.	n.d.	0.88	18.67	17.80	25.25	21.26	14.31	0.31	0.16	0.25	0.28	38.18	38.42	38.31	38.54	38.35
10707	39.783	17.583	1598	0.622	17.26	0.61	23.57	0.06	125	0.59	18.70	17.50	25.50	21.46	14.75	0.29	0.13	0.21	0.24	38.21	38.64	38.36	38.41	38.24
10708	39.808	17.733	686	0.597	16.50	0.56	20.92	0.05	438	0.81	18.70	17.70	25.32	21.33	14.47	0.29	0.15	0.23	0.27	38.21	38.61	38.46	38.55	38.35
10709	39.757	17.893	173	0.591	16.33	0.51	18.03	0.06	396	n.a.	18.81	17.80	25.22	21.30	14.59	0.28	0.15	0.22	0.25	38.23	38.33	38.31	38.51	38.35
10710	39.592	17.683	2040	0.623	17.27	0.61	23.72	0.04	125	0.37	18.81	17.60	25.41	21.44	14.82	0.26	0.12	0.19	0.22	38.23	38.61	38.61	38.59	38.24
10711	39.683	17.800	1049	0.569	15.68	0.61	23.65	0.07	43.9	0.38	18.81	17.80	25.31	21.38	14.82	0.26	0.13	0.20	0.23	38.23	38.55	38.60	38.55	38.37
10712	39.727	17.862	618	0.637	17.69	0.59	22.27	0.05	112	0.71	18.81	17.80	25.22	21.30	14.59	0.28	0.15	0.22	0.25	38.23	38.55	38.60	38.55	38.37
10713	39.692	18.283	127	0.549	15.06	0.52	18.45	0.07	149	0.46	18.83	16.26	25.34	21.18	14.39	0.28	0.16	0.24	0.31	38.24	38.18	37.98	38.31	37.73
10714	39.640	18.283	207	0.631	17.51	0.53	18.83	0.05	82.0	0.33	18.83	16.26	25.34	21.18	14.39	0.28	0.16	0.24	0.31	38.24	38.18	37.98	38.31	37.73
10715	39.559	18.283	697	0.628	17.43	0.59	22.21	0.05	34.4	0.40	18.98	18.20	25.39	21.41	14.92	0.24	0.14	0.18	0.23	38.27	38.30	38.28	38.53	38.12
10716	39.345	18.283	1328	0.544	14.92	0.65	25.60	0.07	133	0.33	18.98	18.20	25.36	21.83	15.11	0.23	0.11	0.15	0.21	38.27	38.38	38.28	38.51	38.34
10717	39.742	18.080	93	0.609	16.86	0.46	15.11	0.08	192	0.45	18.78	18.00	25.14	21.02	13.88	0.33	0.18	0.30	0.39	38.23	38.19	38.31	38.50	38.46
10718	39.693	18.058	220	0.620	17.19	0.48	16.34	0.06	120	0.62	18.78	18.00	25.25	21.24	14.62	0.28	0.15	0.24	0.30	38.23	38.20	38.60	38.52	38.46
10719	39.653	18.042	616	0.658	18.34	0.60	22.95	0.09	143	0.53	18.78	18.00	25.25	21.24	14.62	0.28	0.15	0.24	0.30	38.23	38.27	38.88	38.48	38.72
10720	39.507	17.978	1387	0.578	15.95	0.61	23.63	0.08	38.4	0.28	18.93	18.20	25.34	21.18	14.52	0.26	0.12	0.18	0.23	38.25	38.37	38.88	38.45	38.55
10721	42.166	16.767	203	0.637	17.70	0.52	18.37	0.04	41.6	0.36	18.16	17.90	25.34	21.48	14.99	0.23	0.14	0.20	0.24	38.19	38.36	38.06	38.44	38.44
10722	42.167	16.500	142	0.586	16.17	0.45	14.65	0.05	105	0.45	18.09	16.70	24.76	20.05	14.60	0.25	0.17	0.25	0.28	38.18	38.25	38.11	38.22	38.40

n.d.: not detected

n.a.: not available

^aSST_{UK'37} calculated after Conte et al., 2006^bSST_{TEX86} calculated after Kim et al., 2008^cEnvironmental Data: Chl *a*=Chlorophyll *a*. SSS=Salinity; su=summer (Jun-Jul-Aug), wi=winter (Dec-Jan-Feb) (Zonneveld et al., 2009)

Table II.1 Station data and results of alkenones and GDGT analysis for core top sediments (Part 2/2)

Sample [GeoB]	Lat [°N]	Lon [°E]	Water Depth [m]	U ₃₇ ^K	SST _{UK37} ^a [°C]	TEX ₈₆	SST _{TEX86} ^b [°C]	BIT index	Conc alkenones [µg/g dw]	TOC [%]	SST satellite [°C] ^c					Chl <i>a</i> [mg/dm ³] ^c				SSS [psu] ^c				
											an	sp	su	au	wi	sp	su	au	wi	an	sp	su	au	wi
10723	42.167	16.000	114	0.561	15.42	0.50	17.16	0.07	159	0.67	18.06	16.50	24.73	19.90	14.37	0.32	0.23	0.40	0.44	38.10	37.65	37.85	37.88	38.25
10724	42.001	16.217	50	0.568	15.65	0.49	16.89	0.21	54.8	0.21	18.02	15.10	24.89	20.10	13.73	0.40	0.28	0.48	0.70	38.17	37.04	37.86	37.42	37.90
10725	42.000	16.367	98	0.548	15.04	0.46	15.24	0.20	205	0.70	18.02	16.30	24.79	20.06	13.97	0.34	0.24	0.41	0.43	38.17	38.28	37.92	38.15	38.36
10726	42.000	16.717	183	0.645	17.94	0.44	14.20	0.09	40.6	0.21	n.a.	n.a.	n.a.	n.a.	n.a.	n.a.	n.a.	n.a.	n.a.	n.a.	n.a.	n.a.	n.a.	
10727	41.801	16.617	101	0.589	16.27	0.43	13.14	0.11	122	0.59	18.03	16.60	24.82	19.96	14.16	0.30	0.21	0.32	0.36	38.26	38.02	37.72	38.21	38.47
10728	41.783	16.858	194	0.669	18.66	0.53	18.85	0.05	11.5	0.17	n.a.	n.a.	n.a.	n.a.	n.a.	n.a.	n.a.	n.a.	n.a.	n.a.	n.a.	n.a.	n.a.	
10729	41.647	17.191	712	0.618	17.12	0.59	22.14	0.03	40.6	0.32	18.05	17.10	24.77	20.00	14.39	0.27	0.13	0.18	0.21	38.27	38.31	38.23	38.48	38.53
10730	41.500	17.050	183	0.698	19.52	0.50	17.30	0.06	24.9	0.21	17.93	17.00	24.66	19.96	14.47	0.26	0.13	0.19	0.22	38.28	38.32	38.10	38.37	38.36
10731	41.500	16.658	96	0.578	15.94	0.45	14.68	0.06	224	0.65	17.87	16.60	25.00	20.19	14.10	0.33	0.26	0.39	0.45	38.27	37.92	37.63	38.07	37.08
10732	41.500	16.407	51	0.560	15.40	0.39	10.96	0.14	283	0.79	17.83	16.40	25.13	20.44	13.14	0.59	0.39	0.58	0.91	38.25	37.60	37.42	38.03	37.08
10733	41.500	16.225	23	0.554	15.22	0.45	14.28	0.25	213	0.73	17.83	16.20	25.23	20.56	12.76	0.79	0.47	0.83	1.43	38.29	37.25	37.31	38.29	37.08
10734	41.667	16.242	18	0.583	16.09	0.44	14.08	0.29	127	0.48	17.89	16.20	25.44	20.54	13.07	1.15	0.67	1.00	1.89	38.29	33.93	37.24	37.59	37.97
10735	41.500	17.308	733	0.569	15.68	0.58	21.77	0.02	129	0.74	18.01	17.30	24.81	20.08	14.25	0.29	0.12	0.18	0.21	38.28	38.58	38.24	38.49	38.59
10736	40.758	18.192	123	0.603	16.69	0.49	16.58	0.07	164	0.76	18.57	18.10	24.82	20.54	13.59	0.36	0.22	0.37	0.54	38.21	38.10	38.00	37.86	37.40
10737	40.625	18.329	113	0.599	16.56	0.48	15.93	0.09	236	0.76	18.64	18.30	24.88	20.56	13.73	0.32	0.20	0.30	0.47	38.18	38.12	37.94	37.93	37.45
10738	40.546	18.467	112	0.591	16.31	0.54	19.54	0.08	189	0.80	18.64	18.40	24.87	20.56	13.84	0.32	0.20	0.31	0.46	38.18	38.28	37.86	37.88	37.45
10739	40.500	18.642	565	0.607	16.80	0.55	19.97	0.04	106	0.66	18.64	18.60	24.82	20.42	14.33	0.26	0.16	0.24	0.30	38.17	38.24	38.09	37.96	37.67
10740	40.392	18.583	128	0.576	15.87	0.49	17.01	0.06	143	0.26	18.66	18.50	24.88	20.60	13.76	0.32	0.19	0.32	0.47	38.16	38.19	38.06	37.79	37.56
10741	40.233	18.667	287	0.556	15.26	0.50	17.35	0.05	330	0.67	18.66	18.60	24.84	20.61	14.00	0.29	0.18	0.29	0.40	37.99	38.18	38.07	37.85	37.64
10742	39.716	18.776	599	0.642	17.85	0.58	21.56	0.04	47.2	0.43	18.91	18.70	24.87	21.30	15.14	0.24	0.14	0.18	0.23	38.26	38.25	37.95	38.37	38.08
10743	39.825	18.642	124	0.581	16.02	0.47	15.52	0.05	271	0.75	18.76	18.60	24.86	21.00	14.55	0.26	0.16	0.21	0.30	38.22	38.10	38.03	38.27	37.66
10744	39.850	18.600	117	0.571	15.72	0.49	16.88	0.07	405	0.72	18.76	18.60	24.86	21.00	14.55	0.26	0.16	0.21	0.30	38.22	38.08	38.02	38.20	37.72
10746	39.908	16.758	157	0.630	17.48	0.50	17.12	0.06	120	0.63	18.90	16.70	25.58	21.73	14.54	0.45	0.21	0.27	0.33	38.26	38.26	38.66	38.38	28.39
10747	39.725	16.975	246	0.646	17.95	0.53	19.23	0.04	134	0.65	19.08	16.90	25.65	21.72	14.54	0.39	0.18	0.24	0.27	38.29	38.27	38.66	38.32	28.39
10748	39.667	17.050	288	0.632	17.55	0.55	19.88	0.05	95.9	0.63	19.08	17.00	25.61	21.64	14.56	0.33	0.16	0.23	0.27	38.29	38.27	38.59	38.29	38.20
10749	39.600	17.183	278	0.648	18.03	0.55	20.41	0.05	55.0	0.54	18.87	17.10	25.59	21.62	14.53	0.32	0.16	0.22	0.26	38.26	38.26	38.66	38.37	38.16

n.d.: not detected

n.a.: not available

^aSST_{UK37} calculated after Conte et al., 2006^bSST_{TEX86} calculated after Kim et al., 2008^cEnvironmental Data: Chl *a*=Chlorophyll *a*. SSS=Salinity; su=summer (Jun-Jul-Aug), wi=winter (Dec-Jan-Feb) (Zonneveld et al., 2009)

II.5. RESULTS

II.5.1. Alkenone-based temperatures ($SST_{UK'37}$)

The alkenone-based temperatures range from 14.9 to 19.5 °C with lower temperatures at near-coastal sites (Fig. II.2b, Table II.1). This temperature difference varies between 2 to 4 °C and is largest in transects at the Gargano Promontory sites. At the Strait of Otranto there is no obvious gradient except in the southernmost transect (10744-42; 15.7-17.8 °C). The onshore-offshore gradient also occurs in the eastern part of the Gulf of Taranto. In contrast, temperature differences at the western Gulf of Taranto are not significant (17.5-18.0 °C). The $SST_{UK'37}$ are up to 4 °C lower than the annual average satellite-derived SSTs, and are much closer to the winter/spring SSTs (Fig. II.3.). Correlation of $SST_{UK'37}$ with seasonal satellite-derived SST is poor with the exception of winter SST (Table II.2).

II.5.2. GDGT-based temperatures (SST_{TEX86})

The GDGT-based temperatures vary between 11.0 and 25.8 °C and similar to the alkenone-based SSTs, tend to increase seawards (Fig. II.2c, Table II.1). Lowest SST_{TEX86} (11.0 and 19.5 °C) occur at near-coastal shelf sites (water depth: <220 m); intermediate values (17.4-22.9 °C) at the outer shelf and shelf break sites (220-733 m) and highest values (23.6-25.8 °C) at the deep ocean sites (>733 m). In the Gulf of Taranto this temperature difference between coast and open ocean approaches 10°C (15.1-25.8°C). The comparison with satellite-derived SSTs shows that neither SST_{TEX86} at shallow-shelf sites nor at the offshore sites agree with annually averaged SSTs (Fig. II.2a). The comparison between SST_{TEX86} and water depth shows that calculated temperatures at shallow sites match winter and spring SSTs, whereas sites with water depths exceeding 500 m resemble autumn and summer values (Fig. II.3.). This pattern also persists when using the recently proposed calibration from Kim et al. (2010; Fig. II.S1. and Table II.S1). SST_{TEX86} shows a positive correlation with depth (Table II.2). It is anti-correlated to chlorophyll-*a*, whereas no correlation exists with $SST_{UK'37}$ and TOC.

II.5.3. Alkenone concentrations

Summed concentrations of the di- and triunsaturated C_{37} alkenones range between 10 and 500 ng/g of dry sediment (Fig. II.4b). At the Gargano Promontory highest concentrations of 200-280 ng/g of dry sediment are observed offshore with a cross-shelf decrease towards the near-coastal sites. Similar concentrations are reached in the Strait of Otranto. Maximum concentrations of 400-500 ng/g of dry sediment are observed between Cape St. Maria di

Leuca and Gulf of Taranto, where they decrease seawards and to hardly detectable levels at the deepest sites. The normalization of concentrations to TOC (not shown) does not significantly change the above described pattern based on dry sediment.

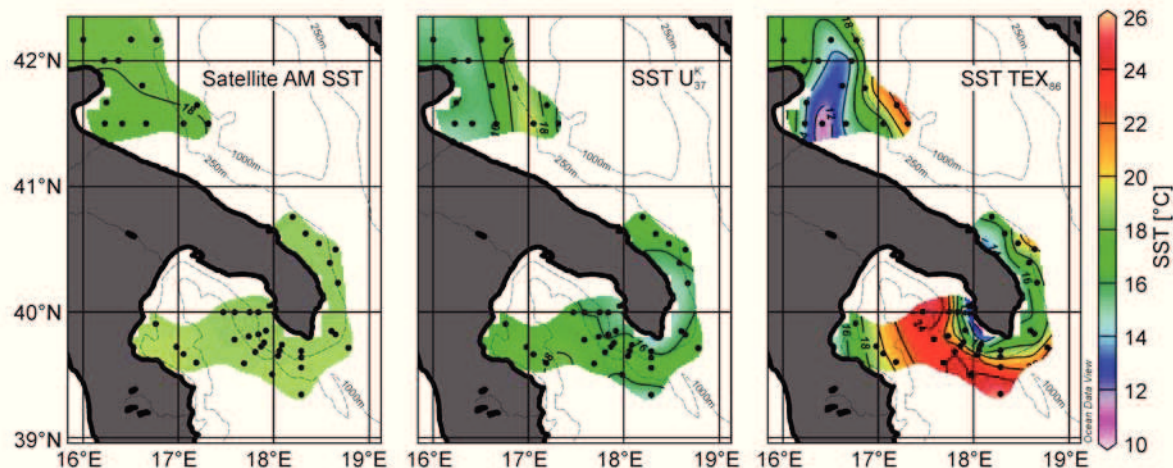


Figure II.2. Contour plots of SST values for surface sediments along the southern Italian shelf: (a) satellite-derived annual mean SST (AM SST); (b) alkenone-based temperature ($SST_{UK'37}$); (c) GDGT-derived temperature (SST_{TEX86}). Dashed lines are water depth contours (250 m and 1000 m).

Table II.2 Pearson correlation coefficient (r) detected between biomarker and environmental data ($p < 0.05$ and $p \leq 0.0001$ with $r > -0.5$ to $r < +0.5$ and $r \geq 0.5$ and $r \leq -0.5$)

	$SST_{UK'37}$	Conc alkenones	SST_{TEX86}	BIT
Conc alkenones	-0.415			
SST_{TEX86}	0.201	-0.145		
BIT	-0.300	0.036	-0.483	
TOC	-0.372	0.437	-0.107	-0.065
Water Depth	0.076	-0.134	0.789	-0.317
SST satellite an	0.237	0.007	0.532	-0.515
SST satellite sp	0.099	0.157	0.350	-0.537
SST satellite su	0.192	-0.052	0.382	-0.069
SST satellite au	0.234	0.023	0.522	-0.368
SST satellite wi	0.381	-0.222	0.637	-0.695
Chl a sp	-0.191	0.070	-0.438	0.789
Chl a su	-0.271	0.098	-0.573	0.853
Chl a au	-0.308	0.097	-0.570	0.878
Chl a wi	-0.275	0.091	-0.510	0.859
SSS an	0.331	-0.269	0.111	0.118
SSS sp	0.166	0.042	0.448	-0.783
SSS su	0.382	-0.144	0.652	-0.609
SSS au	0.251	-0.046	0.499	-0.545
SSS wi	-0.183	0.009	0.127	0.014

TOC=Total Organic Carbon; Chl a =Chlorophyll a ; SST=satellite-derived SST; SSS=Salinity; an=annual, sp=spring (Mar-Apr-May), su=summer (Jun-Jul-Aug), au=autumn (Sep-Oct-Nov), wi=winter (Dec-Jan-Feb) (Zonneveld et al., 2009)

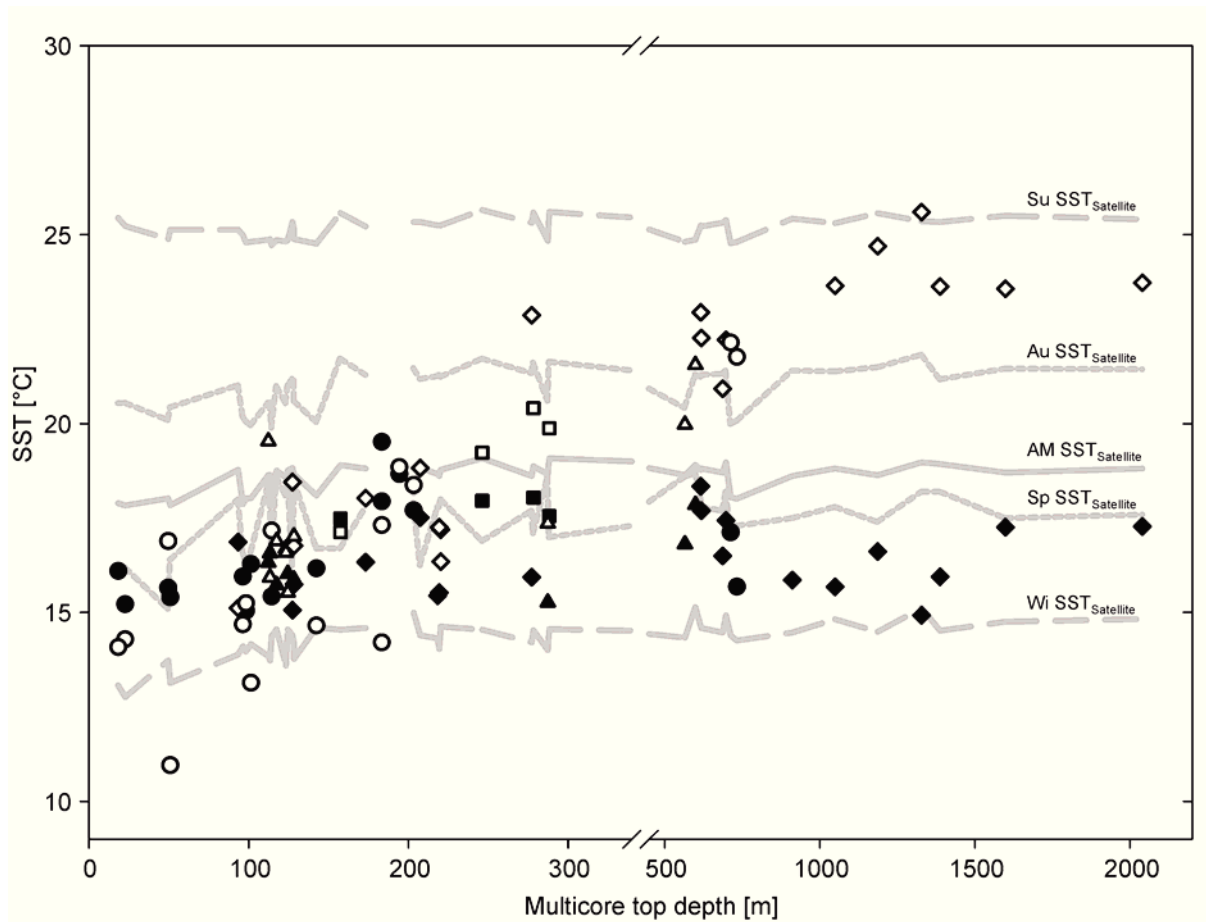


Figure II.3. Seasonal SST and proxy variations for the surface sediment sample locations versus multicore top depth. Curves indicate annual mean (AM SST; solid) and seasonal (Wi SST, Sp SST, Su SST, Au SST; dashed) satellite derived SST. Seasons are defined as: Wi SST: Dec-Jan-Feb, Sp SST: Mar-Apr-May, Su SST: Jun-Jul-Aug, Au SST: Sep-Oct-Nov. SSTs based on $U^{K'}_{37}$ are indicated by filled symbols and TEX_{86} by open symbols, respectively. Different symbols represent the spatial sample distribution within the research area (Fig. II.1.; circles: GP and G. of Manfredonia, triangles: Strait of Otranto, diamonds: E Gulf of Taranto and squares: W Gulf of Taranto). Errors of temperature estimate based on the calibration of Conte et al. (2006) and Kim et al. (2008) are 1.1 °C and 1.7 °C.

II.5.4. GDGT distributions and BIT-Index

The relative abundance of isoprenoidal GDGTs within the surface sediments shows the typical distribution of planktonic archaeal GDGTs and is dominated by GDGT-4 (crenarchaeol) accounting for 50-55% and GDGT-0 representing 25-40% of total GDGTs (Fig. II.A2.).

The BIT index varies between 0.02 and 0.29 (Table II.1) with highest values at the near-coastal sites of the Gargano Promontory and decreasing seaward (Fig. II.5.). At the Strait of Otranto and Gulf of Taranto, BIT is generally lower (0.02 and 0.09), whereas a decrease with increasing distance from the coast was not found. BIT is inversely correlated to $SST_{TEX_{86}}$ and salinity, whereas a positive correlation is present between BIT and chlorophyll-*a* (Table II.2).

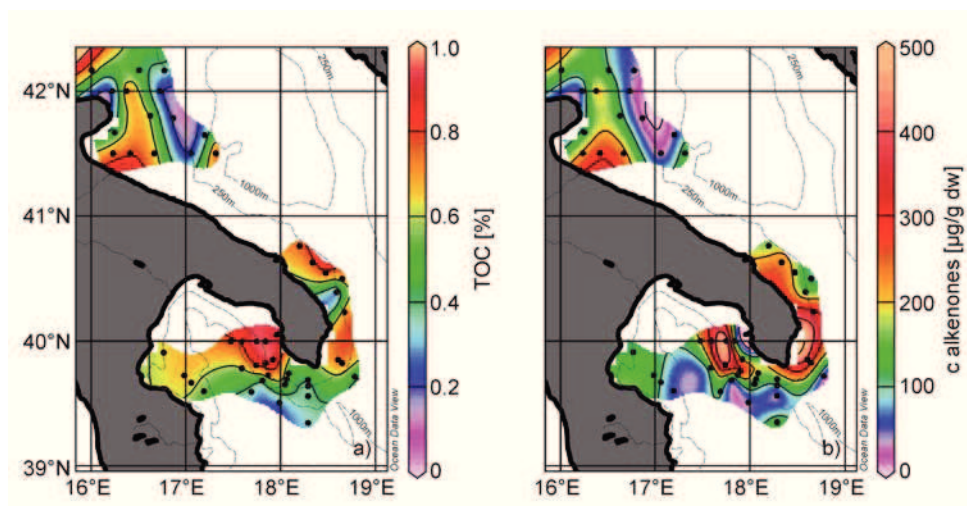


Figure II.4. Distribution of (a) TOC values and (b) content of summed di- and triunsaturated alkenones (in $\mu\text{g/g dw}$) in surface sediments along the southern Italian shelf. Dashed lines are water depth contours (250 m and 1000 m).

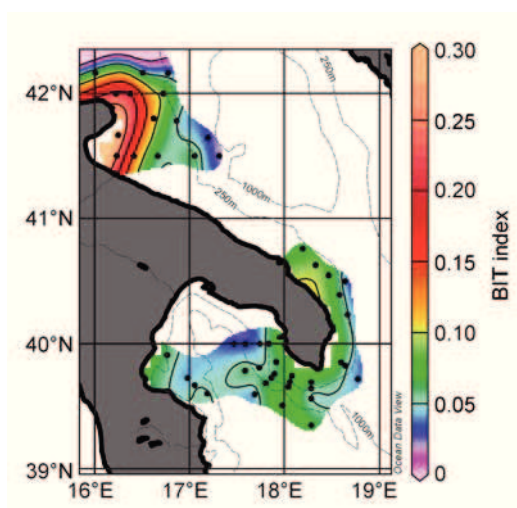


Figure II.5. Contour plot of BIT index values in surface sediments along the southern Italian shelf. Dashed lines are water depth contours (250 m and 1000 m).

II.6. DISCUSSION

The alkenone- and GDGT-based temperature proxies and recent environmental data clearly demonstrate that in the studied region there is no simple relationship with the annual SST usually observed elsewhere. Of the several mechanisms affecting the temperature proxies we will discuss those, which seem to be of major importance: seasonality, subsurface water production of GDGTs, benthic vs. pelagic origin of GDGTs, and bias caused by the presence of terrigenous GDGTs.

II.6.1. Seasonal alkenone production and alkenone preservation

The observation that the $SST_{UK'37}$ are consistently lower than annual mean SST suggests that alkenone production predominantly takes place during the cooler part of the year along the southern Italian shelf.

In the investigated region haptophyte production is dominated by *E. huxleyi* and occurs throughout the whole year with maxima between late autumn and spring based on near-coastal sediment trap stations within the Strait of Otranto and water samples from transects along the southern Adriatic coast (Caroppo et al., 1999; Socal et al., 1999). In the mid Adriatic Sea *E. huxleyi* abundance typically increases in April (Totti et al., 2000). It is also prominent at the Gulf of Manfredonia (Rubino et al., 2009; Balestra et al., 2009). In this region the winter distribution of cold and nutrient-rich Adriatic Surface Water is the main factor promoting phytoplankton growth and controlling the species composition (Socal et al., 1999). Second in importance is the intrusion of nutrient-rich Levantine Intermediate Water by affecting the renewal of water layers during winter turbulence (Caroppo et al., 2001). At the near-coastal stations satellite-derived SSTs for winter and observed $SST_{UK'37}$ are in agreement with each other showing lower temperatures and the influence of Adriatic Surface Water (Fig. II.3.).

In the Mediterranean Sea highest coccolithophore production and fluxes occur during late winter and spring, with *E. huxleyi* as the ubiquitous species in the eastern Mediterranean Sea with its highest abundance within surface waters (Knappertsbusch, 1993; Ziveri et al., 2000). $SST_{UK'37}$ below mean annual values have been reported from particulate material collected in sediment traps and surface sediments of the Mediterranean basin (Ternois et al., 1997; Emeis et al., 2000). Calculating $SST_{UK'37}$ of surface sediments from the northern Ionian Sea (Emeis et al., 2000) and top cm of a sediment core from the Strait of Otranto (Sangiorgi et al., 2003) using the calibration of Conte et al. (2006) provides 16 °C and 14 °C. This also agrees with winter SSTs and with our $SST_{UK'37}$ range of our nearby samples 10716 (14.9 °C) and 10742 (17.8 °C). We estimated the expected sedimentary alkenone composition as a flux-weighted mean on the basis of seasonal cell abundances of *E. huxleyi* and seasonal SSTs from a sediment trap at the Italian shelf in the Strait of Otranto showing maximum cell abundances in November and February (Socal et al., 1999). The estimates are consistent with the alkenone composition in the surface sediments and show a substantially lower SST compared to annual mean SSTs (Table II.3).

Satellite-derived surface pigment concentrations for the years 2002-2006 of the investigated sites show a negative correlation with SSTs also suggesting that the major portion of PP takes

place during the colder seasons with systematically higher chlorophyll-*a* concentrations at the near-coastal sites (Table II.2; Zonneveld et al., 2009). Additionally, TOC and concentrations of alkenones appear higher at near-coastal stations, suggesting a higher PP for this region (Fig. II.4b).

Table II.3 Comparison of seasonal abundance of *E. huxleyi*, influence on the SST signal by calculated weighted SST and SST_{UK'37} of surface sediments

	Average occurrence of <i>E. huxleyi</i> ^a		SST [°C]	SST References
	[cells/dm ⁻³]	[%]		
February	22779	47.7	11.2	Socal et al. (1999)
May	8825	18.5	18.8	OBPG MODIS-Aqua 2002-2006*
August	4412	9.2	28.5	Socal et al. (1999)
November	11767	24.6	18.9	OBPG MODIS-Aqua 2002-2006*
MA SST			19.4	
Weighted SST			16.1	
SST _{UK'37}			16.2±0.7	this study (10743 and -44)

^a Survey from 1994 Socal et al. (1999)

* Monthly means of OBPG MODIS Aqua 2002-2006 for area at Latitude 39.4-39.5 °N/ Longitude 18.3-18.4 °E

In general, chlorophyll-*a* concentrations in the water column follow phytoplankton density. Typically, low values, implying oligotrophic conditions, occur throughout the year, except during winter along the southern Adriatic coast (Caroppo et al., 2001). During winter, highest chlorophyll-*a* concentrations are found within the near-coastal surface layer. This is consistent with high phytoplankton concentrations promoted by the nutrient-rich surface waters of the Western Adriatic Current. Additionally, vertical mixing during winter months brings nutrients into the surface waters (Zonneveld et al., 2009). In summer a deep chlorophyll maximum exists, which can result in underestimation of haptophyte production during warmer seasons as surface waters are depleted in nutrients and alkenone producers may concentrate at the nutricline (Knappertsbusch, 1993). However, observations at the Strait of Otranto imply that coccolithophorids thrive within the surface waters even during summer (Boldrin et al., 2002). Further evidence of the influence of near-coastal Adriatic Surface Water can be observed in the seaward increase in satellite-derived SST during winter (e.g., Gulf of Manfredonia) (Fig. II.3.). This partly may explain the seaward increase of SST_{UK'37}. Since, the SST_{UK'37} increase appears to be 2 °C higher than that observed by satellites an additional explanation is needed. However, considering the calibration error of 1.1 °C, this temperature increase is not significant. Selective degradation of tri-unsaturated alkenones in well oxygenated bottom waters of the Northern Adriatic deep Dense Water and/or Adriatic Deep Water at the deeper sites could lead to an increase of SST_{UK'37} (e.g. Hoefs et al., 1998; Gong & Hollander, 1999; Kim et al., 2009b). The influence of early diagenetic processes at the deeper sites was also

considered as a factor affecting the dinoflagellate cyst associations in the region, but since oxygen penetration depth is not significantly related to the cyst accumulation rates, this mechanism appears to be unlikely (Zonneveld et al., 2009). Therefore, we propose that selective degradation of alkenones plays a minor role. Instead we conclude that the observed alkenone-based SSTs are consistent with the general productivity patterns recording primarily the SST during the colder part of the year when biomass is highest.

II.6.2. Seasonality in production of planktonic archaea

For the offshore sites, the GDGT-derived temperatures agree best with summer SST. The SST_{TEX86} are 7 °C higher than annual mean SST and 10 °C higher than $SST_{UK'37}$ (Fig. II.3.). That leads to the hypothesis that, in contrast to the haptophytes, offshore the export of biomarker signals from planktonic archaea predominantly takes place during the warm season. During this season oligotrophic conditions in the open Adriatic and Ionian Sea prevail, which is also reflected by minimum concentrations of chlorophyll-*a* in surface waters (Socal et al., 1999). Consequently, maxima in growth of planktonic archaea occur when PP is at a minimum. Such inverse correlations between archaeal abundance and chlorophyll-*a* have also been observed elsewhere such as in the polar oceans (Murray et al., 1998), the Santa Barbara Channel (Murray et al., 1999) and the North Sea (Wuchter et al., 2005; Herfort et al., 2007). GDGT-based SSTs in eastern Mediterranean Sea sediments also agree with our observation that the offshore 'open-sea' sites reflect summer conditions (Menzel et al., 2006; Castañeda et al., 2010). Thus we propose that also for the offshore sites in our study the SST_{TEX86} reflects summer planktonic archaeal production.

In contrast, the much lower SST_{TEX86} , at the near-coastal sites, which agree with winter SST, suggest that the maximum archaeal production takes place during the colder part of the year; the period with maximum PP. This is especially pronounced at the Gargano Promontory sites under the direct influence of the Western Adriatic Current. Nutrient concentrations and particle loading in the surface waters appear higher during the colder period (Socal et al., 1999). These conditions may favor the presence of planktonic archaea as reported for coastal waters in the Black Sea (Stoica and Herndl, 2007) and the Canadian Arctic (Wells et al., 2006). Wuchter et al. (2005) observed a positive correlation between chlorophyll-*a* and archaeal lipids in surface waters from the Bermuda Atlantic Time-Series (BATS). At the BATS site, wind-induced convective mixing results in nutrient enrichment of surface waters which promotes PP during winter and possibly also growth of planktonic archaea. At the coastal sites in our region, chlorophyll-*a* concentrations are higher than offshore during the

whole year (Table II.1) and even in summer they exceed offshore winter levels. Consequently, in contrast to the offshore sites, archaeal blooming during the oligotrophic season, as a strategy of minimizing the competition for nutrients (Murray, 1998) is unlikely to occur at the coastal sites. Instead the winter signal may become relatively more important. A crucial process may be the concomitant increased transport of phytoplankton to depth due to aggregation of cells and other suspended matter occurring during higher PP in this coastal shallow setting (Socal et al., 1999). This larger amount of marine snow in combination with a shallow water column would promote an efficient vehicle to carry the GDGTs to the sea floor and primarily export the SST signal during this time of the year (Wuchter et al., 2005; Huguet et al., 2006a, 2007). Further evidence may lie in the biology of planktonic archaea with some members participating in the oxidation of ammonia (Könneke et al., 2005; Wuchter et al., 2006). Especially in shallow and photic estuarine sediments, phytoplankton and microphytobenthos can contribute organic nitrogen (Caffrey et al., 2007). If this nitrogen becomes mineralized to ammonia it supports nitrification by crenarchaeaota (Francis et al., 2005; Nicol & Schleper, 2006).

Alternatively, it is known that crenarchaeaota can reside in deeper water (e.g., Karner et al., 2001) and low reconstructed temperatures could result from subsurface production of GDGTs, which seems to play a major role in upwelling areas where TEX₈₆ systematically underestimates SSTs (Huguet et al., 2007; Lee et al., 2008). However, as our data show, for stations with depths below the thermocline (> 75 m, i.e., the vast majority of our samples), the observed pattern cannot be explained by invoking a substantial contribution of GDGTs produced below the thermocline. Likewise, deep water production is not relevant for the shallowest, coldest stations (< 75 m) that do not reach below the thermocline.

Our observations suggest that there are two modes of planktonic archaeal growth, which are spatially and temporally separated on the southern Italian shelf. One is consistent with the general observation of preferred oligotrophic conditions accompanied by low PP at the offshore sites. The other mode is directly linked to higher nutrient concentrations at the near-coastal sites, where planktonic archaea are rather associated with particle-rich waters of the Adriatic Surface Water and vertical mixing during the colder season.

Future studies on the seasonal abundances and community structure of planktonic archaea within the water column as well as the distribution of GDGTs for near-coastal and offshore sites are required.

II.6.3. GDGTs from benthic and pelagic archaeal communities

All samples showed a characteristic marine archaeal GDGT profile, with abundant GDGT-0 and crenarchaeol and lower contributions of GDGT-1 to GDGT-3 and the crenarchaeol regioisomer. Shallow sites show a higher contribution of GDGT-0 than offshore sites and vice versa (Fig. II.A1.). Although crenarchaeol is a predominant marker for planktonic crenarchaeota affiliated with Marine Group 1 (MG1) (Sinninghe Damsté et al., 2002b), it also is biosynthesized by a thermophilic crenarchaeota living in hot springs (Pearson et al., 2004; Zhang et al., 2006; Schouten et al., 2007b; Pitcher et al., 2009). GDGT-0 has been interpreted as a general archaeal core lipid that is synthesized by members distributed throughout the archaeal domain (Koga et al., 1993). In the oceanic water column this compound is probably derived from both planktonic eury- and crenarchaeota. Furthermore, it is likely that cren- and euryarchaeota, including sedimentary affiliates of the MG1 archaea (Inagaki et al., 2006) and other benthic archaea (Teske & Sorensen, 2008) produce similar lipids as their water column relatives (Biddle et al., 2006; Lipp & Hinrichs, 2009). In our region benthic cren- and euryarchaeotal communities were found in sediments located off the Cape of St. Maria di Leuca and bottom waters east off the Gulf of Manfredonia (Yakimov et al., 2006; Martin-Cuadrado et al., 2008), but their influence on the TEX₈₆ signal still remains unclear. Turich et al. (2007) differentiated between GDGT abundances in epi- and mesopelagic waters based on a data set of particulate organic matter (POM), where higher abundances of GDGT-0 compared to GDGT-1 to GDGT-4 are observed in epipelagic waters indicating a contribution of group II euryarchaeota. Being aware that studies on POM reflect only snapshots it is striking that we observe a similar pattern in the surface sediments. However, without DNA data, a robust link between the microbial ecology of planktonic archaea and GDGT lipids cannot be established.

II.6.4. Cold-biased signature from the terrestrial realm

The BIT values in the range of 0.02-0.29 with a seaward decrease are consistent with previously observed values for coastal to open marine environments (Hopmans et al., 2004; Kim et al., 2006). BIT values for coastal marine settings with a high input of OM from rivers are up to 0.98 (Hopmans et al., 2004; Kim et al., 2006). In comparison BIT values of lake sediments from Italy showed a wide range between 0.08 and 0.99 and a highly variable degree of soil OM input (Blaga et al., 2009). Hence, the values at the southern Adriatic Sea and Gulf of Taranto suggest the sediments contain a low contribution of soil OM; implying that the TEX₈₆ reflects largely a marine signal. Elevated BIT values occur at locations with

higher chlorophyll-*a* concentrations and lower salinity (Table II.2), a pattern which is particularly pronounced at the inner shelf of the Gargano Promontory. This indicates an increased supply of terrestrial OM and nutrients, due to the influence of the Western Adriatic Current that stimulates PP. However, the supply of terrestrial GDGTs by nearby local rivers south of the Gargano Promontory (e.g. Ofanto River) cannot be excluded. The generally lower BIT values in the remainder of the southern Adriatic Sea and Gulf of Taranto, even at near-coastal sites, can be related to the absence of river input due to the lack of major rivers on the Apulian Peninsula (Raicich, 1996). It also indicates that the input of land-derived material from the north is low and, more specifically, that the soil-derived fraction of terrestrial OM is low for the region (Walsh et al., 2008). The latter situation is typical for southern Italy since the landscape of the Apulian peninsula is characterized by complex karst landforms. Additionally, variations in autochthonous crenarchaeol production can affect the BIT as observed from discrepancies between BIT and other soil markers (Schmidt et al., 2009). Interestingly, higher BIT values are associated with low SST_{TEX86} predominantly at the Gargano Promontory area (Table II.2). This is in contrast to the general observation that terrestrial isoprenoid GDGTs may alter the TEX₈₆ signal leading to an increase of estimated temperature with higher BIT values (Herfort et al., 2006; Weijers et al., 2006). Instead our observations suggest the possibility of an allochthonous, cold TEX₈₆ signal that is transported from the continent to shelf sediments. Further investigations on the soils and river sediments in the research area are necessary to reveal their influence on the marine realm.

II.7. CONCLUSIONS

Calibration of the U^K₃₇ and TEX₈₆ temperature proxies using core-tops along the southern Italian shelf to local SSTs shows that both proxies reflect SSTs that considerably differ from annual mean SSTs. SST_{UK'37} values appear lower than annual mean SSTs. This is attributed to predominant production and export of alkenones during winter and spring fuelled by the Adriatic Surface Water and vertical mixing. SST_{TEX86} increases with distance from shore suggesting that at offshore sites the peak of planktonic archaeal production and the export of related signals take place during summer when conditions are oligotrophic. In contrast, SST_{TEX86} at near-coastal sites is low. This is explained by either one or a combination of the following factors: different timing of archaeal production due to particle-rich surface waters and prevailing higher nutrient contents (no oligotrophic conditions) and/or terrestrial input leading to a cold-biased TEX₈₆ signal. Our study demonstrates the importance of constraining

regional factors to arrive at a robust interpretation of past temperature signals and that care has to be taken in applications of SST proxies in near-coastal environments. We suggest that regional studies are needed in coastal to marine transitions showing contrasting water column characteristics. As a corollary, interpretation of molecular SST signals in terms of absolute temperature in ancient environments that are not accessible to an evaluation of regional and seasonal factors will remain problematic. Here, a combination of both molecular temperature proxies provides an opportunity to differentiate between seasonal and/or spatial characteristics of the water column in the past.

Supplementary materials related to this article can be found online at [doi:10.1016/j.epsl.2010.09.042](https://doi.org/10.1016/j.epsl.2010.09.042).

II.8. ACKNOWLEDGEMENTS

We would like to thank M. Elvert, X. Prieto-Mollar and R. Kreutz for lab assistance, E. Schefuß for providing ASE extraction facility and K. Becker for help with sample preparation. Many thanks go to the members of MOCCHA (Multidisciplinary study of continental/ocean climate dynamics using high-resolution records from the eastern Mediterranean) for fruitful discussion at early stages of this study. This work was supported by the Deutsche Forschungsgemeinschaft under the EUROCORES Programme EuroMARC project MOCCHA, through contract No. ERAS-CT-2003-980409 of the European Commission, DG Research, FP6. Additional support was provided by the Bremen International Graduate School for Marine Sciences “Global Change in the Marine Realm” (GLOMAR). We thank John Volkman and one anonymous reviewer for their constructive comments helping to improve this manuscript.

II.9. REFERENCES

- Artegiani, A., Paschini, E., Russo, A., Bregant, D., Raicich, F., Pinardi, N., 1997a. The Adriatic Sea general circulation. Part I: Air–sea interactions and water mass structure. *J. Phys. Oceanogr.* 27, 1492-1514.
- Artegiani, A., Paschini, E., Russo, A., Bregant, D., Raicich, F., Pinardi, N., 1997b. The Adriatic Sea general circulation. Part II: baroclinic circulation structure. *J. Phys. Oceanogr.* 27, 1515-1532.
- Balestra, B., Marino, M., Monechi, S., Marano, C., Locaiono, F., 2009. Coccolithophore communities in the Gulf of Manfredonia (Southern Adriatic Sea): data from water and surface sediments. *Micropaleontology* 54, 377-396.
- Bentaleb, I., Grimalt, J.O., Vidussi, F., Marty, J.C., Martin, V., Denis, M., Hatté, C., Fontugne, M., 1999. The C₃₇ alkenone record of seawater temperature during seasonal thermocline stratification. *Mar. Chem.* 64, 301-313.
- Benthien, A., Müller, P.J., 2000. Anomalously low alkenone temperatures caused by lateral particle and sediment transport in the Malvinas Current region, western Argentine Basin. *Deep-Sea Res. I* 47, 2369-2393.
- Biddle, J.F., Lipp, J.S., Lever, M.A., Lloyd, K.G., Sorensen, K.B., Anderson, R., Fredricks, H.F., Elvert, M., Kelly, T.J., Schrag, D.P., Sogin, M.L., Brenchley, J.E., Teske, A., House, C.H., Hinrichs, K.-U., 2006. Heterotrophic Archaea dominate sedimentary subsurface ecosystems off Peru. *Proc. Natl. Acad. Sci. USA* 103, 3846-3851.
- Bignami, F., Sciarra, R., Carniel, S., Santoleri, R., 2007. Variability of Adriatic Sea coastal turbid waters from SeaWiFS imagery. *J. Geophys. Res.* 112, C03S10, doi: doi:10.1029/2006JC003518.
- Bлага, C., Reichart, G.-J., Heiri, O., Sinninghe Damsté, J.S., 2009. Tetraether membrane lipid distributions in water-column particulate matter and sediments: a study of 47 European lakes along a north–south transect. *J. Paleolimn.* 41, 523-540.
- Boldrin, A., Miserocchi, S., Rabitti, S., Turchetto, M.M., Balboni, V., Socal, G., 2002. Particulate matter in the southern Adriatic and Ionian Sea: characterisation and downward fluxes. *J. Mar. Syst.* 33-34, 389-410.
- Bonino, G., Cini Castagnoli, G., Callegari, E., Zhu, G.-M., 1993. Radiometric and tephroanalysis dating of recent Ionian Sea cores. *Il Nuovo Cimento C*, 16, 155-162.
- Brassell, S.C., Brereton, R.G., Eglinton, G., Grimalt, J., Liebezeit, G., Marlowe, I.T., Pflaumann, U., Sarnthein, M., 1986. Palaeoclimatic signals recognized by chemometric treatment of molecular stratigraphic data. *Org. Geochem.* 10, 649-660.
- Caffrey, J.M., Bano, N., Kalanetra, K., Hollibaugh, J.T., 2007. Ammonia oxidation and ammonia-oxidizing bacteria and archaea from estuaries with differing histories of hypoxia. *ISME J.* 1, 660-662.

- Caroppo, C., Fiocca, A., Sammarco, P., Magazzu, G., 1999. Seasonal variations of nutrients and phytoplankton in the coastal SW Adriatic Sea (1995–1997). *Bot. Mar.* 42, 389-400.
- Caroppo, C., Congestri, R., Bruno, M., 2001. Dynamics of *Dinophysis* sensu lato species (Dinophyceae) in a coastal Mediterranean environment (Adriatic Sea). *Cont. Shelf Res.* 21, 1839-1854.
- Castañeda, I.S., Schefuß, E., Pätzold, J., Sinninghe Damsté, J.S., Weldeab, S., Schouten, S., 2010. Millennial-scale sea surface temperature changes in the eastern Mediterranean (Nile River Delta region) over the last 27,000 years. *Paleoceanography* 25, PA1208.
- Cattaneo, A., Correggiari, A., Langone, L., Trincardi, F., 2003. The late-Holocene Gargano subaqueous delta, Adriatic shelf: Sediment pathways and supply fluctuations. *Mar. Geol.* 193, 61-91.
- Cini Castagnoli, G., Bonino, G., Provenzale, A., Serio, M., 1990. On the presence of regular periodicities in the thermoluminescence profile of a recent sea sediment core. *Phil. Trans. R. Soc. Lond.* 330, 481-486.
- Cini Castagnoli, G., Bonino, G., Provenzale, A., Serio, M., Callegari, E., 1992a. The $CaCO_3$ profiles of deep and shallow Mediterranean sea cores as indicators of past solar-terrestrial relationships. *Nuovo Cimento Soc. Ital. Fis. C* 15, 547-563.
- Cini Castagnoli, G., Bonino, G., Serio, G., Sonett, C.P., 1992b. Common spectral features in the 5500-year record of total carbonate in sea sediments and radiocarbon in tree rings. *Radiocarbon* 34, 798-805.
- Cini Castagnoli, G., Bonino, G., Della Monica, P., Taricco, C., 1997. Record of thermoluminescence in sea sediments in the last millennia. *Nuovo Cimento Soc. Ital. Fis. C* 20, 1-8.
- Cini Castagnoli, G., Bernasconi, S.M., Bonino, G., Della Monica, P., Taricco, C., 1999. 700 year record of the 11 year solar cycle by planktonic foraminifera of a shallow water Mediterranean core. *Adv. Space Res.* 24, 233-236.
- Cini Castagnoli, G., Bonino, G., Della Monica, P., Taricco, C., Bernasconi, S.M., 1999b. Solar activity in the last millennium recorded in the $\delta^{18}O$ profile of planktonic foraminifera of a shallow water Ionian Sea core. *Sol. Phys.* 188, 191-202.
- Cini Castagnoli, G., Bonino, G., Taricco, C., Bernasconi, S.M., 2000. The 11 year solar cycle and the modern Increase in the $\delta^{13}C$ of planktonic foraminifera of a shallow water Mediterranean Sea Core (590-1979). In: *Proc. 1st Solar & Space Weather Euroconference. 'The solar cycle and terrestrial climate', Solar and space weather. Santa Cruz de Tenerife. Tenerife. Spain., ESA SP-463, 481-484.*
- Cini Castagnoli, G., Bonino, G., Taricco, C., Bernasconi, S.M., 2002. Solar radiation variability in the last 1400 years recorded in the carbon isotope ratio of a mediterranean sea core. *Adv. Space Res.* 29, 1989-1994.

- Cini Castagnoli, G., Taricco, C., Alessio, S., 2005. Isotopic record in a marine shallow-water core: Imprint of solar centennial cycles in the past 2 millennia. *Adv. Space Res.* 35, 504-508.
- Civitarese, G., Gačić, M., Vetrano, A., Boldrin, A., Bregant, D., Rabitti, S., Souvermezoglou, E., 1998. Biogeochemical fluxes through the Strait of Otranto (Eastern Mediterranean). *Cont. Shelf Res.* 18, 773-789.
- Conte, M.H., Thompson, A., Lesley, D., Harris, R.P., 1998. Genetic and physiological influences on the alkenone/alkenoate versus growth temperature relationship in *Emiliana huxleyi* and *Gephyrocapsa oceanica*. *Geochim. Cosmochim. Acta* 62, 51-68.
- Conte, M.H., Sicre, M.-A., Rühlemann, C., Weber, J.C., Schulte, S., Schulz-Bull, D., Blanz, T., 2006. Global temperature calibration of the alkenone unsaturation index ($U^{K'_{37}}$) in surface waters and comparison with surface sediments. *Geochem. Geophys. Geosyst.* 7, Q02005, doi: 10.1029/2005GC001054.
- De Long, E.F. (2006). Archaeal mysteries of the deep revealed, *Proc. Natl. Acad. Sci. USA* 103, 6417-6418.
- Elderfield, H., Ganssen, G., 2000. Past temperature and $\delta^{18}O$ of surface ocean waters inferred from foraminiferal Mg/Ca ratios. *Nature*, 405, 442-445.
- Elvert, M., Boetius, A., Knittel, K., Jørgensen, B.B., 2003. Characterization of specific membrane fatty acids as chemotaxonomic markers for sulfate-reducing bacteria involved in anaerobic oxidation of methane. *Geomicrobiol. J.* 20, 403-419.
- Emeis, K.-C., Struck, U., Schulz, H.-M., Rosenberg, R., Bernasconi, S.M., Erlenkeuser, H., Sakamoto, T., Martinez-Ruiz, F., 2000. Temperature and salinity variations of Mediterranean Sea surface waters over the last 16,000 years from records of planktonic stable oxygen isotopes and alkenone unsaturation ratios. *Palaeogeogr., Palaeoclim., Palaeoecol.* 158, 259-280.
- Epstein, B.L., D'Hondt, S., Quinn, J.G., Zhang, J., Hargraves, P.E., 1998. An effect of dissolved nutrient concentrations on alkenone-based temperature estimates. *Paleoceanography* 13, 122-126, PA03358.
- Erez, J., Luz, B., 1983. Experimental paleotemperature equation for planktonic foraminifera. *Geochim. Cosmochim. Acta* 47, 1025-1031.
- Focardi, S., Specchiulli, A., Spagnoli, F., Fiesoletti, F., Rossi, C., 2009. A combined approach to investigate the biochemistry and hydrography of a shallow bay in the South Adriatic Sea: the Gulf of Manfredonia (Italy). *Environ. Monit. Assess.*, 153, 209-220.
- Francis, C.A., Roberts, K.J., Beman, J.M., Santoro, A.E., Oakley, B.B., 2005. Ubiquity and diversity of ammonia-oxidizing archaea in water columns and sediments of the ocean. *Proc. Natl. Acad. Sci. USA* 102, 14683-14688.
- Gong, C., Hollander, D.J., 1999. Evidence for differential degradation of alkenones under contrasting bottom water oxygen conditions: implication for paleotemperature reconstruction. *Geochim. Cosmochim. Acta* 63, 405-411.

- Goñi, M.A., Hartz, D.M., Thunell, R.C., Tappa, E., 2001. Oceanographic considerations for the application of the alkenone-based paleotemperature $U^{K'}_{37}$ index in the Gulf of California. *Geochim. Cosmochim. Acta* 65, 545-557.
- Hainbucher, D., Rubino, A., Klein, B., 2006. Water mass characteristics in the deep layers of the western Ionian Basin observed during May 2003. *Geophys. Res. Lett.*, 33, L05608.
- Hammer, Ø., Harper, D.A.T., Ryan, P.D., 2001. PAST: Paleontological Statistics Software Package for Education and Data Analysis. *Palaeontol. Electr.* 4, 9.
- Haug, G.H., Ganopolski, A., Sigman, D.M., Rosell-Melé, A., Swann, G.E.A., Tiedemann, R., Jaccard, S.L., Bollmann, J., Maslin, M.A., Leng, M.J., 2005. North Pacific seasonality and the glaciation of North America 2.7 million years ago. *Nature* 433, 821-825.
- Herbert, T.D., Heinrich, D.H., Karl, K.T., 2003. Alkenone Paleotemperature Determinations. In: *Treatise on Geochemistry*, pp. 391-432. Pergamon, Oxford.
- Herfort, L., Schouten, S., Boon, J.P., Sinninghe Damsté, J.S., 2006. Application of the TEX_{86} temperature proxy to the southern North Sea. *Org. Geochem.* 37, 1715-1726.
- Herfort, L., Schouten, S., Abbas, B., Veldhuis, M.J.W., Coolen, M.J.L., Wuchter, C., Boon, J.P., Herndl, G.J., Sinninghe Damsté, J.S., 2007. Variations in spatial and temporal distribution of Archaea in the North Sea in relation to environmental variables. *FEMS Microbiol. Ecol.* 62, 242-257.
- Hoefs, M.J.L., Rijpstra, W.I.C., Sinninghe Damsté, J.S., 2002. The influence of oxic degradation on the sedimentary biomarker record I: evidence from Madeira Abyssal Plain turbidites. *Geochim. Cosmochim. Acta* 66, 2719-2735.
- Hopmans, E.C., Schouten, S., Pancost, R.D., van der Meer, M.T.J., Sinninghe Damsté, J.S., 2000. Analysis of intact tetraether lipids in archaeal cell material and sediments by high performance liquid chromatography/atmospheric pressure chemical ionization mass spectrometry. *Rap. Commun. Mass. Spectrom.* 14, 585-589.
- Hopmans, E.C., Weijers, J.W.H., Schefuß, E., Herfort, L., Sinninghe Damsté, J.S., Schouten, S., 2004. A novel proxy for terrestrial organic matter in sediments based on branched and isoprenoid tetraether lipids. *Earth Planet. Sci. Lett.* 224, 107-116.
- Huguet, C., Kim, J.-H., Sinninghe Damsté, J.S., Schouten, S., 2006. Reconstruction of sea surface temperature variations in the Arabian Sea over the last 23 kyr using organic proxies (TEX_{86} and $U^{K'}_{37}$). *Paleoceanography* 21, PA3003.
- Huguet, C., Schimmelmann, A., Thunell, R., Lourens, L.J., Sinninghe Damsté, J.S., Schouten, S., 2007. A study of the TEX_{86} paleothermometer in the water column and sediments of the Santa Barbara Basin. *California. Paleoceanography* 22, PA3203.
- Hurrell, J.W., Van Loon, H., 1997. Decadal variations in climate associated with the North Atlantic Oscillation. *Clim. Change* 36, 301-326.
- Inagaki, F., Nunoura, T., Nakagawa, S., Teske, A., Lever, M., Lauer, A., Suzuki, M., Takai, K., Delwiche, M., Colwell, F.S., Nealson, K.H., Horikoshi, K., D'Hondt, S., Jorgensen, B.B., 2006. Biogeographical distribution and diversity of microbes in

- methane hydrate-bearing deep marine sediments on the Pacific Ocean margin. *Proc. Natl. Acad. Sci. USA* 103, 2815-2820.
- Karner, M.B., DeLong, E.F., Karl, D.M., 2001. Archaeal dominance in the mesopelagic zone of the Pacific Ocean. *Nature* 409, 507-510.
- Kim, J.-H., Schouten, S., Buscail, R., Ludwig, W., Bonnin, J., Sinninghe Damsté, J.S., Bourrin, F., 2006. Origin and distribution of terrestrial organic matter in the NW Mediterranean (Gulf of Lions): Exploring the newly developed BIT index. *Geochem. Geophys. Geosyst.* 7, Q11017, doi: 10.1029/2006GC001306.
- Kim, J.-H., Schouten, S., Hopmans, E.C., Donner, B., Sinninghe Damsté, J.S., 2008. Global sediment core-top calibration of the TEX₈₆ paleothermometer in the ocean. *Geochim. Cosmochim. Acta* 72, 1154-1173.
- Kim, J.-H., Crosta, X., Michel, E., Schouten, S., Duprat, J., Sinninghe Damsté, J.S., 2009a. Impact of lateral transport on organic proxies in the Southern Ocean. *Quat. Res.* 71, 246-250.
- Kim, J.-H., Hugué, C., Zonneveld, K.A.F., Versteegh, G.J.M., Roeder, W., Sinninghe Damsté, J.S., Schouten, S., 2009b. An experimental field study to test the stability of lipids used for the TEX₈₆ and palaeothermometers. *Geochim. Cosmochim. Acta* 73, 2888-2898.
- Kim J.-H., van der Meer, J., Schouten, S., Helmke, P., Willmott, V., Sangiorgi, F., Koç, N., Hopmans, E.C., Sinninghe Damsté, J.S., 2010. New indices and calibrations derived from the distribution of crenarchaeal isoprenoid tetraether lipids: Implications for past sea surface temperature reconstructions. *Geochim. Cosmochim. Acta* 74, 4639-4654.
- Knappertsbusch, M., 1993. Geographic distribution of living and Holocene coccolithophores in the Mediterranean Sea. *Mar. Micropaleontol.* 21, 219-247.
- Koga, Y., Nishihara, M., Morii, H., Akagawa-Matsushita, M., 1993. Ether polar lipids of methanogenic bacteria: structures, comparative aspects, and biosyntheses. *Microbiol. Mol. Biol. Rev.* 57, 164-182.
- Kourafalou, V.H., 2001. River plume development in semi-enclosed Mediterranean regions: North Adriatic Sea and Northwestern Aegean Sea. *J. Mar. Syst.* 30, 181-205.
- Könneke, M., Bernhard, A.E., De la Torre, J.R., Walker, C.B., Waterbury, J.B., Stahl, D.A., 2005. Isolation of an autotrophic ammonia-oxidizing marine archaeon. *Nature* 437, 543-546.
- Lee, K.E., Kim, J.-H., Wilke, I., Helmke, P., Schouten, S., 2008. A study of the alkenone, TEX₈₆, and planktonic foraminifera in the Benguela upwelling system: Implications for past sea surface temperature estimates. *Geochem., Geophys., Geosyst.* 9, Q10019, doi: 10.1029/2008GC002056.
- Lipp, J.S., Hinrichs, K.-U., 2009. Structural diversity and fate of intact polar lipids in marine sediments. *Geochim. Cosmochim. Acta* 73, 6816-6833.
- Lipp, J.S., Morono, Y., Inagaki, F., Hinrichs, K.-U., 2008. Significant contribution of Archaea to extant biomass in marine subsurface sediments. *Nature*, 454, 991-994.

- Manca, B.B., Kovacevic, V., Gačić, M., Viezzoli, D., 2002. Dense water formation in the southern Adriatic Sea and spreading into the Ionian Sea in the period 1997-1999. *J. Mar. Syst.* 33-34, 133-154.
- Marasović, I., Grbec, B., Morović, M., 1995. Long-term production changes in the Adriatic. *Netherl. J. Sea Res.* 34, 267-273.
- Marlowe, I.T., Green, J.C., Neal, A.C., Brassell, S.C., Eglinton, G., Course, P.A., 1984. Long chain($n-C_{37}-C_{39}$) alkenones in the Prymnesiophyceae, distribution of alkenones and other lipids and their taxonomic significance. *Brit. Phycolog. J.* 19, 203-216.
- Martin-Cuadrado, A.-B., Rodriguez-Valera, F., Moreira, D., Alba, J.C., Ivars-Martinez, E., Henn, M.R., Talla, E., Lopez-Garcia, P., 2008. Hindsight in the relative abundance, metabolic potential and genome dynamics of uncultivated marine archaea from comparative metagenomic analyses of bathypelagic plankton of different oceanic regions. *ISME J.* 2, 865-886.
- Menzel, D., Hopmans, E.C., Schouten, S., Sinninghe Damsté, J.S., 2006. Membrane tetraether lipids of planktonic Crenarchaeota in Pliocene sapropels of the Eastern Mediterranean Sea. *Palaeogeogr., Palaeoclim., Palaeoecol.* 239, 1-15.
- Milligan, T.G., Cattaneo, A., 2007. Sediment dynamics in the western Adriatic Sea: From transport to stratigraphy. *Cont. Shelf Res.* 27, 287-295.
- Mollenhauer, G., Inthorn, M., Vogt, T., Zabel, M., Sinninghe Damsté, J.S., Eglinton, T.I., 2007. Aging of marine organic matter during cross-shelf lateral transport in the Benguela upwelling system revealed by compound-specific radiocarbon dating. *Geochem., Geophys., Geosyst.* 8, Q09004, doi:10.1029/2007GC001603.
- Morović, M., 2002. Seasonal and interannual variations in pigments in the Adriatic Sea. *J. Earth Syst. Sci.* 111, 215-225.
- Morović, M., Mati, F., Grbec, B., Dadi, V., Ivankovi, D., 2006. South Adriatic phenomena observable through VOS XBT and other ADRICOSM data. *Acta Adriat.* 47, 33-49.
- Müller, P.J., Kirst, G., Ruhland, G., von Storch, I., Rosell-Melé, A., 1998. Calibration of the alkenone paleotemperature index $U^{K'}_{37}$ based on core-tops from the eastern South Atlantic and the global ocean (60°N-60°S). *Geochim. Cosmochim. Acta* 62, 1757-1772.
- Murray, A.E., Preston, C.M., Massana, R., Taylor, L.T., Blakis, A., Wu, K., DeLong, E.F., 1998. Seasonal and spatial variability of bacterial and archaeal assemblages in the coastal waters near Anvers Island, Antarctica. *Appl. Environ. Microbiol.* 64, 2585-2595.
- Murray, A.E., Blakis, A., Massana, R., Strawzewski, S., Passow, U., Alldredge, A., DeLong, E.F., 1999. A time series assessment of planktonic archaeal variability in the Santa Barbara Channel. *Aq. Microb. Ecol.* 20, 129-145.
- Nicol, G.W., Schleper, C., 2006. Ammonia-oxidising Crenarchaeota: important players in the nitrogen cycle? *Trends Microbiol.*, 14, 207-212.

- Nürnberg, D., Bijma, J., Hemleben, C., 1996. Assessing the reliability of magnesium in foraminiferal calcite as a proxy for water mass temperatures. *Geochim. Cosmochim. Acta* 60, 803-814.
- Ohkouchi, N., Eglinton, T.I., Keigwin, L.D., Hayes, J.M., 2002. Spatial and temporal offsets between proxy records in a sediment drift. *Science* 298, 1224-1227.
- Orlić, M., Gačić, M., La Violette, P.E., 1992. The currents and circulation of the Adriatic Sea. *Oceanolog. Acta* 15, 109-124.
- Pearson, A., McNichol, A.P., Benitez-Nelson, B.C., Hayes, J.M., Eglinton, T.I., 2001. Origins of lipid biomarkers in Santa Monica Basin surface sediment: a case study using compound-specific $\Delta^{14}\text{C}$ analysis. *Geochim. Cosmochim. Acta* 65, 3123-3137.
- Pearson, A., Huang, Z., Ingalls, A.E., Romanek, C.S., Wiegel, J., Freeman, K.H., Smittenberg, R.H., Zhang, C.L., 2004. Nonmarine crenarchaeol in Nevada hot springs. *Appl. Environ. Microbiol.* 70, 5229.
- Pearson, P.N., van Dongen, B.E., Nicholas, C.J., Pancost, R.D., Schouten, S., Singano, J.M., Wade, B.S., 2007. Stable warm tropical climate through the Eocene Epoch. *Geology* 35, 211-214.
- Pitcher, A., Schouten, S., Sinninghe Damsté, J.S., 2009. In situ production of crenarchaeol in two California hot springs. *Appl. Environ. Microbiol.* 75, 4443-4451.
- Popp, B.N., Prah, F.G., Wallsgrove, R.J., Tanimoto, J., 2006. Seasonal patterns of alkenone production in the subtropical oligotrophic North Pacific. *Paleoceanography* 21, PA1004.
- Poulain, P.-M., 2001. Adriatic Sea surface circulation as derived from drifter data between 1990 and 1999. *J. Mar. Syst.* 29, 3-32.
- Powers, L.A., Werne, J.P., Johnson, T.C., Hopmans, E.C., Sinninghe Damsté, J.S., Schouten, S., 2004. Crenarchaeotal membrane lipids in lake sediments: A new paleotemperature proxy for continental paleoclimate reconstruction? *Geology* 32, 613-616.
- Prah, F.G., Wakeham, S.G., 1987. Calibration of unsaturation patterns in long-chain ketone compositions for palaeotemperature assessment. *Nature* 330, 367-369.
- Prah, F.G., Pilskaln, C.H., Sparrow, M.A., 2001. Seasonal record for alkenones in sedimentary particles from the Gulf of Maine. *Deep-Sea Res. I* 48, 515-528.
- Prah, F.G., Wolfe, G.V., Sparrow, M.A., 2003. Physiological impacts on alkenone paleothermometry. *Paleoceanography* 18, PA1025.
- Prah, F.G., Popp, B.N., Karl, D.M., Sparrow, M.A., 2005. Ecology and biogeochemistry of alkenone production at Station ALOHA. *Deep-Sea Res. I* 52, 699-719.
- Raicich, F., 1996. On the fresh balance of the Adriatic Sea. *J. Mar. Syst.* 9, 305-319.
- Rizzoli, P.M., Bergamasco, A., 1983. The Dynamics of the coastal region of the northern Adriatic Sea. *J. Phys. Oceanogr.* 13, 1105-1130.

- Rontani, J.-F., Marty, J.-C., Miquel, J.-C., Volkman, J.K., 2006. Free radical oxidation (autoxidation) of alkenones and other microalgal lipids in seawater. *Org. Geochem.* 37, 354-368.
- Rontani, J.F., Zabeti, N., Wakeham, S.G., 2009. The fate of marine lipids: Biotic vs. abiotic degradation of particulate sterols and alkenones in the Northwestern Mediterranean Sea. *Mar. Chem.* 113, 9-18.
- Rubino, F., Saracino, O.D., Moscatello, S., Belmonte, G., 2009. An integrated water/sediment approach to study plankton (a case study in the southern Adriatic Sea). *J. Mar. Syst.* 78, 536-546.
- Sachs, J.P., Anderson, R.F., 2005. Increased productivity in the subantarctic ocean during Heinrich events. *Nature* 434, 1118-1121.
- Sangiorgi, F., Capotondi, L., Nebout, N.C., Vigliotti, L., Brinkhuis, H., Giunta, S., Lotter, A.F., Morigi, C., Negri, A., Reichert, G.-J., 2003. Holocene seasonal sea-surface temperature variations in the southern Adriatic Sea inferred from a multiproxy approach. *J. Quatern. Sci.* 18, 723-732.
- Schlitzer, R., 2010. Ocean Data View, <http://odw.awi.de> (version 4.3.2).
- Schmidt, F., Hinrichs, K.-U., Elvert, M., 2010. Sources, transport, and partitioning of organic matter at a highly dynamic continental margin. *Mar. Chem.* 118, 37-55.
- Schouten, S., Hopmans, E.C., Pancost, R.D., Sinninghe Damsté, J.S., 2000. Widespread occurrence of structurally diverse tetraether membrane lipids: evidence for the ubiquitous presence of low-temperature relatives of hyperthermophiles. *Proc. Natl. Acad. Sci. USA* 97, 14421-14426.
- Schouten, S., Hopmans, E.C., Schefuss, E., Sinninghe Damsté, J.S., 2002. Distributional variations in marine crenarchaeotal membrane lipids: a new tool for reconstructing ancient sea water temperatures? *Earth Planet. Sci. Lett.* 204, 265-274.
- Schouten, S., Hopmans, E.C., Sinninghe Damsté, J.S., 2004. The effect of maturity and depositional redox conditions on archaeal tetraether lipid palaeothermometry. *Org. Geochem.* 35, 567-571.
- Schouten, S., Huguet, C., Hopmans, E.C., Kienhuis, M.V.M., Sinninghe Damsté, J.S., 2007a. Analytical methodology for TEX₈₆ paleothermometry by High-Performance Liquid Chromatography/Atmospheric Pressure Chemical Ionization-Mass Spectrometry. *Anal. Chem.* 79, 2940-2944.
- Schouten, S., van der Meer, M.T.J., Hopmans, E.C., Rijpstra, W.I.C., Reysenbach, A.-L., Ward, D.M., Sinninghe Damsté, J.S., 2007b. Archaeal and bacterial Glycerol Dialkyl Glycerol Tetraether Lipids in hot springs of Yellowstone National Park. *Appl. Environ. Microbiol.* 73, 6181-6191.
- Schouten, S., Hopmans, E.C., van der Meer, J., Mets, A., Bard, E., Bianchi, T.S., Diefendorf, A., Escala, M., Freeman, K.H., Furukawa, Y., Huguet, C., Ingalls, A., Ménot-Combes, G., Nederbragt, A.J., Oba, M., Pearson, A., Pearson, E.J., Rosell-Melé, A., Schaeffer, P., Shah, S.R., Shanahan, T.M., Smith, R.W., Smittenberg, R., Talbot, H.M., Uchida,

- M., Van Mooy, B.A.S., Yamamoto, M., Zhang, Z., Sinninghe Damsté, J.S., 2009. An interlaboratory study of TEX₈₆ and BIT analysis using high-performance liquid chromatography-mass spectrometry. *Geochem. Geophys. Geosyst.* 10, Q03012, doi: 10.1029/2008GC002221.
- Sellschopp, J. and Álvarez, A., 2003. Dense low-salinity outflow from the Adriatic Sea under mild (2001) and strong (1999) winter conditions. *J. Geophys. Res.* 108(C9), 8104, doi: 10.1029/2002JC001562.
- Shah, S.R., Mollenhauer, G., Ohkouchi, N., Eglinton, T.I., Pearson, A., 2008. Origins of archaeal tetraether lipids in sediments: Insights from radiocarbon analysis. *Geochim. Cosmochim. Acta* 72, 4577-4594.
- Sikes, E.L., Volkman, J.K., Robertson, L.G., Pichon, J.-J., 1997. Alkenones and alkenes in surface waters and sediments of the Southern Ocean: Implications for paleotemperature estimation in polar regions. *Geochim. Cosmochim. Acta* 61, 1495-1505.
- Sinninghe Damsté, J.S., Rijpstra, W.I.C., Reichart, G.-J., 2002a. The influence of oxic degradation on the sedimentary biomarker record II. Evidence from Arabian Sea sediments. *Geochim. Cosmochim. Acta* 66, 2737-2754.
- Sinninghe Damsté, J.S., Schouten, S., Hopmans, E.C., van Duin, A.C.T., Geenevasen, J.A.J., 2002b. Crenarchaeol: the characteristic core glycerol dibiphytanyl glycerol tetraether membrane lipid of cosmopolitan pelagic crenarchaeota. *J. Lipid Res.* 43, 1641-1651.
- Socal, G., Boldrin, A., Bianchi, F., Civitarese, G., De Lazzari, A., Rabitti, S., Totti, C., Turchetto, M.M., 1999. Nutrient, particulate matter and phytoplankton variability in the photic layer of the Otranto strait. *J. Mar. Syst.* 20, 381-398.
- Sorensen, K.B., Teske, A., 2006. Stratified communities of active archaea in deep marine subsurface sediments. *Appl. Environ. Microbiol.* 72, 4596-4603.
- Stoica, E., Herndl, G.J., 2007. Contribution of Crenarchaeota and Euryarchaeota to the prokaryotic plankton in the coastal northwestern Black Sea. *J. Plankton Res.* 29, 699-706.
- Sun, M.Y., Wakeham, S.G., 1994. Molecular evidence for degradation and preservation of organic matter in the anoxic Black Sea basin. *Geochim. Cosmochim. Acta* 58, 3395-3406.
- Ternois, Y., Sicre, M.A., Boireau, A., Conte, M.H., Eglinton, G., 1997. Evaluation of long-chain alkenones as paleo-temperature indicators in the Mediterranean Sea. *Deep-Sea Res. I* 44, 271-286.
- Teske, A., Sorensen, K.B., 2008. Uncultured archaea in deep marine subsurface sediments: have we caught them all? *ISME J.* 2, 3-18.
- Totti, C., Civitarese, G., Aciri, F., Barletta, D., Candelari, G., Paschini, E., Solazzi, A., 2000. Seasonal variability of phytoplankton populations in the middle Adriatic sub-basin. *J. Plankton Res.* 22, 1735-1756.

- Trigo, I.F., Davies, T.D., Bigg, G.R., 1999. Objective climatology of cyclones in the Mediterranean region. *J. Clim.* 12, 1685–1696
- Turich, C., Freeman, K.H., Bruns, M.A., Conte, M., Jones, A.D., Wakeham, S.G., 2007. Lipids of marine archaea: Patterns and provenance in the water-column and sediments. *Geochim. Cosmochim. Acta* 71, 3272–3291.
- Uda, I., Sugai, A., Itoh, Y.H., Itoh, T., 2004. Variation in molecular species of core lipids from the order thermoplasmatales strains depends on the growth temperature. *J. Oleo Sci.* 53, 399–404.
- Versteegh, G.J.M., Riegman, R., de Leeuw, J.W., Jansen, J.H.F., 2001. $U^{K'}_{37}$ values for *Isochrysis galbana* as a function of culture temperature, light intensity and nutrient concentrations. *Org. Geochem.* 32, 785–794.
- Versteegh, G.J.M., de Leeuw, J.W., Taricco, C., Romero, A., 2007. Temperature and productivity influences on $U^{K'}_{37}$ and their possible relation to solar forcing of the Mediterranean winter. *Geochem., Geophys., Geosyst.* 8, Q09005, doi: 10.1029/2006GC001543
- Vilibić, I., Supić, N., 2005. Dense water generation on a shelf: the case of the Adriatic Sea. *Ocean Dyn.* 55, 403–415.
- Viličić, D., Vučak, Z., Škrivanić, A., Gržetić, Z., 1989. Phytoplankton blooms in the oligotrophic open south Adriatic waters. *Mar. Chem.* 28, 89–107.
- Volkman, J.K., Eglinton, G., Corner, E.D.S., Forsberg, T.E.V., 1980. Long-chain alkenes and alkenones in the marine coccolithophorid *Emiliana huxleyi*. *Phytochemistry* 19, 2619–2622.
- Volkman, J.K., Barrerr, S.M., Blackburn, S.I., Sikes, E.L., 1995. Alkenones in *Gephyrocapsa oceanica*: Implications for studies of paleoclimate. *Geochim. Cosmochim. Acta* 59, 513–520.
- Volkman, J.K., 2000. Ecological and environmental factors affecting alkenone distributions in seawater and sediments. *Geochem. Geophys. Geosyst.* 1, 2000GC000061, doi: 10.1029/2000gc000061.
- Walsh, E.M., Ingalls, A.E., Keil, R.G., 2008. Sources and transport of terrestrial organic matter in Vancouver Island fjords and the Vancouver-Washington Margin: A multiproxy approach using $\delta^{13}C_{org}$, lignin phenols, and the ether lipid BIT index. *Limnol. Oceanogr.* 53, 1054–1063.
- Weijers, J.W.H., Schouten, S., Hopmans, E.C., Geenevasen, J., A.J., David, O.R.P., Coleman, J.M., D., P.R., Sinninghe Damsté, J.S., 2006a. Membrane lipids of mesophilic anaerobic bacteria thriving in peats have typical archaeal traits. *Environ. Microbiol.* 8, 648–657.
- Weijers, J.W.H., Schouten, S., Spaargaren, O.C., Sinninghe Damsté, J.S., 2006b. Occurrence and distribution of tetraether membrane lipids in soils: Implications for the use of the TEX_{86} proxy and the BIT index. *Org. Geochem.* 37, 1680–1693.

- Wells, L.E., Cordray, M., Bowerman, S., Miller, L.A., Vincent, W.F., Deming, J.W., 2006. Archaea in Particle-Rich Waters of the Beaufort Shelf and Franklin Bay, Canadian Arctic: Clues to an Allochthonous Origin? *Limnol. Oceanogr.* 51, 47-59.
- Wuchter, C., Schouten, S., Wakeham, S.G., Sinninghe Damsté, J.S., 2005. Temporal and spatial variation in tetraether membrane lipids of marine crenarchaeota in particulate organic matter: Implications for TEX₈₆ paleothermometry. *Paleoceanography* 20, PA3013.
- Wuchter, C., Schouten, S., Wakeham, S.G., Sinninghe Damsté, J.S., 2006. Archaeal tetraether membrane lipid fluxes in the northeastern Pacific and the Arabian Sea: Implications for TEX₈₆ paleothermometry. *Paleoceanography* 21, PA4208.
- Xoplaki, E., González-Rouco, J.F., Luterbacher, J., Wanner, H., 2003. Mediterranean summer air temperature variability and its connection to the large-scale atmospheric circulation and SSTs. *Clim. Dyn.* 20, 723-739.
- Xoplaki, E., González-Rouco, J.F., Luterbacher, J., Wanner, H., 2004. Wet season Mediterranean precipitation variability: influence of large-scale dynamics and trends. *Clim. Dyn.* 23, 63-78.
- Yakimov, M.M., Cappello, S., Crisafi, E., Tursi, A., Savini, A., Corselli, C., Scarfi, S., Giuliano, L., 2006. Phylogenetic survey of metabolically active microbial communities associated with the deep-sea coral *Lophelia pertusa* from the Apulian plateau, Central Mediterranean Sea. *Deep-Sea Res. I* 53, 62-75.
- Zavatarelli, M., Pinardi, N., 2003. The Adriatic Sea modelling system: a nested approach. *Ann. Geophys.* 21, 345-364.
- Zavatarelli, M., Raicich, F., Bregant, D., Russo, A., Artegiani, A., 1998. Climatological biogeochemical characteristics of the Adriatic Sea. *J. Mar. Syst.* 18, 227-263.
- Zhang, C.L., Pearson, A., Li, Y.L., Mills, G., Wiegand, J., 2006. Thermophilic temperature optimum for crenarchaeol synthesis and its implication for archaeal evolution. *Appl. Environ. Microbiol.* 72, 4419.
- Ziveri, P., Rutten, A., de Lange, G.J., Thomson, J., Corselli, C., 2000. Present-day coccolith fluxes recorded in central eastern Mediterranean sediment traps and surface sediments. *Palaeogeogr., Palaeoclim., Palaeoecol.* 158, 175-195.
- Zonneveld, K.A.F., Chen, L., Möbius, J., Mahmoud, M.S., 2009. Environmental significance of dinoflagellate cysts from the proximal part of the Po-river discharge plume (off southern Italy, Eastern Mediterranean). *J. Sea Res.* 62, 189-213.

II.A1. APPENDIX

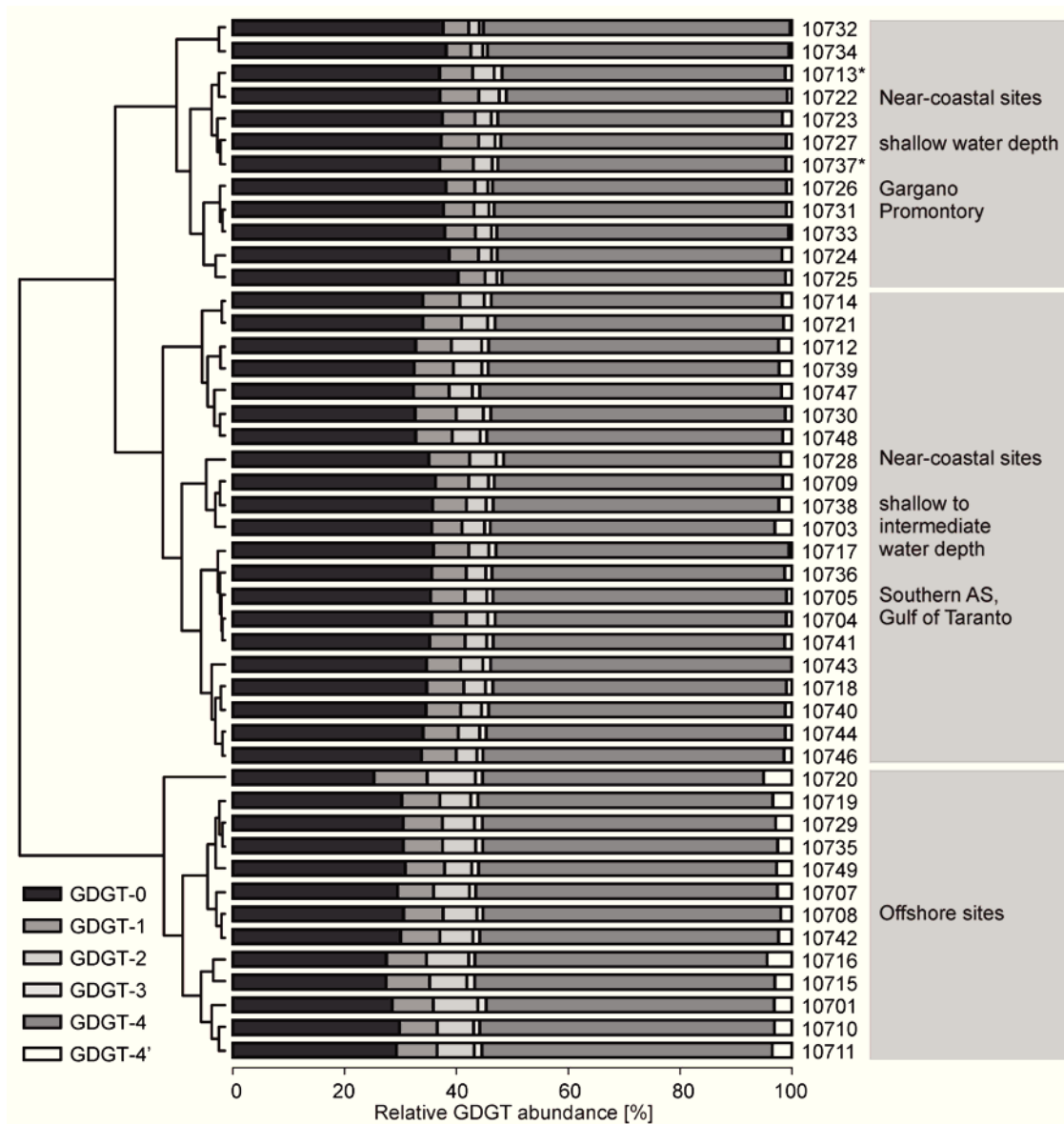


Figure II.A1. Cluster analysis and bar plot of relative GDGT abundance in the analyzed surface sediment samples. Numbers correspond to samples listed in Table II.1.

II.S1. SUPPLEMENTARY MATERIAL (ELECTRONICAL ANNEX)

(available online at doi:10.1016/j.epsl.2010.09.042)

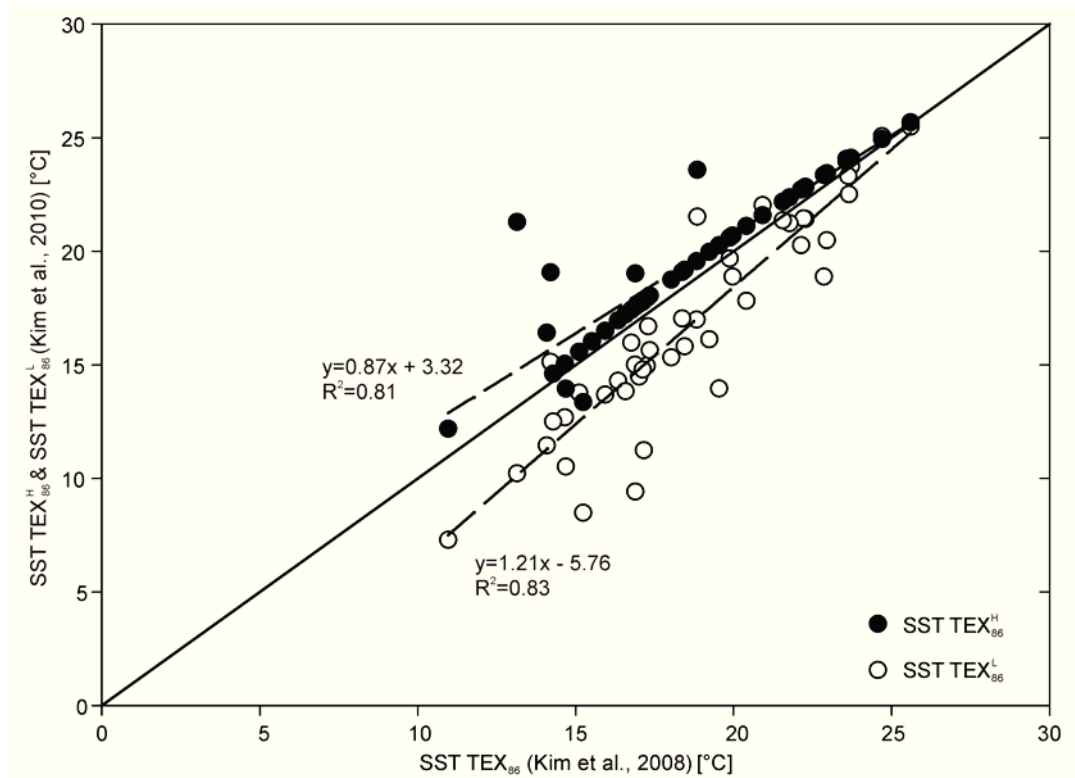


Figure II.S1. SST estimates resulting from the calibration by Kim et al. (2008; x-axis) vs. SST estimates according to two new calibrations by Kim et al. (2010; y-axis; open and black circles are TEX₈₆^L and TEX₈₆^H, based respectively) for the dataset from the southern Italian shelf. The solid line gives the 1:1 line between both temperature estimates. The dashed lines give the linear regression based on the dataset.

Table II.S1 Comparison of TEX_{86} indices and derived temperatures based on the calibrations from Kim et al. (2008, 2010)

Sample	Lat	Lon	Water Depth	TEX_{86}	TEX_{86}^L	TEX_{86}^H	SST TEX_{86}^a	SST $TEX_{86}^L^b$	SST $TEX_{86}^H^b$
[GeoB]	[°N]	[°E]	[m]				[°C]	[°C]	[°C]
10701	40.000	17.467	1186	0.63	-0.32	-0.20	24.70	25.07	24.94
10702	40.000	17.586	911	n.d.	n.d.	n.d.	n.d.	n.d.	n.d.
10703	40.000	17.742	277	0.60	-0.41	-0.22	22.86	18.89	23.36
10704	40.000	17.833	219	0.50	-0.47	-0.30	17.25	14.96	17.93
10705	39.853	17.913	128	0.49	-0.46	-0.31	16.76	15.97	17.41
10706	39.825	17.833	218	n.d.	n.d.	n.d.	n.d.	n.d.	n.d.
10707	39.783	17.583	1598	0.61	-0.34	-0.21	23.57	24.06	23.97
10708	39.808	17.733	686	0.56	-0.37	-0.25	20.92	22.03	21.59
10709	39.757	17.893	173	0.51	-0.47	-0.29	18.03	15.33	18.75
10710	39.592	17.683	2040	0.61	-0.34	-0.21	23.72	23.75	24.11
10711	39.683	17.800	1049	0.61	-0.36	-0.21	23.65	22.51	24.04
10712	39.727	17.862	618	0.59	-0.38	-0.23	22.27	21.43	22.83
10713	39.692	18.283	127	0.52	-0.46	-0.28	18.45	15.81	19.18
10714	39.640	18.283	207	0.53	-0.44	-0.28	18.83	16.99	19.56
10715	39.559	18.283	697	0.59	-0.38	-0.23	22.21	21.44	22.78
10716	39.345	18.283	1328	0.65	-0.32	-0.19	25.60	25.48	25.68
10717	39.742	18.080	93	0.46	-0.49	-0.34	15.11	13.77	15.58
10718	39.693	18.058	220	0.48	-0.48	-0.32	16.34	14.30	16.96
10719	39.653	18.042	616	0.60	-0.39	-0.22	22.95	20.49	23.43
10720	39.507	17.978	1387	0.61	-0.35	-0.21	23.63	23.31	24.03
10721	42.166	16.767	203	0.52	-0.44	-0.29	18.37	17.04	19.09
10722	42.167	16.500	142	0.45	-0.51	-0.34	14.65	12.68	15.04
10723	42.167	16.000	114	0.50	-0.53	-0.30	17.16	11.23	17.84
10724	42.001	16.217	50	0.49	-0.56	-0.29	16.89	9.41	19.02
10725	42.000	16.367	98	0.46	-0.57	-0.37	15.24	8.48	13.35
10726	42.000	16.717	183	0.44	-0.47	-0.29	14.20	15.13	19.07
10727	41.801	16.617	101	0.43	-0.54	-0.25	13.14	10.22	21.29
10728	41.783	16.858	194	0.53	-0.38	-0.22	18.85	21.52	23.59
10729	41.647	17.191	712	0.59	-0.39	-0.23	22.14	20.27	22.71
10730	41.500	17.050	183	0.50	-0.45	-0.30	17.30	16.69	17.99
10731	41.500	16.658	96	0.45	-0.54	-0.36	14.68	10.51	13.95
10732	41.500	16.407	51	0.39	-0.59	-0.39	10.96	7.29	12.18
10733	41.500	16.225	23	0.45	-0.51	-0.35	14.28	12.49	14.61
10734	41.667	16.242	18	0.44	-0.53	-0.32	14.08	11.44	16.41
10735	41.500	17.308	733	0.58	-0.38	-0.24	21.77	21.23	22.37
10736	40.758	18.192	123	0.49	-0.49	-0.31	16.58	13.84	17.22
10737	40.625	18.329	113	0.48	-0.49	-0.32	15.93	13.69	16.50
10738	40.546	18.467	112	0.54	-0.49	-0.27	19.54	13.96	20.27
10739	40.500	18.642	565	0.55	-0.41	-0.26	19.97	18.89	20.69
10740	40.392	18.583	128	0.49	-0.48	-0.31	17.01	14.48	17.68
10741	40.233	18.667	287	0.50	-0.46	-0.30	17.35	15.64	18.05
10742	39.716	18.776	599	0.58	-0.38	-0.24	21.56	21.36	22.18
10743	39.825	18.642	124	0.47	-0.46	-0.33	15.52	16.03	16.04
10744	39.850	18.600	117	0.49	-0.47	-0.31	16.88	15.01	17.55
10746	39.908	16.758	157	0.50	-0.48	-0.30	17.12	14.79	17.77
10747	39.725	16.975	246	0.53	-0.46	-0.27	19.23	16.13	19.97
10748	39.667	17.050	288	0.55	-0.40	-0.26	19.88	19.68	20.60
10749	39.600	17.183	278	0.55	-0.43	-0.26	20.41	17.82	21.11

^a SST TEX_{86} calculated after Kim et al., 2008^b SST TEX_{86}^L and SST TEX_{86}^H calculated after Kim et al., 2010

CHAPTER III

Distribution and stable isotopes of plant wax derived *n*-alkanes in marine surface sediments along a SE Italian transect and their potential to reconstruct the water balance

Arne Leider^{a,*}, Kai-Uwe Hinrichs^a, Enno Schefuß^a and Gerard J.M. Versteegh^{a,*}

Revised version upon acceptance considering major revisions
to *Geochimica et Cosmochimica Acta*

^a MARUM Center for Marine Environmental Sciences & Dept. of Geosciences, University of Bremen, D-28334 Bremen, Germany

* corresponding authors,

E-mail addresses: AL: arneleider@uni-bremen.de; GJMV: versteegh@uni-bremen.de

Phone: +49 421 218 65742 (AL)

Fax: +49 421 218 65715

III.1. ABSTRACT

We investigated to what extent changes in the stable hydrogen and carbon isotope composition and distribution of plant wax derived *n*-alkanes in terrestrial, coastal and offshore surface sediments along a N-S transect in east Italy relate to hydrological variations on land. The *n*-alkanes from the terrestrial and coastal samples show a southward increase of δD of 40‰ VSMOW and an increase in the *n*-alkane average chain length, which is in line with the generally southward increasing δD of precipitation and mean annual air temperature, respectively. However, the trend in δD of precipitation is much smaller than that of the δD of plant waxes. We attributed this difference to an additional effect of increased leaf water transpiration and/or soil water evaporation in S Italy. The $\delta^{13}C$ - δD of plant waxes from the northern Po and Apennine river systems differs considerably from that in south Italian sediments. On the basis of this difference we can characterize plant wax supply from the N Adriatic Sea by the Western Adriatic Current to the offshore sediments of the Gulf of Manfredonia. This is in agreement with maxima in BIT values and the distribution of clay minerals. This supply of plant waxes is negligible for the sediments in the Gulf of Taranto, which is largely influenced by regional southern Italian sources. Our study provides a calibration of δD of plant waxes, which may be used as a proxy for past changes in the Adriatic water balance. The additional use of the plant wax chain length distribution and $\delta^{13}C$ enables the assessment of the contribution by different source areas.

III.2 INTRODUCTION

For the Mediterranean Sea and its adjacent areas evaporation (E) exceeds precipitation (P) and river runoff (Trigo et al., 1999; Boukthir and Barnier, 2000; Mariotti et al., 2002; Struglia et al., 2004; Xoplaki et al., 2004). The Fourth Assessment Report of the IPCC (Intergovernmental Panel on Climate Change) estimates that the upcoming climate change will severely increase this imbalance with highest temperature maxima and moisture loss during summer (IPCC, 2007). Still, climate is complex and response to forcing is hard to model and predict, especially for the water balance. The reconstruction of past climate provides information on responses of climate to forcing mechanisms and can play an important role for the validation of climate models.

The hydrogen isotopic composition (δD) of environmental water is modified by climatic parameters such as evaporation, water vapor sources and precipitation (Craig, 1961; Gat,

1996). By incorporation of source water-derived hydrogen into organic compounds, the δD of lipid biomarkers (Sessions et al., 1999; Sauer et al., 2001) preserved in marine (Schefuß et al., 2005; Pagani et al., 2006; Shuman et al., 2006; Niedermeyer et al., 2010) and lacustrine sediments (Huang et al., 2002; Sachse et al., 2004; Tierney et al., 2008; Tierney et al., 2010) as well as soils (Liu and Huang, 2005; Rao et al., 2009; Smith et al., 2007) shows good agreement to recent environmental conditions in different climates and may provide a powerful proxy for reconstructing the past water cycle. Long chain odd-numbered (C_{27} - C_{33}) *n*-alkanes of vascular plant leaf waxes (Eglinton and Hamilton, 1967) are well suited for such analyses due to their resistance to degradation and hydrogen exchange during diagenesis (e.g., Sessions et al., 2004; Schimmelmann et al., 2006).

Plant waxes are ablated from living plants by rain or wind and can be carried by long-range atmospheric transport to the open ocean (Simoneit, 1977; Gagosian et al., 1981; Ohkouchi et al., 1997; Huang et al., 2000; Rommerskirchen et al., 2003; Schefuß et al., 2003). Additionally, plant waxes found in shallow and near coastal environments can be fluvially transported (e.g., Prah et al., 1994; Bird et al., 1995; Pelejero, 2003; Colombo et al., 2005).

The δD of plant waxes ($\delta D_{\text{plant-wax}}$) is influenced by more factors than the δD of precipitation ($\delta D_{\text{precipitation}}$). Large differences in hydrogen isotope fractionation have been observed between plant types (i.e. trees, shrubs, C_3 and C_4 grass) and between specimens of the same plant species (even at sites receiving the same precipitation). These are linked to plant physiology, microclimates (sunlight exposure, temperature, humidity, wind), location-dependent water use and canopy thickness, demonstrating that changes in vegetation cover can affect sedimentary $\delta D_{\text{plant-wax}}$ values (Chikaraishi & Naraoka, 2003, Bi et al., 2005; Krull et al., 2006; Smith & Freeman, 2006; Hou et al., 2007a, b; Liu & Yang, 2008; McInerney et al., 2011). The effect of C_3 vs. C_4 plant types on the $\delta D_{\text{plant-wax}}$ is not well constrained, mainly due to the comparison between plants showing considerable differences in growth forms (e.g., Chikaraishi & Naraoka, 2003). However, C_4 grasses are generally more D-depleted compared to C_3 grasses (Smith & Freeman, 2006). The processes of soil water evaporation and leaf water transpiration, both leading to D enrichment, are hard to disentangle (Smith and Freeman, 2006; Feakins and Sessions, 2010; Polissar and Freeman, 2010; Seki et al., 2010; McInerney et al., 2011). In arid ecosystems transpiration seems to be more important than the groundwater composition (Feakins and Sessions, 2010). In contrast, Liu and Huang (2005) proposed that increased evapotranspiration leads to D-enriched plant waxes under arid conditions with low atmospheric humidity so that in these cases the $\delta D_{\text{plant-wax}}$ primarily

reflect relative humidity. Additionally, variations in relative humidity are suggested to operate primarily via the modulation of soil water rather than leaf water (McInerney et al., 2011).

To better capture the factors influencing the $\delta D_{\text{plant-wax}}$ additional plant wax parameters can be quantified such as their chain length distribution and stable carbon isotope composition ($\delta^{13}\text{C}$). Environmental factors and related changes in vegetation seem to affect the plant wax distribution leading to a shift to higher homologues and higher values of average chain length (ACL) (Poynter et al., 1989; Poynter and Eglinton, 1990) with higher temperature, aridity and C_4 plant contribution (Cranwell, 1973; Simoneit, 1977; Gagosian and Peltzer, 1986; Hinrichs et al., 1998; Schefuß et al., 2003; Rommerskirchen et al., 2006b; Vogts et al., 2009)

The $\delta^{13}\text{C}$ of plants and their lipids is controlled by concentration and $\delta^{13}\text{C}$ of ambient CO_2 and environmental factors like temperature and aridity, which affect plant physiology (Farquhar and Sharkey, 1982; Farquhar et al., 1989; Cerling et al., 1997; Ehleringer et al., 1997; Eglinton and Eglinton, 2008). Major differences in discrimination against ^{13}C during photosynthesis exist between the C_3 and C_4 pathway (Smith and Epstein, 1971; O'Leary, 1981; Rieley et al., 1993; Collister et al., 1994). This has led to the use of $\delta^{13}\text{C}$ of sedimentary plant waxes to reconstruct past vegetation changes and shifts in the relative contribution of C_3 and C_4 plants (Huang et al., 2000; Schefuß et al., 2003b; Rommerskirchen et al., 2006a).

The main goal of this study is to calibrate the relationship between δD of plant waxes and climate along the eastern Italian coast and to evaluate its imprint on surface sediments from the southern Italian shelf for reconstructions of the past precipitation-evaporation budget at the Gallipoli shelf (Gulf of Taranto, S. Italy; Fig. III.1) (Cini Castagnoli et al., 1999; Versteegh et al., 2007; Taricco et al., 2009). Morphology and southward extension of Italy into the Mediterranean Sea result in a transition from a subcontinental climate in northern

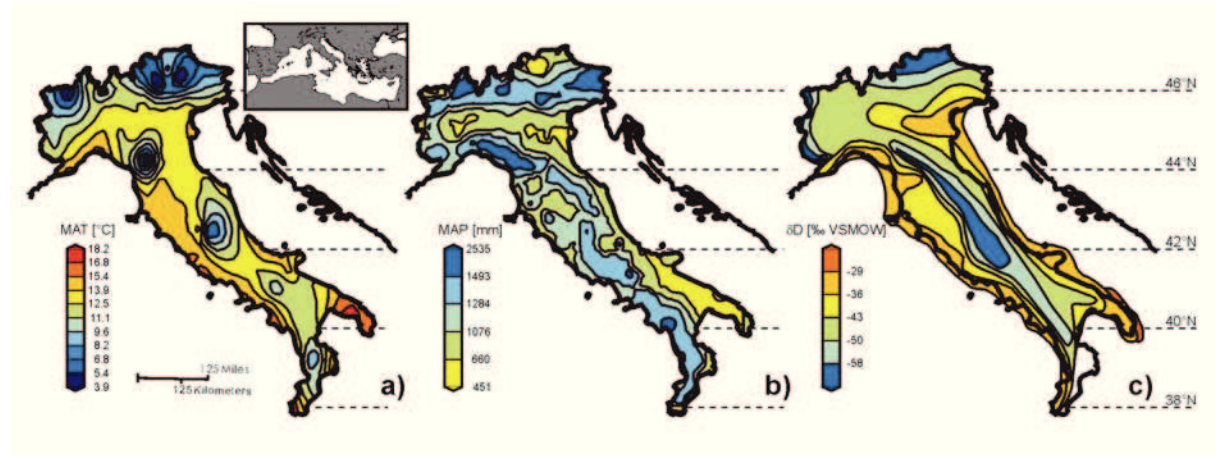


Figure III.1. Map of Italy showing the distribution of (a) mean annual air temperature (MAT), (b) mean annual precipitation (MAP) for the period 1961-1990 (modified from Desiato et al., 2005) and (c) stable hydrogen isotopic composition of precipitation (δD) (map modified by conversion of $\delta^{18}\text{O}$ to δD based on the meteoric water line of Italy; $\delta D = 7.61 \delta^{18}\text{O} + 9.21$, from Longinelli and Selmo, 2003).

Italy to a dry Mediterranean/subtropical climate in southern Italy (Rivas-Martínez et al., 2004; Peel et al., 2007; Todorovic et al., 2007) showing strong gradients in temperature, precipitation and the water budget (Fig. III.1a, b, c). However, a calibration can only be successful by including the contribution of all potential terrestrial source regions and their climate signature. Therefore, we analyzed samples from various terrestrial settings covering a N-S transect in Italy as well as marine sediments from the southern Adriatic Sea and Gulf of Taranto (Fig. III.2).

III.3. STUDY AREA

III.3.1. Climatic setting

The overall warm-temperate climate of Italy is modified by orographic and hydrographic factors e.g., its exposure to the Mediterranean Sea. These factors influence parameters like annual mean air temperature and precipitation (Fig. III.1a, b). As a result the central northern regions including the Po valley are characterized by a subcontinental climate, while a dry semi-arid Mediterranean climate dominates at the central coastal and southern zones (Rivas-Martínez et al., 2004; Peel et al. 2007; Todorovic et al., 2007). This is reflected by the natural vegetation showing a shift from N to S with mesophytic broad-leaved deciduous and mixed broad-leaved / conifer forest at the Po valley to typical Mediterranean sclerophyllous forest and scrubland along the coastal areas of S Italy and S Apulia (Bohn et al., 2004) (Fig. III.2).

Lowest temperatures occur in the northern Alpine and central Italian Apennine mountains. These regions show highest annual mean precipitation rates fuelling the Po and Apennine river systems, which drain into the Adriatic Sea (Fig. 2) (Artegiani et al., 1997a; Zavatarelli et al., 1998; Cattaneo et al., 2003; Zavatarelli and Pinardi, 2003). Highest temperatures occur along the western coast and in southern Italy (Apulian peninsula). Especially the southern Italian region with its subtropical climate experiences low precipitation, which results in drier conditions and a more negative water balance (Marsico et al., 2007). This is also expressed in deviations from the global meteoric water line (Craig et al., 1961), showing an increase in deuterium excess, a measure for kinetic evaporation processes on precipitation, from N to S Italy (Longinelli and Selmo, 2003, 2010). $\delta D_{\text{precipitation}}$ in Italy ranges from -60‰ VSMOW to -25‰ VSMOW. Additionally, it is mainly modulated by altitude with lowest values for the Alps and Apennine mountains (Fig. III.1c) (Longinelli and Selmo, 2003). These trends are in line with the general global δD pattern (e.g., Bowen and Revenaugh, 2003).

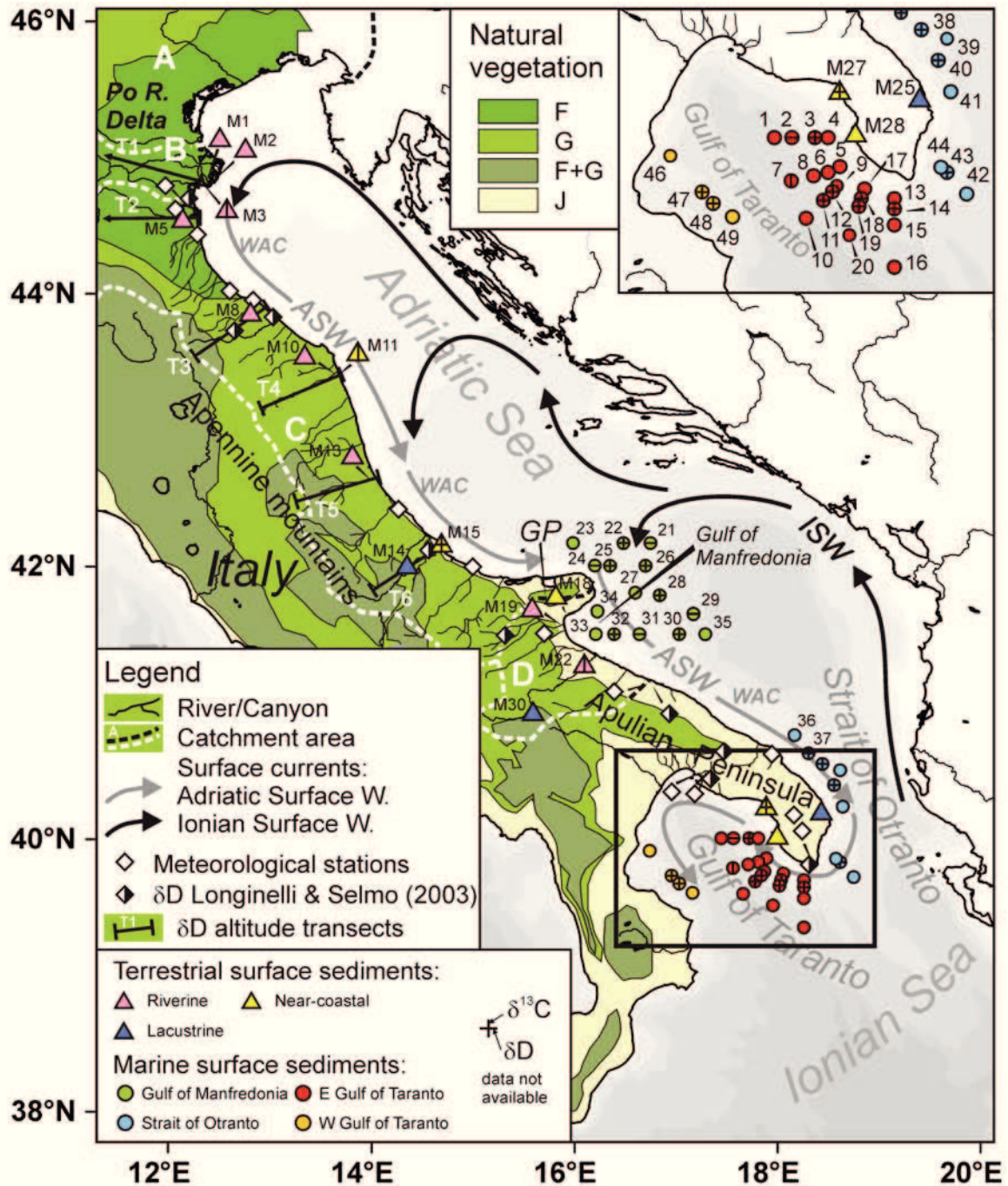


Figure II.2. Map of Central and Southern Italy, the Adriatic and Ionian Sea indicating the study area and general circulation pattern (ISW: Ionian Surface Water, ASW: Adriatic Surface Water, WAC: Western Adriatic Current; redrawn from Artegiani et al., 1997b; Poulain, 2001). Natural vegetation is shown according to the classification of Bohn et al. (2004) with F: Mesophytic deciduous broad-leaved and mixed broad-leaved coniferous forests, G: Thermophilous mixed deciduous broad-leaved forests, J: Mediterranean sclerophyllous forests and scrub. Major catchment areas are indicated by thick dashed curves redrawn from Cattaneo et al. (2003) with A: Alpine rivers, B: Po river, C: Apennine rivers, D: rivers south of Gargano. Diamonds show meteorological stations with available data of mean annual air temperature, precipitation and humidity (open diamonds); δD of precipitation (half open diamonds). Transects (T1-T6) indicate Po River and Apennine rivers regions, where the δD of precipitation has been averaged based on data from Online Isotope Precipitation Calculator (OIPC). Filled triangles indicate terrestrial surface sediments of lacustrine, riverine and near coastal origin. Filled circles indicate locations of marine surface sediments. Marine samples were grouped in accordance to their spatial distribution within the southern Adriatic Sea (green: Gargano Promontory (GP) and Gulf of Manfredonia, blue: Strait of Otranto) and Gulf of Taranto (red: E Gulf of Taranto, yellow: W Gulf of Taranto). Signature within triangles and circles refers to samples without δD and/or $\delta^{13}C$ data.

III.3.2. Oceanographic setting

The Adriatic Sea is a narrow semi-enclosed sub-basin of the northeastern Mediterranean Sea (Artegiani et al., 1997a; Cattaneo et al., 2003) (Fig. III.2.). Freshwater supply to the western Adriatic Sea is dominated by the Po River and Apennine rivers located north of the Gargano Promontory (Zavatarelli and Pinardi, 2003; Milligan and Cattaneo, 2007). They contribute more than 70% of the total runoff and $\sim 51.7 \times 10^6$ t/yr of mean suspended load to the Adriatic Sea (e.g., Cattaneo et al., 2003 and references therein). At the southwestern Adriatic Sea, rivers are nearly absent and contributions of sediments from Croatian margin are assumed to be negligible (Cattaneo et al., 2003; Raicich, 1996). River runoff is highest during late autumn and late spring corresponding to maxima in precipitation and snow melting (Cattaneo et al., 2003; Nittrouer, 2004). This creates the coastal Western Adriatic Current (WAC) characterized as Adriatic Surface Water, which is confined to a narrow coastal strip flowing southwards along the Italian eastern margin through the Strait of Otranto into the Gulf of Taranto where it mixes with Ionian Sea water masses (e.g., Morovic et al., 2006). The WAC controls the distribution of sediments from the northern entry points along the western Adriatic shelf (e.g. Tomadin, 2000). Along shore transport is assumed to transfer $\sim 35\%$ of the river supply from the north to the central Adriatic Sea (Frignani et al., 2005). Wind-induced resuspension events promoted by Bora and Sirocco winds lead to a southward movement of sediments (Fain et al., 2007; Tesi et al., 2007). As a result, there is a distinct organic matter-rich mud deposit consisting of deltaic and shallow marine sediments along the western Adriatic Sea reaching as far as southeast of the Gargano Promontory (Trincardi et al., 1994; Cattaneo et al., 2003; Nittrouer, 2004).

III.4. MATERIAL AND METHODS

III.4.1. Sample sites

Terrestrial samples have been collected during a land survey in October 2009 covering a north to south transect (45 to 40 °N) along the east coast of Italy (Fig. III.2., Table 1). These samples represent the top 1 cm of sediments from Po and Apennine rivers, lakes, beaches and other near coastal environments. The marine offshore sediments analyzed represent the top 2 cm of multicores from 48 stations obtained from the southern Adriatic Sea to the Gulf of Taranto. They have been collected during P339 POSEIDON cruise “CAPPUCCINO” in June 2006 (Fig. 2, Table 2) (Zonneveld et al., 2009; Grauel and Bernasconi, 2010; Leider et al.,

2010). The material was frozen to -20 °C directly upon collection and remained at this temperature until geochemical processing.

III.4.2. Sample Preparation

5-15 g of freeze dried and homogenized sediment were extracted using an accelerated solvent extractor (ASE 200, DIONEX) with a mixture of dichloromethane (DCM):methanol (MeOH) 9:1 (v/v, three cycles of 5 min each, 100 °C and 7.6×10^6 Pa). Before extraction known amounts of *n*-hexatriacontane, 2-nonadecanone, *n*-nonadecanol and *n*-nonadecanoic acid were added as internal standards. The obtained total lipid extracts (TLE) were dried using a Turbovap LV (Zymark Corp.) at 35 °C under a nitrogen stream.

III.4.3. Sample preparation, identification and quantification of *n*-alkanes

Saponification of the TLE was performed adding 2 ml 6% KOH in MeOH and reaction at 80°C for 3 h. After cooling and subsequent dilution with 2 ml 0.05 M KCl solution, neutral lipids were released by extracting four times using 2 ml *n*-hexane (Elvert et al., 2003). The resulting fraction was separated in DCM-soluble asphaltenes and *n*-hexane-soluble maltenes. The maltenes were desulfurized with activated copper powder and separated by solid phase extraction (Supelco LC-NH₂ glass cartridges; 500 mg sorbent). Four fractions of increasing polarity (hydrocarbons, ketones, alcohols, and fatty acids) were obtained according to the protocol by Hinrichs et al. (2000).

Gas chromatography was performed by using a Trace GC Gas Chromatograph equipped with a 30 m DB-5MS fused silica column (0.32 mm ID, 0.25 µm film thickness) and a flame ionization detector using He as carrier gas with a flow rate of 1 ml/min. The GC temperature program for hydrocarbons was: injection at 60 °C, 1 min isothermal; from 60 °C to 150 °C at 10 °C/min; from 150 °C to 310 °C at 4 °C/min; 25 min isothermal with a total oven run time of 75 min. Peak identification of compounds was based on retention time and comparison with parallel GC-MS runs. Compounds were quantified by peak integration and by assuming the same response factor as the internal standard (*n*-hexatriacontane). Contents of the *n*-C₂₉ and *n*-C₃₁ alkanes are reported in µg/g dry mass sediment.

If coelution was evident in the FID chromatogram the hydrocarbon fraction was treated using urea adduction for separation of straight chained *n*-alkanes before analyzing their compound-specific stable isotopic composition. Non-adducts were separated by rinsing the urea crystals with *n*-hexane/DCM (2:1, v/v). Adducted *n*-alkanes were partitioned into *n*-hexane/DCM (4:1, v/v) after addition of H₂O to dissolve the urea crystals.

III.4.4. Gas Chromatography Isotope Ratio Monitoring Mass Spectrometry (GC-IRMS)

III.4.4.1. Analysis of $\delta^{13}\text{C}$ values of the *n*-alkanes

For the analysis of $\delta^{13}\text{C}$ values of individual *n*-alkanes hydrocarbon fractions were injected into a Trace GC equipped with a 30 m DB-5MS fused silica column (0.32 mm ID, 0.25 μm film thickness), coupled to an isotope ratio mass spectrometer (IRMS) (Delta^{plus}XP, Finnigan MAT, Bremen, Germany) via a Finnigan GC III Combustion interface at 940 °C. The injector was operated at 310 °C in splitless mode. The oven was maintained for 1 min at 60 °C then heated at 10 °C/min to 150 °C followed by 4 °C/min to 320 °C and held for 17.5 min at the final temperature. The column flow was held constant at 1.2 ml/min throughout the run. All $\delta^{13}\text{C}$ values were normalized to the VPDB scale using multiple pulses of CO_2 reference gas. Samples were analyzed with two replicate measurements. The standard deviations of the replicate measurements are reported individually for the *n*-C₂₉ and *n*-C₃₁ alkanes, and are generally $< \pm 0.3\text{‰}$ ($n = 150$, 92 runs with 1-2 peaks each). Weighted mean $\delta^{13}\text{C}$ values were calculated for the *n*-C₂₉ and *n*-C₃₁ alkane (WM $\delta^{13}\text{C}$ *n*-C_{29, 31}).

III.4.4.2. Analysis of δD values of the *n*-alkanes

For δD analysis of *n*-alkanes, hydrocarbon fractions were injected into a Trace GC equipped with a 30 m DB-5MS fused silica column (0.32 mm ID, 0.25 μm film thickness). The injector was operated at 300 °C in splitless mode and the same oven and column parameters were used as for $\delta^{13}\text{C}$ analyses. The eluting compounds were transferred to a pyrolysis conversion furnace operated at 1440 °C (Burgoyne and Hayes, 1998; Hilkert et al., 1999; Sessions, 2006) and quantitatively converted to H_2 , which was introduced into an isotope ratio mass spectrometer (IRMS) (Delta^{plus}XP, Finnigan MAT, Bremen, Germany). Each sample was analyzed with two to three replicate measurements. All δD values were normalized to the VSMOW scale using C_{30:0} FAME as reference standard (A. Schimmelmann, Indiana University, Bloomington, USA). The precision of the instrument was determined by analysis of a standard mixture of *n*-alkane homologues (Mixture B including *n*-C₁₆ to *n*-C₃₀; A. Schimmelmann, Indiana University, Bloomington, USA).

Injection of the standard mixture showed a standard deviation of 3.2‰ and a root-mean-squared accuracy of 5.7‰. The H_3^+ factor was determined once a day and stayed constant within the analytical error of the instrument at 4.53 (SD = 0.15; $n = 33$) during the first measurement series and at 3.01 (SD = 0.05; $n = 6$) during the second measurement period.

Achieved precision, expressed as the average standard deviation for the n -C₂₉ and n -C₃₁ alkanes for the samples was 2.5‰ ($n = 161$, 91 runs with 1–2 peaks each). Weighted mean δD values were calculated for the n -C₂₉ and n -C₃₁ alkane (WM δD n -C_{29,31}).

III.4.5. Definition of CPI and ACL

Carbon preference indices (CPIs) for the n -alkanes were calculated as:

$$\text{CPI}_{25-33} = [0.5 ((X_i + X_{i+2} + \dots + X_n) / (X_{i-1} + X_{i+1} + \dots + X_{n-1})) + 0.5 ((X_i + X_{i+2} + \dots + X_n) / (X_{i+1} + X_{i+3} + \dots + X_{n+1}))] \quad (\text{III.1})$$

for n -alkanes with carbon number range from $i = 25$ to $n = 35$ (Bray and Evans, 1961; Schefuß et al., 2001; Boot et al., 2006).

Average Chain Lengths (ACLs) were calculated as:

$$\text{ACL}_{25-33} = (25[C_{25}] + 27[C_{27}] + 29[C_{29}] + 31[C_{31}] + 33[C_{33}]) / ([C_{25}] + [C_{27}] + [C_{29}] + [C_{31}] + [C_{33}]) \quad (\text{III.2})$$

with $[C_x]$ indicating the area of the n -alkane with x carbon atoms (Poynter et al., 1989; Poynter and Eglinton, 1990).

III.4.6. δD values of precipitation

For δD of precipitation for the terrestrial sample locations in our study, we used the annual mean δD retrieved from the Online Isotope in Precipitation Calculator (OIPC) database available at <http://wateriso.eas.purdue.edu/waterisotopes/> (Bowen and Revenaugh, 2003; Bowen, 2011) (Table 1). Additionally, we calculated an average δD of precipitation along altitudinal transects (maximum distance to coast: ~70 and 200 km) in the catchment areas of the Po River and the Apennine rivers to account for plant-wax contributions from higher altitudes. For comparison annual mean precipitation δD values have been extracted from the isotope mapping of Italy by Longinelli and Selmo (2003). The data are presented in Supplementary data EA-III.1 (Fig. III.2.).

III.4.7. Mean air temperature, precipitation and relative humidity

Mean annual air temperatures (MAT), annual precipitation (MAP) and relative humidity (RH) of coastal meteorological stations along a N-S transect in Italy (Fig. III.2) were obtained from the meteorological and climatic database available at the webpage of SCIA (Sistema nazionale per la raccolta, l'elaborazione e la diffusione di dati Climatologici di Interesse Ambientale; www.scia.sinanet.it) provided by the ISPRA (Institute for Environmental

Protection and Research, Italy). The values represent averages for the period from 1961 to 2000. The data are presented in Supplementary data EA-III.2.

III.5. RESULTS

III.5.1. Molecular distributions (CPI, ACL) and concentrations

All samples show *n*-alkane distributions with a clear odd-over-even predominance with CPI values ranging from 1.7 to 8.7 (Table 1 and 2). The average CPI for terrestrial samples is 6.1 ± 1.8 (with highest values in river sediments and Lago di Monticchio; CPI = 19.8), the average for marine samples is 3.9 ± 0.8 . Concentrations of summed *n*-C₂₉ and *n*-C₃₁ alkanes ($\sum n\text{-C}_{29,31}$) of terrestrial sediments (0.03 to 6.7 $\mu\text{g/g}$) are mostly higher and cover a larger range than those of marine sediments (0.1 to 1.4 $\mu\text{g/g}$) (Table 1 and 2). In the terrestrial sediments highest concentrations are associated with high CPI values and near shore terrestrial sediments show concentrations similar to those of the marine sediments at the Italian shelf.

The long chain *n*-alkane abundances are dominated by the *n*-C₂₇, *n*-C₂₉ and *n*-C₃₁ alkanes (Supplementary data EA-III.3). Northern Italian river sediments show maxima at the *n*-C₂₉ alkane, whereas central and southern terrestrial samples are mainly dominated by the *n*-C₃₁ alkane (Fig. III.3a-f). Lake sediments at Lago di Bomba and Lago di Monticchio are dominated by the *n*-C₂₇ alkane (Fig. III.3g-h). In contrast, the Lago Alimini Grande situated in S Italy shows higher ACL dominated by the *n*-C₃₁ alkane. Marine sediments show a tendency to longer chain homologues compared to northern and central Italian terrestrial samples (Fig. III.3i).

This pattern is expressed by an increase with decreasing latitude of ACL and $n\text{-C}_{31}/\sum n\text{-C}_{29,31}$ from 28.3 to 30.1 and 0.3 to 0.6, respectively (Fig. III.4a and b; Lago di Monticchio: ACL = 27.3, $n\text{-C}_{31}/\sum n\text{-C}_{29,31} = 0.1$, since C_{max} is at *n*-C₂₇). The distribution of long chain *n*-alkanes in the marine surface sediments shows a narrow range in ACL (29.3 to 30.1) and $n\text{-C}_{31}/\sum n\text{-C}_{29,31}$ (0.5 to 0.6). These ranges are similar to those in central Italian river and southern coastal samples.

Table III.I Location of terrestrial sediment samples along the Italian N-S transect, CPI, ACL, ratio between $n\text{-C}_{31}$ and $n\text{-C}_{29}$ alkane, concentration of summed $n\text{-C}_{29}$ and $n\text{-C}_{31}$ alkane, stable $\delta^{13}\text{C}$ and δD composition of $n\text{-C}_{29}$ and $n\text{-C}_{31}$ alkane and δD of precipitation

Station	Type	Lat [°N]	Lon [°E]	Altitude [m asl]	CPI ₂₅₋₃₃	ACL ₂₅₋₃₃	$n\text{-C}_{31}/$ $\Sigma n\text{-C}_{29,31}$	c $\Sigma n\text{-C}_{29,31}$ [$\mu\text{g/g}$]	$\delta^{13}\text{C}$ of $n\text{-alkanes}$ [‰ VPDB]						δD of $n\text{-alkanes}$ [‰ VSMOW]						δD precipitation [‰ VSMOW]	
									$n\text{-C}_{29}$	SD	$n\text{-C}_{31}$	SD	WM	$n\text{-C}_{29,31}$	SD	$n\text{-C}_{29}$	SD	$n\text{-C}_{31}$	SD	WM	$n\text{-C}_{29,31}$	SD
M1	Riverine	44.84	12.38	0	7.8	28.9	0.32	3.54	-33.9	0.1	-34.3	0.3	-34.0	0.3	-170	8.0	-165	10.6	-169	13.2	-43	2
M2	Riverine	44.84	12.34	0	8.1	29.0	0.38	5.23	-33.5	0.4	-35.0	0.0	-34.1	0.4	-182	3.3	-175	0.7	-180	3.4	-43	2
M3	Near-coastal	44.82	12.35	0	4.4	29.5	0.49	1.26	-32.2	0.0	-33.7	0.0	-32.9	0.1							-43	2
M5	Riverine	44.55	12.14	2	6.8	28.8	0.32	1.71	-33.0	0.2	-34.5	0.0	-33.5	0.2	-172	0.5	n.a.	n.a.	n.a.	n.a.	-42	2
M8	Riverine	43.87	12.81	25	7.7	28.9	0.36	2.51	-33.1	0.1	-34.9	0.2	-33.7	0.2	-167	1.4	-155	n.a.	-163	1.4	-41	2
M10	Riverine	43.42	13.65	0	7.5	29.0	0.41	1.39	-34.0	0.0	-35.1	0.0	-34.5	0.0	-164	4.7	-158	0.2	-161	4.7	-39	2
M11	Near-coastal	43.41	13.68	0	4.9	28.6	0.44	1.81	-27.7	n.a.	-31.6	n.a.	-29.4	n.a.							-39	2
M13	Riverine	42.65	13.99	15	5.3	29.1	0.47	0.74	-32.8	0.3	-33.5	0.1	-33.1	0.3	-152	0.1	-156	1.1	-154	1.1	-38	2
M14	Lacustrine	42.01	14.36	269	4.6	28.3	0.34	1.18	-31.4	0.1	-33.0	0.0	-31.9	0.1	-156	3.9	-147	n.a.	-153	3.9	-40	2
M15	Near-coastal	42.17	14.71	0	6.5	28.6	0.39	0.69													-36	2
M18	Near-coastal	41.62	15.90	0	5.9	29.2	0.46	4.65	-33.5	n.a.	-33.3	n.a.	-33.4	n.a.	-159	3.7	-154	1.4	-157	3.9	-35	2
M19	Riverine	41.57	15.89	0	8.7	29.7	0.57	6.67	-32.7	0.2	-34.7	0.6	-33.8	0.7	-175	0.2	-162	0.4	-168	0.4	-35	2
M22	Riverine	41.29	16.11	23	6.6	29.4	0.56	3.50	-32.5	0.0	-33.0	0.3	-32.7	0.3							-35	2
M25	Lacustrine	40.20	18.45	0	7.5	30.0	0.56	6.24	-31.6	0.1	-34.5	0.0	-33.2	0.1	-159	2.6	-146	3.1	-152	4.0	-33	3
M 27	Near-coastal	40.03	18.02	0	1.7	29.4	0.52	0.03													-32	3
M 28	Near-coastal	40.24	17.91	0	4.0	30.1	0.57	0.30	-31.5	0.2	-32.1	0.9	-31.8	0.9	-134	2.4	-139	0.6	-137	2.5	-33	3
M30	Lacustrine	40.93	15.60	659	19.8	27.3	0.14	2.39	-31.0	0.0	-35.9	0.0	-31.7	0.1	-170	0.7	n.a.	n.a.	n.a.	n.a.	-43	3

m asl: meters above sea level

δD C₂₉ and C₃₁ are reported as mean values from multiple measurements

WM: weighted mean

SD: standard deviation

AM: annual mean

CI: confidence interval

n.a.: not available

^a data from Online Isotope in Precipitation Calculator (OIPC)

Table III.2 Location of marine sediment samples along the eastern Italian shelf, CPI, ACL, ratio between *n*-C₃₁ and *n*-C₂₉ alkane, concentration of summed *n*-C₂₉ and *n*-C₃₁ alkane, stable δ¹³C and δD composition of *n*-C₂₉ and *n*-C₃₁ alkane (1/2)

Station [GeoB]	Location	Type	Lat [°N]	Lon [°E]	Depth [m bsl]	CPI ₂₅₋₃₃	ACL ₂₅₋₃₃	C ₃₁ / Σ C _{29,31}	c Σ C _{29,31} [μg/g]	δ ¹³ C of <i>n</i> -alkanes [‰ VPDB]						δD of <i>n</i> -alkanes [‰ VSMOW]					
										<i>n</i> -C ₂₉	SD	<i>n</i> -C ₃₁	SD	WM	<i>n</i> -C _{29,31}	SD	<i>n</i> -C ₂₉	SD	<i>n</i> -C ₃₁	SD	WM
10701	G. of Taranto	Marine	40.000	17.467	1186	4.2	29.8	0.54	0.69	-31.5	0.0	-31.2	0.2	-31.3	0.2	-141	0.5	-149	1.1	-145	1.2
10702	G. of Taranto	Marine	40.000	17.586	911	3.4	29.8	0.53	0.85	-31.6	0.2	-31.7	0.1	-31.6	0.3						
10703	G. of Taranto	Marine	40.000	17.742	277	3.1	29.8	0.54	1.04												
10704	G. of Taranto	Marine	40.000	17.833	219	1.9	29.8	0.53	1.18	-30.6	0.6	-30.6	0.5	-30.6	0.8	-129	6.4	-123	n.a.	-126	6.4
10705	G. of Taranto	Marine	39.853	17.913	128	2.8	30.0	0.55	0.42	-30.6	0.0	-31.6	1.0	-31.2	1.0	-150	2.1	-150	0.5	-150	2.1
10706	G. of Taranto	Marine	39.825	17.833	218	3.8	29.8	0.52	0.97	-30.1	0.1	-30.5	0.3	-30.3	0.3	-153	2.1	-155	2.1	-154	3.0
10707	G. of Taranto	Marine	39.783	17.583	1598	3.7	29.6	0.53	0.85							-132	n.a.	-147	n.a.	-140	n.a.
10708	G. of Taranto	Marine	39.808	17.733	686	3.3	29.9	0.55	0.89	-29.7	0.4	-30.2	0.1	-29.9	0.4	-146	0.7	-144	1.3	-145	1.5
10709	G. of Taranto	Marine	39.757	17.893	173	3.9	29.8	0.54	0.71	-30.5	0.6	-30.8	0.7	-30.7	0.9	-152	1.1	-147	0.8	-149	1.3
10710	G. of Taranto	Marine	39.592	17.683	2040	3.8	29.5	0.50	0.67	-31.0	0.1	-31.4	0.2	-31.2	0.2	-140	3.4	-141	6.5	-140	7.3
10711	G. of Taranto	Marine	39.683	17.800	1049	5.9	29.8	0.54	0.39												
10712	G. of Taranto	Marine	39.727	17.862	618	3.5	30.0	0.55	0.36												
10713	G. of Taranto	Marine	39.692	18.283	127	4.3	30.1	0.57	0.34	-29.8	0.1	-30.2	0.2	-30.0	0.2	-153	2.9	-147	1.9	-149	3.5
10714	G. of Taranto	Marine	39.640	18.283	207	4.2	29.9	0.56	0.32												
10715	G. of Taranto	Marine	39.559	18.283	697	5.7	30.1	0.59	0.32	-31.8	0.4	-32.0	0.7	-31.9	0.8						
10716	G. of Taranto	Marine	39.345	18.283	1328	5.9	30.0	0.58	0.33	-32.6	0.3	-31.7	0.3	-32.1	0.5	-128	n.a.	-142	n.a.	-136	n.a.
10717	G. of Taranto	Marine	39.742	18.080	93	3.0	29.7	0.55	0.25	-31.1	0.4	-31.0	0.1	-31.1	0.4	-145	8.4	-144	2.6	-144	8.8
10718	G. of Taranto	Marine	39.693	18.058	220	3.3	30.0	0.54	0.39												
10719	G. of Taranto	Marine	39.653	18.042	616	3.5	29.8	0.55	0.51												
10720	G. of Taranto	Marine	39.507	17.978	1387	4.7	29.6	0.52	0.47	-31.1	0.2	-31.2	0.1	-31.2	0.2	-142	3.8	-154	5.4	-148	6.6
10721	Gargano P.	Marine	42.166	16.767	203	4.1	29.8	0.54	0.26	-31.7	0.3	-31.8	0.0	-31.7	0.3						
10722	Gargano P.	Marine	42.167	16.500	142	3.6	29.9	0.55	0.47												
10723	Gargano P.	Marine	42.167	16.000	114	4.0	29.8	0.54	0.55	-31.8	0.2	-31.2	0.4	-31.4	0.4	-161	2.0	-156	0.7	-159	2.2
10724	Gargano P.	Marine	42.001	16.217	50	4.1	29.6	0.52	0.26	-31.6	0.1	-32.4	0.0	-32.0	0.1						
10725	Gargano P.	Marine	42.000	16.367	98	3.8	29.7	0.53	0.82												
10726	Gargano P.	Marine	42.000	16.717	183	3.9	29.9	0.56	0.12												
10727	Gargano P.	Marine	41.801	16.617	101	3.7	29.9	0.55	0.47							-152	5.3	-152	7.5	-152	9.2
10728	Gargano P.	Marine	41.783	16.858	194	3.9	29.9	0.54	0.06												
10729	Gargano P.	Marine	41.647	17.191	712	4.0	29.9	0.55	0.18	-30.1	0.6	-30.4	0.2	-30.2	0.6						
10730	Gargano P.	Marine	41.500	17.050	183	3.7	29.9	0.55	0.14												
10731	Gargano P.	Marine	41.500	16.658	96	3.3	29.6	0.51	0.74	-29.4	0.5	-31.5	0.3	-30.5	0.6						
10732	Gargano P.	Marine	41.500	16.407	51	3.5	29.5	0.49	1.17												
10733	Gargano P.	Marine	41.500	16.225	23	3.7	29.6	0.51	0.93	-32.0	0.2	-32.8	0.2	-32.4	0.2	-154	2.8	-153	0.4	-154	2.9
10734	Gargano P.	Marine	41.667	16.242	18	3.8	29.4	0.48	0.61	-32.0	0.0	-32.6	0.2	-32.3	0.2	-169	0.1	-163	0.7	-166	0.7
10735	Gargano P.	Marine	41.500	17.308	733	4.0	29.7	0.54	0.60	-31.7	0.8	-32.2	0.4	-32.0	0.9	-138	0.7	-141	1.1	-140	1.3

Table III.2 Location of marine sediment samples along the eastern Italian shelf , CPI, ACL, ratio between n -C₃₁ and n -C₂₉ alkane, concentration of summed n -C₂₉ and n -C₃₁ alkane, stable $\delta^{13}\text{C}$ and δD composition of n -C₂₉ and n -C₃₁ alkane (2/2).

Station [GeoB]	Location	Type	Lat [°N]	Lon [°E]	Depth [m bsl]	CPI ₂₅₋₃₃	ACL ₂₅₋₃₃	C ₃₁ / Σ C _{29,31}	c Σ C _{29,31} [μg/g]	$\delta^{13}\text{C}$ of n -alkanes [‰ VPDB]						δD of n -alkanes [‰ VSMOW]					
										n -C ₂₉	SD	n -C ₃₁	SD	WM n -C _{29,31}	SD	n -C ₂₉	SD	n -C ₃₁	SD	WM n -C _{29,31}	SD
10736	Strait of Otranto	Marine	40.758	18.192	123	5.4	29.8	0.55	0.80	-31.2	0.4	-31.6	0.0	-31.5	0.4	-158	2.4	-156	1.3	-157	2.7
10737	Strait of Otranto	Marine	40.625	18.329	113	5.1	29.9	0.58	0.81												
10738	Strait of Otranto	Marine	40.546	18.467	112	4.6	29.5	0.55	1.39												
10739	Strait of Otranto	Marine	40.500	18.642	565	4.5	29.8	0.55	0.54	-30.8	0.1	-31.1	0.1	-31.0	0.1	-156	2.0	-159	3.5	-158	4.0
10740	Strait of Otranto	Marine	40.392	18.583	128	4.4	29.6	0.51	0.26												
10741	Strait of Otranto	Marine	40.233	18.667	287	3.7	29.5	0.51	0.83	-31.3	0.2	-32.2	0.3	-31.7	0.3	-157	4.3	-154	1.5	-155	4.6
10742	Strait of Otranto	Marine	39.716	18.776	599	3.8	29.8	0.54	0.42	-31.5	0.4	-32.0	0.1	-31.8	0.4	-144	0.9	-141	0.3	-142	0.9
10743	Strait of Otranto	Marine	39.825	18.642	124	3.0	29.6	0.53	0.76												
10744	Strait of Otranto	Marine	39.850	18.600	117	4.9	29.7	0.50	1.07	-30.3	0.2	-30.6	0.1	-30.4	0.2	-152	2.0	-152	1.4	-152	2.4
10746	W G. of Taranto	Marine	39.908	16.758	157	2.6	29.3	0.53	0.68	-30.2	1.3	-30.6	1.3	-30.4	1.9	-138	4.8	-138	3.3	-138	5.9
10747	W G. of Taranto	Marine	39.725	16.975	246	3.3	29.6	0.53	0.62												
10748	W G. of Taranto	Marine	39.667	17.050	288	3.6	29.5	0.52	0.73												
10749	W G. of Taranto	Marine	39.600	17.183	278	4.1	29.6	0.52	0.73	-30.7	0.3	-31.8	0.2	-31.3	0.4	-138	0.1	-140	2.9	-139	2.9

m bsl: meters below sea level

δD C₂₉ and C₃₁ are reported as mean values from multiple measurements

WM: weighted mean

SD: standard deviation

n.a.: not available

III.5.2. $\delta^{13}\text{C}$ of plant wax *n*-alkanes

In the terrestrial samples the carbon isotopic composition for the *n*-C₂₉ alkane ranges from -33.9‰ to -27.7‰ and for the *n*-C₃₁ alkane from -35.9‰ to -31.6‰ (sample M30) (Table 1). Weighted mean values of both *n*-alkanes (WM $\delta^{13}\text{C}$ *n*-C_{29, 31}) vary between -34.5‰ and -29.4‰ and show a slight increase from N to S Italy for samples of riverine origin, although the correlation is poor, as well as more enriched values in near coastal sample M28 (Fig. III.4c). For the marine samples the $\delta^{13}\text{C}$ of the *n*-C₂₉ alkane ranges from -32.6‰ to -29.4‰ and for the *n*-C₃₁ alkanes from -32.8‰ to -30.2‰ (Table 2). Here, the WM $\delta^{13}\text{C}$ *n*-C_{29, 31} varies between -32.4‰ and -29.9‰.

III.5.3. δD of plant wax *n*-alkanes

The δD of the *n*-C₂₉ alkane in terrestrial samples varies between -182‰ and -134‰, that for the *n*-C₃₁ alkane between -175‰ and -139‰, which results in weighted mean values (WM δD *n*-C_{29, 31}) from -180‰ to -137‰ (Table 1). From N to S Italy δD values become more positive (Fig. III.4d and III.5e). The lowest WM δD *n*-C_{29, 31} value is from the northern Po area (-180‰), whereas the southernmost terrestrial sample M28 shows a value of -137‰. The maximum range including all terrestrial samples is ~40‰ from 45 °N to 40 °N

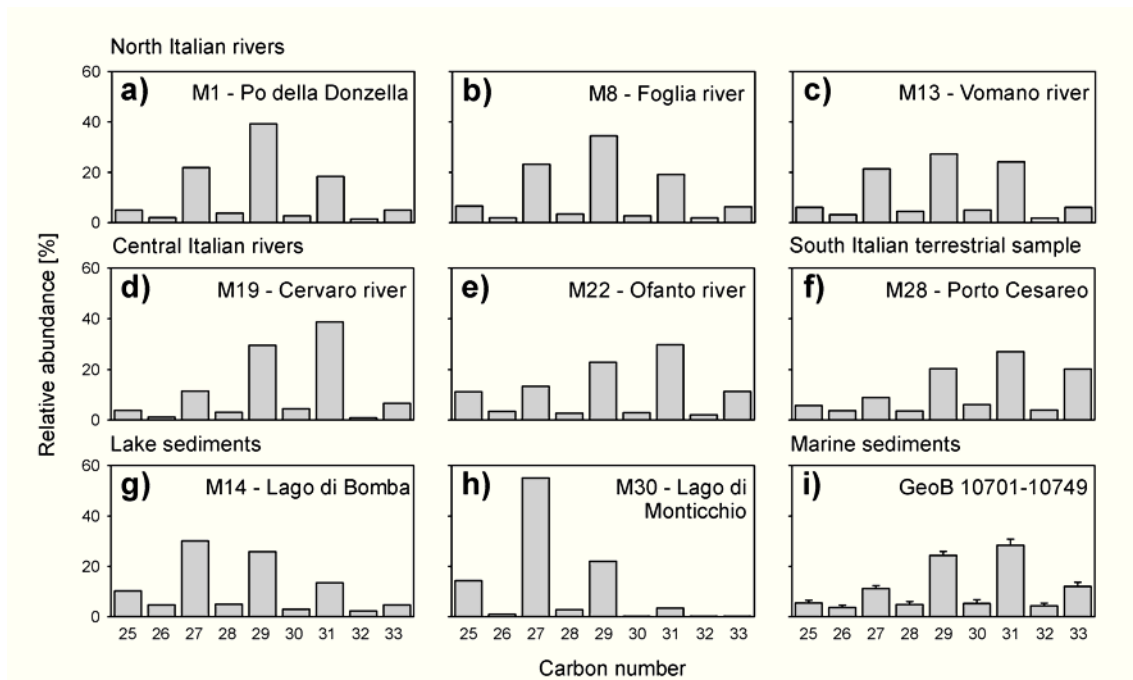


Figure III.3. Representative molecular distribution of long chain *n*-alkanes in northern and central Italian rivers (a-e), southern Italian terrestrial samples (f), lake (g-h) and marine (i) sediments along the southern Italian shelf. Error bars in (i) give standard deviation of relative *n*-alkane abundance in all marine sediment samples.

($y = -0.12x + 24.1$; $R^2 = 0.62$), resulting in a trend of about $-8\text{‰} / \text{°Latitude}$. The δD of marine samples varies between -169‰ to -128‰ for the $n\text{-C}_{29}$ alkane and between -163‰ to -123‰ for the $n\text{-C}_{31}$ alkane (Table 2). The WM $\delta\text{D } n\text{-C}_{29,31}$ varies from -166‰ to -126‰ and is more positive than the N Italian terrestrial samples (Fig. III.4d). A linear relationship between $\delta^{13}\text{C}$ vs. δD has been found for plant waxes in terrestrial and marine sediments albeit with a considerable scatter (Fig. III.6).

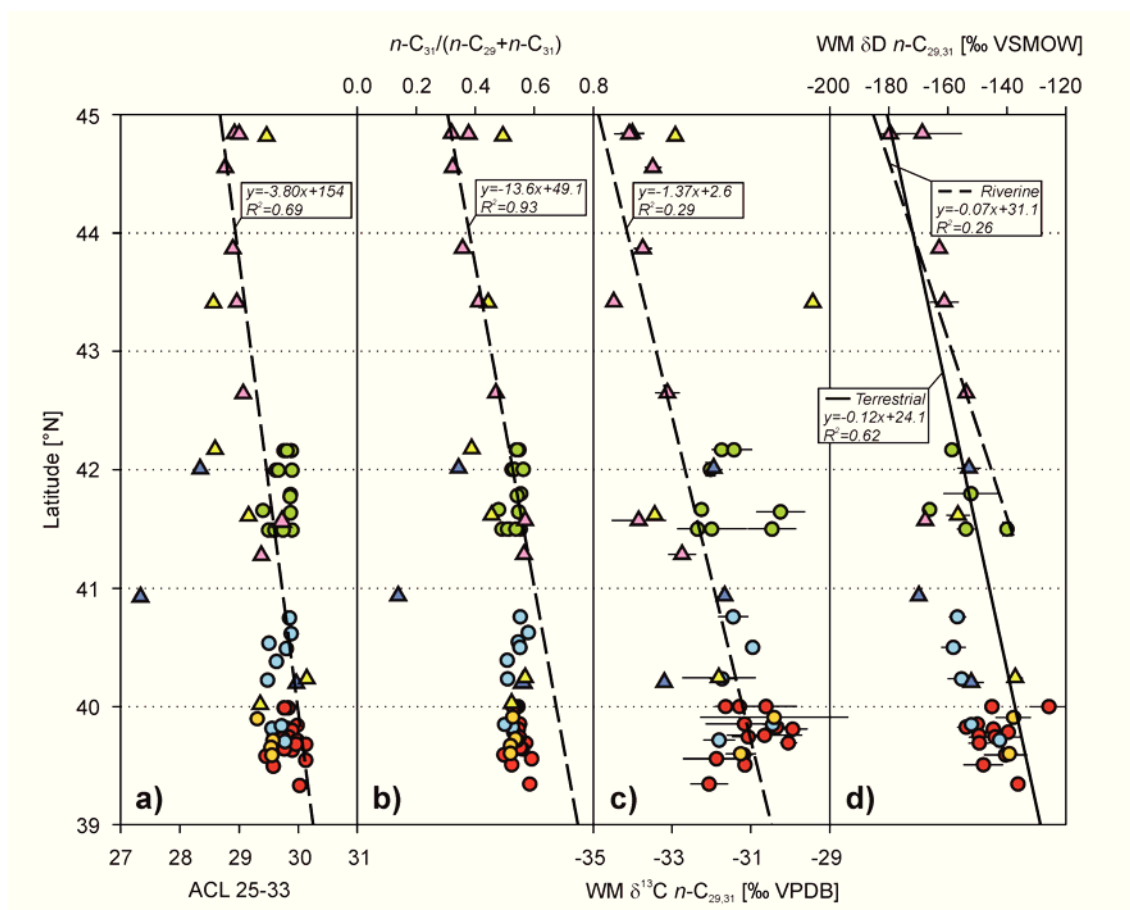


Figure III.4. Variation of (a) Average Chain Length (ACL₂₅₋₃₃), (b) ratio between the $n\text{-C}_{31}$ and $n\text{-C}_{29}$ alkane, (c) weighted mean carbon isotopic composition of the $n\text{-C}_{29}$ and $n\text{-C}_{31}$ alkane (WM $\delta^{13}\text{C } n\text{-C}_{29,31}$), (d) weighted mean hydrogen isotopic composition of the $n\text{-C}_{29}$ and $n\text{-C}_{31}$ alkane (WM $\delta\text{D } n\text{-C}_{29,31}$) in terrestrial (triangles) and marine (circles) sediment samples along the Italian N-S transect (see Fig. III.2 for color code). Dashed lines in (a-d) give regressions and corresponding R^2 values including only river samples. Solid line in (d) gives regression and corresponding R^2 value including all terrestrial samples. Error bars indicate standard deviation of WM $\delta^{13}\text{C } n\text{-C}_{29,31}$ and $\delta\text{D } n\text{-C}_{29,31}$.

III.6. DISCUSSION

III.6.1. Control on the molecular distribution of plant waxes

High CPI values and ACL distributions dominated by the $n\text{-C}_{27}$, $n\text{-C}_{29}$ and $n\text{-C}_{31}$ alkanes indicate a higher plant origin (Bray and Evans, 1961; Eglington and Hamilton, 1963; Simoneit, 1984). The distribution of n -alkanes in the terrestrial samples shows a trend to

longer chain homologues from N to S Italy, with the *n*-C₃₁ alkane as the dominant one in southern samples (Table 1, Fig. III.4a and b). Changes in ACL in dust samples from the Pacific and Atlantic Ocean and sediments have been attributed to temperature and aridity variations at the source regions (Simoneit, 1977; Gagosian et al., 1981; Gagosian et al., 1987; Poynter et al., 1989). Biosynthesis of long-chain plant waxes in response to higher ambient temperature is thought to prevent water loss during respiration and to maintain the hardness of the waxes (e.g., Kozłowski and Pallardy, 1997; Kawamura et al., 2003). ACL in dust samples off NW Africa decrease in front of the tropical rain forest, suggesting that plant waxes regulate the plants moisture balance. This is influenced by the precipitation regime rather than temperature (Schefuß et al., 2003a). Furthermore, the occurrence of longer chained *n*-alkanes has been attributed to increased contributions from C₄ vegetation (Rommerskirchen et al., 2006a; Vogts et al., 2009). However, the increase in ACL is also found in broadleaf trees from temperate to tropical environments and deciduous tree leaves along a N-S transect in Europe (Kawamura et al., 2003; Sachse et al., 2006). The shift in ACL co-occurs with a MAT increase of 4°C (13.1 °C to 17.5 °C) along the coastal N-S transect, while precipitation shows no significant trend (Fig. 5 a, b). Additionally, RH decreases from the N Italian Po River to the Taranto area (Fig. III.5c). Therefore, we propose that the ACL increase is controlled by higher temperature/aridity and associated changes in vegetation in S Italy.

The dominance of the *n*-C₂₇ alkane in lake sediments from Lago di Bomba (M14) and Lago di Monticchio (M30) has also been found for other sediments of Italian lakes that are surrounded by deciduous trees (Sachse et al., 2006). The *n*-alkane distribution in leaves of the tree *Fagus sylvatica* as the dominant species (ACL 26.9; CPI 26.7) agrees well with that of the lake sediments at Lago di Monticchio, which is not surprising since *Fagus sylvatica* is the dominant tree species in the catchment area of the lake (Sachse et al., 2004). At Lago di Monticchio the CPI of 19.8 and ACL of 27.3 suggest a similar tree leaf source for our samples and that ACL in the lake is influenced by vegetation due to the restricted catchment areas of the lake. However, *n*-alkanes in lake sediments can integrate over diverse sources and dominance of the *n*-C₂₇ alkane has been documented for other trees, shrubs and emergent water plants (Rieley et al., 1991; Ficken et al., 2000), which limit the use of distributions as a paleoenvironmental tool for vegetation types. Multiple sources for the *n*-C₂₇ alkane may play a role at the Lago di Bomba sampling site, since here large beech stands are absent and the artificial lake holds a larger catchment area including the high altitude hinterland. Different surrounding vegetation dominated by reeds, i.e. *Phragmites australis*, may have resulted in the higher ACL at Lago Alimini Grande. Alternatively, this may be interpreted as an

environmental change from the high altitude lakes Lago di Bomba and Lago di Monticchio, experiencing higher precipitation rates and lower temperatures, to the lake at lower altitudes (Fig. III.1a and b), which is in line with the overall southward increase in ACL.

III.6.2. Control on $\delta^{13}\text{C}$ of plant waxes

An important factor influencing the $\delta^{13}\text{C}$ of plants is the photosynthetic pathway. For this reason the $\delta^{13}\text{C}$ of *n*-alkanes has been used to calculate the relative contribution from C_4 and C_3 plants (Huang et al., 2000; Rommerskirchen et al., 2003; Schefuß et al., 2004; Vogts et al., 2009). For our dataset, the same calculation based on averaged endmember values for C_3 and C_4 plants from the literature, i.e. -36‰ for C_3 and -21.5‰ for C_4 plants (Rieley et al., 1993; Collister et al., 1994), and using WM $\delta^{13}\text{C}$ *n*- $\text{C}_{29, 31}$ values would lead to an average C_4 plant contribution of 21% for our terrestrial sample set and 33% for marine sediments (related to more enriched $\delta^{13}\text{C}$ values). This is highly unrealistic since C_4 plants make up to 1.5% of the total flora of Italy and C_4 vegetation is absent at the sampling sites (Collins and Jones, 1985; Woodward et al., 2004). Italy with its typical Mediterranean vegetation is mainly dominated by forests and shrubland accounting for approximately 40% of the ecosystem types, while 56% are covered by cropland or crops with natural vegetation mosaics (World Resources Institute, 2007), which complicates the association to specific vegetation types. Major crop areas growing C_4 plants (e.g., maize) can be found in N Italy, whereas fruits, olive trees and wine dominates the coastal areas of central and S Italy (Maricchiolo et al., 2005; Todorovic et al., 2007; European Environmental Agency (EEA), 2010). As a consequence we would expect that C_4 plants play only a significant role in N Italy, which cannot explain the observed $\delta^{13}\text{C}$ trend (Fig. III.4.).

The $\delta^{13}\text{C}$ in C_3 plants has been used to estimate the water use efficiency, as ^{13}C is enriched due to lower stomatal conductance for CO_2 in response to water stress (Farquhar and Sharkey, 1982). A similar mechanism has been suggested to explain enrichments of plant waxes of 3-4‰ in gymnosperms compared to angiosperms (Chikaraishi & Naraoka, 2003; Pedentchouk et al., 2008). The southward increase in $\delta^{13}\text{C}_{\text{plant-wax}}$ may thus reflect intensified drought, which is supported by the above described increase in MAT and ACL. However, the correlation of $\delta^{13}\text{C}_{\text{plant-wax}}$ with latitude is poor, possibly reflecting the shift in natural vegetation, which changes along the N-S transect from mesophytic and mixed forests to Mediterranean sclerophyllous forest and scrubs (Bohn et al., 2004). As the vegetation pattern is also controlled by the environmental conditions, it is hard to separate the mechanisms controlling $\delta^{13}\text{C}$.

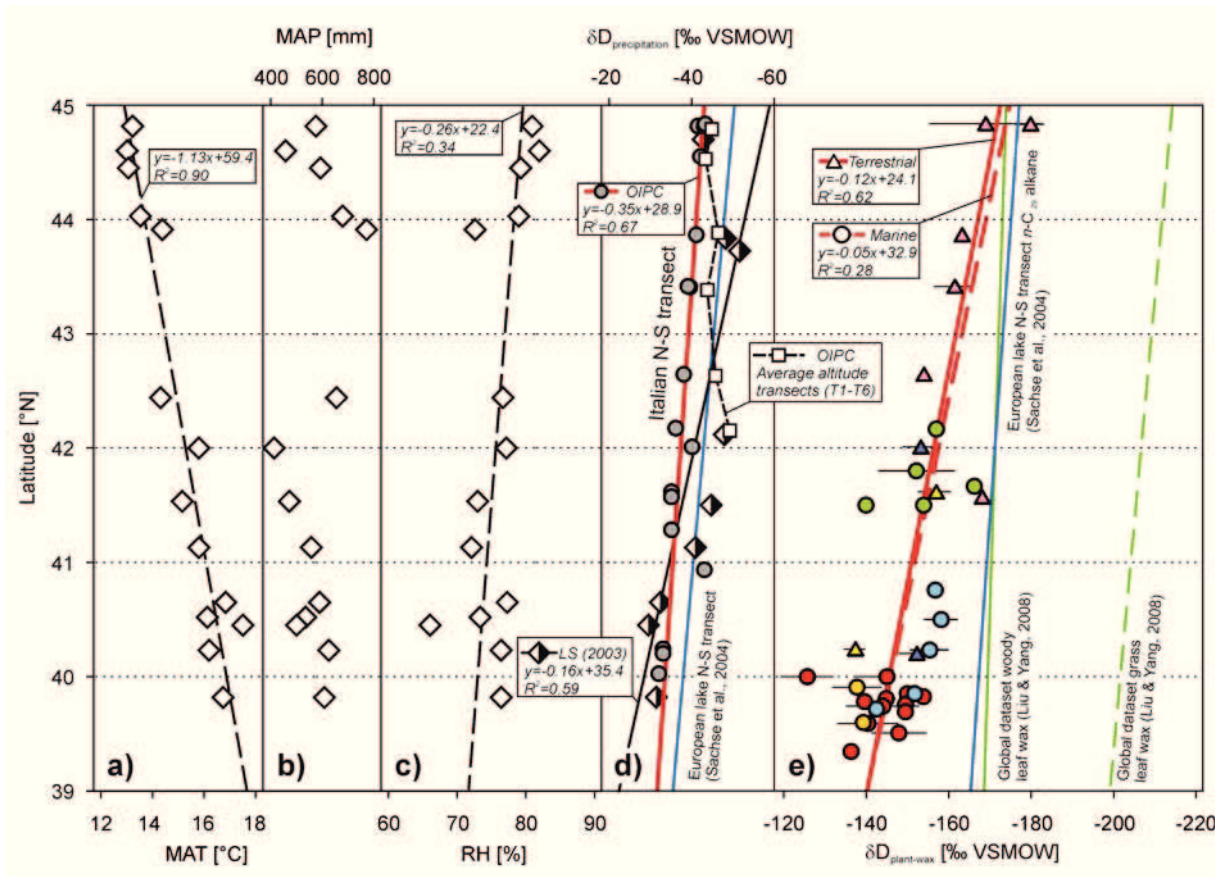


Figure III.5. Variation of environmental and plant wax data along the N-S Italian transect. Environmental data includes (a) mean annual temperature (MAT), (b) mean annual precipitation (MAP) and (c) relative humidity (RH) averaged for the period from 1961-2000 (see Supplementary data EA-2); regression lines are represented by dashed lines. δD values of (d) annual precipitation at terrestrial sample sites (grey filled circles and red solid line) and averaged precipitation along altitudinal transect of Po River and Apennine river catchments (open squares and dashed line) derive from the Online Isotope in Precipitation Calculator (OIPC). Annual δD precipitation values are reported from near-by meteorological stations based on IAEA-GNIP and Longinelli and Selmo (LS), (2003) (diamonds and black solid line); the regression line of the δD of meteoric water from a European lake transect is given as blue solid line (Sachse et al., 2004). δD of (e) plant wax *n*-alkanes in terrestrial and marine sediments in this study are indicated by colored triangles and circles, respectively (see Fig. III.1. for color code); regression lines for terrestrial and marine WM δD n -C_{29,31} are shown by thick red solid and dashed lines; error bars indicate standard deviation of WM δD n -C_{29,31}; regression line of the n -C₂₉ alkane from a European lake transect is given as blue solid line (Sachse et al., 2004); regressions of woody plants and grass leaf waxes from a global dataset are represented by green solid and dashed lines (Liu & Yang, 2008). Note that the δD axis is reverse.

III.6.3. Control on δD of plant waxes

In general, in the terrestrial transect we observe an increase in both $\delta D_{\text{plant-wax}}$ and $\delta D_{\text{precipitation}}$ estimates with decreasing latitude (Fig. III.5d and e) (Longinelli and Selmo, 2003, Bowen, 2011). This suggests that the $\delta D_{\text{precipitation}}$ plays a dominant role in controlling the $\delta D_{\text{plant-wax}}$ along the transect, as shown for sedimentary and plant leaf waxes in regional (Sachse et al., 2004, 2006; Smith and Freeman, 2006; Hou et al., 2008; Rao et al., 2009) and global scale studies (Liu & Yang, 2008). The latitudinal D enrichments of precipitation from 45°N to 40°N based on OIPC is 15‰ and that based on water samples is 30‰ compared to $\delta D_{\text{plant-wax}}$

of 40‰. The differences can be attributed to the fact that the sample set based on measured values also includes stations situated at higher altitudes experiencing more depleted precipitation (Fig. III.2, Supplementary data EA-1) and excluding those samples results in a lower enrichment more comparable to the OIPC data. The $\delta D_{\text{precipitation}}$ based on OIPC can only account for 40% of the observed D enrichment of plant waxes, indicating that additional factors influence the isotopic composition.

This may derive from more D-depleted plant waxes in the northern part of the transect, since here the Po River and Apennine rivers potentially carry plant-waxes from higher elevations. Therefore, the altitudinal averaged $\delta D_{\text{precipitation}}$ for the catchment areas may reveal potential contributions. However, the data shows no increase along the N-S transect, due to the more D-depleted values from the Apennine mountains compared to the Po River region. Additionally, averaged $\delta D_{\text{precipitation}}$ for the Po River catchment do not differ significantly from values at the sample location. Hence, a contribution from plant waxes that derive from higher elevations in N Italy is unlikely. The OIPC based $\delta D_{\text{precipitation}}$ along the Italian N-S (our sites) and an European N-S lake transect (Sachse et al., 2004) are offset, which is mainly due to the fact that the lakes sampled for *n*-alkanes occur at higher altitudes than the stations in our study and thus experience more depleted precipitation (Fig. III.5d). Higher elevation also explains the lower $\delta D_{\text{plant-wax}}$ at Lago di Monticchio (sample M30) compared to near coastal samples at the same latitude. For this lake we report $\delta D_{\text{plant-wax}}$ values similar to Sachse et al. (2004). While the offset between $\delta D_{\text{plant-wax}}$ and $\delta D_{\text{precipitation}}$ stays nearly constant along the European lake transect, we observe that $\delta D_{\text{plant-wax}}$ shows a stronger increase to the south (Fig. III.5e). Therefore, further south and at the coastal sites the influence of the Mediterranean climate seems to dominate.

The comparison to global northern hemispheric variations in $\delta D_{\text{plant-wax}}$ of woody and grass leaf waxes (Liu and Yang, 2008) shows that the observed δD values are closer to that of woody plants and that vegetation shifts between both plant life forms are insufficient to explain the observed amplitude in δD (Fig. III.5e). Additionally, the $\delta^{13}\text{C}$ - δD relationship of plant waxes along the transect compared to data from regional studies on different plant leaves and soil types shows that the Italian terrestrial samples correspond to that of C_3 plant leaves in line with being the dominant *n*-alkane source (Fig. III.6a).

Relative humidity along the N-S transect ranges between of 65 to 80% (Fig. III.5c). The seasonal distribution of precipitation showing peaks during April-June and October-November in N Italy and only one pronounced peak during autumn in Central and S Italy leads to an extension of the dry period increasing soil moisture depletion in the south (Salvati

et al., 2008). This is also indicated by semi-arid and dry conditions in southern Italy (Racioppi and Simeone, 2003; Salvati, 2009; Salvati and Bajocco, 2011). Additionally, regional estimates of evapotranspiration in Italy show for N Italy slightly more than 50% of the precipitation is evapotranspired. In contrast, maximum values of 75% are observed at the Apulian Peninsula (Portoghese et al., 2005; Venezian Scarascia et al., 2006). Relative humidity can influence $\delta D_{\text{plant-wax}}$ via soil-evaporation and/or transpiration rather than evaporative enrichment of leaf water (Liu & Huang, 2005; Smith & Freeman, 2006; Hou et al., 2008; McInerney et al., 2011). Additionally, the evapotranspiration of leaf water is considered to be of major importance to δD isotope values in arid climate ecosystems, but a strong change is not found across aridity/temperature gradients (Feakins and Sessions, 2010). We propose that enhanced soil-evaporation and/or evapotranspiration explain the stronger increase of $\delta D_{\text{plant-wax}}$ compared to $\delta D_{\text{precipitation}}$ along the N-S transect.

III.6.4. Origin of plant waxes along the Italian shelf

Plant waxes from N Africa and waxes transported by the south-easterly Sirocco winds could also affect the δD and $\delta^{13}C$ in southern Italian sediments. Unfortunately, we have no information on plant wax content of Saharan dust reaching the Italian peninsula. However, Saharan dust has a characteristic clay and trace metal signature. On the basis of this signature it has been inferred that the African dust contributions to the southern Adriatic Sea ranges between 2-5% compared to the river input into the Adriatic basin (e.g., Correggiari et al., 1989; Tomadin, 2000) so that already on this basis a significant influence of African dust-derived waxes on our *n*-alkane proxies is unlikely.

Po and Apennine river sediments show higher concentrations in plant waxes than the rivers south of the Gargano Promontory so that in the Adriatic Sea the sedimentary *n*-alkane signal may be biased towards northern values due to southward transport. This is in agreement with higher sediment loads related to larger catchment areas in the North, which makes these rivers the main sediment source for the Adriatic Sea (Cattaneo et al., 2003; Frignani et al., 2005). The lower concentrations of long chain *n*-alkanes in marine sediments may reflect a generally low supply from the northern and central Adriatic shelf areas whereas the narrow range of marine ACL values suggest a well-mixed signal from diverse source areas. Nevertheless, the marine ACL values are mostly higher than those from the Po and Apennine rivers suggesting a source from warmer and more arid regions in Italy.

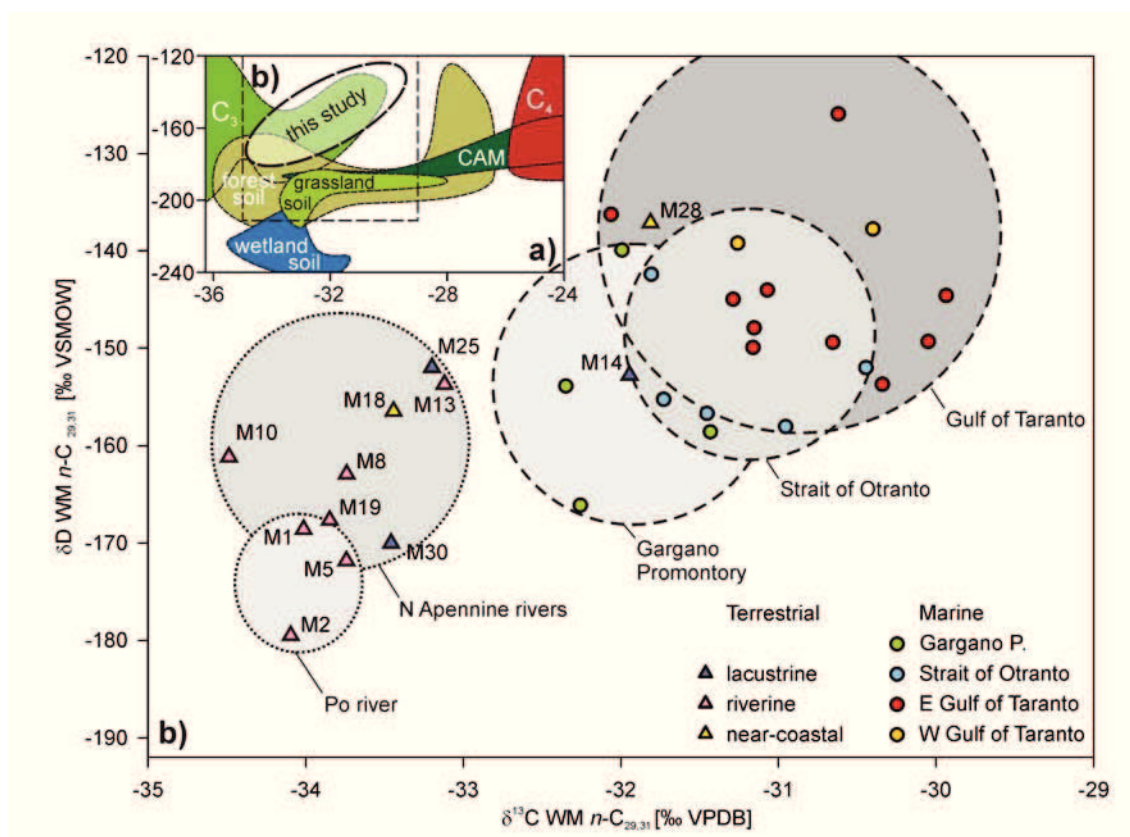


Figure III.6. Plot between $\delta^{13}\text{C}$ and δD of plant wax n -alkanes shown as weighted mean values of $n\text{-C}_{29}$ and $n\text{-C}_{31}$ alkanes. (a) Range of mean values of $n\text{-C}_{29}$ and $n\text{-C}_{31}$ alkanes in this study indicated by thick dashed curve compared to the range of mean values of $n\text{-C}_{29}$ and $n\text{-C}_{31}$ alkanes in leaves and soils from the literature (C_3 and C_4 leaves: Bi et al., 2005; Chikaraishi & Naraoka, 2003; Krull et al., 2006. CAM leaves: Bi et al., 2005; Chikaraishi & Naraoka, 2003. Forest soil: Seki et al., 2010; Krull et al., 2006; Rao et al., 2009. Grassland soil: Rao et al., 2009; Krull et al., 2006. Wetland soil: Seki et al., 2010). (b) Zoom-in plot of weighted mean values of $n\text{-C}_{29}$ and $n\text{-C}_{31}$ alkanes of terrestrial and marine samples in this study with indicated geographical separation represented by dotted and dashed circles. Triangles indicate terrestrial samples according to their origin type (δD values of samples M5 and M30 are only available for the $n\text{-C}_{29}$ alkane). Colored circles indicate marine samples along the southern Italian shelf.

The combined use of compound-specific $\delta^{13}\text{C}$ vs. δD shows clearly the differences between plant waxes at the northern/central Italian rivers and the Italian shelf (Fig. III.6). In detail, the gradual shift to more positive isotope values persists in the marine sediments from the southern Adriatic Sea to the Gulf of Taranto. Several explanations for relationships between the $\delta^{13}\text{C}$ and δD of plant waxes have been proposed. In plant leaves, major differences are observed between C_3 and C_4 plants mainly based on the $\delta^{13}\text{C}$ rather than δD (Chikaraishi and Naraoka, 2003). Though, C_4 grasses have been found to be more D-depleted compared to C_3 grasses (Smith and Freeman, 2006). No obvious relation is observed in C_3 plants except for a positive relation between $\delta^{13}\text{C}$ and δD in trees (Bi et al., 2005). The same study showed a strong inverse correlation in C_4 plants. Inverse correlations between $\delta^{13}\text{C}$ and δD are assumed to reflect differences in water use strategies of trees experiencing the same water source and environmental conditions, with more positive $\delta^{13}\text{C}$ (and more negative δD) indicative of

higher water use efficiencies (Hou et al., 2007a). The effect of higher water use efficiency is also proposed for gymnosperms compared to angiosperms showing higher $\delta^{13}\text{C}$ and lower δD in a semi-desert environment (Pedentchouk et al., 2008).

The northern and central river samples are isotopically more similar to the marine samples at the Gargano Promontory than to the marine samples from the Gulf of Taranto. As a consequence, the progressive relationship of $\delta^{13}\text{C}$ and δD in combination with increasing ACL values as well as the ratio between the *n*-C₃₁ and *n*-C₂₉ alkanes, suggests a restricted delivery of plant waxes from the northern Adriatic Sea to southern Adriatic sediments. This is also supported by the use of the BIT-Index, an organic geochemical proxy for fluvial soil input to the ocean (Hopmans et al., 2004), and its application to the same marine sample set at the southern Italian shelf (Leider et al., 2010). Maximum BIT values of ~0.3 reported at the near coastal sites at the Gargano Promontory are related to the influence of the WAC system and/or local river inputs, whereas the remaining marine samples show low BIT values. Marine samples with highest BIT values yield the lowest $\delta\text{D}_{\text{plant-wax}}$ values, suggesting that the fluvial input controls the distribution of both soil and plant waxes at the Gargano Promontory. In contrast, transport of sediment and plant waxes by the southward moving WAC does not seem to impact the Gulf of Taranto area. Consequently, plant waxes in the southernmost shelf sediments derive from a local southern Italian source. The exclusion of plant-wax supply from additional source regions allows a subsequent reconstruction of paleohydrological changes in the Central Mediterranean.

III.7. CONCLUSIONS

Long chained *n*-alkanes show a shift to more positive $\delta\text{D}_{\text{plant-wax}}$ values and higher ACL values along the terrestrial N-S transect in agreement with a D enrichment of precipitation and increases in mean annual air temperature, respectively. Since, C₄ plants constitute an insignificant part of the Italian vegetation the $\delta^{13}\text{C}_{\text{plant-wax}}$ and ACL data have been interpreted in terms of C₃ vegetation changes and physiological adaptation along the altitudinal and latitudinal environmental gradients in Italy. So far, the stronger D enrichment observed in plant waxes compared to precipitation implies an additional factor, than variations in $\delta\text{D}_{\text{precipitation}}$, explainable by enhanced soil water evaporation and/or leaf water evapotranspiration. These changes are interpreted to reflect the southward increase in aridity in Italy and thus provide a proxy for the Mediterranean P-E balance.

III.8. ACKNOWLEDGEMENTS

We thank M. Elvert, X. Prieto-Mollar and J. Wendt for lab assistance during stable isotope analysis. Many thanks go to the scientific party of RV POSEIDON 'CAPPUCCINO' cruise and the land survey team for sample collection. The members of MOCCHA (Multidisciplinary study of continental/ocean climate dynamics using high-resolution records from the eastern Mediterranean) are thanked for contributions at early stages of this study. This work was supported by the Deutsche Forschungsgemeinschaft under the EUROCORES Programme EuroMARC project MOCCHA, through contract No. ERAS-CT-2003-980409 of the European Commission, DG Research, FP6. Additional support was provided by the Bremen International Graduate School for Marine Sciences "Global Change in the Marine Realm" (GLOMAR).

III.9. REFERENCES

- Artegiani, A., Paschini, E., Russo, A., Bregant, D., Raicich, F., and Pinardi, N., 1997a. The Adriatic Sea general circulation. Part I: Air-sea interactions and water mass structure. *J. Phys. Oceanogr.* 27, 1492-1514.
- Artegiani, A., Paschini, E., Russo, A., Bregant, D., Raicich, F., and Pinardi, N., 1997b. The Adriatic Sea general circulation. Part II: baroclinic circulation structure. *J. Phys. Oceanogr.* 27, 1515-1532.
- Bi, X., Sheng, G., Liu, X., Li, C., and Fu, J., 2005. Molecular and carbon and hydrogen isotopic composition of n-alkanes in plant leaf waxes. *Org. Geochem.* 36, 1405-1417.
- Bird, M. I., Summons, R. E., Gagan, M. K., Roksandic, Z., Dowling, L., Head, J., Keith Fifield, L., Cresswell, R. G., and Johnson, D. P., 1995. Terrestrial vegetation change inferred from n-alkane $\delta^{13}\text{C}$ analysis in the marine environment. *Geochim. Cosmochim. Acta* 59, 2853-2857.
- Bohn, U., Neuhäusl, R., Gollub, G., Hettwer, C., Neuhäuslová, Z., Raus, T., Schlüter, H., and Weber, H., 2004. Map of the Natural Vegetation of Europe. 1: 2 500 000. Bundesamt für Naturschutz (BfN), Bonn, Germany.
- Boot, C. S., Ettwein, V. J., Maslin, M. A., Weyhenmeyer, C. E., and Pancost, R. D., 2006. A 35,000 year record of terrigenous and marine lipids in Amazon Fan sediments. *Org. Geochem.* 37, 208-219.
- Boukthir, M. and Barnier, B., 2000. Seasonal and inter-annual variations in the surface freshwater flux in the Mediterranean Sea from the ECMWF re-analysis project. *J. Mar. Syst.* 24, 343-354.

- Bowen, G. J., 2011. The Online Isotopes in Precipitation Calculator, version 2.2. <http://www.waterisotopes.org>.
- Bowen, G. J. and Revenaugh, J., 2003. Interpolating the isotopic composition of modern meteoric precipitation. *Water Resour. Res.* 39, 1299. doi:10.1029/2003WR002086.
- Bray, E. E. and Evans, E. D., 1961. Distribution of *n*-paraffins as a clue to recognition of source beds. *Geochim. Cosmochim. Acta* 22, 2-15.
- Burgoyne, T. W. and Hayes, J. M., 1998. Quantitative Production of H₂ by Pyrolysis of Gas Chromatographic Effluents. *Anal. Chem.* 70, 5136-5141.
- Camuffo, D., Bertolin, C., Barriendos, M., Dominguez-Castro, F., Cocheo, C., Enzi, S., Sghedoni, M., della Valle, A., Garnier, E., Alcoforado, M. J., Xoplaki, E., Luterbacher, J., Diodato, N., Maugeri, M., Nunes, M., and Rodriguez, R., 2010. 500-year temperature reconstruction in the Mediterranean Basin by means of documentary data and instrumental observations. *Clim. Change* 101, 169-199.
- Cattaneo, A., Correggiari, A., Langone, L., and Trincardi, F., 2003. The late-Holocene Gargano subaqueous delta, Adriatic shelf: Sediment pathways and supply fluctuations. *Mar. Geol.* 193, 61-91.
- Cerling, T. E., Harris, J. M., MacFadden, B. J., Leakey, M. G., Quade, J., Eisenmann, V., and Ehleringer, J. R., 1997. Global vegetation change through the Miocene/Pliocene boundary. *Nature* 389, 153-158.
- Chikaraishi, Y. and Naraoka, H., 2003. Compound-specific δD - $\delta^{13}C$ analyses of *n*-alkanes extracted from terrestrial and aquatic plants. *Phytochemistry* 63, 361-371.
- Cini Castagnoli, G., Bonino, G., Della Monica, P., Taricco, C., and Bernasconi, S. M., 1999. Solar activity in the last millennium recorded in the $\delta^{18}O$ profile of planktonic foraminifera of a shallow water Ionian Sea core. *Sol. Phys.* 188, 191-202.
- Collins, R. P. and Jones, M. B., 1985. The influence of climatic factors on the distribution of C₄ species in Europe. *Plant Ecol.* 64, 121-129.
- Collister, J. W., Rieley, G., Stern, B., Eglinton, G., and Fry, B., 1994. Compound-specific $\delta^{13}C$ analyses of leaf lipids from plants with differing carbon dioxide metabolisms. *Org. Geochem.* 21, 619-627.
- Colombo, J. C., Cappelletti, N., Laschi, J., Migoya, M. C., Speranza, E., and Skorupka, C. N., 2005. Sources, Vertical Fluxes, and Accumulation of Aliphatic Hydrocarbons in Coastal Sediments of the Río de la Plata Estuary, Argentina. *Environ. Sci. Tech.* 39, 8227-8234.
- Correggiari, A., Guerzoni, S., Lenaz, R., Quarantotto, G., and Rampazzo, G., 1989. Dust deposition in the central Mediterranean, Tyrrhenian and Adriatic Seas.: Relationships with marine sediments and riverine input. *Terra Nova* 1, 549-558.
- Craig, H., 1961. Isotopic Variations in Meteoric Waters. *Science* 133, 1702-1703.
- Cranwell, P. A., 1973. Chain-length distribution of *n*-alkanes from lake sediments in relation to post-glacial environmental change. *Freshwater Biol.* 3, 259-265.

- Desiato, F., Lena, F., Baffo, F., Suatoni, B., and Toreti, A., 2005. Indicatori del CLIMA in Italia - elaborati attraverso il sistema SCIA. APAT - Agenzia per la Protezione dell'Ambiente e per i servizi Tecnici, Rome.
- Eglinton, G. and Hamilton, R. J., 1963.. The distribution of alkanes. In: Chemical plant taxonomy (Ed. Swain, T.). Academic Press. pp. 187-217.
- Eglinton, G. and Hamilton, R. J., 1967) Leaf Epicuticular Waxes. *Science* 156, 1322-1335.
- Eglinton, T. I. and Eglinton, G., 2008. Molecular proxies for paleoclimatology. *Earth Planet. Sci. Lett.* 275, 1-16.
- Ehleringer, J. R., Cerling, T. E., and Helliker, B. R., 1997. C 4 photosynthesis, atmospheric CO 2, and climate. *Oecologia* 112, 285-299.
- Elvert, M., Boetius, A., Knittel, K., and Jørgensen, B. B., 2003. Characterization of specific membrane fatty acids as chemotaxonomic markers for sulfate-reducing bacteria involved in anaerobic oxidation of methane. *Geomicrobiol. J.* 20, 403-419.
- European Environmental Agency (EEA), 2010) Corine land cover 2006, version 13. Raster data 250 x 250 meters. Accessible at: <http://www.eea.europa.eu/>.
- Fain, A. M. V., Ogston, A. S., and Sternberg, R. W., 2007. Sediment transport event analysis on the western Adriatic continental shelf. *Cont. Shelf Res.* 27, 431-451.
- Farquhar, G. D., Ehleringer, J. R., and Hubick, K. T., 1989. Carbon isotope discrimination and photosynthesis. *Annu. Rev. Plant Biol.* 40, 503-537.
- Farquhar, G. D. and Sharkey, T. D., 1982. Stomatal conductance and photosynthesis. *Annu. Rev. Plant Physiol.* 33, 317-345.
- Feakins, S. J. and Sessions, A. L., 2010. Controls on the D/H ratios of plant leaf waxes in an arid ecosystem. *Geochim. Cosmochim. Acta* 74, 2128-2141.
- Ficken, K. J., Li, B., Swain, D. L., and Eglinton, G., 2000. An n-alkane proxy for the sedimentary input of submerged/floating freshwater aquatic macrophytes. *Org. Geochem.* 31, 745-749.
- Frignani, M., Langone, L., Ravaioli, M., Sorgente, D., Alvisi, F., and Albertazzi, S., 2005. Fine-sediment mass balance in the western Adriatic continental shelf over a century time scale. *Mar. Geol.* 222-223, 113-133.
- Gagosian, R. B. and Peltzer, E. T., 1986. The importance of atmospheric input of terrestrial organic material to deep sea sediments. *Org. Geochem.* 10, 661-669.
- Gagosian, R. B., Peltzer, E. T., and Merrill, J. T., 1987. Long-range transport of terrestrially derived lipids in aerosols from the south Pacific. *Nature* 325, 800-803.
- Gagosian, R. B., Peltzer, E. T., and Zafiriou, O. C., 1981. Atmospheric transport of continentally derived lipids to the tropical North Pacific. *Nature* 291, 312-314.
- Gat, J. R., 1996. Oxygen and hydrogen isotopes in the hydrologic cycle. *Annu. Rev. Earth Planet. Sci.* 24, 225-262.

- Grauel, A. L. and Bernasconi, S. M., 2010. Core-top calibration of $\delta^{18}\text{O}$ and $\delta^{13}\text{C}$ of *G. ruber*, white. and *U. mediterranea* along the southern Adriatic coast of Italy. *Mar. Micropaleontol.* 77, 175-186.
- Hilkert, A. W., Douthitt, C. B., Schlüter, H. J., and Brand, W. A., 1999. Isotope ratio monitoring gas chromatography/Mass spectrometry of D/H by high temperature conversion isotope ratio mass spectrometry. *Rapid Commun. Mass Spectrom.* 13, 1226-1230.
- Hinrichs, K.-U., Rinna, J., and Rullkötter, J., 1998. Late Quaternary paleoenvironmental conditions indicated by marine and terrestrial molecular biomarkers in sediments from the Santa Barbara basin. In: Proceedings of the Fourteenth Annual Pacific Climate, (PACLIM) Workshop, April 6–9, 1997 (eds. Wilson, R.C. & Tharp, V.L.), Interagency Ecological Program, Technical Report 57, California Department of Water Resources. pp. 125–133.
- Hinrichs, K.-U., Summons, R. E., Orphan, V., Sylva, S. P., and Hayes, J. M., 2000. Molecular and isotopic analysis of anaerobic methane-oxidizing communities in marine sediments. *Org. Geochem.* 31, 1685-1701.
- Hopmans, E. C., Weijers, J. W. H., Schefuß, E., Herfort, L., Sinninghe Damsté, J. S., and Schouten, S., 2004. A novel proxy for terrestrial organic matter in sediments based on branched and isoprenoid tetraether lipids. *Earth Planet. Sci. Lett.* 224, 107-116.
- Hou, J., D'Andrea, W. J., MacDonald, D., and Huang, Y., 2007a. Evidence for water use efficiency as an important factor in determining the δD values of tree leaf waxes. *Org. Geochem.* 38, 1251-1255.
- Hou, J., D'Andrea, W. J., MacDonald, D., and Huang, Y., 2007b. Hydrogen isotopic variability in leaf waxes among terrestrial and aquatic plants around Blood Pond (Massachusetts, USA). *Org. Geochem.* 38, 977-984.
- Huang, Y., Dupont, L., Sarnthein, M., Hayes, J. M., and Eglinton, G., 2000) Mapping of C_4 plant input from North West Africa into North East Atlantic sediments. *Geochim. Cosmochim. Acta* 64, 3505-3513.
- Huang, Y., Shuman, B., Wang, Y., and Webb, T., 2002. Hydrogen isotope ratios of palmitic acid in lacustrine sediments record late Quaternary climate variations. *Geology* 30, 1103-1106.
- IAEA/WMO, 2006. Global Network of Isotopes in Precipitation. The GNIP Database. Accessible at: <http://www.iaea.org/water>.
- IPCC, 2007. Climate Change 2007: The physical science basis. Contribution of working group I to the fourth assessment report of the intergovernmental panel on climate change, eds. Solomon, S., Qin, D., Manning, M., Chen, Z., Marquis, M., Averyt, K. B., Tignor, M., and Miller, H. L.. New York: Cambridge University Press.
- Kawamura, K., Ishimura, Y., and Yamazaki, K., 2003. Four years' observations of terrestrial lipid class compounds in marine aerosols from the western North Pacific. *Global Biogeochem. Cycles* 17, 1003.

- Kozłowski, T. T. and Pallardy, S. G., 1997. Growth control in woody plants. Academic Press, San Diego, California, USA.
- Krull, E., Sachse, D., Mügler, I., Thiele, A., and Gleixner, G., 2006. Compound-specific $\delta^{13}\text{C}$ and $\delta^2\text{H}$ analyses of plant and soil organic matter: A preliminary assessment of the effects of vegetation change on ecosystem hydrology. *Soil Biol. Biochem.* 38, 3211-3221.
- Leider, A., Hinrichs, K.-U., Mollenhauer, G., and Versteegh, G. J. M., 2010. Core-top calibration of the lipid-based U^{K}_{37} and TEX_{86} temperature proxies on the southern Italian shelf (SW Adriatic Sea, Gulf of Taranto). *Earth Planet. Sci. Lett.* 300, 112-124.
- Liu, W. and Huang, Y., 2005. Compound specific D/H ratios and molecular distributions of higher plant leaf waxes as novel paleoenvironmental indicators in the Chinese Loess Plateau. *Org. Geochem.* 36, 851-860.
- Liu, W. and Yang, H., 2008. Multiple controls for the variability of hydrogen isotopic compositions in higher plant n-alkanes from modern ecosystems. *Global Change Biol.* 14, 2166-2177.
- Longinelli, A. and Selmo, E., 2003. Isotopic composition of precipitation in Italy: a first overall map. *J. Hydrol.* 270, 75-88.
- Longinelli, A. and Selmo, E., 2010. Isotope geochemistry and the water cycle: a short review with special emphasis on Italy. *Mem. Descr. Carta Geol. d'It.* XC, 153-164.
- Maricchiolo, C., Sambucini, V., Pugliese, A., Munafò, M., Cecchi, G., Rusco, E., Blasi, C., Marchetti, M., Chirici, G., and Corona, P., 2005. La realizzazione in Italia del progetto europeo Corine Land Cover 2000. *Rapporti APAT* 61.
- Mariotti, A., Struglia, M. V., Zeng, N., and Lau, K. M., 2002. The Hydrological Cycle in the Mediterranean Region and Implications for the Water Budget of the Mediterranean Sea. *J. Clim.* 15, 1674-1690.
- Marsico, A., Caldara, M., Capolongo, D., and Pennetta, L., 2007. Climatic characteristics of middle-southern Apulia (southern Italy). *J. Maps*, 342-348.
- McInerney, F. A., Helliker, B. R., and Freeman, K. H., 2011. Hydrogen isotope ratios of leaf wax n-alkanes in grasses are insensitive to transpiration. *Geochim. Cosmochim. Acta* 75, 541-554.
- Milligan, T. G. and Cattaneo, A., 2007. Sediment dynamics in the western Adriatic Sea: From transport to stratigraphy. *Cont. Shelf Res.* 27, 287-295.
- Morovic, M., Mati, F., Grbec, B., Dadi, V., and Ivankovi, D., 2006. South Adriatic phenomena observable through VOS XBT and other ADRICOSM data. *Acta Adriat.* 47, 33-49.
- Niedermeyer, E. M., Schefuß, E., Sessions, A. L., Mulitza, S., Mollenhauer, G., Schulz, M., and Wefer, G., 2010. Orbital- and millennial-scale changes in the hydrologic cycle and vegetation in the western African Sahel: insights from individual plant wax δD and $\delta^{13}\text{C}$. *Quat. Sci. Rev.* 29, 2996-3005.

- Nittrouer, C. A., Miserocchi, S. and Trincardi, F., 2004. The PASTA Project: Investigation of Po and Apennine sediment transport and accumulation. *Oceanography* 17, 46-57.
- O'Leary, M. H., 1981. Carbon isotope fractionation in plants. *Phytochemistry* 20, 553-567.
- Ohkouchi, N., Kawamura, K., Kawahata, H., and Taira, A., 1997. Latitudinal distributions of terrestrial biomarkers in the sediments from the Central Pacific. *Geochim. Cosmochim. Acta* 61, 1911-1918.
- Orlic, M., Gacic, M., and La Violette, P. E., 1992. The currents and circulation of the Adriatic Sea. *Oceanolog. acta* 15, 109-124.
- Pagani, M., Pedentchouk, N., Huber, M., Sluijs, A., Schouten, S., Brinkhuis, H., Sinninghe Damste, J. S., Dickens, G. R., and Scientists, E., 2006. Arctic hydrology during global warming at the Palaeocene/Eocene thermal maximum. *Nature* 442, 671-675.
- Pedentchouk, N., Sumner, W., Tipple, B., and Pagani, M., 2008. $\delta^{13}\text{C}$ and δD compositions of *n*-alkanes from modern angiosperms and conifers: An experimental set up in central Washington State, USA. *Org. Geochem.* 39, 1066-1071.
- Peel, M. C., Finlayson, B. L., and McMahon, T. A., 2007. Updated world map of the Köppen-Geiger climate classification. *Hydrol. Earth Syst. Sci.* 4, 439-473.
- Pelejero, C., 2003. Terrigenous *n*-alkane input in the South China Sea: high-resolution records and surface sediments. *Chem. Geol.* 200, 89-103.
- Polissar, P. J. and Freeman, K. H., 2010. Effects of aridity and vegetation on plant-wax δD in modern lake sediments. *Geochim. Cosmochim. Acta* 74, 5785-5797.
- Portoghese, I., Uricchio, V., and Vurro, M., 2005. A GIS tool for hydrogeological water balance evaluation on a regional scale in semi-arid environments. *Comp. & Geosci.* 31, 15-27.
- Poulain, P.-M., 2001. Adriatic Sea surface circulation as derived from drifter data between 1990 and 1999. *J. Mar. Syst.* 29, 3-32.
- Poynter, J. and Eglinton, G., 1990. Molecular composition of three sediments from hole 717C: the Bengal Fan. *Proc. ODP Sci. Results* 116, 155-161.
- Poynter, J. G., Farrimond, P., Robinson, N., and Eglinton, G., 1989. Aeolian-derived higher plant lipids in the marine sedimentary record: Links with palaeoclimate. In: *Palaeoclimatology and Palaeometeorology: Modern and Past Patterns of Global Atmosphere Transport* (eds. Leinen, M. & Sarnthein, M.). Kluwer. pp. 435-462.
- Prahl, F. G., Ertel, J. R., Goni, M. A., Sparrow, M. A., and Eversmeyer, B., 1994. Terrestrial organic carbon contributions to sediments on the Washington margin. *Geochim. Cosmochim. Acta* 58, 3035-3048.
- Racioppi, R. and Simeone, V., 2003.. Desertification risk in southern apulia rainfall decreasing analysis. In: *Local resources and global trades: Environments and agriculture in the Mediterranean region* (eds. Camarda, D., C. and Grassini, L.). CIHEAM-IAMB, Bari. pp. 429-440.
- Raicich, F., 1996. On the fresh balance of the Adriatic Sea. *J. Mar. Syst.* 9, 305-319.

- Rao, Z., Zhu, Z., Jia, G., Henderson, A. C. G., Xue, Q., and Wang, S., 2009. Compound specific δD values of long chain n-alkanes derived from terrestrial higher plants are indicative of the δD of meteoric waters: Evidence from surface soils in eastern China. *Org. Geochem.* 40, 922-930.
- Rieley, G., Collier, R. J., Jones, D. M., Eglinton, G., Eakin, P. A., and Fallick, A. E., 1991. Sources of sedimentary lipids deduced from stable carbon-isotope analyses of individual compounds. *Nature* 352, 425-427.
- Rieley, G., Collister, J. W., Stern, B., and Eglinton, G., 1993. Gas chromatography/isotope ratio mass spectrometry of leaf wax n-alkanes from plants of differing carbon dioxide metabolisms. *Rapid Commun. Mass Spectrom.* 7, 488-491.
- Rinna, J., Güntner, U., Hinrichs, K.-U., Mangelsdorf, -U., van der Smissen, K., and Rullkötter, J. H., 1999. Temperature related molecular proxies: degree of alkenone unsaturation and average chain length of n-alkanes. In: *Proceedings of the Sixteenth Annual Pacific Climate (PACLIM) Workshop, May 24–27, 1999* (eds. Wilson, R.C. and Tharp, V.L... Technical Report, California Department of Water Resources, pp. 183–192.
- Rivas-Martínez, S., Penas, A., and Díaz, T. E., 2004) Bioclimatic map of Europe-Thermoclimatic belts 1:16 000 000. Accessible at: www.globalclimatics.org.
- Rizzoli, P. M. and Bergamasco, A., 1983. The Dynamics of the Coastal Region of the Northern Adriatic Sea. *J. Phys. Oceanogr.* 13, 1105-1130.
- Rommerskirchen, F., Eglinton, G., Dupont, L., Güntner, U., Wenzel, C., and Rullkötter, J., 2003. A north to south transect of Holocene southeast Atlantic continental margin sediments: Relationship between aerosol transport and compound-specific $\delta^{13}C$ land plant biomarker and pollen records. *Geochem. Geophys. Geosyst.* 4, 1101. doi:10.1029/2003GC000541.
- Rommerskirchen, F., Eglinton, G., Dupont, L., and Rullkötter, J., 2006a. Glacial/interglacial changes in southern Africa: Compound-specific $\delta^{13}C$ land plant biomarker and pollen records from southeast Atlantic continental margin sediments. *Geochem. Geophys. Geosyst.* 7, Q08010. doi:10.1029/2005GC001223.
- Rommerskirchen, F., Plader, A., Eglinton, G., Chikaraishi, Y., and Rullkötter, J., 2006b. Chemotaxonomic significance of distribution and stable carbon isotopic composition of long-chain alkanes and alkan-1-ols in C_4 grass waxes. *Org. Geochem.* 37, 1303-1332.
- Sachse, D., Radke, J., and Gleixner, G., 2004. Hydrogen isotope ratios of recent lacustrine sedimentary n-alkanes record modern climate variability. *Geochim. Cosmochim. Acta* 68, 4877-4889.
- Sachse, D., Radke, J., and Gleixner, G., 2006. δD values of individual n-alkanes from terrestrial plants along a climatic gradient - Implications for the sedimentary biomarker record. *Org. Geochem.* 37, 469-483.

- Salvati, L., 2009. Are Mediterranean Coastal Regions More Exposed to Land Degradation in Recent Years? *J. Coast. Res.* 56, 262-266.
- Salvati, L. and Bajocco, S., 2011. Land sensitivity to desertification across Italy: Past, present, and future. *Appl. Geogr.* 31, 223-231.
- Salvati, L., Petitta, M., Ceccarelli, T., Perini, L., Di Battista, F., and Scarascia, M. E. V., 2008. Italy's renewable water resources as estimated on the basis of the monthly water balance. *Irrig. and Drain.* 57, 507-515.
- Sauer, P. E., Eglinton, T. I., Hayes, J. M., Schimmelmann, A., and Sessions, A. L., 2001. Compound-specific D/H ratios of lipid biomarkers from sediments as a proxy for environmental and climatic conditions. *Geochim. Cosmochim. Acta* 65, 213-222.
- Schefuß, E., Ratmeyer, V., Stuut, J.-B. W., Jansen, J. H. F., and Sinninghe Damsté, J. S., 2003. Carbon isotope analyses of *n*-alkanes in dust from the lower atmosphere over the central eastern Atlantic. *Geochim. Cosmochim. Acta* 67, 1757-1767.
- Schefuß, E., Schouten, S., and Schneider, R. R., 2005. Climatic controls on central African hydrology during the past 20,000 years. *Nature* 437, 1003-1006.
- Schefuß, E., Versteegh, G. J. M., Jansen, J. H. F., and Sinninghe Damsté, J. S., 2001. Marine and terrigenous lipids in Southeast Atlantic sediments (Leg 175). as paleoenvironmental indicators: Initial results. *Proc. ODP Sci. Results* 175, 1-34.
- Schefuß, E., Versteegh, G. J. M., Jansen, J. H. F., and Sinninghe Damsté, J. S., 2004. Lipid biomarkers as major source and preservation indicators in SE Atlantic surface sediments. *Deep Sea Res. I* 51, 1199-1228.
- Schimmelmann, A., Sessions, A. L., and Mastalerz, M., 2006. Hydrogen isotopic (D/H) composition of organic matter during diagenesis and thermal maturation. *Annu. Rev. Earth Planet. Sci.* 34, 501-533.
- Schlitzer, R., 2010. Ocean Data View. Accessible at: <http://odw.awi.de>
- Seki, O., Nakatsuka, T., Shibata, H., and Kawamura, K., 2010. A compound-specific *n*-alkane $\delta^{13}\text{C}$ and δD approach for assessing source and delivery processes of terrestrial organic matter within a forested watershed in northern Japan. *Geochim. Cosmochim. Acta* 74, 599-613.
- Sessions, A. L., 2006. Isotope-ratio detection for gas chromatography. *J. Sep. Sci.* 29, 1946-1961.
- Sessions, A. L., Burgoyne, T. W., Schimmelmann, A., and Hayes, J. M., 1999. Fractionation of hydrogen isotopes in lipid biosynthesis. *Org. Geochem.* 30, 1193-1200.
- Sessions, A. L., Sylva, S. P., Summons, R. E., and Hayes, J. M., 2004. Isotopic exchange of carbon-bound hydrogen over geologic timescales. *Geochim. Cosmochim. Acta* 68, 1545-1559.
- Shuman, B., Huang, Y., Newby, P., and Wang, Y., 2006. Compound-specific isotopic analyses track changes in seasonal precipitation regimes in the Northeastern United States at ca. 8200 cal yr BP. *Quat. Sci. Rev.* 25, 2992-3002.

- Simoneit, B. R. T., 1977. Organic matter in eolian dusts over the Atlantic Ocean. *Mar. Chem.* 5, 443-464.
- Simoneit, B. R. T., 1984. Organic matter of the troposphere - III. Characterization and sources of petroleum and pyrogenic residues in aerosols over the western United States. *Atmos. Environ.* 18, 51-67.
- Smith, B. N. and Epstein, S., 1971. Two categories of $^{13}\text{C}/^{12}\text{C}$ ratios for higher plants. *Plant Physiol.* 47, 380.
- Smith, F. A. and Freeman, K. H., 2006. Influence of physiology and climate on δD of leaf wax n-alkanes from C_3 and C_4 grasses. *Geochim. Cosmochim. Acta* 70, 1172-1187.
- Smith, F. A., Wing, S. L., Freeman, K. H., 2007. Magnitude of the carbon isotope excursion at the Paleocene-Eocene thermal maximum: The role of plant community change, *Earth Planet. Sci. Lett.* 262, 50-65.
- Struglia, M. V., Mariotti, A., and Filograsso, A., 2004. River discharge into the Mediterranean Sea: Climatology and aspects of the observed variability. *J. Clim.* 17, 4740-4751.
- Taricco, C., Ghil, M., and Vivaldo, G., 2009. Two millennia of climate variability in the Central Mediterranean. *Clim. Past* 5, 171-181.
- Tesi, T., Miserocchi, S., Goñi, M. A., Langone, L., Boldrin, A., and Turchetto, M., 2007. Organic matter origin and distribution in suspended particulate materials and surficial sediments from the western Adriatic Sea (Italy). *Estuar. Coast. Shelf Sci.* 73, 431-446.
- Tierney, J. E., Oppo, D. W., Rosenthal, Y., Russell, J. M., and Linsley, B. K., 2010. Coordinated hydrological regimes in the Indo-Pacific region during the past two millennia. *Paleoceanography* 25, PA1102. doi:10.1029/2009PA001871.
- Tierney, J. E., Russell, J. E., Huang, Y., Damste, J. S. S., Hopmans, E. C., and Cohen, A. S., 2008. Northern Hemisphere Controls on Tropical Southeast African Climate During the Past 60,000 Years. *Science*. 322, 252-255.
- Todorovic, M., Calciandro, A., and Albrizio, R., 2007. Irrigated agriculture and water use efficiency in Italy. In: *Water Use Efficiency and Water Productivity. Proceedings of 4th WASAMED Workshop* (eds. Lamaddalena, N., Shatanawi, M., Todorovic, M., Bogliotti, C. and Albrizio, R). *Options Méditerranéennes Séries B* 57, pp. 102-138.
- Tomadin, L., 2000. Sedimentary fluxes and different dispersion mechanisms of the clay sediments in the Adriatic Basin. *Rend. Fis. Acc. Lincei* 11, 161-174.
- Trigo, I. F., Davies, T. D., and Bigg, G. R., 1999. Objective climatology of cyclones in the Mediterranean region. *J. Clim.* 12, 1685-1696.
- Trincardi, F., Correggiari, A., and Roveri, M., 1994. Late Quaternary transgressive erosion and deposition in a modern epicontinental shelf: The Adriatic semienclosed basin. *Geo-Mar. Lett.* 14, 41-51.
- Venezian Scarascia, M. E., Battista, F. D., and Salvati, L., 2006. Water resources in Italy: availability and agricultural uses. *Irrig. and Drain.* 55, 115-127.

- Versteegh, G. J. M., de Leeuw, J. W., Taricco, C., and Romero, A., 2007. Temperature and productivity influences on $U^{K'}_{37}$ and their possible relation to solar forcing of the Mediterranean winter. *Geochem. Geophys. Geosyst.* 8, Q09005. doi:10.1029/2006GC001543.
- Vogts, A., Moossen, H., Rommerskirchen, F., and Rullkötter, J., 2009. Distribution patterns and stable carbon isotopic composition of alkanes and alkan-1-ols from plant waxes of African rain forest and savanna C_3 species. *Org. Geochem.* 40, 1037-1054.
- Woodward, F. I., Lomas, M. R., and Kelly, C. K., 2004. Global climate and the distribution of plant biomes. *Philos. Trans. R. Soc. Lond. B* 359, 1465-1476.
- World Resources Institute, 2007. EarthTrends: Environmental Information, Forests, grasslands and drylands-Italy. Accessible at: <http://earthtrends.wri.org>.
- Xoplaki, E., González-Rouco, J. F., Luterbacher, J., and Wanner, H., 2004. Wet season Mediterranean precipitation variability: influence of large-scale dynamics and trends. *Clim. Dyn.* 23, 63-78.
- Zavatarelli, M. and Pinardi, N., 2003. The Adriatic Sea modelling system: a nested approach. *Ann. Geophys.* 21, 345-364.
- Zavatarelli, M., Raicich, F., Bregant, D., Russo, A., and Artegiani, A., 1998. Climatological biogeochemical characteristics of the Adriatic Sea. *J. Mar. Sys.* 18, 227-263.
- Zonneveld, K. A. F., Chen, L., Möbius, J., and Mahmoud, M. S., 2009. Environmental significance of dinoflagellate cysts from the proximal part of the Po-river discharge plume, off southern Italy (Eastern Mediterranean). *J. Sea Res.* 62, 189-213.

SUPPLEMENTARY DATA EA-III.1

Compilation of analyzed stable hydrogen isotope composition of precipitation at coastal terrestrial stations from northern to southern Italy (see Fig.III.2.)

Station	Lat [°N]	Lon [°E]	Altitude [m asl]	δD precipitation [‰ VSMOW]	Sampling Period	Reference
COM (Comacchio Stat. No. 32)	44.70	12.18	1	-42	06/2000-05/2001	^a
URB (Urbino Stat. No. 40)	43.73	12.64	485	-51	10/1998-10/2001	^a
FAN (Fano Stat. No. 41)	43.83	13.02	12	-48	01/1995-12/1999	^a
SCE (Scerni Stat. No. 53)	42.12	14.57	287	-48	09/1998-09/2001	^a
LUC (Lucera Stat. No. 56)	41.50	15.33	219	-44	12/1997-11/1998	^a
BAR2 (Bari Stat. No. 63)	41.13	16.78	24	-40	01/1998-12/2001	^a
CME (Ceglie Messapico Stat. No. 66)	40.65	17.50	302	-32	11/1998-10/1999	^a
TAR2 (S. Giorgio Ionico Stat. No. 64)	40.45	17.37	26	-29	Incomplete year	^a
SML2 (S. Maria di Leuca Stat. No. 65)	39.82	18.35	59	-31	11/1998-10/1999	^a

m asl: meters above sea level

^a Longinelli and Selmo, 2003)

Averaged stable hydrogen isotope composition of precipitation from OIPC along altitudinal transects in the Po River and Apennine river catchments (see Fig. III.2.).

Transect	Lat [°N]	Lon [°E]	Altitude range [m asl]	Distance to coast [km]	δD precipitation [‰ VSMOW]	Reference
T1 (Po River)	44.79/45.29	12.28/9.83	0-257	200	-44	^b
T2 (Po River)	44.53/44.52	12.28/11.01	0-186	100	-43	^b
T3 (Apennine rivers)	43.89/43.51	12.95/12.24	19-786	70	-46	^b
T4 (Apennine rivers)	43.39/43.14	13.68/12.90	1-662	70	-43	^b
T5 (Apennine rivers)	42.64/42.46	14.05/13.24	2-1297	70	-45	^b
T6 (Apennine rivers)	42.16/41.81	14.71/13.99	4-2047	70	-48	^b

^b OIPC

SUPPLEMENTARY DATA EA-III.2

Mean annual air temperature (MAT), mean annual precipitation (MAP) and relative humidity (RH) covering the period from 1961 to 2000 at meteorological stations along a coastal N-S Italian transect (see Fig. III.2.)

Station	Lat [°N]	Lon [°E]	Altitude [m asl]	MAT		MAP		RH	
				[°C]	SD	[mm]	SD	[%]	SD
Volano	44.82	12.25	3	13.2	0.9	579	188	81	2
C.A.M.S.E. 2	44.60	12.08	-1	13.1	0.2	461	69	82	1
Punta Marina	44.45	12.30	2	13.1	0.2	592	140	79	2
Rimini	44.03	12.62	12	13.5	0.5	683	166	79	3
Pesaro	43.91	12.88	40	14.4	0.6	775	166	73	2
Pescara	42.44	14.20	10	14.3	0.4	659	140	77	2
Termoli	42.00	15.00	44	15.8	0.5	417	152	77	4
Amendola	41.53	15.72	57	15.2	0.4	471	109	73	3
Bari/Palese Macchie	41.13	16.78	34	15.8	0.5	561	165	72	2
Brindisi	40.65	17.95	15	16.9	0.5	593	125	77	2
Grottaglie	40.52	17.40	64	16.2	0.4	534	171	73	3
Taranto	40.45	17.30	22	17.5	0.6	504	152	66	3
Lecce	40.23	18.15	48	16.2	0.4	629	176	76	3
S. Maria di Leuca	39.82	18.35	65	16.8	0.3	611	196	77	3

m asl: meters above sea level

MAT: mean annual air temperature

MAP: mean annual precipitation

RH: relative humidity

SD: standard deviation

SUPPLEMENTARY DATA EA-III.3 (1/2)

Relative abundance of *n*-C₂₅ to *n*-C₃₃ alkanes at coastal terrestrial stations from northern to southern Italy and marine core tops at the southern Italian shelf (see Fig. III.2.)

Station	Location	Type	Lat [°N]	Lon [°E]	Altitude/Depth [m asl/ m bsl]	<i>n</i> -C ₂₅ alkane [%]	<i>n</i> -C ₂₆ alkane [%]	<i>n</i> -C ₂₇ alkane [%]	<i>n</i> -C ₂₈ alkane [%]	<i>n</i> -C ₂₉ alkane [%]	<i>n</i> -C ₃₀ alkane [%]	<i>n</i> -C ₃₁ alkane [%]	<i>n</i> -C ₃₂ alkane [%]	<i>n</i> -C ₃₃ alkane [%]
M1	Po della Donzella	Riverine	44.840	12.380	0	5.0	2.1	21.9	3.9	39.2	2.8	18.4	1.5	5.1
M2	Po di Goro	Riverine	44.836	12.344	0	5.4	2.1	21.7	3.4	35.6	2.9	21.6	1.6	5.6
M3	Po di Goro harbour	Near-coastal	44.818	12.352	0	5.6	3.8	14.0	4.4	28.1	5.0	27.4	3.2	8.5
M5	Reno river	Riverine	44.552	12.141	2	6.1	2.6	23.9	4.6	36.5	3.1	17.4	1.5	4.2
M8	Foglia river	Riverine	43.867	12.812	25	6.6	2.0	23.2	3.5	34.5	2.7	19.1	1.9	6.3
M10	Potenza river	Riverine	43.415	13.655	0	6.3	2.9	22.1	3.6	33.0	2.6	23.1	1.3	5.1
M11	Porto Recanati	Near-coastal	43.409	13.678	0	9.3	3.8	26.1	7.4	24.8	5.0	19.8	0.5	3.4
M13	Vomano river	Riverine	42.645	13.990	15	6.1	3.3	21.4	4.6	27.3	5.1	24.2	1.8	6.2
M14	Lago di Bomba	Lacustrine	42.011	14.362	269	10.3	4.8	30.2	5.0	25.9	3.1	13.5	2.4	4.8
M15	Punta della Penna	Near-coastal	42.174	14.707	0	3.2	4.3	31.4	4.8	31.9	4.2	20.2		
M18	Manfredonia Lido	Near-coastal	41.618	15.904	0	7.7	2.9	18.0	3.9	29.0	3.6	24.2	2.6	8.1
M19	Cervaro river	Riverine	41.573	15.886	0	3.9	1.2	11.6	3.1	29.4	4.5	38.7	1.0	6.6
M22	Ofanto river	Riverine	41.285	16.114	23	11.2	3.5	13.4	2.8	22.9	3.0	29.7	2.2	11.4
M25	Alimini Grande	Lacustrine	40.203	18.455	0	2.9	1.0	7.9	2.6	30.3	4.8	38.7	2.6	9.1
M 27	Gallipoli Beach	Near-coastal	40.027	18.019	0	10.5	6.0	10.9	7.5	16.6	7.2	18.3	9.9	13.1
M 28	Porto Cesareo	Near-coastal	40.242	17.910	0	5.7	3.8	9.0	3.6	20.5	6.2	27.0	4.0	20.3
M30	Lago di Monticchio	Lacustrine	40.935	15.604	659	14.4	1.0	55.2	2.9	22.1	0.3	3.6	0.3	0.4
10701	G. of Taranto	Marine	40.000	17.467	1186	4.9	3.3	11.2	4.8	24.8	4.3	29.6	3.9	13.1
10702	G. of Taranto	Marine	40.000	17.586	911	5.0	4.2	11.3	5.8	24.2	5.4	27.0	4.9	12.3
10703	G. of Taranto	Marine	40.000	17.742	277	4.9	3.7	10.2	5.7	23.8	6.0	27.6	5.7	12.4
10704	G. of Taranto	Marine	40.000	17.833	219	3.4	4.6	10.5	9.3	20.9	9.3	23.4	8.7	10.0
10705	G. of Taranto	Marine	39.853	17.913	128	4.9	3.7	9.9	4.1	20.9	8.1	25.5	6.8	16.1
10706	G. of Taranto	Marine	39.825	17.833	218	4.9	3.2	10.6	5.0	25.5	4.3	28.2	5.3	12.8
10707	G. of Taranto	Marine	39.783	17.583	1598	5.9	4.1	13.0	5.4	24.5	4.6	27.6	4.3	10.6
10708	G. of Taranto	Marine	39.808	17.733	686	4.1	3.6	9.9	6.1	24.2	5.5	29.0	5.1	12.4
10709	G. of Taranto	Marine	39.757	17.893	173	4.8	2.8	9.8	5.4	26.0	4.1	30.6	4.7	11.7
10710	G. of Taranto	Marine	39.592	17.683	2040	7.6	5.4	12.0	4.9	26.5	4.0	26.1	3.6	9.8
10711	G. of Taranto	Marine	39.683	17.800	1049	4.5	3.3	11.0	3.6	26.9	3.0	32.0	3.4	12.3
10712	G. of Taranto	Marine	39.727	17.862	618	4.4	2.9	10.1	4.2	22.8	6.6	27.9	5.7	15.3
10713	G. of Taranto	Marine	39.692	18.283	127	6.0	2.6	10.4	6.2	23.9	3.4	31.8	4.2	11.5
10714	G. of Taranto	Marine	39.640	18.283	207	5.1	3.5	10.7	4.3	23.6	4.0	29.9	4.5	14.3
10715	G. of Taranto	Marine	39.559	18.283	697	3.7	2.0	9.3	2.9	23.8	4.0	34.2	4.6	15.6
10716	G. of Taranto	Marine	39.345	18.283	1328	3.8	2.3	10.4	3.0	24.4	2.9	34.2	4.9	14.1

SUPPLEMENTARY DATA EA-III.3 (2/2)

Relative abundance of *n*-C₂₅ to *n*-C₃₃ alkanes at coastal terrestrial stations from northern to southern Italy and marine core tops at the southern Italian shelf (see Fig. III.2.)

Station	Location	Type	Lat [°N]	Lon [°E]	Altitude/Depth [m asl/ m bsl]	<i>n</i> -C ₂₅ alkane [%]	<i>n</i> -C ₂₆ alkane [%]	<i>n</i> -C ₂₇ alkane [%]	<i>n</i> -C ₂₈ alkane [%]	<i>n</i> -C ₂₉ alkane [%]	<i>n</i> -C ₃₀ alkane [%]	<i>n</i> -C ₃₁ alkane [%]	<i>n</i> -C ₃₂ alkane [%]	<i>n</i> -C ₃₃ alkane [%]
10717	G. of Taranto	Marine	39.742	18.080	93	5.7	3.9	10.9	5.2	22.2	7.4	27.0	5.4	12.1
10718	G. of Taranto	Marine	39.693	18.058	220	4.2	3.2	10.3	4.3	23.3	7.5	26.9	5.4	14.9
10719	G. of Taranto	Marine	39.653	18.042	616	5.3	3.7	11.2	4.2	23.3	7.2	28.6	4.5	11.9
10720	G. of Taranto	Marine	39.507	17.978	1387	6.2	4.1	12.6	4.0	26.5	4.3	29.2	3.0	10.1
10721	Gargano P.	Marine	42.166	16.767	203	5.3	3.6	11.1	3.6	25.3	6.3	29.5	3.6	11.7
10722	Gargano P.	Marine	42.167	16.500	142	4.8	3.4	10.0	4.0	24.0	6.5	29.1	5.3	13.0
10723	Gargano P.	Marine	42.167	16.000	114	5.4	3.5	11.0	3.6	24.2	6.5	28.7	3.9	13.1
10724	Gargano P.	Marine	42.001	16.217	50	5.5	3.3	13.2	5.7	24.9	5.5	27.4	3.2	11.3
10725	Gargano P.	Marine	42.000	16.367	98	5.7	4.2	12.6	4.5	23.9	6.3	27.1	3.7	11.8
10726	Gargano P.	Marine	42.000	16.717	183	5.1	3.3	10.2	3.9	23.2	6.3	29.8	4.7	13.5
10727	Gargano P.	Marine	41.801	16.617	101	4.3	3.6	11.1	3.9	23.4	6.6	29.1	5.2	12.8
10728	Gargano P.	Marine	41.783	16.858	194	5.7	3.8	10.0	3.8	23.9	6.4	28.3	3.8	14.2
10729	Gargano P.	Marine	41.647	17.191	712	4.9	3.3	10.3	3.8	24.5	5.8	29.5	4.9	13.1
10730	Gargano P.	Marine	41.500	17.050	183	4.9	3.6	9.7	4.1	23.7	6.7	29.3	4.9	13.1
10731	Gargano P.	Marine	41.500	16.658	96	6.5	5.0	12.0	6.8	24.2	5.7	25.6	3.4	10.8
10732	Gargano P.	Marine	41.500	16.407	51	6.1	4.4	13.4	6.7	25.5	6.1	24.5	2.7	10.6
10733	Gargano P.	Marine	41.500	16.225	23	5.6	4.1	13.0	5.9	24.8	6.1	25.7	3.5	11.4
10734	Gargano P.	Marine	41.667	16.242	18	7.1	3.9	13.6	6.1	26.2	6.2	24.0	2.9	10.0
10735	Gargano P.	Marine	41.500	17.308	733	6.4	3.3	10.9	5.6	24.1	4.6	27.9	3.8	13.2
10736	Strait of Otranto	Marine	40.758	18.192	123	5.0	2.7	10.9	3.8	25.9	3.7	31.9	3.3	12.9
10737	Strait of Otranto	Marine	40.625	18.329	113	5.6	3.0	10.7	4.0	23.6	3.5	32.4	3.7	13.5
10738	Strait of Otranto	Marine	40.546	18.467	112	6.5	3.7	13.6	4.6	25.3	3.9	30.3	3.2	8.8
10739	Strait of Otranto	Marine	40.500	18.642	565	5.1	2.8	11.0	4.1	25.1	4.7	30.8	4.4	12.0
10740	Strait of Otranto	Marine	40.392	18.583	128	6.2	4.2	12.1	4.8	26.7	4.0	27.5	2.9	11.7
10741	Strait of Otranto	Marine	40.233	18.667	287	6.6	4.2	12.9	5.0	25.4	6.2	26.3	3.8	9.6
10742	Strait of Otranto	Marine	39.716	18.776	599	5.4	3.7	10.8	4.9	24.5	4.5	29.0	5.0	12.1
10743	Strait of Otranto	Marine	39.825	18.642	124	6.5	5.2	11.7	5.3	23.7	7.2	26.3	4.1	10.0
10744	Strait of Otranto	Marine	39.850	18.600	117	5.6	3.6	10.2	5.1	29.1	2.3	29.0	3.7	11.4
10746	W G. of Taranto	Marine	39.908	16.758	157	9.0	7.2	12.6	7.0	21.1	5.7	23.4	4.6	9.3
10747	W G. of Taranto	Marine	39.725	16.975	246	6.9	5.6	11.8	5.5	23.4	5.0	27.0	4.1	10.7
10748	W G. of Taranto	Marine	39.667	17.050	288	6.9	4.9	12.0	5.8	24.2	4.2	28.4	3.9	9.6
10749	W G. of Taranto	Marine	39.600	17.183	278	6.5	4.3	12.2	4.9	26.2	4.0	28.2	3.9	10.0

m asl: meters above sea level

m bsl: meters below sea level

CHAPTER IV

Multiproxy environmental reconstructions: What do SST proxies really tell us (a high-resolution comparison of U^{K'}₃₇, TEX^H₈₆ and foraminiferal based $\delta^{18}\text{O}$ during the last 500 years in the Gulf of Taranto)

Anna-Lena Grauel^{a,*,1}, Arne Leider^{b,*,1}, Marie-Louise S. Goudeau^c, Inigo Müller^d, Stefano M. Bernasconi^a, Kai-Uwe Hinrichs^b, Gert J. De Lange^c and Gerard J.M. Versteegh^b

Draft for submission to *Paleoceanography*

^a *Geological Institute, ETH Zurich, 8092 Zurich, Switzerland*

^b *MARUM Center for Marine Environmental Sciences & Dept. of Geosciences, University of Bremen, 28334 Bremen, Germany*

^c *Dept. of Geosciences, Utrecht University, Utrecht, The Netherlands*

^d *Max-Planck-Institute for Marine Microbiology, 28359 Bremen, Germany*

** corresponding authors, ¹ equal contribution to this work*

E-mail addresses: ALG: anna.grauel@erdw.ethz.ch; AL: arneleider@uni-bremen.de

Tel.: +41 44 632 8607 (ALG)

Fax: +41 44 632 1075 (ALG)

IV.1. ABSTRACT

We present a multiproxy reconstruction of sea surface temperatures (SST) and coastal environmental changes covering the last 500 years from sediments in the Gulf of Taranto (central Mediterranean) based on $U^{K'}_{37}$ (alkenones from haptophytes), TEX^H_{86} (membrane lipids of marine crenarchaeota), and $\delta^{18}O$ and $\delta^{13}C$ of *Globigerinoides ruber* (*white and pink*) and *Uvigerina mediterranea*. The changes in SSTs reconstructed from $\delta^{18}O$ of *G. ruber* (*white*), TEX^H_{86} and $U^{K'}_{37}$ exceed the variability observed in other local and global Northern Hemisphere temperature reconstructions. The $U^{K'}_{37}$ reflects temperatures during the cooler part of the year, which is when atmospheric circulation leads to nutrient supply by vertical mixing and runoff, which, in turn, induce haptophyte growth. TEX^H_{86} -based temperatures are higher than the $U^{K'}_{37}$ -based SSTs and reflect summer conditions. Co-variation between both SST records suggests a common environmental mechanism during the last 500 years. SSTs reconstructed from the $\delta^{18}O$ of *G. ruber* (*white*) record summer conditions and are in good agreement to summer temperature reconstructions from the European Alps. Moreover, the $\delta^{18}O$ and $\delta^{13}C$ of *G. ruber* (*white*) and *U. mediterranea* are influenced by changes in salinity and food availability related to variations of the major circulation patterns in the Gulf of Taranto on decadal- to centennial-scale. In addition, a negative correlation between SSTs based on TEX^H_{86} and $\delta^{18}O$ of *G. ruber* (*white*) over large parts of the record suggests that changes in circulation in the Gulf of Taranto occurred several times during the last 500 years. The foraminifera and biomarker records indicate a steady increase in eutrophication and terrestrial input during the last 200 years. This is attributed to an increasing human impact on the region.

IV.2. INTRODUCTION

Understanding the mechanisms, causes and amplitude of natural climate variability is one of the major challenges in paleoclimate research as this knowledge can be used to reduce the uncertainties in the prediction of future climate change. Especially, climate variations of the past millennium deserve a careful consideration since this period comprises the transition from pre-industrial times to 20th century global warming. This period includes the Little Ice Age (LIA), which is the most recent period of glacier advances since the late Pleistocene, when European climate experienced periods of cooler conditions with a decrease in Northern Hemisphere (NH) temperatures of about 0.6 °C during the 15th to 19th century relative to late

20th century (e.g., Grove, 1988; Bradley and Jones, 1993; Pfister, 1995; Jones et al., 1998; Crowley, 2000; Wanner et al., 2000; Luterbacher et al., 2004). Cooling culminated during the Maunder Minimum (1645-1715), a phase of reduced solar activity, associated with an increase in climate variability in Europe (Luterbacher et al., 2001). Likely contributors to the global LIA cooling were a lower total solar irradiance (e.g., Eddy, 1976; Lean et al., 1992), increased volcanic activity (Crowley, 2000) and a slowdown of the thermohaline circulation (Bianchi and McCave, 1999; Broecker, 2000), whereby regional climate dynamics were determined by atmosphere-ocean feedbacks (e.g., Luterbacher et al., 1999; Shindell et al., 2001; Luterbacher et al., 2002). Historical documentary accounts, instrumental measurements and proxy records show that there is no continuous period of lower global temperatures synchronous with cold conditions in Europe (Houghton et al., 2001). Instead the LIA is conceived as a period showing significantly increased climate variability, rather than changes in average climate, where timing and amplitude were highly variable between regions (e.g., Mann, 2002; Bradley et al., 2003). Additionally, climatic variations and responses to climate forcing may not be the same over the entire year as suggested by multiproxy reconstructions of seasonal air temperatures (Briffa and Osborn, 2002; Esper et al., 2002; Luterbacher et al., 2004), precipitation (Pauling et al., 2006) and simulations (Hegerl et al., 2011; Palastanga et al., 2011) for the last 500 years.

The Mediterranean Sea is situated at the transition between the subtropical high-pressure belt and mid-latitude westerlies (Trigo et al., 1999; Xoplaki et al., 2003). Hence, variations in atmospheric circulation have a significant influence on its climate (e.g., Hurrell, 1995; Jacobeit et al., 2001, 2002; Dünkeloh and Jacobeit, 2003; Xoplaki et al., 2003, 2004; Alpert et al., 2006; Lionello et al., 2006). Documentary sources indicate a higher frequency of floods, droughts and frosts in Mediterranean Europe's mountainous regions during the LIA (Grove et al., 2001). Anomalous drought, heavy rainfall and storm activity are reported for large parts of the Mediterranean during the last 500 years (e.g., Enzi and Camuffo, 1995; Camuffo et al., 2000; Rodrigo et al., 2000; Barriendos and Llasat, 2003; Lionello et al., 2006 and references therein; Brewer et al., 2007; Diodato, 2007; Nicault et al., 2008). In large parts these studies focus on the terrestrial environment. In contrast, little is known about the influences on the marine environment in the Mediterranean due to this increased variability during the last 500 years (Schilman et al., 2001; Incarbona et al., 2010).

The reconstruction of past sea surface temperatures (SST) is a key issue for paleoceanographic studies. Commonly used geochemical SST proxies in marine sediments are the oxygen stable isotopic composition ($\delta^{18}\text{O}$) of planktonic foraminifera (Emiliani, 1955;

Shackleton, 1967; Ravelo and Hillaire-Marcel, 2007), the lipid $U^{K'}_{37}$ index based on alkenones produced by haptophyte algae (Brassel et al., 1986; Prahl and Wakeham, 1987) and the TEX_{86} index based on glycerol dialkyl glycerol tetraethers (GDGTs) from planktonic crenarchaeota (Schouten et al., 2002).

Core top calibrations along the southern Italian shelf showed clear discrepancies between these SST proxies, due to different ecologies (production season, water depth) of the organisms from which the proxies have been derived (Grauel and Bernasconi, 2011; Leider et al., 2010) (Fig. IV.1. and IV.2.). We use these differences between the SST proxies to reconstruct the marine response to the climatic and anthropogenic changes that occurred in the south Italian region during the last 500 years. We take advantage of the high sedimentation rates on the Gallipoli shelf (e.g., Cini Castagnoli et al., 1999; Versteegh et al., 2007; Zonneveld et al., 2012; Goudeau et al., *subm.*) to create the first reconstruction of SSTs in the Mediterranean Sea at sub-decadal resolution covering the last 500 years based on a direct comparison of $\delta^{18}O$ of *G. ruber* (*white*), $U^{K'}_{37}$ and TEX_{86} indices. In this coastal setting terrestrial input may modify our proxies. Riverine input may reduce salinity, modifying the oxygen isotopic composition of foraminifera. Terrestrial organic matter input may influence the TEX_{86} (through soil-derived lipids). Furthermore, nutrient input may change species abundances (timing, duration and amplitude) and through this the recorded signals. To assess the impact of these terrestrial influences we determined the BIT index, a proxy for soil organic matter input, and concentrations of long-chain *n*-alkanes, derived from leaf waxes of higher land plants (Eglinton and Hamilton, 1967; Hopmans et al., 2004). Finally, we discuss our results in the context of other regional and NH climate reconstructions to disentangle local and ecological effects from ocean climate variability.

IV.3. SST PROXIES AND THEIR BIASES

The oxygen isotope geochemistry of foraminifera is a well-established paleoceanographic tool (e.g. Emiliani, 1955; Shackleton, 1967; Zachos et al., 1994; Ravelo and Hillaire-Marcel, 2007), but because the $\delta^{18}O$ of foraminifera is influenced by both ambient water temperature and by the oxygen isotopic composition of the water in which calcite precipitation takes place (Epstein and Mayeda, 1953), temperature reconstructions are not straightforward. In pelagic settings variations in $\delta^{18}O$ of seawater can be due to changes in the global ice volume (Shackleton and Opdyke, 1973) and in salinity due to regional hydrological changes in evaporation and/or freshwater input and/or large scale oceanic circulation (Craig and Gordon,

1965; Broecker et al., 1986). Consequently, not knowing past variations in the $\delta^{18}\text{O}$ of seawater introduces a significant error in the interpretation of $\delta^{18}\text{O}$ -based temperatures. The interpretation of foraminiferal $\delta^{18}\text{O}$ records in near coastal settings is even more complex due to a strong variability in environmental parameters such as salinity, $\delta^{18}\text{O}$ of the water, temperature and availability of nutrients affecting their seasonal abundance and depth habitat (Martinez et al., 1998; Ding et al., 2006).

The lipid-based $U_{37}^{K'}$ index is defined as the ratio of di- ($C_{37:2}$) to triunsaturated ($C_{37:3}$) alkenones in which the relative proportion of the $C_{37:3}$ alkenone decreases with increasing water temperature (Prahl and Wakeham, 1987; Müller et al., 1998; Conte et al., 2006). Alkenones are synthesized by a small group of haptophyte algae mainly the coccolithophore *Emiliana huxleyi* and related species growing in the ocean surface waters (Volkman et al., 1980; Marlowe et al., 1984; Brassell et al., 1986; Prahl and Wakeham, 1987; Conte et al., 1998). Global core top calibrations show a linear correlation between $U_{37}^{K'}$ and mean annual SSTs (Müller et al., 1998; Conte et al., 2006) and the successful application of the $U_{37}^{K'}$ in various marine settings (Herbert et al., 2003 and references therein) indicate its reliability as a paleoceanographic tool. Factors that lead to discrepancies between $U_{37}^{K'}$ based temperatures and mean annual SSTs are related to preferential degradation of the $C_{37:3}$ alkenone (Sun and Wakeham, 1994; Gong and Hollander, 1999; Hoefs et al., 2002; Rontani et al., 2006, Kim et al., 2009a; Rontani et al., 2009), nutrient and light availability (Epstein et al., 1998; Versteegh et al., 2001; Prahl et al., 2003), transport of alkenones (Benthien and Müller, 2000; Goñi et al., 2001; Ohkouchi et al., 2002; Mollenhauer et al., 2007), differences in species composition (Volkman et al., 1995; Conte et al., 1998), production at greater depth in the mixed layer (Ternois et al., 1997; Bentaleb et al., 1999; Prahl et al., 2005) or seasonal blooming of haptophytes (Sikes et al., 1997; Bentaleb et al., 1999; Prahl et al., 2001; Popp et al., 2006 and references therein).

The TEX_{86} temperature proxy is based on archaeal GDGTs, which are abundant in marine sediments (Schouten et al., 2000, 2002). These isoprenoid GDGTs are produced by marine Crenarchaeota, a major group of prokaryotes in today's ocean (Karner et al., 2001). The relative proportion of cyclopentane moieties of isoprenoid GDGTs increases with growth temperature in mesocosm experiments (Wuchter et al., 2005) and this proportion in core tops correlates linearly to mean annual temperatures of the overlying surface waters, worldwide. This observation leads to the establishment of the TEX_{86} index and a global calibration of TEX_{86} to SST (Schouten et al., 2002; Kim et al., 2008, 2010). Deviations in TEX_{86} derived temperatures from mean annual SSTs are explained by crenarchaeotal production below the

mixed layer prevalent in upwelling areas (Huguet et al., 2007a; Lee et al., 2008; Lopes dos Santos, 2010; Rommerskirchen et al., 2011) and differences in growth season (Menzel et al., 2006; Castañeda et al., 2010; Leider et al., 2010; Huguet et al., 2011). Terrestrial soil organic matter (OM) can constitute a potential source of isoprenoid GDGTs affecting the TEX₈₆ signal in marine settings with large soil input (Weijers et al., 2006). This can be verified by the application of the Branched and Isoprenoid Tetraether (BIT) index, a ratio between terrestrial and marine GDGTs (Hopmans et al., 2004). Additionally, GDGTs may also derive from benthic archaea living in marine sediments (Lipp et al., 2008; Lipp and Hinrichs, 2009; Liu et al., 2011).

The above discussion highlights that only a multiproxy approach allows unraveling of environmental and biological factors influencing these proxies and through this can provide more confident climate reconstructions.

IV.4. STUDY AREA

IV.4.1. Oceanography

The Gulf of Taranto is situated in the northwestern Ionian Sea between Calabria and Apulia (Fig. IV.1a). It can be divided into three distinct geological provinces, the Apulian Slope, the Taranto Valley and eastern Calabrian Margin. The cores NU04 and GeoB10709-4 are located on the Apulian Margin, a wide continental shelf with a slight gradient towards the deep Taranto Valley (Rossi et al., 1983).

The circulation in the Gulf of Taranto is characterized by a complex water mass distribution as a consequence of plume dynamics and mixing of surface and dense bottom water currents (Sellschopp and Álvarez, 2003) with high seasonal variability (Milligan and Cattaneo, 2007). The main surface water masses are the Western Adriatic Current (WAC), a less saline, nutrient-rich water mass flowing in a narrow coastal band from the northern Adriatic Sea into the Gulf of Taranto and the warmer and more saline Ionian Surface Water (ISW) from the central Ionian Sea (Poulain, 2001; Bignami et al., 2007; Turchetto et al., 2007). The WAC, with the primary fluvial contribution being the Po River in the north and additional input from many smaller Alpine and Apennine rivers flowing into the Northern Adriatic Sea (Turchetto et al., 2007), drives the primary productivity along the coasts of the western Adriatic Sea (e.g., Boldrin et al., 2005). The coastal waters show higher chlorophyll concentrations during all seasons (Marini et al., 2008). The WAC achieves maximal flow rate and volume during

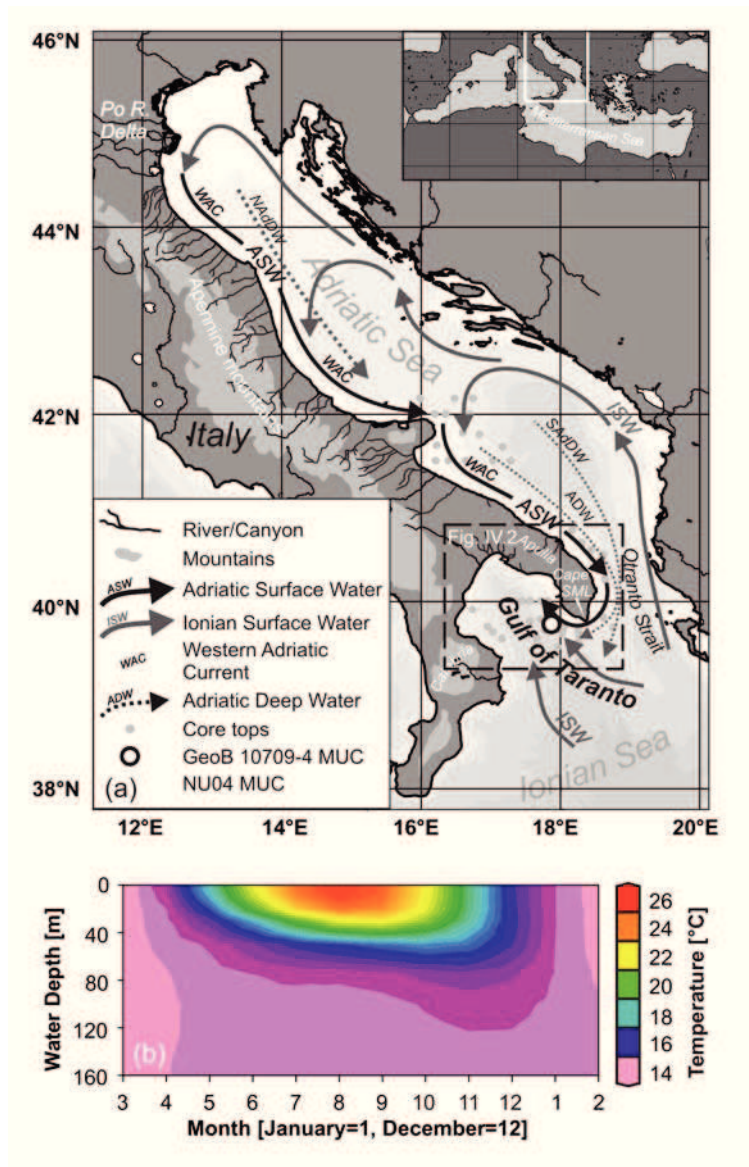


Figure IV.1. (a) Partial map of Italy showing the Adriatic Sea and Ionian Sea, general surface water circulation, water masses and core locations in the Gulf of Taranto (SAdDW: Southern Adriatic Dense Water; NAdDW: Northern Adriatic Dense Water; Cape SML: Cape St. Maria di Leuca) (after Artegiani et al., 1997b; Poulain et al., 2001; Vilibić et al., 2005). (b) Monthly distribution of water column temperature in the Gulf of Taranto (Locarnini et al., 2009; data retrieved from World Ocean Atlas, 2009 database accessible at <http://www.nodc.noaa.gov>, averaged for 38.875°N/17.125°E – 40.375°E/18.375°E).

winter and spring (Poulain, 2001). It can then be traced along the entire eastern Italian coastline down to the Cape Santa Maria di Leuca and into the Gulf of Taranto (Poulain, 2001). The WAC is weaker and located more offshore during summer as a consequence of reduced river discharge (Poulain, 2001) leading to a decreased inflow into the Gulf of Taranto (Poulain, 2001). The highly saline Levantine Intermediate Water (LIW), which flows from the central Ionian Sea into the Gulf of Taranto, is present between 200 m and 600 m water depth (Savini and Corselli, 2010). The bottom waters are characterized by the Adriatic Deep Water (ADW), a dense water mass which is formed by the Northern Adriatic Dense Water

(NAdDW) and Southern Adriatic Dense Water (SAdDW) (Grbec et al., 2007; Turchetto et al., 2007). The NAdDW is formed as a response to wintertime NE Bora wind events in the northern Adriatic Sea (Turchetto et al., 2007). It has an enhanced current and particle flux southward and can be observed in the southern Adriatic Sea during spring (Turchetto et al., 2007). The SAdDW represents a deep-convection water mass formed during late winter/early spring in the southern Adriatic Sea (Turchetto et al., 2007). Annual mean SSTs in the Gulf of Taranto are ~ 18.7 °C. During summer (June-August) the water column is highly stratified and SSTs vary between 26 °C at the surface and 15 °C at 50 m water depth (Zonneveld et al., 2008; Grauel and Bernasconi, 2010) (Fig. IV.1b). During winter (December-February) SSTs vary between 13 and 15 °C and the influence of the WAC is stronger. Seasonal temperature variations can affect the water column up to ~ 100 m water depth (Socal et al., 1999; Locarnini et al., 2009).

IV.4.2. Previous core top calibrations

Core-top calibrations based on $U^{K'_{37}}$, TEX_{86} and $\delta^{18}O$ and $\delta^{13}C$ of *G. ruber* (white) showed that the different proxies reflect seasonal SSTs and environmental conditions in the Gulf of Taranto (Fig. IV.2.). The alkenone-based SSTs ($SST_{UK'37}$) reflect maxima in haptophyte production during the colder seasons (Leider et al., 2010). The TEX_{86} -derived temperatures (SST_{TEX86}) increase with distance from shore, so that at least offshore SST_{TEX86} reflects summer temperatures in the stratified and oligotrophic water column of the Ionian Sea (Leider et al., 2010). The BIT index and the chlorophyll-a concentrations indicate a shoreward increasing impact of seasonal and spatial variability in nutrients suggesting a control of planktonic archaeal abundance by primary productivity (Leider et al., 2010).

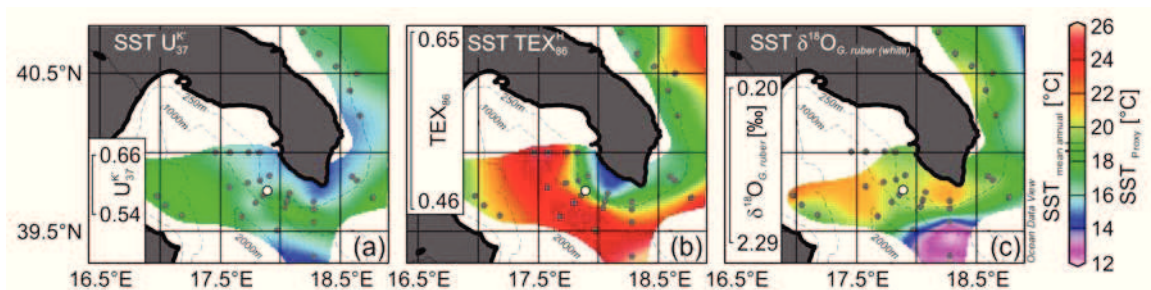


Figure IV.2. Contour plots of reconstructed SSTs based on core tops (0-2 cm) along the southern Italian shelf and Gulf of Taranto. (a) Alkenone-based temperature ($SST_{UK'37}$), (b) GDGT-based temperature (SST_{TEX86}) and (c) $\delta^{18}O$ based temperature of *G. ruber* (white) ($SST_{\delta^{18}O_{G. ruber}}$) (modified from Grauel and Bernasconi, 2010; Leider et al., 2010). Ranges of $U^{K'_{37}}$ and TEX_{86} index values and $\delta^{18}O$ of *G. ruber* (white) are given showing minimum and maximum values relative to the corresponding SST scale. Dashed lines are water depth contours (250 m, 1000 m and 2000 m). For comparison mean annual satellite-derived SSTs of the study area are indicated with pointed lines on the color bar.

Temperature reconstructions based on $\delta^{18}\text{O}$ ($\text{SST}_{\delta^{18}\text{O}}$) of *G. ruber (white)* also reflect a summer signal in the center of the Gulf of Taranto with additional influences from variations in salinity and nutrient distributions related to circulation patterns of the WAC and ISW (Grauel and Bernasconi, 2010). *G. ruber (white)* inhabit the first 30 m of the water column in the Gulf of Taranto but tend to dwell in deeper habitats with distance to the coast (30-50 m water depth) due to lower food availability (Grauel and Bernasconi, 2010). Additionally, the influence of the more saline and oligotrophic ISW has to be considered offshore. Both, the lower nutrient availability and higher salinity lead to an increase in $\delta^{18}\text{O}$ and decrease in SST estimates (Grauel and Bernasconi, 2010).

IV.5. MATERIAL AND METHODS

IV.5.1. Multicores

Sediments analyzed for alkenones and GDGTs are from multicore GeoB 10709-4 (39.757°N, 17.893°E, water depth 173 m; Fig. IV.1). GeoB 10709-4 has been collected during RV POSEIDON cruise P339 'CAPPUCCINO' in June 2006 (Zonneveld et al., 2008). The multicore was frozen directly upon collection and was stored at -20°C until sampling. Sampling for lipid biomarkers was performed on the frozen core on a 2.5 mm resolution. Samples for planktic and benthic foraminifera are from a nearby multicore NU04 (39.764°N, 17.892°E, water depth 160 m) during RV UNIVERSITATIS cruise 'ESPRESSO' in 2005 (Fig. 1). Sampling was performed at 3 mm resolution.

IV.5.2. Radioisotope dating

The XRF analyses of several cores from the eastern Gulf of Taranto (Goudeau et al., submitted) demonstrates that sedimentation rates vary considerably more than suggested previously (Cini Castagnoli et al., 1990; Bonino et al., 1993). Therefore, the cores were dated with ^{210}Pb -dating (core NU04) and AMS ^{14}C -dating (Table IV.1). ^{210}Pb -dating of NU04 results in a sedimentation rate of 0.85 mm/year (de Lange, unpubl.).

For each core the bottom age (last cm) was additionally dated by AMS ^{14}C -analyses. Bulk planktic foraminifera samples were picked and analyzed with a miniaturized radiocarbon dating system (MICADAS) (Ruff et al., 2007; Synal et al., 2007) at the AMS Radiocarbon Dating Laboratory at ETH Zurich. Two samples were measured as solid graphite targets (NU04 and GeoB10709-4) and one sample was measured directly as CO_2 (GeoB10709-5) where MICADAS was equipped with a gas ion source. The ^{14}C -ages were calibrated with the

Table IV.1 Locations of cores, sedimentation rates in the Gulf of Taranto and comparison to sedimentation rates from the literature

	Latitude	Longitude	Depth	Dating method	LSR ²¹⁰ Pb	Depth of ¹⁴ C AMS sampling	ETH N ^o	Year	Error (95%)	LSR ¹⁴ C AMS	References
	[°N]	[°E]	[m]		[mm/yr]	[mm]		[AD]	[+/-yr]	[mm/yr]	
NU04	39.764	17.892	160	²¹⁰ Pb, ¹⁴ C	0.85	460	40265	1260	150	0.62	This study
GeoB 10709-4	39.757	17.893	173	¹⁴ C	-	442.5	39677	1385	105	0.71	This study
GeoB 10709-5	39.757	17.893	173	²¹⁰ Pb and ¹³⁷ Cs, ¹⁴ C	1.17	400	39817	1465	155	0.74	Zonneveld et al. (2012)
GT89-3 (GT90-3)	39.762	17.897	178	²¹⁰ Pb, ¹³⁷ Cs and Pyroxenes	0.64	-	-	-	-	-	Cini Castagnoli et al. (1990), Bonino et al. (1993)
GT 91-1	39.990	17.757	250								

LSR: Linear sedimentation rate

program OxCal v3.10 (Bronk Ramsey, 2005; 2009), with the references of atmospheric data from Reimer et al., (2004) and the curve Marine04 with the marine data from Hughen et al., (2004) ($\Delta R=121\pm 60$ years).

IV.5.3. Stable oxygen ($\delta^{18}\text{O}$) and carbon ($\delta^{13}\text{C}$) isotopic composition of foraminifera

The sample material of core NU04 was freeze-dried and subsequently wet sieved into size fractions of $>600\mu\text{m}$, $600\text{-}150\mu\text{m}$, $250\text{-}200\mu\text{m}$ and $150\text{-}63\mu\text{m}$. The abundance of *G. ruber* (*pink*) was determined in the size fraction 400 to $300\mu\text{m}$ in all samples.

For the isotopic analyses around 10-20 specimens of *G. ruber* (*white*), *G. ruber* (*pink*) and *U. mediterranea* were picked under the microscope from the fractions $600\mu\text{m}$ to $300\mu\text{m}$. To avoid variations in $\delta^{18}\text{O}$ and $\delta^{13}\text{C}$ caused by different morphotypes for *G. ruber* (*white*), we selected only the morphotype platys (according to the nomenclature of Numberger et al. (2009)). The foraminifera shells were thoroughly cleaned with a procedure modified from Barker et al. (2003) which includes: (i) cracking of the chambers to remove internal filling, (ii) cleaning twice with ultrapure water in an ultrasonic bath for one minute (if necessary repeating this step until the water is clear and no contaminations are visible under the microscope) and (iii) cleaning twice with methanol in an ultrasonic bath for 30 seconds. The cleaning procedure has been chosen after several tests where the efficiency of the procedure was checked by scanning electron microscopy.

All samples were measured with a Thermo Fisher Scientific® Kiel IV carbonate device connected to a Thermo Fisher Scientific® MAT 253 dual inlet mass spectrometer. $150\mu\text{g}$ to $200\mu\text{g}$ of shell material was dissolved in vacuum with two drops of $\sim 103\%$ phosphoric-acid at 70°C , cleaned cryogenically and then transferred to the mass spectrometer. The system is calibrated with the international standards NBS19 ($\delta^{13}\text{C}$ VPDB $+1.95\%$, $\delta^{18}\text{O}$ VPDB -2.2%) and L-SVEC ($\delta^{13}\text{C}$ VPDB -46.6% , $\delta^{18}\text{O}$ VPDB -26.41%). All $\delta^{18}\text{O}$ and $\delta^{13}\text{C}$ results are reported in the conventional delta notation with respect to VPDB. The reproducibility of the $\delta^{18}\text{O}$ and $\delta^{13}\text{C}$ is based on repeated measurements of an internal Carrara marble standard (MS2), a laboratory standard calibrated to the international standards, and was better than 0.1% (1σ). For the temperature reconstruction we used the paleotemperature equation of Shackleton (1974):

$$T=16.9-4.38*(\delta^{18}\text{O}_c-\delta^{18}\text{O}_w)+0.1*(\delta^{18}\text{O}_c-\delta^{18}\text{O}_w) \quad (\text{IV.1})$$

where T is the temperature in °C, $\delta^{18}\text{O}_c$ is the $\delta^{18}\text{O}$ of the carbonate of the shells, and $\delta^{18}\text{O}_w$ is the $\delta^{18}\text{O}$ of the ambient seawater. For the temperature reconstruction based on $\delta^{18}\text{O}$ of *G. ruber (white)* we assume a constant $\delta^{18}\text{O}_w$ of 1.4‰ (the modern water value in the Gulf of Taranto), $\delta^{18}\text{O}_w$ of 1.3‰ for *G. ruber (pink)* and $\delta^{18}\text{O}_w$ of 1.5‰ for *U. mediterranea* (Grauel and Bernasconi, 2010). The $\delta^{18}\text{O}_w$ -values are based on direct water measurements and represent the average value in the Gulf of Taranto at 0-5 m for *G. ruber (pink)*, 0-50 m for *G. ruber (white)* and at the bottom for *U. mediterranea*. Sampling and measurement of the water are described in Grauel and Bernasconi (2010). The data for NU04 are reported in the supplementary Table IV.S1.

IV.5.4. Lipid biomarker analysis

For alkenone, *n*-alkane and GDGT analyses, 1-7 g of freeze dried and homogenized sediment were extracted using an accelerated solvent extractor (ASE 200, DIONEX) with a mixture of dichloromethane (DCM):methanol (MeOH) 9:1 (v/v, three cycles of 5 min each) at 100 °C and 7.6×10^6 Pa. Before extraction known amounts of 2-nonadecanone, *n*-hexatriacontane and C_{46} -GDGT were added as internal standards. The obtained total lipid extracts (TLE) were subdivided into two aliquots for further purification.

For alkenone and *n*-alkane analysis alkenoates were removed by base hydrolysis of the TLE fraction following the procedure described by Elvert et al., (2003). The resulting fraction was separated in DCM-soluble asphaltenes and *n*-hexane-soluble maltenes. The maltenes were desulfurized with activated copper powder and separated by solid phase extraction (Supelco LC-NH₂ glass cartridges; 500 mg sorbent). Four fractions of increasing polarity (hydrocarbons, ketones, alcohols, and fatty acids) were obtained by elution with 4 ml *n*-hexane, 6 ml *n*-hexane:DCM 3:1 (v/v), 7 ml DCM:acetone 9:1 (v/v), and 8 ml 2% formic acid in DCM (v/v). The ketone and hydrocarbon fraction were dissolved in 20 μl *n*-hexane prior to capillary gas chromatography (GC).

Gas chromatography was performed with a Trace GC Gas Chromatograph (ThermoQuest) equipped with a 30 m DB-5MS fused silica capillary column (0.32 mm ID, 0.25 μm film thickness) and a flame ionization detector (FID), He as carrier gas with a flow rate of 1 ml/min. The GC temperature program for alkenones and *n*-alkanes used was: injection at 60 °C, 1 min isothermal; from 60 °C to 150 °C at 15 °C/min; from 150 °C to 310 °C at 4 °C/min; 28 min isothermal with a total oven run-time of 75 min. Peak identification of di- and tri-unsaturated C_{37} alkenones ($\text{C}_{37:2}$ and $\text{C}_{37:3}$) and *n*- C_{27} , *n*- C_{29} and *n*- C_{31} alkanes was based on retention time and comparison with parallel GC-MS runs. Quantification was by peak

integration and by assuming the same response factor as the internal standards (2-nonadecanone and *n*-hexatriacontane). Concentrations of di- and triunsaturated C₃₇ alkenones and *n*-alkanes are given as sum in µg/g dw (dry weight) sediment.

The U^{K'}₃₇ was calculated according to Prahl and Wakeham (1987):

$$U_{37}^{K'} = (C_{37:2}) / ((C_{37:2}) + (C_{37:3})) \quad (\text{IV.2})$$

and converted into SSTs with the sediment core top transfer function of Conte et al. (2006):

$$T = 29.876 * U_{37}^{K'} - 1.334 \quad (r^2 = 0.97, n = 592, SD = 1.1 \text{ } ^\circ\text{C}) \quad (\text{IV.3})$$

Analytical precision of duplicate runs was better than ±0.24 °C.

For GDGT analysis, TLE aliquots were separated by alumina oxide column chromatography (activated Al₂O₃, basic, ~150 mesh, 5.8 nm, Type 5016A, Sigma Aldrich) into an apolar and polar fraction using *n*-hexane:DCM 9:1 (v/v) and DCM:MeOH 1:1 (v/v), respectively. The polar fraction was dried under a stream of nitrogen, weighed and dissolved ultrasonically in *n*-hexane:isopropanol 99:1 (v/v) (Schouten et al., 2009). Analyses were performed by high performance liquid chromatography/atmospheric pressure chemical ionization-mass spectrometry (HPLC/APCI-MS) using an Agilent 1200 series HPLC coupled to an HP 6130 MSD equipped with automatic injector and HP Chemstation software. 10 µl aliquots were injected on to an Alltech Prevail Cyano column (2.1x150 mm, 3 µm; Grace) maintained at 30 °C. GDGTs were eluted using the following gradient with solvent A (*n*-hexane) and solvent B (*n*-hexane:isopropanol, 90:10 (v/v)): A: 100% with a linear gradient to 10% B in 35 min. Flow rate was 0.2 ml/min. After each analysis the column was cleaned by back-flush of solvent B at 0.2 ml/min for 8 min.

Conditions for APCI-MS were as follows: nebulizer pressure 4.1x10⁵ Pa, vaporizer temperature 250 °C, drying gas (N₂) flow 6 l/min and temperature 200 °C, capillary voltage - 3 kV, corona 5 µA. For isoprenoid and non-isoprenoid GDGTs peak integration of their (M+H)⁺ ions (m/z 1302, 1300, 1298, 1296, 1292, 1022, 1036, 1050) detected in selective ion monitoring (SIM) mode was used (Schouten et al., 2007).

The TEX₈₆ ratio was calculated according to Schouten et al. (2002):

$$\text{TEX}_{86} = \frac{[\text{GDGT} - 2] + [\text{GDGT} - 3] + [\text{GDGT} - 4']}{[\text{GDGT} - 1] + [\text{GDGT} - 2] + [\text{GDGT} - 3] + [\text{GDGT} - 4']} \quad (\text{IV.4})$$

where numbers represent the number of cyclopentane moieties and GDGT-4' the crenarchaeol-isomer, respectively. For temperature conversion we used the calibration with annual mean SST using marine sediment core tops based on the $\text{TEX}_{86}^{\text{H}}$, defined as the logarithm of TEX_{86} after Kim et al. (2010):

$$T = 68.4 * \log(\text{TEX}_{86}) + 38.6 \quad (r^2 = 0.86, n = 255, \text{SD} = 2.5 \text{ } ^\circ\text{C}) \quad (\text{IV.5})$$

To examine the potential influence of terrestrial archaeal GDGTs we applied the BIT index (Hopmans et al., 2004):

$$\text{BIT} = \frac{[\text{GDGT - I}] + [\text{GDGT - II}] + [\text{GDGT - III}]}{[\text{GDGT - I}] + [\text{GDGT - II}] + [\text{GDGT - III}] + [\text{GDGT - 4}]} \quad (\text{IV.6})$$

where GDGT-I, -II, and -III represent branched GDGTs with different degrees of methylation and GDGT-4 crenarchaeol. Selected samples were analyzed in duplicate and analytical precision was determined by replicate injections of laboratory internal reference material with known TEX_{86} and BIT values. Mean standard deviation of the corresponding temperature was $\pm 0.4 \text{ } ^\circ\text{C}$. Concentrations of crenarchaeol were calculated assuming a linear response to the C_{46} -GDGT standard. Data for GeoB 10709-4 are given in the supplementary: Table IV.S1.

IV.5.5. Total Organic Carbon (TOC)

Analyses on TOC were performed on 14 samples from GeoB 10709-4 (Table S1). 300 mg of sample was decalcified using 1 M HCl to remove inorganic carbon dried at 60°C and finely ground using an agate mortar. Percentages of organic carbon and nitrogen were determined with a Fisons NCS NA 1500 analyzer using dry combustion at 1030°C with a precision of better than 3%.

IV.6. RESULTS

IV.6.1. Age model

The ^{210}Pb age model shows a sedimentation of 0.85 mm/year for NU04, which is considerably less than the 1.17 mm/year for GeoB10709-5 ($39^\circ 45.39'\text{N}$, $17^\circ 53.57'\text{E}$, 172 m water depth) (Zonneveld et al., 2012) (Table IV.1). The AMS ^{14}C -dating indicates similar

bottom ages for all three multicores, and a lower sedimentation rate for NU04 than for the GeoB-cores, but the differences are still within the error (Table IV.1). Due to the higher uncertainty of the AMS ^{14}C -dates it is not clear if the lower sedimentation rate ($\sim 0.7\text{mm/year}$) is a signal of compaction and lower water content at the bottom of the cores. As the ^{210}Pb data of NU04 and the AMS ^{14}C -dates of the multicores indicate a lower sedimentation rate than estimated by Zonneveld et al. (2012), we additionally compared our $\text{U}^{\text{K}'}_{37}$ record with the $\text{U}^{\text{K}'}_{37}$ record by Versteegh et al. (2007) from an adjacent core in the Gulf of Taranto where a sedimentation rate of 0.64mm/yr was assumed (Cini Castagnoli et al. 1990) (Table IV.1). The comparison of the two $\text{U}^{\text{K}'}_{37}$ records (Fig. IV.6a and b) shows that the best curve fit is obtained when using the age model based on ^{210}Pb dating of NU04 with a sedimentation rate of 0.85mm/year . We therefore decided to discuss the data assuming a fixed sedimentation rate of 0.85mm/year . The 2.5mm and 3mm sampling interval, respectively, corresponds to a temporal resolution <4 years per sample and allows an investigation on decadal timescales.

IV.6.2. Alkenone-derived temperatures ($\text{SST}_{\text{UK}'37}$)

Mean $\text{SST}_{\text{UK}'37}$ is $16.5\text{ }^\circ\text{C}$ and $2.2\text{ }^\circ\text{C}$ lower than the present mean annual SST calculated for the entire 500-year period from 1488 to 2006 (Fig. IV.3a). The $\text{SST}_{\text{UK}'37}$ varies by $5\text{ }^\circ\text{C}$ ($14.6\text{--}19.4\text{ }^\circ\text{C}$) with maxima near 1490, 1580, 1780, 1950 and 2006 and minima near 1540, 1680, 1910 and 1980. $\text{SST}_{\text{UK}'37}$ shows a pronounced decrease of $4.5\text{ }^\circ\text{C}$ from 1488 to 1550. The period from 1620 to 1720 shows relatively low $\text{SST}_{\text{UK}'37}$ followed by a maximum increase of $3\text{ }^\circ\text{C}$ to 1780. From 1800 to present a long-term decrease in $\text{SST}_{\text{UK}'37}$ is superimposed by 2 to $3\text{ }^\circ\text{C}$ shifts.

IV.6.3. GDGT-derived temperatures ($\text{SST}_{\text{TEXH86}}$)

Mean $\text{SST}_{\text{TEXH86}}$ is $20.5\text{ }^\circ\text{C}$ and in general higher than the $\text{SST}_{\text{UK}'37}$ and $1.8\text{ }^\circ\text{C}$ higher than the present mean annual SST (Fig. IV.3b). $\text{SST}_{\text{TEXH86}}$ varies by $4\text{ }^\circ\text{C}$ ($18.7\text{--}22.6\text{ }^\circ\text{C}$) with maxima between 1488 and 1520 and from 1660 to 1800. The $\text{SST}_{\text{TEXH86}}$ are $3\text{ }^\circ\text{C}$ lower from 1520 to 1540. Like the $\text{SST}_{\text{UK}'37}$, the $\text{SST}_{\text{TEXH86}}$ decreases from 1800, the $3\text{ }^\circ\text{C}$ decrease is more pronounced than for the $\text{SST}_{\text{UK}'37}$. Comparison of the 5-years running means shows that the decadal trends in $\text{SST}_{\text{TEXH86}}$ are synchronous to those of $\text{SST}_{\text{UK}'37}$ from 1860 AD to present, but show a smaller amplitude. $\text{SST}_{\text{TEXH86}}$ and $\text{SST}_{\text{UK}'37}$ anti-correlate between 1560 and 1720. Nevertheless, a clear linear correlation between both records is apparent upon cross-plotting their smoothed records (Fig. 4a).

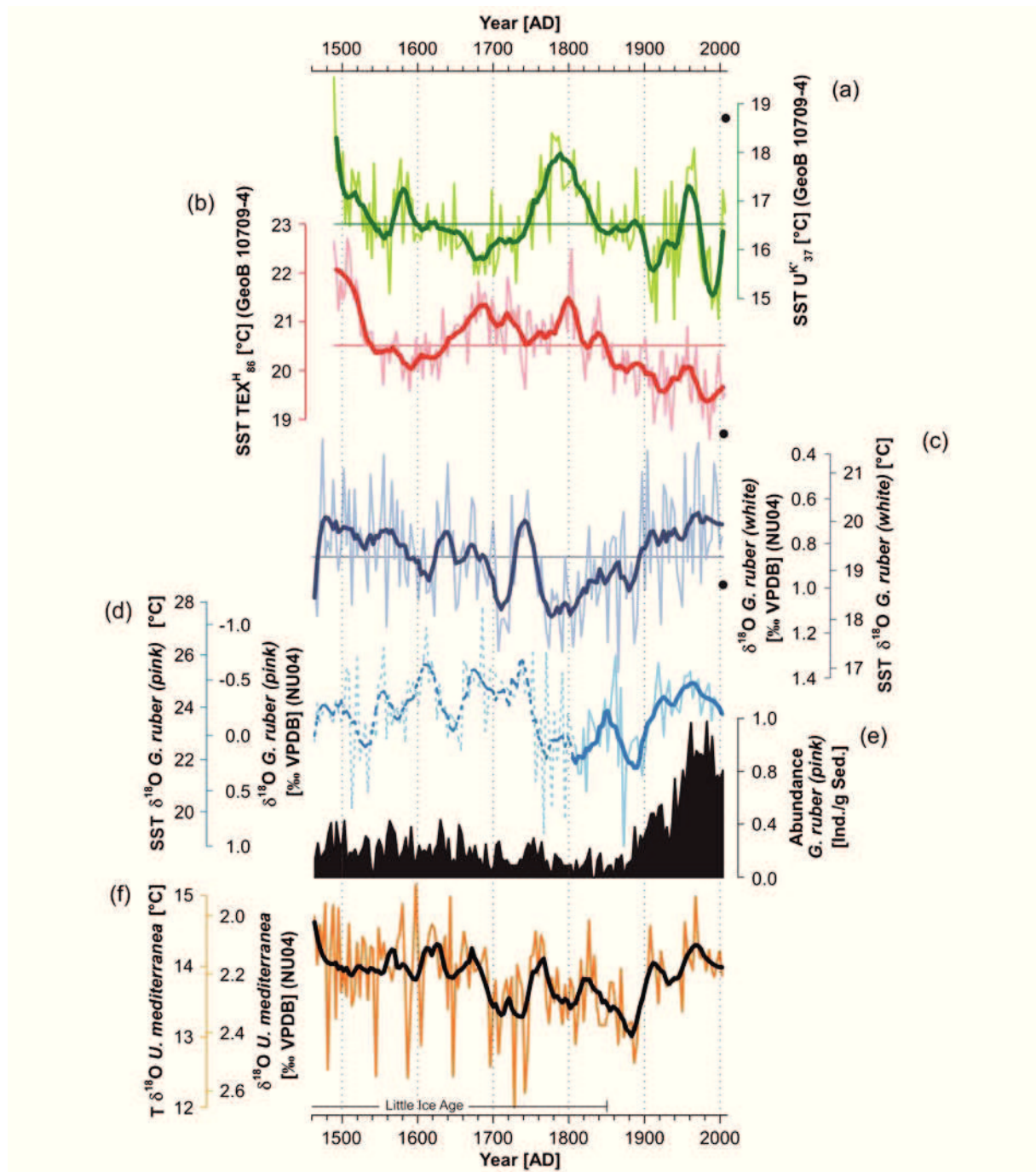


Figure IV.3. Temperature reconstructions in the Gulf of Taranto based on organic and inorganic geochemical proxies for the last 500 years. (a) $SST_{UK^{37}}$ and (b) $SST_{TEX^{H86}}$ records in GeoB 10709-4 are based on the calibration from Conte et al. (2006) and Kim et al. (2010), respectively. Errors of temperature estimate based on the calibration of Conte et al. (2006) and Kim et al. (2010) are 1.1 °C and 2.5 °C. (c) $\delta^{18}O$ record and corresponding SSTs of *G. ruber* (white) and (d) *G. ruber* (pink); dashed curves represent interval with disregarded data due to low abundances of *G. ruber* (pink), (e) abundances of *G. ruber* (pink) and (f) $\delta^{18}O$ record and corresponding temperatures of *U. mediterranea* in NU04. Horizontal lines indicate averaged values of the investigated time interval. Filled circles represent present mean annual SSTs in the Gulf of Taranto compiled from SeaWiFS satellite data for 2002-2006 (Zonneveld et al., 2009). Thin curves indicate raw data. Thick curves represent a polynomial smoothing.

IV.6.4. $\delta^{18}\text{O}$ -based temperatures and abundance of foraminifera

The $\delta^{18}\text{O}$ of *G. ruber (white)* varies between 0.34‰ to 1.4‰ with a mean value of 0.86 ± 0.23 ‰, resulting in a temperature range from 15.9 to 21.7 °C with an average temperature of 19.3 ± 1 °C (Fig. IV.3c) using a $\delta^{18}\text{O}$ of the water of 1.4‰. A maximum increase in $\delta^{18}\text{O}$ of 0.96‰ occurs from 1463 to 1800, while $\delta^{18}\text{O}$ values decrease from 1800 onward. The highest $\delta^{18}\text{O}$ values are observed from 1601-1622, 1707-1717, 1774-1806 and 1866-1887, whereas lower $\delta^{18}\text{O}$ values are from 1500-1580, 1626-1640, 1724-1753 and from 1901 onward. The variability of short-term shifts in $\text{SST}_{\delta^{18}\text{O}}$ of *G. ruber (white)* appears higher than in the $\text{SST}_{\text{UK}'37}$ and $\text{SST}_{\text{TEXH86}}$. Additionally, the smoothed $\text{SST}_{\delta^{18}\text{O}}$ record of *G. ruber (white)* significantly anti-correlates with $\text{SST}_{\text{UK}'37}$ and $\text{SST}_{\text{TEXH86}}$, (Fig. IV.4b and c).

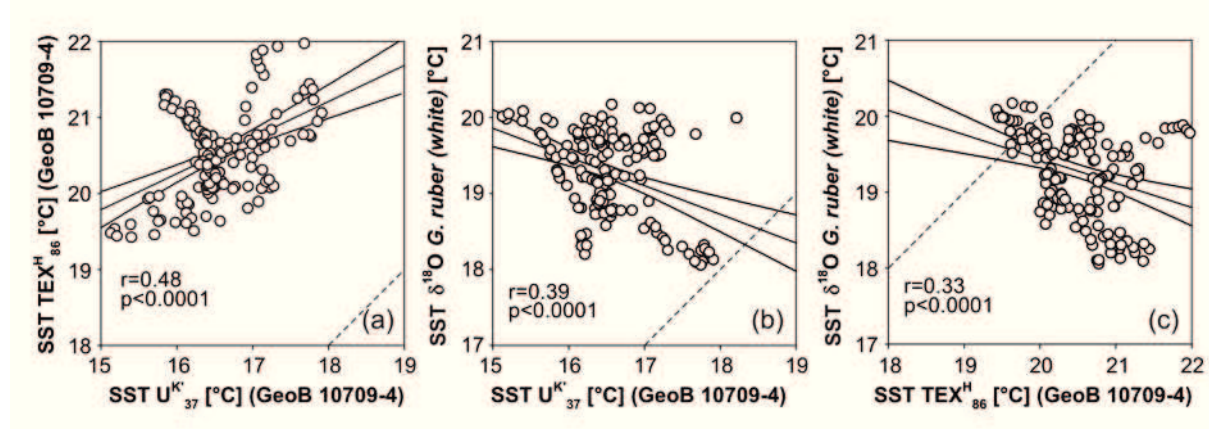


Figure IV.4. Correlations between the different SST proxies in GeoB 10709-4 and NU04 during the last 500 years. (a) $\text{SST}_{\text{UK}'37}$ and $\text{SST}_{\text{TEXH86}}$, (b) $\text{SST}_{\text{UK}'37}$ and $\text{SST}_{\delta^{18}\text{O}}$ of *G. ruber (white)* and (c) $\text{SST}_{\text{TEXH86}}$ and $\text{SST}_{\delta^{18}\text{O}}$ of *G. ruber (white)*. Open circles indicate data derived after polynomial smoothing for intercomparison of cores GeoB 10709-4 and NU04. Solid curves give linear regression and 95% confidence interval. Dashed lines indicate 1:1 line.

The $\delta^{18}\text{O}$ of *G. ruber (pink)* shows a clear offset in $\delta^{18}\text{O}$ of ~ 1 ‰ compared to the $\delta^{18}\text{O}$ of *G. ruber (white)* resulting in higher reconstructed average temperatures of 23.8 ± 2 °C (Fig. IV.3d) using a $\delta^{18}\text{O}$ of the water of 1.3‰. $\delta^{18}\text{O}$ values vary between -1.14‰ to 1.0‰ and show a larger scatter than the $\delta^{18}\text{O}$ of *G. ruber (white)*. *G. ruber (pink)* is almost absent during the LIA, therefore $\delta^{18}\text{O}$ values of *G. ruber (pink)* before 1800 are not included in the discussion (Fig. IV.3g). The total abundance of *G. ruber (pink)* considerably increases at the end of the 19th century coinciding with the decrease in $\delta^{18}\text{O}$ of *G. ruber (white)* and *U. mediterranea*.

The $\delta^{18}\text{O}$ of the benthic species *U. mediterranea* varies between 1.8 and 2.6‰, which corresponds to a temperature range of 12 to 15.2 °C (Fig. IV.3f) (using a $\delta^{18}\text{O}$ of the water of 1.5‰). Between 1663 and 1689 and from 1904 onward the $\delta^{18}\text{O}$ are relatively constant (2.16 ± 0.14 ‰ and 2.17 ± 0.08 ‰, respectively). A maximum increase in $\delta^{18}\text{O}$ occurs between

1696 and 1742 ($2.34 \pm 0.16\text{‰}$), 1774 and 1809 ($2.29 \pm 0.08\text{‰}$), and 1866 and 1890 ($2.39 \pm 0.1\text{‰}$).

IV.6.5. The $\delta^{13}\text{C}$ of *G. ruber* (white and pink) and *U. mediterranea*

The $\delta^{13}\text{C}$ of *G. ruber* (white and pink) decreases over the whole period and varies between 0-1.03‰ and 0.34-1.46‰, respectively (Fig. IV.5a and b). The $\delta^{13}\text{C}$ of *U. mediterranea* decreases over the whole period (-0.45-0.5‰) but changes markedly to lower values from 1850/1900 onward (Fig. 5c). Overall the $\delta^{13}\text{C}$ of *G. ruber* (white) and the *U. mediterranea* decrease around 0.2‰ during the last 200 years.

IV.6.6. TOC, biomarker concentrations and BIT index

TOC values vary between 0.8 to 1.4% and increase from ~1800 (Fig. IV.5d). Lowest concentrations of summed di- and triunsaturated alkenones (0.03 to 0.14 $\mu\text{g/g}$ dry sediment) occur from 1488 to 1820 and are followed by a first increase to 0.27 $\mu\text{g/g}$ until 1940 (Fig. IV.5e). The last decades show rapid increases in concentrations reaching maximum values of 1.69 and 2.25 $\mu\text{g/g}$. Lowest crenarchaeol concentrations (0.07 to 0.13 ng/g dry sediment) occur from 1488 to 1800 and are followed by an increase to 0.27 ng/g (Fig. IV.5f). BIT index values vary between 0.12 and 0.34, with almost constant values of 0.3 from 1488 to 1800 and are followed by a decrease to minimum values (Fig. IV.5g). Concentrations of the summed *n*- C_{27} , *n*- C_{29} and *n*- C_{31} alkanes (*n*- C_{27-31} alkanes) range between 0.31 and 1.37 $\mu\text{g/g}$ dry sediment (Fig. IV.5h). Major variations occur between 1500 and 1600. Concentrations show a maximum between 1800 and 1900 and increase again during the 20th century. This pattern is similar to the decrease in $\delta^{13}\text{C}$ of *U. mediterranea* starting between 1800 and 1900. Additionally, concentrations of *n*- C_{27-31} alkanes and BIT index values show an opposite trend from 1800.

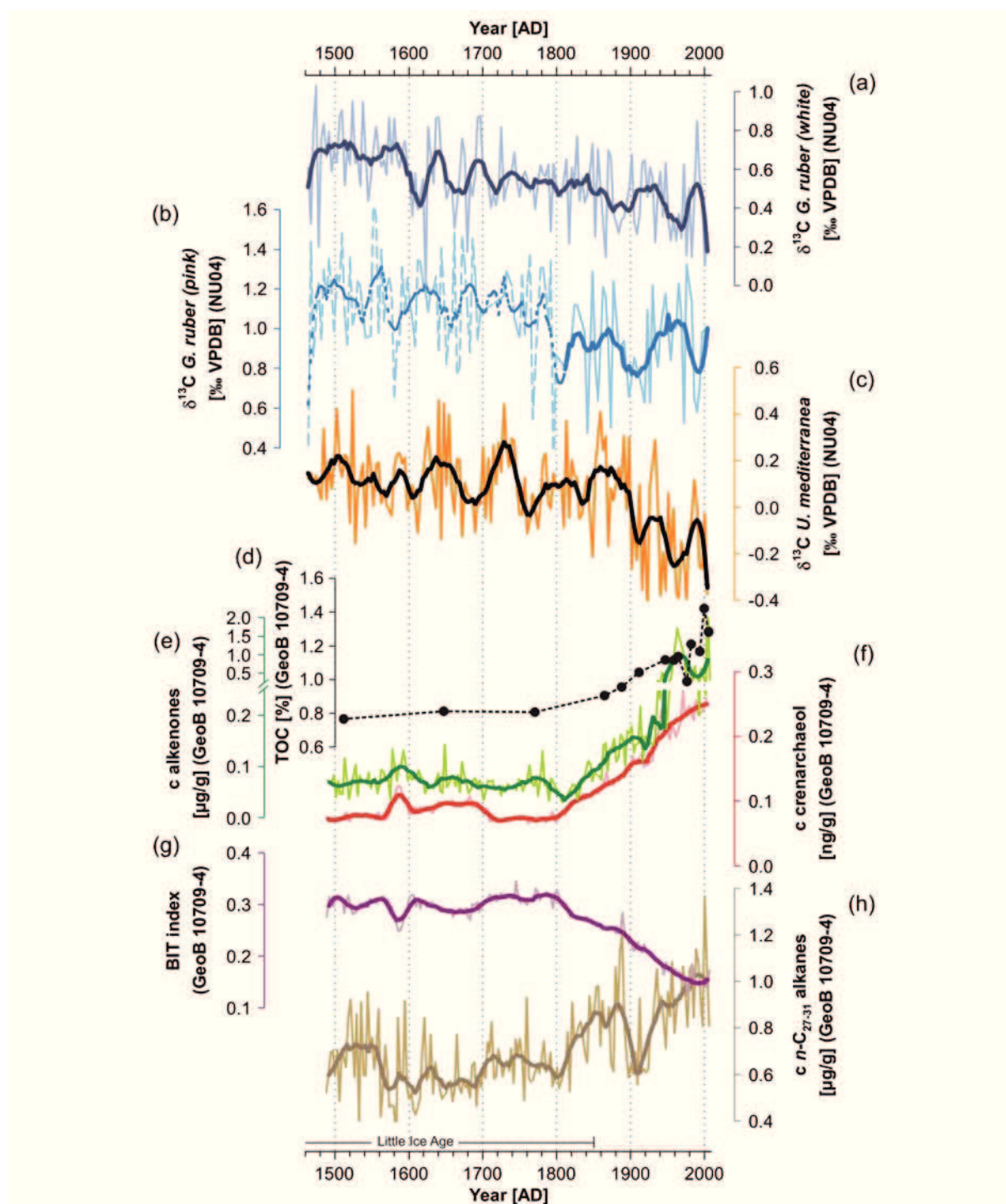


Figure IV.5. Variations in $\delta^{13}\text{C}$ of (a) *G. ruber* (white), (b) *G. ruber* (pink) and (c) *U. mediterranea* in NU04. (d) Total Organic Carbon (TOC), (e) Concentrations of summed di- and triunsaturated alkenones and (f) crenarchaeol for GeoB 10709-4. Note the axis break in concentrations of alkenones. (g) BIT index and (h) concentrations of summed $n\text{-C}_{27}$, C_{29} and C_{31} alkanes for GeoB 10709-4. Thin curves indicate raw data. Thick curves represent a polynomial smoothing.

IV.7. DISCUSSION

Among the potential uncertainties of each proxy used in this study are biases due to the near coastal environment of the study site which imposes seasonally highly variable terrestrial and marine inputs. Therefore biases may derive from past salinity variations, changes in terrestrial input or nutrient availability. Accordingly, the proxies may reflect SSTs on a seasonal scale but also circulation changes, e.g., shifts between wetter and drier conditions along the southern Italian coast. In the following, we will discuss the seasonal climate history and environmental evolution since 1460 AD in the Gulf of Taranto.

IV.7.1. SST proxy records and climatic forcing of the marine environment in the Gulf of Taranto

IV.7.1.1. Variability in SST_{UK'37} and SST_{TEXH86}

Our SST_{UK'37} record is from the same location as the upper part (from core GT89-3) of the composite SST_{UK'37} record by Versteegh et al. (2007). Both records agree well in peak timing and amplitude, which demonstrates the robustness of our methods and justifies the higher sedimentation rate for our core (Fig. IV.6a and b). In contrast, major discrepancies occur with the lower part of the composite record which is from core GT91-1. This latter core is located ~30 km NNW from GeoB 10709-4 and the age model of GT91-1 assumes the same sedimentation rate as for GT89-3, a hypothesis that can be rejected on the basis of more detailed analyses since Goudeau et al. (subm.). The core top calibration in the Gulf of Taranto shows that SST_{UK'37} are below the annual mean SST which reflects that in this region the alkenone producing haptophytes produce primarily during the colder part of the year (Leider et al., 2010). This derives from the dominant nutrient delivery by the WAC and vertical mixing during the colder seasons (Leider et al., 2010). The mean SST_{UK'37} of core GeoB 10709-4 (16.5 °C) is close to the core top calibration (16.3 °C) so that there is no long term trend in either winter temperatures or seasonal timing of alkenone production during the last 500 years. However, decadal to centennial deviations from this mean value occur and their amplitude is much larger than observed for other reconstructions of Mediterranean climate (Brunetti et al., 2004; Camuffo et al., 2010) (Fig. IV.6c and d). Today's SST vary from 13 to 18 °C between late autumn and late spring (Fig. 1), which covers the entire amplitude of our SST_{UK'37} record. This implies that apart from climatic changes in the winter temperatures,

shifts in the timing of alkenone production could also substantially modify the SST_{UK'37}. Higher SST_{UK'37} can be achieved with alkenone production starting earlier in autumn and/or extending into late spring - early summer whereas lower SST_{UK'37} may be recorded when alkenone production is restricted to winter. Such shifts in winter primary production, to which alkenone production is closely tied, do occur indeed (Versteegh et al., 2007). Covariance between timing of alkenone production and winter temperature may amplify the amplitude of the SST_{UK'37} record if the main period of alkenone production gets increasingly focused to the coldest part of the year when winters get colder (Versteegh et al., 2007).

The SST_{UK'37} record corresponds well to the mean annual temperature anomalies of S Italy based on instrumental data since 1850 (Brunetti et al., 2004) and to mean annual air temperature reconstructions from 1500 extracted from the Northern Hemisphere air temperature grid (Luterbacher et al., 2004) (Fig. IV.6d and e). The comparison to the Luterbacher et al. (2004) data shows that the SST_{UK'37} records the major variations in mean annual air temperature during the LIA. Most pronounced are a stable phase of low SST_{UK'37} at ~1700 co-occurring with the Maunder Minimum (suggested to be the coldest period of the LIA in Europe) and the broad temperature maximum around 1800. During the late 20th century the SST_{UK'37} record seems to lag behind the increase in air temperature which may be due to uncertainties in the age model. Major discrepancies occur prior to 1660 which might be due to the increasing uncertainty of the local air temperature reconstructions (Luterbacher et al., 2006). This does not inevitably indicate that SST_{UK'37} reflects mean annual SSTs as mean annual and seasonal temperatures are interdependent (e.g., Brunetti et al., 2000). Furthermore, maximum amplitudes of winter and mean annual air temperatures are too small to solely explain the variations in SST_{UK'37}. Thus, the SST_{UK'37} record reflects the climatic temperature changes, it only has a larger amplitude, which indeed suggests that an amplifying mechanism exists.

Primary productivity is stimulated by a combination of light and nutrients. As such it may be stimulated by wind induced vertical mixing which increases nutrients in the photic zone (e.g., Klein and Coste, 1994; Bakun and Agostini, 2001; Boldrin et al., 2002; Katara et al., 2010). Additionally, the nutrient content can increase due to increased river runoff. In the Adriatic, this leads to a southward extension of the WAC and an increased WAC influence in the Gulf of Taranto. Low-pressure systems bring both wind (turbulence) and rainfall and their dynamics may thus be considered of particular interest. Historical records indicate more late autumn to winter storms in the Adriatic Sea and a higher flooding intensity at the Venice lagoon during the first half of the 1500s and late 1700s (Camuffo et al., 2000) (Fig. IV.6f).

Both periods also show maxima in $SST_{UK'37}$ in the Gulf of Taranto. Furthermore, flooding is more frequent during the late 20th century, while the variability in $SST_{UK'37}$ increases, again indicating that $SST_{UK'37}$ is modulated by storm activity. Storm activity and surges can partly be related to increased relative sea level as a result of Sirocco and Bora winds or intense cyclones in the NW Mediterranean (Camuffo et al., 2000; Lionello et al., 2006). Additionally, southern Italy is a local centre of cyclogenesis during winter (Trigo et al., 1999).

Storm frequency and cyclogenesis in the Mediterranean winter is modulated by the North Atlantic Oscillation (NAO); the pressure gradient between the Azores and Iceland (Hurrell, 1995; Hurrell and van Loon, 1997). In general, the NAO exerts a strong influence on cold season temperature and precipitation in the Mediterranean region, though the strength varies spatially (Dünkeloh and Jacobeit, 2003; Xoplaki et al., 2004; Trigo et al., 2006). Periods of negative NAO, show a weakening of the mid-latitude westerlies causing a southward shift of North Atlantic storm tracks into the Mediterranean region. As may be expected, a negative NAO correlates with more precipitation in Italy and the western Mediterranean (Hurrell and van Loon, 1997; Quadrelli et al., 2001; Brunetti et al., 2002; Mariotti et al., 2002; Trigo et al., 2003) and with higher river discharge across most of the Mediterranean catchment basin during the 20th century also for the Po River (Struglia et al., 2004; Supić et al., 2004; Zanchettin et al., 2008). In the middle Adriatic Sea a negative NAO correlates with higher chlorophyll-a concentrations during spring, and since chlorophyll-a correlates well with alkenone production, this suggests that a negative NAO leads to more intense alkenone production during the warmer and final part of the colder season. A mechanism may be that a negative NAO leads to more snow in the Alps and Apennines which induces a more intense and longer lasting meltwater pulse in the Adriatic Sea and a stronger WAC influence in the Gulf of Taranto, extending the periods of high phytoplankton productivity. This may explain higher $SST_{UK'37}$ when the reconstructed winter NAO is in a negative mode (Luterbacher et al., 2002) (Fig. IV.6g). During a positive NAO central and southern Europe and the Mediterranean are drier, while northern Europe experience wetter conditions (Hurrell, 1995). A positive NAO implies a less turbulent cold season. This may lead to a later breakdown of the summer stratification and earlier stratification in spring, both restricting the alkenone production to the cooler part of winter, resulting in a lower $SST_{UK'37}$. Indeed primary productivity during winter is higher when the NAO is in a positive mode (Ninčević Gladan et al., 2010). Although, this mechanism explains the high variability in $SST_{UK'37}$ it does not seem to be valid for the Maunder Minimum, where low $SST_{UK'37}$ are associated with a

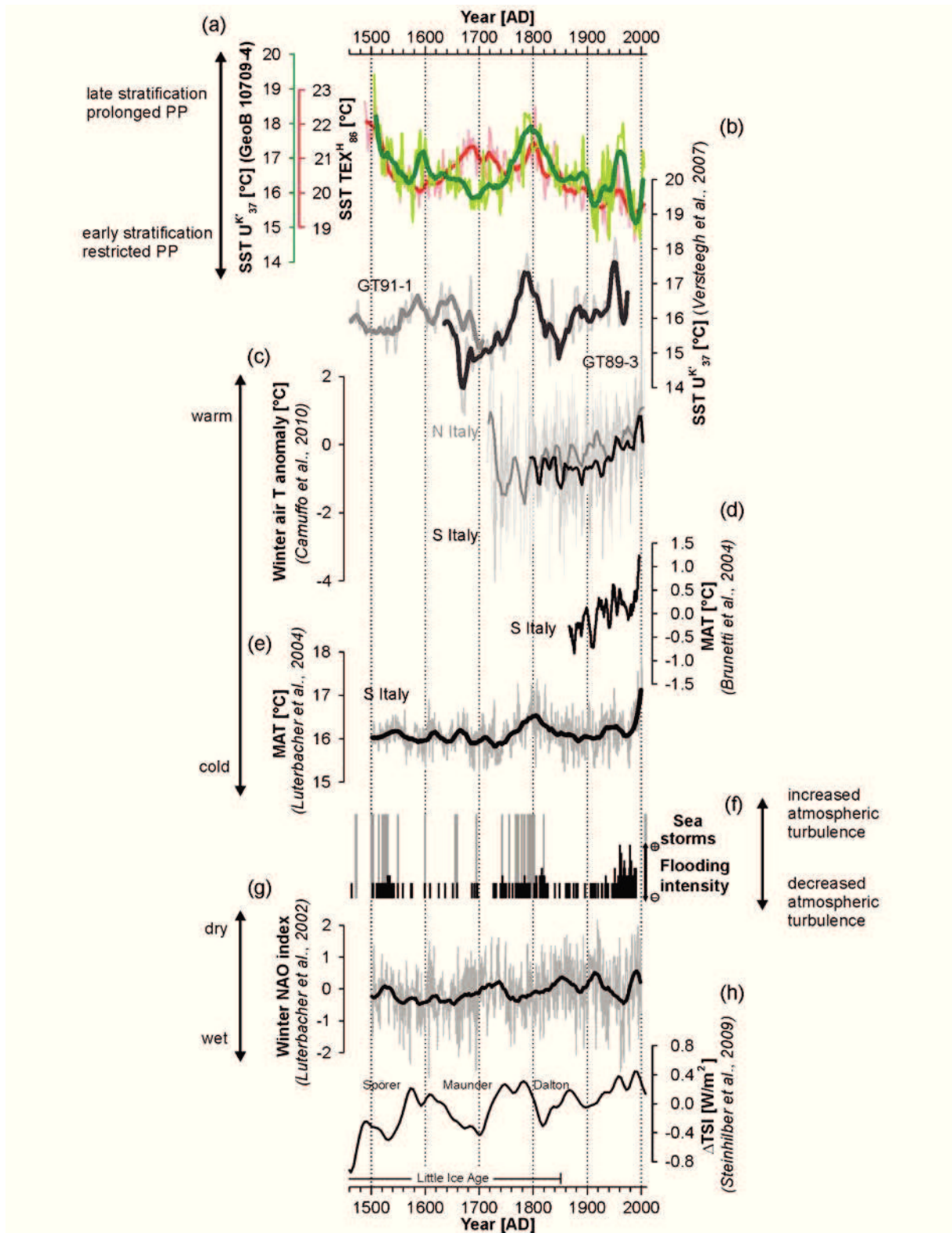


Figure IV.6. SSTs based on $U^{K'_{37}}$ ($SST_{UK'37}$) and $TEX^{H_{86}}$ (SST_{TEXH86}) in (a) GeoB 10709-4 and comparison to climate records during the last 500 years. (b) $SST_{UK'37}$ record from near-by cores in the Gulf of Taranto (Versteegh et al., 2007). (c) Winter air temperature anomaly for N and S Italy (anomalies from reference period 1961-1990, Camuffo et al., 2010). (d) Mean annual air temperature (MAT) of S Italy (5-year running means of yearly anomalies, Brunetti et al., 2004) and (e) MAT of S Italy extracted from the Northern Hemisphere grid from Luterbacher et al. (2004) (for the region 39.5°N/18.0°E – 40°N/18.5°E; accessible at <http://climexp.knmi.nl>). (f) Frequency of seas storms in the Adriatic Sea and flooding intensity of the Venice lagoon from historical data (Camuffo et al., 2000). (g) Winter North Atlantic Oscillation (NAO) index

(Luterbacher et al., 2002). (h) Reconstructed Total Solar Irradiation (TSI) and phases of solar minima (relative to 1986, Steinhilber et al., 2009).

negative winter NAO. During the Maunder Minimum, a negative NAO occurred more frequently. This is partly explained by a reduced solar irradiance (Rind et al., 2004; Shindell et al., 2001) (Fig. IV.6h). In the Mediterranean, the Maunder Minimum is wet and has exceptionally low air temperatures (Luterbacher et al., 2006). Here, a general decrease in SSTs may have overruled the prolonged production season, e.g. while autumn and spring waters were also much cooler than outside the Maunder Minimum.

We are aware that the NAO forcing alone does not affect the Mediterranean climate. Further its interaction may not be stationary during the last 500 years (Luterbacher et al., 2006; Roberts et al., 2012; Trigo et al., 2006). Nonetheless, we observe that the SST_{UK'37} reflects multidecadal variations in winter NAO and reveals a link between productivity modulations in the Gulf of Taranto and the atmospheric circulation of the Northern Hemisphere.

The SST_{TEXH86} are 2-6 °C higher than the SST_{UK'37} record. This is consistent with the core tops calibration which demonstrated that the TEX₈₆ reflects summer SST (Leider et al., 2010). This has also been observed in other regions of the Mediterranean Sea (Menzel et al., 2006; Castañeda et al., 2010; Huguet et al., 2011). The co-variation between SST_{TEXH86} and SST_{UK'37} over large parts of the record might be related to the negative correlation between crenarchaeotal abundance and phytoplankton as reported in several studies (Fig. IV.6a) (e.g., Murray et al., 1999; Wuchter et al., 2006b). This has been explained by suggesting that phytoplankton outcompetes crenarchaeota when productivity is high so that the latter are restricted to warmer parts of the year when the waters are stratified. In case higher SST_{UK'37} during the last 500 year reflect an extension of the main algal primary production period this automatically implies that planktonic crenarchaeotal production is further shifted to the more oligotrophic and warmer summer season, resulting in higher SST_{TEXH86}. In contrast, when algal primary production is confined to the colder parts of the year (low SST_{UK'37}), archaeal growth may already occur during spring and continue into late autumn when SSTs are lower, resulting in lower SST_{TEXH86}.

During the Maunder Minimum this relationship breaks down, the difference between the temperature proxies increases suggesting a larger seasonal contrast (Fig. IV.6a). As described previously, this period is characterized by low air temperatures and increased precipitation during winter, which results in a decrease of SST_{UK'37} despite a longer season of alkenone production. This may reflect an increased seasonality between haptophyte and planktonic crenarchaeota presumably indicating a more dominant influence of ISW compared to WAC during this period.

Thus, we suggest that variations in $SST_{UK'37}$ point to differences in the timing of haptophyte production and primary productivity. This simultaneously modulates archaeal production explaining the covariance between $SST_{UK'37}$ and SST_{TEXH86} . Here, the seasonal differences in water column characteristics modulated by atmospheric circulation may play a more important role for the haptophyte production resulting in an integrated productivity temperature signal.

IV.7.1.2. $SST_{\delta 180}$ of *G. ruber* (white) and SST_{TEXH86}

The reconstructed mean $SST_{\delta 180}$ of *G. ruber* (white) of 19.3 ± 1 °C is very close to the mean annual SST in the Gulf of Taranto. The $SST_{\delta 180}$ of *G. ruber* (white) of 20 ± 1 °C observed in the top part (first cm) of core NU04 is in good agreement with the value based on surface sediments (20.3 °C; first cm) from the Gulf of Taranto (Grauel and Bernasconi, 2010). SST_{TEXH86} shows even higher values, while the top part of the core is in the same range compared to $SST_{\delta 180}$ of *G. ruber* (white). In general, this supports that both SST proxies indicate summer conditions, but trends observed during the last 500 years are considerably different.

The LIA is characterized by a higher climate variability with wetter and colder conditions in northern- and drier summer conditions in southern Europe, but no significant temperature changes (~ 0.4 °C during summer) (Mann et al., 2002; Luterbacher et al., 2004; Raible et al., 2006; Hegerl et al., 2011). Compared to model simulations over the last 500 years the $SST_{\delta 180}$ of *G. ruber* (white) and SST_{TEXH86} scatter around 6 °C and 4 °C, respectively, which is too much for being a pure temperature signal. Furthermore, a negative correlation between $SST_{\delta 180}$ of *G. ruber* (white) and SST_{TEXH86} is observed over large parts of the record (Fig. IV.7a and c). The local core-top calibration showed that the $\delta^{18}O$ of *G. ruber* (white) is influenced by salinity changes in the Gulf of Taranto (Grauel and Bernasconi, 2010). Hence, higher $\delta^{18}O$ values of *G. ruber* (white) could indicate drier conditions due to evaporation and a possibly less intense WAC. Additionally, the core-top calibration determined that the $\delta^{13}C$ of *U. mediterranea* is a good indicator to detect water mass characteristics, e.g. nutrient content and salinity, and their variations along the southern Italian coast (Grauel and Bernasconi, 2010). Today, the coastal areas along the southern Italian coast are influenced by the less saline, nutrient-rich WAC. Thus, the $\delta^{13}C$ and $\delta^{18}O$ of *G. ruber* (white) and *U. mediterranea* increase with distance from the coast due to higher salinity and less nutrients (Grauel and Bernasconi, 2010). Therefore, a reduced influence of the WAC in the Gulf of Taranto could cause heavier $\delta^{13}C$ and $\delta^{18}O$ values of both species and moreover signalize a

higher influence of the ISW and LIW. In this respect, the core top calibration of SST_{TEXH86} showed that SST_{TEXH86} increase with distance to the coast reaching maximum temperatures in the ISW (Leider et al., 2010). Accordingly, heavier $\delta^{18}\text{O}$ values of *G. ruber (white)* associated with higher SST_{TEXH86} support a higher influence of the ISW compared to WAC and the negative correlation suggests that shifts in the relative contribution of water masses in the Gulf of Taranto occurred more regularly.

The reconstructed SST _{$\delta^{18}\text{O}$} of *G. ruber (white)* indicate a general cooling of ~2-3 °C with a high variability from 1460 to 1700 (Fig. IV.7a). This trend is comparable with tree ring data from the European Alps which indicate a prolonged summer cooling (~2 °C) between 1350 and 1700 (Büntgen et al., 2006). The $\delta^{18}\text{O}$ record of *G. ruber (white)* shows a trend to heavier $\delta^{18}\text{O}$ during the Spörer Minimum (1460-1550) (Fig. IV.7i). Around 1530 to 1600 lighter $\delta^{18}\text{O}$ values of *G. ruber (white)* suggest warmer and/or wetter conditions which are associated with a decrease in $\delta^{13}\text{C}$ of *U. mediterranea* (Fig. IV.7e). The $\delta^{18}\text{O}$ record of *G. ruber (white)* shows lower temperatures around 1600 and in the first phase of the Maunder Minimum (1645-1655) (Fig. IV.7i). The sharp increase in $\delta^{18}\text{O}$ suggests a negative temperature anomaly of over 1 °C and/or extremely dry conditions around 1710 coinciding with the Late Maunder Minimum (1675-1715) representing the climax of the LIA accompanied by persisting cold conditions over Europe (Luterbacher et al., 2001). Simultaneously, a maximum in SST_{TEXH86} suggests an increased contribution of the ISW (Fig. IV.7c). Regarding the $\delta^{18}\text{O}$ and $\delta^{13}\text{C}$ records of *U. mediterranea* we observe an increase to higher values (1698-1742) which additionally supports the potentially higher influence of Ionian Sea water masses in the Gulf

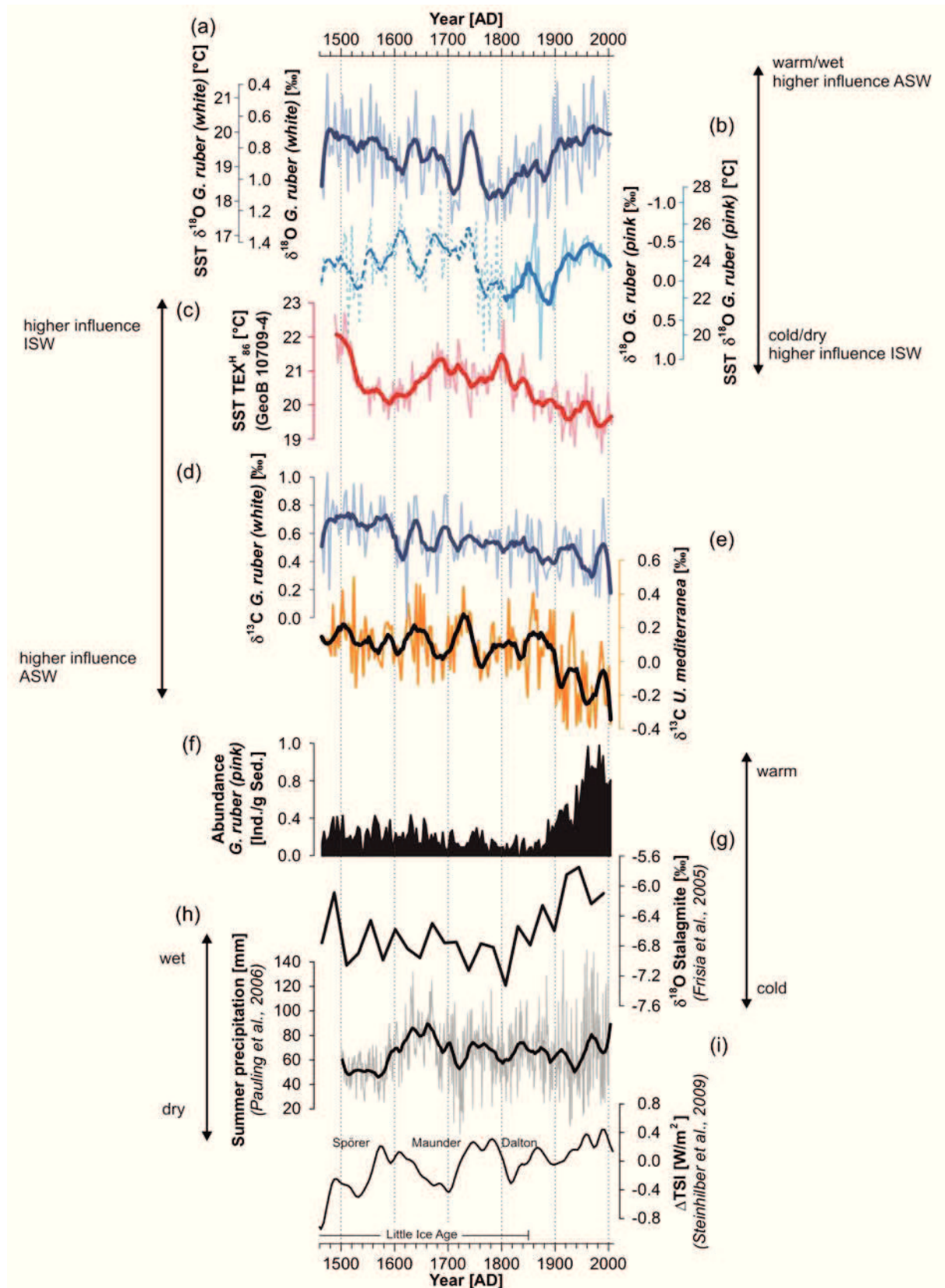


Figure IV.7. $\delta^{18}\text{O}$ record of *G. ruber* (white) in (a), $\delta^{18}\text{O}$ record of *G. ruber* (pink) in (b), SST_{TEX₈₆^H} (c), $\delta^{13}\text{C}$ record of *G. ruber* (white) in (d), $\delta^{13}\text{C}$ record of *U. mediterranea* in (e) and total abundance of *G. ruber* (pink) in (f) of NU04 and comparison to climate records during the last 500 years. (g) $\delta^{18}\text{O}$ stalagmite record from the SE Alps of Italy by Frisia et al. (2005). (h) Summer precipitation (June-July-August) of S Italy (Pauling et al., 2006) extracted from the Northern Hemisphere grid from Luterbacher et al. (2004) (for the region 39°75N/17°75E; accessible at <http://climexp.knmi.nl>). (i) Reconstructed Total Solar Irradiation (TSI) and phases of solar minima (relative to 1986, Steinhilber et al., 2009).

of Taranto that affects the entire water column (Fig. IV.3f and IV.5c). This is followed by a warmer and/or wetter phase ~1730/40 as indicated by the decrease in $\delta^{18}\text{O}$ record of *G. ruber* (*white*) and $\text{SST}_{\text{TEXH86}}$ both suggesting a decrease in the relative contribution of the ISW. However, the still higher $\delta^{18}\text{O}$ values of *U. mediterranea* possibly indicate a decoupling of surface and bottom water masses during this time period.

Mann (2009) described the 17th century in Europe as being the coldest during the LIA, while the $\delta^{18}\text{O}$ record shows the highest variability during this time period and the trend to lower $\delta^{18}\text{O}$ values of *G. ruber* (*white*) possibly indicating wetter conditions rather than higher SSTs, especially from 1630-1650 and the beginning of the Maunder Minimum (1670-1690). Additionally, the lighter $\delta^{13}\text{C}$ values of *U. mediterranea* suggest an increased influence of the WAC during the first phase of the Maunder Minimum possibly related to higher precipitation in the Alps and thus a higher Po discharge. Indeed, the summer precipitation (June-July-August) shows a maximum between 1580 and 1710 (Pauling et al., 2006) (Fig. IV.7h), and Holzhauser et al. (2005) described a glacier maximum around 1640 to 1670 due to low winter and summer temperatures and summer snow fall in the high Alps. The warmer and/or wetter phase ~1730/40 suggesting a decrease in ISW coincides with a glacier retreat in the Alps (Holzhauser et al., 2005). The high variability between wet and dry conditions has also been described by Dominguez-Castro et al. (2008) who characterized the 17th and 18th century as a period where floods and droughts alternate quickly in Central Spain. Between 1750 and 1810 the $\delta^{18}\text{O}$ record of *G. ruber* (*white*) shows a relatively stable phase. The higher $\delta^{18}\text{O}$ values and maximum in $\text{SST}_{\text{TEXH86}}$ are possibly due to a higher influence of the ISW indicating drier conditions (Fig. IV.7a and c). This can be observed in the higher $\delta^{18}\text{O}$ values of *U. mediterranea* (~1774-1809) as well indicating a higher influence of Ionian Sea water masses (Fig. IV.3f). Kress et al. (2010) reconstructed extremely dry summers during the second half of the 18th century from Alpine tree ring stable isotopes and Büntgen et al. (2006) reconstructed a temperature depression around 1810-20 from their tree ring data from the European Alps. This coincides with the Dalton Minimum (1790-1830). However, compared to our record the dry period lasts much longer (1760-1810) than the Dalton Minimum (Fig. IV.7i).

The trend to heavier $\delta^{18}\text{O}$ values of *G. ruber* (*white*) between 1860 and 1880 with a maximum ~1880 indicates colder and/or drier conditions which can be associated with the last glacier advance in the European Alps around this time (1855 to 1860) before the onset of the glacier retreat to today's conditions (Holzhauser et al., 2005). Coevally the $\delta^{18}\text{O}$ values of *U. mediterranea* indicate higher values suggesting a higher influence from the Ionian Sea water

masses also in the deeper layers of the water column. Since 1900 the decrease in $\delta^{18}\text{O}$ of *G. ruber (white)* co-occurs with the decrease in $\delta^{13}\text{C}$ of *U. mediterranea* and *G. ruber (white)* suggesting an enhanced nutrient supply by the WAC. This is also reflected by a decrease in $\text{SST}_{\text{TEXH86}}$ and with the general increasing trend of the different lipid biomarker concentrations, (Fig. IV.5; see discussion IV.7.2). The comparison of the $\delta^{13}\text{C}$ values of *U. mediterranea* with the summer precipitation by Pauling et al. (2006) shows that more negative $\delta^{13}\text{C}$ values are associated with higher precipitation rates during the last 100 years suggesting a link between the nutrient input and precipitation (Fig. IV.7e and h).

Frisia et al. (2005) described the LIA as the coldest period of the past 2000 years and reported temperature anomalies of $-1\text{ }^{\circ}\text{C}$ for extremes. Since 1800 both $\delta^{18}\text{O}$ records indicate a trend to warmer conditions (Fig. IV.7a and g). This increase is comparable to the total amount of *G. ruber (pink)* (Fig. IV.7f). *G. ruber (pink)* is a tropical/subtropical species with an optimum temperature of $\sim 27\text{ }^{\circ}\text{C}$ and it is quite sensitive to temperature variations (Mulitza et al., 1998). This might explain the small amount and the partially totally absence of *G. ruber (pink)* during the LIA. Furthermore, the increase in the abundance of *G. ruber (pink)* since 1800 supports a trend to warmer conditions in the Gulf of Taranto (Fig. IV.7f). The reconstructed $\text{SST}_{\delta^{18}\text{O}}$ of *G. ruber (pink)* shows a temperature increase ($\sim 2\text{ }^{\circ}\text{C}$) over the past 200 years and especially since 1900 (Fig. IV.7b). The comparison of the $\delta^{18}\text{O}$ records of *G. ruber (white)* and *G. ruber (pink)* to the $\delta^{18}\text{O}$ record of *G. ruber* from a nearby core in the Gulf of Taranto by Taricco et al. (2009) shows that in all three records the $\delta^{18}\text{O}$ values decreases from 1800 onward. However, the amplitude of the $\delta^{18}\text{O}$ record of *G. ruber* by Taricco et al. (2009) is much higher ($-0.33 - 1.03\text{‰}$) compared to our $\delta^{18}\text{O}$ record of *G. ruber (white)*. One possible explanation for this high amplitude is that Taricco et al. (2009) used mixed samples of the pink and white variety of *G. ruber* in their analyses.

We conclude that the $\delta^{18}\text{O}$ record of *G. ruber (white)* is a composite record of temperature, precipitation and circulation changes. The latter is also supported by variations in $\text{SST}_{\text{TEXH86}}$, suggesting that shifts in water masses, induced by fluctuations between warm/wet and cold/dry modes, influence the $\text{SST}_{\text{TEXH86}}$ signal. This additionally coincides with variations in the $\delta^{13}\text{C}$ and $\delta^{18}\text{O}$ record of *U. mediterranea* indicating phases of circulation changes that affect the entire water column in the Gulf of Taranto. The recent salinity gradient between the coastal regions along the southern Italian coast and the offshore regions in the central Ionian Sea is $\sim 2\text{psu}$ (Grauel and Bernasconi, 2010) which shows that salinity changes of $1\text{-}2\text{psu}$ during the LIA would have been possible. Therefore, a $\sim 0.25\text{‰}$ shift in $\delta^{18}\text{O}$ could also correspond to a $\sim 1\text{psu}$ shift in salinity (Pierre, 1999) and hence could indicate a change in

circulation. A higher influence from ISW and LIW could induce an increase of the depth habitat of the species which could influence the calcification depths and temperature (Grauel and Bernasconi, 2010). Especially during the last 200 years, where $\delta^{13}\text{C}$ of the benthic and planktic foraminifera decrease and the various lipid biomarker concentrations used in this study indicate an increasing trend. This could be a signal for a higher nutrient availability and thus a change to a shallower depth habitat of the planktic species.

IV.7.2. Environmental changes in the Gulf of Taranto over the past 200 years

A prominent characteristic of the foraminiferal and lipid biomarker records is a major change occurring from 1800 onward. The beginning decrease in $\delta^{13}\text{C}$ of *U. mediterranea* associated with an increase in TOC is a strong indication that there is an increase in productivity during the last 200 years (Fig. IV.5c and d). The increasing concentrations of alkenones and crenarchaeol also suggest an enhanced productivity of haptophytes and crenarchaeota indicating that the whole marine productivity is affected (Fig. IV.5e and f).

The depletion in ^{13}C of *U. mediterranea* can be explained by higher nutrient inputs derived from the WAC. As previously described, this is consistent with the decrease in $\delta^{18}\text{O}$ of *G. ruber* (white) and decreasing SST_{TEXH86}. Higher nutrients will increase the marine productivity and the flux of ^{13}C -depleted OM to the sediment which upon oxidation leads to a lower $\delta^{13}\text{C}$ of DIC in bottom and pore waters, where it is recorded by benthic foraminifera (e.g., Shackleton, 1977; Luz and Reiss, 1983; Loubere, 1996). At the same time the higher OM flux and burial into the sediments increases OM preservation leading to higher TOC values. Alternatively, this effect can also be magnified by progressive degradation of OM with depth resulting in an underestimation of the initial productivity signal. Signs of potential aerobic degradation have been proposed on the basis of degradation sensitive dinoflagellate cysts analyzed on a parallel core of GeoB 10709-4 (Zonneveld et al., 2012). However, the good agreement between the $\delta^{13}\text{C}$, TOC and lipid biomarker records suggests that we indeed observe a change in productivity.

We propose a higher nutrient content carried by the WAC from 1800 which presumably indicates a stronger influence from the Northern Adriatic Sea, where nutrient supply is controlled by run-off from the Po River. This is in agreement with negative $\delta^{13}\text{C}$ values and high summer precipitation rates. However, there is no consistent relation to annual mean precipitation in N and S Italy (Brunetti et al., 2004) or Po River discharge (Zanchettin et al., 2008). Negative and more prolonged precipitation anomalies occurred more often during the last 100 years (Brunetti et al., 2004) suggesting that here the nutrient load may play a more

important role. Therefore we may consider that the observed environmental change derive from anthropogenic influences.

Beside the general decreasing trend in $\delta^{13}\text{C}$ of *U. mediterranea* there are two major phases of increasing productivity occurring from 1850 to 1920 and starting from 1940. The second period is also associated by an even stronger concentration increase of alkenones and crenarchaeol. The general increase in productivity may derive from demographic changes. The human population size in Italy and surrounding countries already increased from 1800 (Lotze et al., 2011). This could have been accompanied by land-use-changes affecting the nutrient load and water management of the major rivers along the eastern Italian coast. Different phases of trophic changes are also observed in the Northern Adriatic Sea from 1830 onward but timing of the onset differs between different studies. Barmawidjaja et al. (1995) suggested that a decrease in the abundance of epiphytic foraminifera off the Po delta indicated higher sediment and nutrient loads of the Po River from 1840 to 1870. Additionally, Sangiorgi and Donders (2004) showed that the total abundance of dinoflagellates increased from the 1830s while eutrophic species increased from 1930 onwards, whereas pollen indicated environmental changes due to land reclamation after 1910. Abundances of coccolithophorids started to increase from the late 1800s followed by diatoms and siliceous plankton increasing in the 20th century (Puskaric et al., 1990). A long-term enrichment of nutrients is suggested by an increasing frequency of anoxic events in the Northern Adriatic Sea between 1911 and 1982 (Justić, 1987). Additionally, increases in dinoflagellate cysts, indicating a higher productivity along the southern Italian shelf and in the Gulf of Taranto, have been attributed to the industrialization and urbanization of Italy and the increased usage of fertilizers (Zonneveld et al., 2012).

The observed shift also occurs in the BIT index and in the concentrations of long-chain *n*-alkanes. The BIT index values during the last 500 years agree with values found in coastal to open marine environments and the southern Italian shelf (Leider et al., 2010; Hopmans et al., 2004) (Fig. 5g). Branched GDGTs are suggested to be transported by rivers and the BIT has been successfully applied to characterize the soil OM supply to near-coastal environments (e.g., Hopmans et al., 2004; Herfort et al., 2006; Kim et al., 2006). Larger rivers are absent in the eastern part of the Gulf of Taranto and are confined to the north-western part of the Gulf. Here, the prevailing anticlockwise circulation prevents soil OM to reach the core location. This is supported by the distribution of heavy metals in surface sediments in the Gulf of Taranto (Buccolieri et al., 2006). The BIT values in core tops from the Gulf of Taranto also show a low contribution of soil OM and document soil OM input by the WAC and local river

supply (Leider et al., 2010). The BIT record seems to suggest that soil OM input started to decrease at 1800. However, a closer look at the concentration profiles of the GDGTs constituting the BIT shows a weaker increase of the soil markers (branched GDGTs) compared to the marine crenarchaeol. Thus the decreased BIT reflects increased marine archaeal production or preferential preservation of marine GDGTs (Huguet et al., 2007b; 2009; Castañeda et al., 2010). This BIT offset by a larger marine compared to terrestrial contribution has also been observed in several other shelf areas. Our study again shows the care that should be taken when interpreting the BIT index in areas with varying marine productivity (Walsh et al., 2008; Schmidt et al., 2010; Smith et al., 2012). Whereas the BIT index provides no evidence for increasing soil input, the increasing concentrations of plant-wax derived *n*-alkanes suggest an enhanced supply of land plant material into the Gulf of Taranto from 1800 and more significantly from the 20th century (Fig. IV.5g). Plant-waxes can be carried to the sea by long-range atmospheric transport (e.g., Simoneit, 1977; Gagosian et al., 1981; Schefuß et al., 2003), or by river transport to shallow and near-coastal environments (e.g., Prahl et al., 1994; Bird et al., 1995; Pelejero, 2003; Colombo et al., 2005). Analyses of stable C and H isotopes in plant-waxes from Italian lakes, rivers, coastal and shelf sediments show that the plant-waxes in the Gulf of Taranto sediments originate from local southern Italian sources and that conclusions only based on *n*-alkane concentrations have to be drawn with caution (Leider et al., *subm.*). Determining the compound-specific stable hydrogen and carbon isotopic composition of the *n*-alkanes will be needed to assess if the observed concentration increase is due to a stronger influence of the WAC.

IV.8. CONCLUSIONS

Using a multiproxy approach based on the TEX₈₆ and U^{K'}₃₇ indices and δ¹⁸O of *G. ruber* (*white*) we obtained a complex picture of SST proxies and how they are influenced by climatic conditions, circulation changes, nutrient distribution and human impact for the last 500 years in the Gulf of Taranto (central Mediterranean Sea).

The reconstructed SST_{UK'37} reflects the SST of the main period of haptophyte production. In the Gulf of Taranto this occurs during the cooler part of the year. Higher SST_{UK'37} occur during periods of frequent storms and flooding events in the Northern Adriatic Sea. Higher SST_{UK'37} values and more frequent flooding and storm events occur when the winter NAO index is in a negative mode. This climatic configuration influences the timing and duration of vertical mixing of the surface waters and continental runoff introducing nutrients in the photic

zone. This modulates the timing in haptophyte production which amplifies the SST_{UK'37} signal compared to air temperature reconstructions. Hence, variations in SST_{UK'37} can provide information on past winter turbulence and associated nutrients supplied by the WAC. SST_{TEXH86} reflect summer conditions. They co-vary with SST_{UK'37} although instrumental records show that summer and winter temperatures are independent. A logical explanation is that an expansion of the season of haptophyte production (towards the warmer parts of autumn and spring, leading to higher SST_{UK'37}) simultaneously reduces the season of archaeal production (towards high summer, resulting in higher SST_{TEXH86}). During the Maunder Minimum this mechanism seems to break down, which is explained by the overall lower temperatures of the unstratified water column indicating an enhanced seasonality.

SST_{δ18O} of *G. ruber (white)* record primarily summer SSTs, but moreover the δ¹⁸O of this species reflects changes in salinity and nutrient distributions related to circulation patterns of the WAC and ISW. The SST_{δ18O} record shows a prolonged summer cooling with a high internal variability between wet/warm and dry/cold conditions from 1350 to 1700, which is in good agreement with tree ring data from the European Alps. Higher δ¹⁸O values between 1750 and 1810 are possibly due to a higher influence of the ISW indicating drier conditions which coincides with a maximum in SST_{TEX86}. A negative correlation of SST_{TEX86} and SST_{δ18O} *G. ruber (white)* is observed over large parts of the record, which suggests that shifts in the strength of water masses in the Gulf of Taranto occurred more regularly during the last 500 years. Here, the combination of both SST proxies provides a detailed view on circulation changes. In this respect, the decrease in SST_{TEX86} and the decrease in δ¹⁸O of *G. ruber (white)* reflect an increase in the dominance of the WAC inflow relative to the ISW into the Gulf of Taranto since 1800. The depletion in δ¹³C of *U. mediterranea* suggests that this co-occurs with an increase in nutrient supply.

The records of TOC, marine and terrestrial lipid biomarker concentrations, BIT index and the δ¹³C of *G. ruber (white and pink)* and *U. mediterranea* show a persisting shift from 1800 onward indicating an increase in productivity and terrestrial supply which we attributed to the steady increasing human impact on the region.

IV.9. ACKNOWLEDGEMENTS

This project was financially supported by the SNSF (Swiss National Science Foundation Project 20MA21-115934), by the DFG (Deutsche Forschungsgemeinschaft Project grant VE 486/1-1), and the ESF (European Science Foundation) within the EuroMARC project

'Multidisciplinary study of continent-ocean climate dynamics using high-resolution records from the eastern Mediterranean' (MOCCHA). We thank E. Ufke for her help with the sample preparation and picking of the foraminifera of NU04 at Utrecht University. Special thanks go to S. Brönnimann, Bern University, for the helpful discussions and the supply of the precipitation and temperature grid data. We thank K. Becker and C. Peters for help with sample preparation for lipid analysis and J. Lipp for assistance during HPLC-MS analysis. M. Elvert, X. Prieto-Mollar, J. Schmal and J. Wendt are thanked for lab assistance. Authors are grateful to Captains, Crew and Colleagues onboard RV *Universitatis* during 'ESPRESSO' cruise 2005 coordinated by G.J. de Lange and RV *Poseidon* during 'CAPPUCCINO' cruise 2006 coordinated by K.A.F. Zonneveld.

Further remarks on the manuscript

Since this manuscript is in a draft version it is subject to modifications. At the moment the age model of NU04 and resulting sedimentation rate is only mentioned as de Lange (unpubl.). For the future we will provide a full description of the methods and include the ^{210}Pb data. Currently, the age model is under review. We proposed an increase in productivity from 1800, this would result in higher sedimentation rates suggesting that sedimentation rates are not linear.

IV.10. REFERENCES

- Alpert, P., Baldi, M., Ilani, R., Krichak, S., Price, C., Rodó, X., Saaroni, H., Ziv, B., Kishcha, P., Barkan, J., Mariotti, A., Xoplaki, E., P. Lionello, P.M.-R., Boscolo, R., 2006. Chapter 2 Relations between climate variability in the Mediterranean region and the tropics: ENSO, South Asian and African monsoons, hurricanes and Saharan dust. In: *Mediterranean Climate Variability* (eds P. Lionello, P. Malanotte-Rizzoli and R. Boscolo), pp. 149-177, Elsevier.
- Artegiani, A., Paschini, E., Russo, A., Bregant, D., Raicich, F., Pinardi, N., 1997b. The Adriatic Sea general circulation. Part II: baroclinic circulation structure. *J. Phys. Oceanogr.* 27, 1515-1532.
- Bakun, A., Agostini, V.N., 2001. Seasonal patterns of wind-induced upwelling/downwelling in the Mediterranean Sea. *Sci. Mar.* 65, 243-257.
- Barmawidjaja, D., G. Van der Zwaan, F. Jorissen, and S. Puskaric (1995), 150 years of eutrophication in the northern Adriatic Sea: evidence from a benthic foraminiferal record, *Marine Geology*, 122(4), 367-384.

- Barriendos, M., Llasat, M.C., 2003. The case of the 'Maladá' anomaly in the western Mediterranean Basin (AD 1760-1800): An example of a strong climatic variability, *Clim. Change* 61, 191-216.
- Barker, S., Greaves, M., Elderfield, H., 2003. A study of cleaning procedures used for foraminiferal Mg/Ca paleothermometry, *Geochem. Geophys. Geosyst.* 4, 1-20.
- Bentaleb, I., Grimalt, J.O., Vidussi, F., Marty, J.C., Martin, V., Denis, M., Hatté, C., Fontugne, M., 1999. The C₃₇ alkenone record of seawater temperature during seasonal thermocline stratification. *Mar. Chem.* 64, 301-313.
- Benthien, A., Müller, P.J., 2000. Anomalously low alkenone temperatures caused by lateral particle and sediment transport in the Malvinas Current region, western Argentine Basin. *Deep-Sea Res. I* 47, 2369-2393.
- Bianchi, G.G., McCave, I.N., 1999. Holocene periodicity in North Atlantic climate and deep-ocean flow south of Iceland. *Nature* 397, 515-517.
- Bignami, F., Sciarra, R., Carniel, S., Santoleri, R., 2007. Variability of Adriatic Sea coastal turbid waters from SeaWiFS imagery. *J. Geophys. Res.* 112, C03S10, doi: doi:10.1029/2006JC003518.
- Bijma, J., Faber, W.W., Hemleben, C., 1990. Temperature and salinity limits for growth and survival of some planktonic foraminifers in laboratory cultures. *Journal of Foraminiferal Research* 20, 95-116.
- Bird, M.I., Summons, R.E., Gagan, M.K., Roksandic, Z., Dowling, L., Head, J., Keith Fifield, L., Cresswell, R.G., Johnson, D.P., 1995. Terrestrial vegetation change inferred from *n*-alkane $\delta^{13}\text{C}$ analysis in the marine environment. *Geochim. Cosmochim. Acta* 59, 2853-2857.
- Boldrin, A., Miserocchi, S., Rabitti, S., Turchetto, M.M., Balboni, V., Socal, G., 2002. Particulate matter in the southern Adriatic and Ionian Sea: characterisation and downward fluxes. *J. Mar. Syst.* 33-34, 389-410.
- Boldrin, A., Langone, L., Miserocchi, S., Turchetto, M., Acri, F., 2005. Po River plume on the Adriatic continental shelf: dispersion and sedimentation of dissolved and suspended matter during different river discharge rates. *Mar. Geol.* 222, 135-158.
- Bonino, G., Cini Castagnoli, G., Callegari, E., Zhu, G.-M., 1993. Radiometric and tephroanalysis dating of recent Ionian Sea cores. *Il Nuovo Cimento C*, 16, 155-162.
- Bradley, R.S., Jones, P.D., 1993. 'Little Ice Age' summer temperature variations: their nature and relevance to recent global warming trends. *The Holocene* 3, 367-376.
- Bradley, R.S., Briffa, K.R., Cole, J., Hughes, M.K., Osborn, T.J., 2003. The climate of the last millennium. *Paleoclim. Glob. Change and the Future*, 105-141.
- Brassell, S.C., Brereton, R.G., Eglinton, G., Grimalt, J., Liebezeit, G., Marlowe, I.T., Pflaumann, U., Sarnthein, M., 1986. Palaeoclimatic signals recognized by chemometric treatment of molecular stratigraphic data. *Org. Geochem.* 10, 649-660.

- Brewer, S., Alleaume, S., Guiot, J., Nicault, A., 2007. Historical droughts in Mediterranean regions during the last 500 years: a data/model approach. *Clim. Past* 3, 355-36
- Briffa, K.R., Osborn, T.J., 2002. Blowing Hot and Cold. *Science* 295, 2227-2228.
- Broecker, W.S., 1986. Oxygen isotope constraints on surface ocean temperatures. *Quat. Res.* 26, 121-134.
- Broecker, W.S., 2000. Was a change in thermohaline circulation responsible for the Little Ice Age? *Proc. Nat. Ac. Sci.* 97, 1339-1342.
- Bronk Ramsey, C., 2005. Improving the resolution of radiocarbon dating by statistical analysis, In: *The Bible and Radiocarbon dating: Archaeology, Text and Science* (eds T.E. Levy, T.F.G. Higham), pp. 57-64, London, Equinox.
- Bronk Ramsey, C., Higham, T.F.G., Brock, F., Baker, D., and Ditchfield, P., 2009. Radiocarbon dates from the Oxford AMS System: *Archaeometry Datelist 33*, *Archaeometry* 51(2), 323-349.
- Brunetti, M., Buffoni, L., Mangianti, F., Maugeri, M., Nanni, T., 2004. Temperature, precipitation and extreme events during the last century in Italy. *Glob. Planet. Change* 40, 141-149.
- Buccolieri, A., Buccolieri, G., Cardellicchio, N., Dell'Atti, A., Di Leo, A., Maci, A., 2006. Heavy metals in marine sediments of Taranto Gulf (Ionian Sea, Southern Italy). *Mar. Chem.* 99, 227-235.
- Büntgen, U., Frank, D.C., Nievergelt, D., Esper, J., 2006. Summer Temperature Variations in the European Alps, A.D. 755-2004. *J. Climate* 19, 5606-5623.
- Camuffo, D., Secco, C., Brimblecombe, P., Martin-Vide, J., 2000. Sea Storms in the Adriatic Sea and the Western Mediterranean during the Last Millennium. *Clim. Change* 46, 209-223
- Camuffo, D., Bertolin, C., Barriendos, M., Dominguez-Castro, F., Cocheo, C., Enzi, S., Sghedoni, M., della Valle, A., Garnier, E., Alcoforado, M.J., Xoplaki, E., Luterbacher, J., Diodato, N., Maugeri, M., Nunes, M., Rodriguez, R., 2010. 500-year temperature reconstruction in the Mediterranean Basin by means of documentary data and instrumental observations. *Clim. Change* 101, 169-199.
- Caroppo, C., Fiocca, A., Sammarco, P., Magazzu, G., 1999. Seasonal variations of nutrients and phytoplankton in the coastal SW Adriatic Sea (1995–1997). *Bot. Mar.* 42, 389-400.
- Castañeda, I.S., Schefuß, E., Pätzold, J., Sinninghe Damsté, J.S., Weldeab, S., Schouten, S., 2010. Millennial-scale sea surface temperature changes in the eastern Mediterranean (Nile River Delta region) over the last 27,000 years. *Paleoceanography* 25, PA1208.
- Cini Castagnoli, G., Bonino, G., Caprioglio, F., Provenzale, A., Serio, M., Guang, and Mei, Z., 1990. The carbonate profile of two recent Ionian Sea cores: Evidence that the sedimentation rate is constant over the last millennia. *Geophys. Res. Lett.* 17, 1937-1940.

- Cini Castagnoli, G., Bernasconi, S.M., Bonino, G., Della Monica, P., Taricco, C., 1999. 700 year record of the 11 year solar cycle by planktonic foraminifera of a shallow water Mediterranean core. *Adv. Space Res.* 24, 233-236.
- Colombo, J.C., Cappelletti, N., Laschi, J., Migoya, M.C., Speranza, E., Skorupka, C.N., 2005. Sources, Vertical Fluxes, and Accumulation of Aliphatic Hydrocarbons in Coastal Sediments of the Río de la Plata Estuary, Argentina. *Environmental Science & Technology* 39, 8227-8234.
- Conte, M.H., Thompson, A., Lesley, D., Harris, R.P., 1998. Genetic and physiological influences on the alkenone/alkenoate versus growth temperature relationship in *Emiliania huxleyi* and *Gephyrocapsa oceanica*. *Geochim. Cosmochim. Acta* 62, 51-68.
- Conte, M.H., Sicre, M.-A., Rühlemann, C., Weber, J.C., Schulte, S., Schulz-Bull, D., Blanz, T., 2006. Global temperature calibration of the alkenone unsaturation index ($U^{K_{37}}$) in surface waters and comparison with surface sediments. *Geochem. Geophys. Geosyst.* 7, Q02005, doi: 10.1029/2005GC001054.
- Craig, H., Gordon, L.I., 1965. Deuterium and oxygen 18 variations in the ocean and the marine atmosphere. Consiglio nazionale delle ricerche, Laboratorio de geologia nucleare.
- Crowley, T.J., 2000. Causes of Climate Change Over the Past 1000 Years. *Science* 289, 270-277.
- Deuser, W., Ross, E., Hemleben, C. and Spindler M., 1981. Seasonal changes in species composition, numbers, mass, size, and isotopic composition of planktonic foraminifera settling into the deep Sargasso Sea, *Palaeogeogr. Palaeoclimatol. Palaeoecol.*, 33, 103-127.
- Ding, X., Bassinot, F., Guichard, F., Li, Q.Y., Fang, N.Q., Labeyrie, L., Xin, R.C., Adisaputra, M.K., Hardjawidjaksana, K., 2006. Distribution and ecology of planktonic foraminifera from the seas around the Indonesian Archipelago. *Mar. Micropaleontol.* 58, 114-134.
- Diodato, N., 2007. Climatic fluctuations in southern Italy since the 17th century: reconstruction with precipitation records at Benevento. *Clim. Change* 80, 411-431.
- Domínguez-Castro, F., Santisteban, J.I., Barriendos, M., Mediavilla, R., 2008. Reconstruction of drought episodes for central Spain from rogation ceremonies recorded at the Teledo Cathedral from 1506 to 1900: A methodological approach, *Glob. Planet. Change* 63, 230-242.
- Dünkeloh, A., Jacobeit, J., 2003. Circulation dynamics of Mediterranean precipitation variability 1948–98. *Int. J. Climatol.* 23, 1843-1866.
- Eddy J.E., 1976. The Maunder Minimum, *Science* 192(4245), 1189-1202.
- Eglinton, G. and Hamilton, R. J., 1967. Leaf Epicuticular Waxes. *Science* 156, 1322-1335.
- Elderfield, H., Ganssen, G., 2000. Past temperature and $\delta^{18}\text{O}$ of surface ocean waters inferred from foraminiferal Mg/Ca ratios. *Nature*, 405, 442-445.

- Elvert, M., Boetius, A., Knittel, K., Jørgensen, B.B., 2003. Characterization of specific membrane fatty acids as chemotaxonomic markers for sulfate-reducing bacteria involved in anaerobic oxidation of methane. *Geomicrobiol. J.* 20, 403-419.
- Emiliani, C., 1955. Pleistocene Temperatures. *J. Geol.* 63, 538-578.
- Enzi, S., Camuffo D. (1995), Documentary sources of the sea surges in Venice from AD 787 to 1867, *Nat. Hazards*, 12, 225-287.
- Epstein, S., Mayeda T. (1953), Variation of ^{18}O content of waters from natural sources, *Geochim. Cosmochim. Acta*, 4, 213-224.
- Epstein, B.L., D'Hondt, S., Quinn, J.G., Zhang, J., Hargraves, P.E., 1998. An effect of dissolved nutrient concentrations on alkenone-based temperature estimates. *Paleoceanography* 13, 122-126, PA03358.doi: 10.1029/97pa03358.
- Erez, J., Luz, B., 1983. Experimental paleotemperature equation for planktonic foraminifera. *Geochim. Cosmochim. Acta* 47, 1025-1031.
- Esper, J., Cook, E.R., Schweingruber, F.H., 2002. Low-Frequency Signals in Long Tree-Ring Chronologies for Reconstructing Past Temperature Variability. *Science* 295, 2250-2253.
- Frisia, S., Borsato, A., Spötl, C., Villa, I.M., Cucchi, F., 2005. Climate variability in the SE Alps of Italy over the past 17 000 years reconstructed from a stalagmite record. *Boreas* 34, 445-455.
- Gagosian, R.B., Peltzer, E.T., Merrill, J.T., 1987. Long-range transport of terrestrially derived lipids in aerosols from the south Pacific. *Nature* 325, 800-803.
- Gong, C., Hollander, D.J., 1999. Evidence for differential degradation of alkenones under contrasting bottom water oxygen conditions: implication for paleotemperature reconstruction. *Geochim. Cosmochim. Acta* 63, 405-411.
- Goñi, M.A., Hartz, D.M., Thunell, R.C., Tappa, E., 2001. Oceanographic considerations for the application of the alkenone-based paleotemperature U_{37}^K index in the Gulf of California. *Geochim. Cosmochim. Acta* 65, 545-557.
- Goudeau, M.-L.S., Grauel, A.L., Tessarolo, C., Leider, A., Chen, L., Bernasconi, S.M., Versteegh, G.J.M., Zonneveld, K.A.F., De Lange, G.J., 2012. Environmental changes observed by high-resolution XRF core-scanning in Holocene (0-16 ka cal. BP) sediments from the Gulf Of Taranto, Central Mediterranean, (subm.).
- Grauel, A.L., Bernasconi, S.M., 2010. Core-top calibration of $\delta^{18}\text{O}$ and $\delta^{13}\text{C}$ of *G. ruber* (white) and *U. mediterranea* along the southern Adriatic coast of Italy. *Mar. Micropaleontol.* 77, 175-186.
- Grbec, B., Vilibić, I., Bajić, A., Morović, M., Bec Paklar, G.B., Matić, E., Dadić, V., 2007. Response of Adriatic Sea to the atmospheric anomaly in 2003. *Ann. Geophys.* 25, 835-846.
- Grove, J. M. (1988), *The Little Ice Age*, Methuen, New York.

- Grove, A.T., 2001. The "Little Ice Age" and its Geomorphological Consequences in Mediterranean Europe. *Clim. Change* 48, 121-136.
- Hegerl, G., Luterbacher, J., Gonzalez-Rouco, F., Tett, S.F.B., Crowley, T., Xoplaki, E., 2011. Influence of human and natural forcing on European seasonal temperatures. *Nature Geosci.* 4, 99-103.
- Herbert, T.D., Heinrich, D.H., Karl, K.T., 2003. Alkenone Paleotemperature Determinations. In: *Treatise on Geochemistry*, pp. 391-432. Pergamon, Oxford.
- Herfort, L., Schouten, S., Boon, J.P., Sinninghe Damsté, J.S., 2006. Application of the TEX₈₆ temperature proxy to the southern North Sea. *Org. Geochem.* 37, 1715-1726.
- Hoefs, M.J.L., Rijpstra, W.I.C., Sinninghe Damsté, J.S., 2002. The influence of oxic degradation on the sedimentary biomarker record I: evidence from Madeira Abyssal Plain turbidites. *Geochim. Cosmochim. Acta* 66, 2719-2735.
- Holzhauser, H., Magny, M., Zumbuhl, H.J., 2005. Glacier and lake-level variations in west-central Europe over the last 3500 years. *The Holocene* 15, 789-801.
- Houghton, J. T., et al., 2001. Climate change 2001: the scientific basis. In: *IPCC Third Assessment report – Climate change 2001*, Cambridge University Press Cambridge, New York.
- Hopmans, E.C., Weijers, J.W.H., Schefuß, E., Herfort, L., Sinninghe Damsté, J.S., Schouten, S., 2004. A novel proxy for terrestrial organic matter in sediments based on branched and isoprenoid tetraether lipids. *Earth Planet. Sci. Lett.* 224, 107-116.
- Huguet, C., Schimmelmann, A., Thunell, R., Lourens, L.J., Sinninghe Damsté, J.S., Schouten, S., 2007. A study of the TEX₈₆ paleothermometer in the water column and sediments of the Santa Barbara Basin. *California. Paleoceanography* 22, PA3203.
- Huguet, C., Smittenberg, R.H., Boer, W., Sinninghe Damsté, J.S., Schouten, S., 2007. Twentieth century proxy records of temperature and soil organic matter input in the Drammensfjord, southern Norway. *Org. Geochem.* 38, 1838-1849.
- Huguet, C., Kim, J.-H., de Lange, G.J., Sinninghe Damsté, J.S., Schouten, S., 2009. Effects of long term oxic degradation on the TEX₈₆ and BIT organic proxies. *Org. Geochem.* 40, 1188-1194.
- Huguet, C., Martrat, B., Grimalt, J.O., Sinninghe Damsté, J.S., Schouten, S., 2011. Coherent millennial-scale patterns in UK'37; and TEX₈₆ temperature records during the penultimate interglacial-to-glacial cycle in the western Mediterranean. *Paleoceanography* 26, PA2218.doi: 10.1029/2010pa002048.
- Hughen, K.A., Baillie, M.G.L., Bard, E., Beck, J.W., Bertrand, C.J.H., Blackwell, P.G., Buck, C.E., Burr, G.S., Cutler, K.B., Damon, P.E., Edwards, R.L., Fairbanks, R.G., Friedrich, M., Guilderson, T.P., Kromer, B., McCormac, G., Manning, S., Ramsey, C.B., Reimer, P.J., Reimer, R.W., Remmele, S., Southon, J.R., Stuiver, M., Talamo, S., Taylor, F.W., van der Plicht, J., and Weyhenmeyer, C.E., 2004. Marine04 marine radiocarbon age calibration, 0-26 cal kyr BP, *Radiocarbon* 46, 1059-1086.

- Hurrell, J. W., 1995. Decadal Trends in the North Atlantic Oscillation: Regional Temperatures and Precipitation, *Science*, 269, 676-679.
- Hurrell, J.W., Van Loon, H., 1997. Decadal variations in climate associated with the North Atlantic Oscillation. *Clim. Change* 36, 301-326
- Incarbona, A., Ziveri, P., Di Stefano, E., Lirer, F., Mortyn, G., Patti, B., Pelosi, N., Sprovieri, M., Tranchida, G., Vallefucio, M., 2010. The Impact of the Little Ice Age on Coccolithophores in the Central Mediterranean Sea. *Clim. Past* 6, 795-805.
- IPCC, 2001. *Climate Change 2001: The physical science basis. Contribution of working group I to the fourth assessment report of the intergovernmental panel on climate change.* (Eds Solomon, S., Qin, D., Manning, M., Chen, Z., Marquis, M., Averyt, K.B., Tignor M. and Miller H.L.), p. 996 pp., New York: Cambridge University Press.
- Jacobeit, J., Jönsson, P., Barring, L., Beck, C., Ekström, M., 2001. Zonal Indices for Europe 1780–1995 and Running Correlations with Temperature. *Clim. Change* 48, 219-241.
- Jacobeit, J., Glaser, R., Luterbacher, J., Wanner, H., 2003. Links between flood events in central Europe since AD 1500 and large-scale atmospheric circulation modes. *Geophys. Res. Lett* 30, 1172.
- Jones, P.D., New, M., Parker, D.E., Martin, S., Rigor, I.G., 1999. Surface air temperature and its changes over the past 150 years. *Rev. Geophys.* 37, 173-199.
- Justic, D., Legovic, T., Rottini-Sandrini, L., 1987. Trends in oxygen content 1911-1984 and occurrence of benthic mortality in the northern Adriatic Sea. *Estuarine, Coast. Shelf Sci.* 25, 435-445.
- Karner, M.B., DeLong, E.F., Karl, D.M., 2001. Archaeal dominance in the mesopelagic zone of the Pacific Ocean. *Nature* 409, 507-510.
- Katara, I., Illian, J., Pierce, G., Scott, B., Wang, J., 2008. Atmospheric forcing on chlorophyll concentration in the Mediterranean. *Hydrobiologia* 612, 33-48.
- Kim, J.-H., Schouten, S., Buscail, R., Ludwig, W., Bonnin, J., Sinninghe Damsté, J.S., Bourrin, F., 2006. Origin and distribution of terrestrial organic matter in the NW Mediterranean (Gulf of Lions): Exploring the newly developed BIT index. *Geochem. Geophys. Geosyst.* 7, Q11017, doi: 10.1029/2006GC001306.
- Kim, J.-H., Schouten, S., Hopmans, E.C., Donner, B., Sinninghe Damsté, J.S., 2008. Global sediment core-top calibration of the TEX₈₆ paleothermometer in the ocean. *Geochim. Cosmochim. Acta* 72, 1154-1173.
- Kim, J.-H., Huguet, C., Zonneveld, K.A.F., Versteegh, G.J.M., Roeder, W., Sinninghe Damsté, J.S., Schouten, S., 2009b. An experimental field study to test the stability of lipids used for the TEX₈₆ and palaeothermometers. *Geochim. Cosmochim. Acta* 73, 2888-2898.
- Kim J.-H., van der Meer, J., Schouten, S., Helmke, P., Willmott, V., Sangiorgi, F., Koç, N., Hopmans, E.C., Sinninghe Damsté, J.S., 2010. New indices and calibrations derived

- from the distribution of crenarchaeal isoprenoid tetraether lipids: Implications for past sea surface temperature reconstructions. *Geochim. Cosmochim. Acta* 74, 4639-4654.
- Klein, P., Coste, B., 1984. Effects of wind-stress variability on nutrient transport into the mixed layer. *Deep-Sea Res.* 31, 21-37.
- Kress, A., Saurer, M., Siegwolf, R.T.W., Frank, D.C., Esper, J., Bugmann, H., 2010. A 350 year drought reconstruction from Alpine tree ring stable isotopes, *Global Biogeochem. Cycles* 24, GB2011.
- Lean, J., Skumanich, A., White, O., 1992. Estimating the Sun's radiative output during the Maunder Minimum. *Geophys. Res. Lett.* 19, 1591-1594.
- Lee, K.E., Kim, J.-H., Wilke, I., Helmke, P., Schouten, S., 2008. A study of the alkenone, TEX₈₆, and planktonic foraminifera in the Benguela upwelling system: Implications for past sea surface temperature estimates. *Geochem., Geophys., Geosyst.* 9, Q10019, doi: 10.1029/2008GC002056.
- Leider, A., Hinrichs, K.-U., Mollenhauer, G., Versteegh, G.J.M., 2010. Core-top calibration of the lipid-based U^K₃₇ and TEX₈₆ temperature proxies on the southern Italian shelf (SW Adriatic Sea, Gulf of Taranto). *Earth Planet. Sci. Lett.* 300, 112-124.
- Leider, A., K.-U. Hinrichs, E. Schefuß, G. J. M. Versteegh, Distribution and stable isotopes of plant wax-derived *n*-alkanes in marine surface sediments along a SE Italian transect and their potential to reconstruct the water balance, *subm.*
- Lionello, P., Malanotte-Rizzoli, P., Boscolo, R., Alpert, P., Artale, V., Li, L., Luterbacher, J., May, W., Trigo, R., Tsimplis, M., Ulbrich, U., Xoplaki, E., P. Lionello, P.M.-R., Boscolo, R., (2006), The Mediterranean climate: An overview of the main characteristics and issues, In: *Mediterranean Climate Variability* (eds P. Lionello, P. Malanotte-Rizzoli and R. Boscolo), pp. 1-26, Elsevier.
- Lipp, J.S., Hinrichs, K.-U., 2009. Structural diversity and fate of intact polar lipids in marine sediments. *Geochim. Cosmochim. Acta* 73, 6816-6833.
- Lipp, J.S., Morono, Y., Inagaki, F., Hinrichs, K.-U., 2008. Significant contribution of Archaea to extant biomass in marine subsurface sediments. *Nature*, 454, 991-994.
- Liu, X., Lipp, J.S., Hinrichs, K.-U., 2011. Distribution of intact and core GDGTs in marine sediments. *Org. Geochem.* 42, 368-375.
- Locarnini, R.A., Mishonov, A.V., Antonov, J.I., Boyer, T.P., Garcia, H.E., Baranova, O.K., Zweng, M.M. and Johnson, D.R., 2010. *World Ocean Atlas 2009, Volume 1: Temperature*. S. Levitus, Ed. NOAA Atlas NESDIS 68, U.S. Government Printing Office, Washington, D.C., 184 pp.
- Lopes dos Santos, R.A., Prange, M., Castañeda, I.S., Schefuß, E., Mulitza, S., Schulz, M., Niedermeyer, E.M., Sinninghe Damsté, J.S., Schouten, S., 2010. Glacial-interglacial variability in Atlantic meridional overturning circulation and thermocline adjustments in the tropical North Atlantic. *Earth Planet. Sci. Lett.* 300, 407-414.

- Lotze, H., Coll, M., Dunne, J., 2011. Historical Changes in Marine Resources, Food-web Structure and Ecosystem Functioning in the Adriatic Sea, Mediterranean. *Ecosystems* 14, 198-222.
- Loubere, P., 1996. The surface ocean productivity and bottom water oxygen signals in deep water benthic foraminiferal assemblages. *Mar. Micropaleontol.* 28, 247-261.
- Luterbacher, J., Schmutz, C., Gyalistras, D., Xoplaki, E., Wanner, H., 1999. Reconstruction of monthly NAO and EU indices back to AD 1675. *Geophys. Res. Lett.* 26, 2745-2748.
- Luterbacher, J., Rickli, R., Xoplaki, E., Tinguely, C., Beck, C., Pfister, C., Wanner, H., 2001. The Late Maunder Minimum (1675–1715) – A Key Period for Studying Decadal Scale Climatic Change in Europe. *Clim. Change* 49, 441-462.
- Luterbacher, Xoplaki, Dietrich, Rickli, Jacobeit, Beck, Gyalistras, Schmutz, Wanner, 2002. Reconstruction of sea level pressure fields over the Eastern North Atlantic and Europe back to 1500. *Clim. Dyn.* 18, 545-561.
- Luterbacher, J., Dietrich, D., Xoplaki, E., Grosjean, M., Wanner, H., 2004. European Seasonal and Annual Temperature Variability, Trends, and Extremes Since 1500. *Science* 303, 1499-1503.
- Luterbacher, J., et al., 2006. Chapter 1 Mediterranean climate variability over the last centuries: A review. In: *Mediterranean Climate Variability* (eds P. Lionello, P. Malanotte-Rizzoli and R. Boscolo), pp. 27-148, Elsevier.
- Luz, B., Reiss, Z., 1983. Stable carbon isotopes in Quaternary foraminifera from the Gulf of Aqaba (Elat), Red Sea. *Utrecht Micropaleontol. Bull.* 30, 129-140.
- Mann, M.E. (2002), Little Ice Age, in *The Earth System: physical and chemical dimensions of global environmental change Vol. 1*. In: *Encyclopedia of Global Environmental Change* (eds MacCracken, M.C., Perry, J.S.) pp 504-509, John Wiley & Sons, Ltd, Chichester.
- Mann, M.E., Zhang, Z., Rutherford, S., Bradley, R.S., Hughes, M.K., Shindell, D., Ammann, C., Faluvegi, G., Ni, F., 2009. Global Signatures and Dynamical Origins of the Little Ice Age and Medieval Climate Anomaly. *Science* 326, 1256-1260
- Marini, M., Jones, B.H., Campanelli, A., Grilli, F., Lee, C.M., 2008. Seasonal variability and Po River plume influence on biochemical properties along western Adriatic coast. *J. Geophys. Res.* 113. doi:10.1029/2007JC004370.
- Mariotti, A., Struglia, M.V., Zeng, N., Lau, K.M., 2002. The Hydrological Cycle in the Mediterranean Region and Implications for the Water Budget of the Mediterranean Sea. *J. Clim.* 15, 1674-1690.
- Marlowe, I.T., Green, J.C., Neal, A.C., Brassell, S.C., Eglinton, G., Course, P.A., 1984. Long chain(n-C₃₇-C₃₉) alkenones in the Prymnesiophyceae, distribution of alkenones and other lipids and their taxonomic significance. *Brit. Phycolog. J.* 19, 203-216.

- Martinez, J.I., Taylor, L., De Deckker, P., Barrows, T., 1998. Planktonic foraminifera from the eastern Indian Ocean: distribution and ecology in relation to the western Pacific Warm Pool (WPWP), *Mar. Micropaleontol.* 34, 121-151.
- Menzel, D., Hopmans, E.C., Schouten, S., Sinninghe Damsté, J.S., 2006. Membrane tetraether lipids of planktonic Crenarchaeota in Pliocene sapropels of the Eastern Mediterranean Sea. *Palaeogeogr., Palaeoclim., Palaeoecol.* 239, 1-15.
- Milligan, T.G., Cattaneo, A., 2007. Sediment dynamics in the western Adriatic Sea: From transport to stratigraphy. *Cont. Shelf Res.* 27, 287-295.
- Mollenhauer, G., Inthorn, M., Vogt, T., Zabel, M., Sinninghe Damsté, J.S., Eglinton, T.I., 2007. Aging of marine organic matter during cross-shelf lateral transport in the Benguela upwelling system revealed by compound-specific radiocarbon dating. *Geochim., Geophys., Geosyst.* 8, Q09004, doi:10.1029/2007GC001603.
- Mulitza, S., Wolff, T., Pätzold, J., Hale, W., Wefer, G., 1998. Temperature sensitivity of planktonic foraminifera and its influence on the oxygen isotope record, *Mar. Micropaleontol.* 33, 223-240.
- Murray, A.E., Blakis, A., Massana, R., Strawzewski, S., Passow, U., Alldredge, A., DeLong, E.F., 1999. A time series assessment of planktonic archaeal variability in the Santa Barbara Channel. *Aq. Microb. Ecol.* 20, 129-145.
- Müller, P.J., Kirst, G., Ruhland, G., von Storch, I., Rosell-Melé, A., 1998. Calibration of the alkenone paleotemperature index U^{K}_{37} based on core-tops from the eastern South Atlantic and the global ocean (60°N-60°S). *Geochim. Cosmochim. Acta* 62, 1757-1772.
- Nicault, A., Alleaume, S., Brewer, S., Carrer, M., Nola, P., Guiot, J., 2008. Mediterranean drought fluctuation during the last 500 years based on tree-ring data. *Clim. Dyn.* 31, 227-245.
- Ninčević Gladan, Ž., Marasović, I., Grbec, B., Skejić, S., Bužančić, M., Kušpilić, G., Matijević, S. and Matic F., 2010. Inter-decadal variability in phytoplankton community in the Middle Adriatic (Kaštela Bay) in relation to the North Atlantic Oscillation. *Estuar. coasts*, 33, 376-383.
- Numberger, L., Hemleben, C., Hoffmann, R., Mackensen, A., Schulz, H., Wunderlich, J.-M., Kucera, M., 2009. Habitats, abundance patterns and isotopic signals of morphotypes of the planktonic foraminifer *Globigerinoides ruber* (d'Orbigny) in the eastern Mediterranean Sea since the Marine Isotopic Stage 12. *Mar. Micropaleontol.* 73, 90-104.
- Ohkouchi, N., Eglinton, T.I., Keigwin, L.D., Hayes, J.M., 2002. Spatial and temporal offsets between proxy records in a sediment drift. *Science* 298, 1224-1227.
- Pauling, A., Luterbacher, J., Casty, C., Wanner, H., 2006. Five hundred years of gridded high-resolution precipitation reconstructions over Europe and the connection to large-scale circulation. *Clim. Dyn.* 26, 387-405.

- Palastanga, V., van der Schrier, G., Weber, S., Kleinen, T., Briffa, K., Osborn, T., 2011. Atmosphere and ocean dynamics: contributors to the European Little Ice Age? *Clim. Dyn.* 36, 973-987.
- Pelejero, C., 2003. Terrigenous n-alkane input in the South China Sea: high-resolution records and surface sediments. *Chem. Geol.* 200, 89-103.
- Pfister, C. (1995), Monthly Temperature and Precipitation in Central Europe 1525–1979: Quantifying Documentary Evidence on Weather and its Effects. In: *Climate Since A.D. 1500* (eds R. S. Bradley and P. D. Jones), Routledge, London, 118–142.
- Pierre, C., 1999. The oxygen and carbon isotope distribution in the Mediterranean water masses. *Mar. Geol.* 153, 41-45.
- Popp, B.N., Prah, F.G., Wallsgrove, R.J., Tanimoto, J., 2006. Seasonal patterns of alkenone production in the subtropical oligotrophic North Pacific. *Paleoceanography* 21, PA1004.
- Poulain, P.-M., 2001. Adriatic Sea surface circulation as derived from drifter data between 1990 and 1999. *J. Mar. Syst.* 29, 3-32.
- Prah, F.G., Wakeham, S.G., 1987. Calibration of unsaturation patterns in long-chain ketone compositions for palaeotemperature assessment. *Nature* 330, 367-369.
- Prah, F.G., Pilskaln, C.H., Sparrow, M.A., 2001. Seasonal record for alkenones in sedimentary particles from the Gulf of Maine. *Deep-Sea Res. I* 48, 515-528.
- Prah, F.G., Wolfe, G.V., Sparrow, M.A., 2003. Physiological impacts on alkenone paleothermometry. *Paleoceanography* 18, PA1025.
- Prah, F.G., Popp, B.N., Karl, D.M., Sparrow, M.A., 2005. Ecology and biogeochemistry of alkenone production at Station ALOHA. *Deep-Sea Res. I* 52, 699-719.
- Puškarić, S., Berger, G.W., Jorissen, F.J., 1990. Successive appearance of subfossil phytoplankton species in Holocene sediments of the northern Adriatic and its relation to the increased eutrophication pressure. *Estuar. Coast. Shelf Sci.* 31, 177-187.
- Quadrelli, R., Pavan, V., Molteni, F., 2001. Wintertime variability of Mediterranean precipitation and its links with large-scale circulation anomalies. *Clim. Dyn.* 17, 457-466.
- Raible, C., Casty, C., Luterbacher, J., Pauling, A., Esper, J., Frank, D., Büntgen, U., Roesch, A., Tschuck, P., Wild, M., Vidale, P.-L., Schär, C., Wanner, H., 2006. Climate Variability-Observations, Reconstructions, and Model Simulations for the Atlantic-European and Alpine Region from 1500-2100 AD. *Clim. Change* 79, 9-29.
- Ravelo, A.C., Hillaire-Marcel, C. (2007). The use of oxygen and carbon isotopes of foraminifera in paleoceanography. In: *Developments in Marine Geology: Proxies in Late Cenozoic Paleocanography Vol. 1* (eds C. Hillaire-Marcel, A. de Vernal), pp. 735-764, Elsevier.
- Reimer, P.J., Baillie, M.G.L., Bard, E., Bayliss, A., Beck, J.W., Bertrand, C.J.H., Blackwell, P.G., Buck, C.E., Burr, G.S., Cutler, K.B., Damon, P.E., Edwards, R.L., Fairbanks,

- R.G., Friedrich, M., Guilderson, T.P., Hogg, A.G., Hughen, K.A., Kromer, B., McCormac, G., Manning, S., Ramsey, C.B., Reimer, R.W., Remmele, S., Southon, J.R., Stuiver, M., Talamo, S., Taylor, F.W., van der Plicht, J., and Weyhenmeyer, C.E., 2004. IntCal04 terrestrial radiocarbon age calibration, 0-26 cal kyr BP, *Radiocarbon* 46, 1029-1058.
- Richey, J.N., Hollander, D.J., Flower, B.P., Eglinton, T.I., 2011. Merging late Holocene molecular organic and foraminiferal-based geochemical records of sea surface temperature in the Gulf of Mexico. *Paleoceanography* 26, PA1209. Doi: 10.1029/2010pa002000.
- Rind, D., Shindell, D., Perlwitz, J., Lerner, J., Lonergan, P., Lean, J., McLinden, C., 2004. The Relative Importance of Solar and Anthropogenic Forcing of Climate Change between the Maunder Minimum and the Present. *J. Clim.* 17, 906-929.
- Roberts, N., Moreno, A., Valero-Garcés, B.L., Corella, J.P., Jones, M., Allcock, S., Woodbridge, J., Morellón, M., Luterbacher, J., Xoplaki, E., Türkeş, M., 2012. Palaeolimnological evidence for an east-west climate see-saw in the Mediterranean since AD 900. *Glog. Planet. Change* 84-85, 23-34.
- Rodrigo, F.S., Esteban-Parra, M.J., Pozo-Vázquez, D., Castro-Díez, Y., 2000. Rainfall variability in southern Spain on decadal to centennial time scales. *Int. J. Climatol.* 20, 721-732.
- Rohling, E., Jorissen, F., Grazzini, C.V., Zachariasse, W., 1993. Northern Levantine and Adriatic Quaternary planktic foraminifera; Reconstruction of paleoenvironmental gradients. *Mar. Micropaleontol.* 21, 191-218.
- Rommerskirchen, F., Condon, T., Mollenhauer, G., Dupont, L., Schefuss, E., 2011. Miocene to Pliocene development of surface and subsurface temperatures in the Benguela Current system. *Paleoceanography* 26, PA3216. doi: 10.1029/2010pa002074.
- Rontani, J.-F., Marty, J.-C., Miquel, J.-C., Volkman, J.K., 2006. Free radical oxidation (autoxidation) of alkenones and other microalgal lipids in seawater. *Org. Geochem.* 37, 354-368.
- Rontani, J.F., Zabeti, N., Wakeham, S.G., 2009. The fate of marine lipids: Biotic vs. abiotic degradation of particulate sterols and alkenones in the Northwestern Mediterranean Sea. *Mar. Chem.* 113, 9-18.
- Rossi, S., Auroux, C., Mascle, J., 1983. The Gulf of Taranto (Southern Italy): Seismic stratigraphy and shallow structure. *Mar Geol.* 51, 327-346.
- Ruff, M., Wacker, L., Gäggeler, H.W., Suter, M., Synal, H.A., and Szidat, S., 2007. A gas ion source for radiocarbon measurements at 200 kV, *Radiocarbon* 49, 307-314.
- Sangiorgi, F., Donders, T.H., 2004. Reconstructing 150 years of eutrophication in the north-western Adriatic Sea (Italy) using dinoflagellate cysts, pollen and spores. *Estuarine, Coast. Shelf Sci.* 60, 69-79.

- Savini, A., Corselli, C., 2010. High-resolution bathymetry and acoustic geophysical data from Santa Maria di Leuca Cold Water Coral province (Northern Ionian Sea--Apulian continental slope). *Deep-Sea Res. II* 57, 326-344.
- Schefuß, E., Ratmeyer, V., Stuut, J.-B.W., Jansen, J.H.F., Sinninghe Damsté, J.S., 2003. Carbon isotope analyses of n-alkanes in dust from the lower atmosphere over the central eastern Atlantic. *Geochim. Cosmochim. Acta* 67, 1757-1767.
- Schilman, B., Almogi-Labin, A., Bar-Matthews, M., Labeyrie, L., Paterne, M., Luz, B., 2001. Long- and short-term carbon fluctuations in the Eastern Mediterranean during the late Holocene. *Geology* 29, 1099-1102.
- Schmidt, F., Hinrichs, K.-U., Elvert, M., 2010. Sources, transport, and partitioning of organic matter at a highly dynamic continental margin. *Mar. Chem.* 118, 37-55.
- Schouten, S., Hopmans, E.C., Pancost, R.D., Sinninghe Damsté, J.S., 2000. Widespread occurrence of structurally diverse tetraether membrane lipids: evidence for the ubiquitous presence of low-temperature relatives of hyperthermophiles. *Proc. Natl. Acad. Sci. USA* 97, 14421-14426.
- Schouten, S., Hopmans, E.C., Schefuss, E., Sinninghe Damsté, J.S., 2002. Distributional variations in marine crenarchaeotal membrane lipids: a new tool for reconstructing ancient sea water temperatures? *Earth Planet. Sci. Lett.* 204, 265-274.
- Schouten, S., Huguet, C., Hopmans, E.C., Kienhuis, M.V.M., Sinninghe Damsté, J.S., 2007a. Analytical methodology for TEX₈₆ paleothermometry by High-Performance Liquid Chromatography/Atmospheric Pressure Chemical Ionization-Mass Spectrometry. *Anal. Chem.* 79, 2940-2944.
- Schouten, S., Hopmans, E.C., van der Meer, J., Mets, A., Bard, E., Bianchi, T.S., Diefendorf, A., Escala, M., Freeman, K.H., Furukawa, Y., Huguet, C., Ingalls, A., Ménot-Combes, G., Nederbragt, A.J., Oba, M., Pearson, A., Pearson, E.J., Rosell-Melé, A., Schaeffer, P., Shah, S.R., Shanahan, T.M., Smith, R.W., Smittenberg, R., Talbot, H.M., Uchida, M., Van Mooy, B.A.S., Yamamoto, M., Zhang, Z., Sinninghe Damsté, J.S., 2009. An interlaboratory study of TEX₈₆ and BIT analysis using high-performance liquid chromatography-mass spectrometry. *Geochem. Geophys. Geosyst.* 10, Q03012, doi: 10.1029/2008GC002221.
- Sellschopp, J. and Álvarez, A., 2003. Dense low-salinity outflow from the Adriatic Sea under mild (2001) and strong (1999) winter conditions. *J. Geophys. Res.* 108(C9), 8104, doi: 10.1029/2002JC001562.
- Shackleton, N.J., 1967. Oxygen isotope analyses and Pleistocene temperatures re-assessed. *Nature* 215, 15-17.
- Shackleton, N.J., Opdyke, N.D., 1973. Oxygen isotope and palaeomagnetic stratigraphy of Equatorial Pacific core V28-238: Oxygen isotope temperatures and ice volumes on a 10⁵ year and 10⁶ year scale. *Quat. Res.* 3, 39-55.

- Shackleton, N. J., 1977. Carbon-13 in *Uvigerina*: Tropical rainforest history and the equatorial Pacific carbonate dissolution cycle. In: *The fate of fossil fuel CO₂ in the oceans* (eds. N. R. Anderson and A. Malahoff), pp. 401–428, New York, Plenum.
- Shindell, D.T., Schmidt, G.A., Mann, M.E., Rind, D., Waple, A., 2001. Solar Forcing of Regional Climate Change During the Maunder Minimum. *Science* 294, 2149-2152.
- Sikes, E.L., Volkman, J.K., Robertson, L.G., Pichon, J.-J., 1997. Alkenones and alkenes in surface waters and sediments of the Southern Ocean: Implications for paleotemperature estimation in polar regions. *Geochim. Cosmochim. Acta* 61, 1495-1505.
- Simoneit, B.R.T., 1977. Organic matter in eolian dusts over the Atlantic Ocean. *Mar. Chem.* 5, 443-464
- Socal, G., Boldrin, A., Bianchi, F., Civitarese, G., De Lazzari, A., Rabitti, S., Totti, C., Turchetto, M.M., 1999. Nutrient, particulate matter and phytoplankton variability in the photic layer of the Otranto strait. *J. Mar. Syst.* 20, 381-398.
- Smith, R.W., Bianchi, T.S., Li, X., 2012. A re-evaluation of the use of branched GDGTs as terrestrial biomarkers: Implications for the BIT Index, *Geochim. Cosmochim. Acta*, 80, 14-29.
- Steinhilber, F., Beer, J., Fröhlich, C., 2009. Total solar irradiance during the Holocene. *Geophys. Res. Lett.* 36, L19704.doi:10.1029/2009GL040142.
- Struglia, M.V., Mariotti, A., Filograsso, A., 2004. River discharge into the Mediterranean Sea: Climatology and aspects of the observed variability. *J. Clim.* 17, 4740-4751.
- Sun, M.Y., Wakeham, S.G., 1994. Molecular evidence for degradation and preservation of organic matter in the anoxic Black Sea basin. *Geochim. Cosmochim. Acta* 58, 3395-3406.
- Supić, N., Grbec, B., Vilibić, I. and Ivančić, I., 2004. Long-term changes in hydrographic conditions in northern Adriatic and its relationship to hydrological and atmospheric processes, *Ann. Geophys.*, 22, 733-745, doi:10.5194/angeo-22-733-2004.
- Synal, H.-A., Stocker, M., and Suter, M. (2007), MICADAS: A new compact radiocarbon AMS system, *Nuclear Instruments and Methods in Physics Research B* 259, 7-13.
- Taricco, C., Ghil, M., Vivaldo, G., 2009. Two millennia of climate variability in the Central Mediterranean. *Clim. Past* 5, 171-181.
- Ternois, Y., Sicre, M.A., Boireau, A., Conte, M.H., Eglinton, G., 1997. Evaluation of long-chain alkenones as paleo-temperature indicators in the Mediterranean Sea. *Deep-Sea Res. I* 44, 271-286.
- Trigo, I.F., Davies, T.D., Bigg, G.R., 1999. Objective climatology of cyclones in the Mediterranean region. *Journal of Climate* 12, 1685–1696.
- Trigo, R., Xoplaki, E., Zorita, E., Luterbacher, J., Krichak, S.O., Alpert, P., Jacobeit, J., Sáenz, J., Fernández, J., González-Rouco, F., Garcia-Herrera, R., Rodo, X., Brunetti, M., Nanni, T., Maugeri, M., Türkes, M., Gimeno, L., Ribera, P., Brunet, M., Trigo,

- I.F., Crepon, M., Mariotti, A (2006), Chapter 3 Relations between variability in the Mediterranean region and mid-latitude variability. In: Mediterranean Climate Variability (eds. P. Lionello, P. Malanotte-Rizzoli and R. Boscolo), pp. 179-226, Elsevier.
- Turchetto, M., Boldrin, A., Langone, L., Miserocchi, S., Tesi, T., Fogliani, F., 2007. Particle transport in the Bari Canyon (southern Adriatic Sea). *Marine Geology* 246, 231-247.
- Versteegh, G.J.M., Riegman, R., de Leeuw, J.W., Jansen, J.H.F., 2001. $U^{K'}_{37}$ values for *Isochrysis galbana* as a function of culture temperature, light intensity and nutrient concentrations. *Org. Geochem.* 32, 785-794.
- Versteegh, G.J.M., de Leeuw, J.W., Taricco, C., Romero, A., 2007. Temperature and productivity influences on $U^{K'}_{37}$ and their possible relation to solar forcing of the Mediterranean winter. *Geochem., Geophys., Geosyst.* 8, Q09005, doi: 10.1029/2006GC001543.
- Vilibić, I., Supić, N., 2005. Dense water generation on a shelf: the case of the Adriatic Sea. *Ocean Dyn.* 55, 403-415.
- Volkman, J.K., Eglinton, G., Corner, E.D.S., Forsberg, T.E.V., 1980. Long-chain alkenes and alkenones in the marine coccolithophorid *Emiliana huxleyi*. *Phytochemistry* 19, 2619-2622.
- Volkman, J.K., Barrerr, S.M., Blackburn, S.I., Sikes, E.L., 1995. Alkenones in *Gephyrocapsa oceanica*: Implications for studies of paleoclimate. *Geochim. Cosmochim Acta* 59, 513-520.
- Walsh, E.M., Ingalls, A.E., Keil, R.G., 2008. Sources and transport of terrestrial organic matter in Vancouver Island fjords and the Vancouver-Washington Margin: A multiproxy approach using $\delta^{13}C_{org}$, lignin phenols, and the ether lipid BIT index. *Limnol. Oceanogr.* 53, 1054-1063.
- Wanner, H., Holzhauser, H., Pfister, C., Zumbühl, H., 2000. Interannual to Century Scale Climate Variability in the European Alps (Die Klimavariabilität im europäischen Alpenraum auf der Zeitskala von Jahren bis Jahrhunderten). *Erdkunde*, 62-69.
- Waelbroeck, C., Mulitza, S., Spero, H., Dokken, T., Kiefer, T., Cortijo, E., 2005. A global compilation of late Holocene planktonic foraminiferal ^{18}O : relationship between surface water temperature and ^{18}O . *Quat. Sci. Rev.* 24, 853-868.
- Weijers, J.W.H., Schouten, S., Spaargaren, O.C., Sinninghe Damsté, J.S., 2006b. Occurrence and distribution of tetraether membrane lipids in soils: Implications for the use of the TEX₈₆ proxy and the BIT index. *Org. Geochem.* 37, 1680-1693.
- Wuchter, C., Schouten, S., Wakeham, S.G., Sinninghe Damsté, J.S., 2005. Temporal and spatial variation in tetraether membrane lipids of marine crenarchaeota in particulate organic matter: Implications for TEX₈₆ paleothermometry. *Paleoceanography* 20, PA3013.

- Wuchter, C., Schouten, S., Wakeham, S.G., Sinninghe Damsté, J.S., 2006. Archaeal tetraether membrane lipid fluxes in the northeastern Pacific and the Arabian Sea: Implications for TEX₈₆ paleothermometry. *Paleoceanography* 21, PA4208.
- Wuchter, C., Abbas, B., Coolen, M.J.L., Herfort, L., van Bleijswijk, J., Timmers, P., Strous, M., Teira, E., Herndl, G.J., Middelburg, J.J., Schouten, S., Sinninghe Damsté, J.S., 2006. Archaeal nitrification in the ocean. *Proc. N. Ac. Sci.* 103, 12317-12322.
- Xoplaki, E., Maheras, P., Luterbacher, J., 2001. Variability of climate in meridional Balkans during the periods 1675-1715 and 1780-1830 and its impact on human life. *Clim. Change* 48, 581-615.
- Xoplaki, E., González-Rouco, J.F., Luterbacher, J., Wanner, H., 2003. Mediterranean summer air temperature variability and its connection to the large-scale atmospheric circulation and SSTs. *Clim. Dyn.* 20, 723-739.
- Xoplaki, E., González-Rouco, J.F., Luterbacher, J., Wanner, H., 2004. Wet season Mediterranean precipitation variability: influence of large-scale dynamics and trends. *Clim. Dyn.* 23, 63-78.
- Zachos, J.C., Stott, L.D., Lohmann, K.C., 1994. Evolution of early Cenozoic marine temperatures. *Paleoceanography* 9, 353-387.
- Zanchettin, D., Traverso, P., Tomasino, M., 2008. Po River discharges: a preliminary analysis of a 200-year time series. *Clim. Change* 89, 411-433.
- Ziveri, P., Rutten, A., de Lange, G.J., Thomson, J., Corselli, C., 2000. Present-day coccolith fluxes recorded in central eastern Mediterranean sediment traps and surface sediments. *Palaeogeogr., Palaeoclim., Palaeoecol.* 158, 175-195.
- Zonneveld, K.A.F., and cruise participants, 2008. Report and preliminary results of R/V POSEIDON Cruise P339, Piräus - Messina, 16 June - 2 July 2006. *Berichte, Fachbereich Geowissenschaften, Universität Bremen* 268, 61.
- Zonneveld, K.A.F., Chen, L., Möbius, J., Mahmoud, M.S., 2009. Environmental significance of dinoflagellate cysts from the proximal part of the Po-river discharge plume (off southern Italy, Eastern Mediterranean). *J. Sea Res.* 62, 189-213.
- Zonneveld, K.A.F., Chen, L., Elshanawany, R., Fischer, H.W., Hoins, M., Ibrahim, M.I., Pittauerova, D., Versteegh, G.J.M., 2012. The use of dinoflagellate cysts to separate human-induced from natural variability in the trophic state of the Po River discharge plume over the last two centuries. *Mar. Poll. Bull.* 64, 114-132.

IV.S1. SUPPLEMENTARY MATERIAL (ELECTRONICAL ANNEX)

Table IV.S1 Numerical data of cores NU04 and GeoB 10709-4

Core	Depth [mm]	Year [AD]	<i>G. ruber (white)</i>				<i>G. ruber (pink)</i>				<i>U. mediterranea</i>					
			$\delta^{18}\text{O}$ [‰ VPDB]	SD	SST $\delta^{18}\text{O}$ [°C]	$\delta^{13}\text{C}$ [‰ VPDB]	SD	$\delta^{18}\text{O}$ [‰ VPDB]	SST $\delta^{18}\text{O}$ [°C]	$\delta^{13}\text{C}$ [‰ VPDB]	Abundance Individuals/g dry weight	$\delta^{18}\text{O}$ [‰ VPDB]	T $\delta^{18}\text{O}$ [°C]	$\delta^{13}\text{C}$ [‰ VPDB]	SD	
NU04	1.5	2003	0.78	0.01	19.7	0.27	0.01	-0.19	23.6	0.91		0.81	2.21	13.9	-0.37	0.01
NU04	4.5	2000	0.82	0.01	19.5	0.10	0.01	-0.26	24.0	1.00		0.74	2.12	14.2	-0.03	0.01
NU04	7.5	1996	0.54	0.02	20.7	0.48	0.01	-0.29	24.1	0.98		0.77	2.16	14.1	-0.26	0.01
NU04	10.5	1993	0.44	0.01	21.2	0.56	0.00	-0.35	24.4	0.70		0.73	2.21	13.8	-0.26	0.01
NU04	13.5	1989	0.79	0.02	19.6	0.85	0.01	-0.14	23.4	0.58		1.06	2.18	14.0	-0.01	0.01
NU04	16.5	1986	0.81	0.01	19.5	0.45	0.01	-0.47	25.0	0.66		0.81	2.12	14.2	0.12	0.01
NU04	19.5	1982	0.88	0.02	19.2	0.15	0.01	-0.40	24.6	1.14		1.18	2.19	13.9	-0.04	0.01
NU04	22.5	1979	0.59	0.01	20.5	0.50	0.01					0.89	2.13	14.2	-0.13	0.01
NU04	25.5	1975	0.99	0.01	18.7	0.16	0.01	-0.19	23.6	1.32		0.93	2.15	14.1	-0.40	0.01
NU04	28.5	1971	0.35	0.01	21.6	0.62	0.01	-0.51	25.1	0.53		0.93	2.12	14.2	-0.23	0.01
NU04	31.5	1968	0.42	0.03	21.3	0.24	0.01	-0.48	25.0	1.07		0.95	1.93	15.0	-0.15	0.01
NU04	34.5	1964	0.94	0.02	18.9	0.37	0.01	-0.34	24.3	1.23		0.82	2.19	13.9	-0.39	0.01
NU04	37.5	1961	0.64	0.02	20.3	0.23	0.01	-0.58	25.5	1.00		1.17	2.16	14.1	-0.37	0.01
NU04	40.5	1957	0.89	0.01	19.2	0.34	0.01	-0.54	25.3	1.02		0.94	2.12	14.2	-0.01	0.01
NU04	43.5	1954	0.40	0.01	21.4	0.23	0.01	-0.54	25.3	0.84		0.67	2.02	14.6	-0.22	0.01
NU04	46.5	1950	1.10	0.01	18.2	0.35	0.01					0.81	2.33	13.3	0.06	0.01
NU04	49.5	1947				0.63	0.01	-0.21	23.7	1.18		0.60	2.19	13.9	-0.36	0.01
NU04	52.5	1943	0.92	0.02	19.0	0.35	0.01					0.44	2.21	13.8	-0.19	0.01
NU04	55.5	1940	0.66	0.01	20.2	0.59	0.01	-0.28	24.1	1.00		0.74	2.23	13.8	-0.38	0.01
NU04	58.5	1936	0.60	0.01	20.5	0.49	0.01	-0.18	23.6	0.81		0.41	2.22	13.8	0.01	0.01
NU04	61.5	1933	0.89	0.01	19.2	0.22	0.01	-0.49	25.1	0.91		0.22	2.23	13.7	0.29	0.01
NU04	64.5	1929	0.58	0.01	20.6	0.55	0.01	-0.35	24.4	1.22		0.38	2.24	13.7	0.19	0.01
NU04	67.5	1926	0.54	0.02	20.8	0.61	0.01	0.01	22.7	0.63		0.32	2.18	14.0	0.09	0.01
NU04	70.5	1922	1.17	0.01	17.9	0.46	0.01	-0.39	24.6	1.10		0.55	2.12	14.2	-0.46	0.01
NU04	73.5	1919	0.90	0.01	19.1	0.65	0.01	-0.66	25.9	0.63		0.53	2.30	13.5	-0.08	0.01
NU04	76.5	1915	0.79	0.02	19.6	0.63	0.01					0.42	2.17	14.0	-0.36	0.01
NU04	79.5	1911	0.66	0.02	20.2	0.36	0.00	-0.17	23.6	0.75		0.48	2.17	14.0	0.10	0.01
NU04	82.5	1908	0.94	0.03	18.9	0.27	0.01					0.48	2.03	14.6	-0.23	0.02
NU04	85.5	1904	0.39	0.02	21.5	0.33	0.01	-0.06	23.0	0.86		0.39	2.23	13.8	-0.05	0.02
NU04	88.5	1901	1.02	0.01	18.6	0.68	0.01					0.34	2.23	13.7	-0.26	0.02

NU04	91.5	1897	0.48	0.02	21.0	0.50	0.01	0.37	21.1	0.66	0.27	2.27	13.6	0.30	0.01
NU04	94.5	1894									0.31	2.29	13.5	-0.01	0.02
NU04	97.5	1890	1.17	0.01	17.9	0.35	0.01	0.01	22.7	0.94	0.14	2.43	12.9	0.31	0.02
NU04	100.5	1887	1.26	0.01	17.5	0.34	0.01				0.38	2.50	12.6	0.08	0.02
NU04	103.5	1883	0.89	0.01	19.2	0.27	0.00	0.06	22.5	0.90	0.13	2.36	13.2	0.17	0.02
NU04	106.5			0.04	15.9	0.19	0.01				0.08	2.39	13.1	0.13	0.02
NU04	109.5	1876	1.06	0.01	18.4	0.38	0.00	0.27	21.5	1.24	0.10	2.38	13.1	0.03	0.02
NU04	112.5	1873	0.66	0.02	20.2	0.66	0.01	1.05	18.0	0.51	0.00	2.42	13.0	0.08	0.02
NU04	115.5	1869	0.77	0.01	19.7	0.70	0.01	-0.43	24.8	0.93	0.17	2.18	14.0	-0.17	0.02
NU04	118.5	1866	1.40	0.01	16.9	0.15	0.01	0.28	21.5	1.16	0.13	2.44	12.9	0.31	0.02
NU04	121.5	1862	0.78	0.02	19.7	0.33	0.00	-0.72	26.2	1.21	0.14	2.31	13.4	0.24	0.01
NU04	124.5	1859	0.77	0.02	19.7	0.52	0.01				0.00	2.23	13.8	0.41	0.02
NU04	127.5	1855	0.82	0.02	19.5	0.70	0.01	-0.24	23.9	0.64	0.09	2.23	13.8	0.29	0.02
NU04	130.5	1851	1.26	0.01	17.5	0.25	0.01	0.14	22.1	0.84	0.09	2.34	13.3	0.17	0.02
NU04	133.5	1848	0.80	0.01	19.6	0.73	0.01	-0.32	24.3	1.29	0.05	2.38	13.1	-0.21	0.02
NU04	136.5	1844									0.00				
NU04	139.5	1841	1.02	0.01	18.6	0.47	0.01	0.10	22.3	0.48	0.18	2.37	13.1	0.13	0.02
NU04	142.5	1837	1.09	0.02	18.3	0.43	0.01	0.00	22.8	0.98	0.13	2.31	13.4	0.07	0.02
NU04	145.5	1834	0.88	0.02	19.2	0.55	0.01				0.00	2.14	14.2	-0.03	0.02
NU04	148.5	1830	1.06	0.01	18.4	0.44	0.01				0.00	2.26	13.6	-0.05	0.02
NU04	151.5	1827	0.73	0.02	19.9	0.77	0.01	-0.23	23.8	1.12	0.22	2.02	14.7	0.13	0.01
NU04	154.5	1823	0.94	0.00	18.9	0.53	0.01	0.51	20.4	1.12	0.14	2.23	13.8	0.14	0.02
NU04	157.5	1820	1.13	0.02	18.1	0.61	0.01	-0.06	23.1	0.96	0.10	2.36	13.2	0.20	0.02
NU04	160.5	1816	1.23	0.01	17.6	0.22	0.01	0.35	21.2	0.86	0.08	2.15	14.1	-0.05	0.02
NU04	163.5	1813	0.93	0.01	19.0	0.65	0.01	0.35	21.2	0.81	0.04	2.32	13.4	0.37	0.02
NU04	166.5	1809						0.10	22.3	0.81	0.13	2.44	12.9	-0.09	0.02
NU04	169.5	1806	1.28	0.01	17.4	0.46	0.01				0.00	2.25	13.7	0.11	0.01
NU04	172.5	1802	1.07	0.01	18.4	0.48	0.01				0.09	2.21	13.8	0.10	0.01
NU04	175.5	1799	1.02	0.02	18.6	0.53	0.01	-0.19	23.7	0.87	0.09	2.35	13.2	0.08	0.01
NU04	178.5	1795	0.86	0.01	19.3	0.63	0.01	0.74	19.4	0.23	0.09	2.24	13.7	0.15	0.01
NU04	181.5	1791	1.30	0.01	17.3	0.28	0.01	-0.56	25.4	1.34	0.09	2.37	13.2	-0.01	0.01
NU04	184.5	1788	1.18	0.02	17.9	0.62	0.01	-0.05	23.0	1.05	0.13	2.29	13.5	0.02	0.02
NU04	187.5	1784	1.04	0.02	18.5	0.56	0.01	0.22	21.8	1.20	0.15	2.18	14.0	0.23	0.01
NU04	190.5	1781	1.07	0.01	18.4	0.58	0.01	-0.20	23.7	1.31	0.18	2.30	13.5	0.21	0.01
NU04	193.5	1777	1.02	0.01	18.6	0.62	0.01	0.63	19.9	1.30	0.04	2.21	13.8	0.02	0.03
NU04	196.5	1774	1.28	0.01	17.4	0.53	0.01				0.05	2.37	13.2	-0.09	0.01
NU04	199.5	1770	1.20	0.01	17.8	0.39	0.01	-0.74	26.3	0.80	0.13	2.29	13.5	0.00	0.02
NU04	202.5	1767	1.05	0.02	18.5	0.53	0.01	0.89	18.7	0.55	0.09	2.10	14.3	0.06	0.03
NU04	205.5	1763	0.86	0.02	19.3	0.48	0.01	-0.14	23.4	1.37	0.27	2.07	14.5	-0.05	0.01
NU04	208.5	1760	1.05	0.01	18.5	0.56	0.01	0.09	22.3	1.22	0.17	2.21	13.9	-0.11	0.01

Chapter IV

NU04	211.5	1756	0.95	0.01	18.9	0.59	0.01	0.41	20.9	0.97	0.17	2.05	14.5	0.13	0.01
NU04	214.5	1753	0.79	0.01	19.6	0.55	0.01	-0.75	26.3	1.27	0.30	2.13	14.2	-0.03	0.01
NU04	217.5	1749	0.81	0.03	19.5	0.46	0.00	-0.36	24.5	0.96	0.22	2.14	14.1	-0.03	0.01
NU04	220.5	1746	0.56	0.01	20.6	0.54	0.01	-0.48	25.0	1.00	0.26	2.45	12.8	0.09	0.06
NU04	223.5	1742	0.67	0.01	20.1	0.69	0.01	-0.39	24.6	1.06	0.21	2.61	12.2	0.28	0.01
NU04	226.5	1739	0.77	0.01	19.7	0.59	0.01	-0.67	25.9	1.22	0.13	2.25	13.7	0.30	0.01
NU04	229.5	1735									0.14	2.21	13.8	0.17	0.01
NU04	232.5	1731	0.76	0.02	19.7	0.51	0.01	-0.44	24.8	1.29	0.09	2.17	14.0	0.27	0.18
NU04	235.5	1728	0.99	0.03	18.7	0.44	0.00	-0.35	24.4	1.16	0.09	2.66	12.0	0.44	0.01
NU04	238.5	1724	0.59	0.02	20.5	0.82	0.01				0.09	2.21	13.8	0.15	0.01
NU04	241.5	1721	1.21	0.01	17.7	0.49	0.01				0.09	2.29	13.5	0.28	0.01
NU04	244.5	1717	1.18	0.02	17.9	0.41	0.01				0.13	2.22	13.8	0.10	0.01
NU04	247.5	1714	1.15	0.02	18.0	0.47	0.01				0.12	2.26	13.6	0.27	0.01
NU04	250.5	1710	1.15	0.01	18.0	0.40	0.01				0.15	2.34	13.3	-0.07	0.01
NU04	253.5	1707	1.30	0.01	17.3	0.54	0.01				0.27	2.47	12.7	0.21	0.01
NU04	256.5	1703	0.92	0.02	19.1	0.56	0.01				0.25	2.22	13.8	-0.05	0.01
NU04	259.5	1700	0.71	0.01	20.0	0.57	0.01				0.09	2.30	13.5	0.26	0.01
NU04	262.5	1696	0.85	0.02	19.3	0.88	0.01	-0.60	25.6	1.08	0.04	2.52	12.5	0.01	0.01
NU04	265.5	1693	1.00	0.02	18.7	0.87	0.01	-0.21	23.7	0.95	0.10	2.20	13.9	0.05	0.01
NU04	268.5	1689	0.96	0.02	18.9	0.57	0.01	-0.04	23.0	1.26	0.25	2.11	14.3	-0.11	0.01
NU04	271.5	1686	0.90	0.01	19.1	0.46	0.01	-1.14	28.2	1.45	0.05	2.15	14.1	0.04	0.01
NU04	274.5	1682	0.88	0.01	19.2	0.54	0.01	-0.44	24.8	0.88	0.14	2.18	14.0	0.04	0.01
NU04	277.5	1679	1.06	0.02	18.4	0.17	0.01				0.13	2.18	14.0	0.06	0.01
NU04	280.5	1675	0.64	0.02	20.3	0.67	0.01	-0.49	25.1	1.32	0.24	2.19	13.9	0.11	0.01
NU04	283.5	1671	0.60	0.02	20.5	0.76	0.01	-0.57	25.5	1.46	0.14	2.11	14.3	-0.13	0.01
NU04	286.5	1668	0.87	0.02	19.3	0.56	0.01	-0.35	24.4	0.80	0.22	2.25	13.7	0.20	0.05
NU04	289.5	1664	0.96	0.02	18.9	0.41	0.01	-0.63	25.7	0.78	0.14	2.11	14.3	0.21	0.05
NU04	292.5	1661	0.80	0.02	19.6	0.30	0.01	-0.67	25.9	1.48	0.18	2.05	14.5	-0.03	0.05
NU04	295.5	1657	0.85	0.01	19.3	0.53	0.01	0.13	22.2	0.98	0.33	2.14	14.1	0.07	0.05
NU04	298.5	1654	1.08	0.01	18.3	0.50	0.01	0.03	22.6	1.00	0.40	2.25	13.7	0.40	0.01
NU04	301.5	1650	1.11	0.01	18.2	0.45	0.01	-0.12	23.3	0.82	0.09	2.16	14.0	0.10	0.05
NU04	304.5	1647	0.75	0.01	19.8	0.60	0.01	-0.16	23.5	1.17	0.14	2.55	12.4	0.45	0.05
NU04	307.5	1643	0.86	0.01	19.3	0.68	0.01	-0.19	23.7	1.41	0.09	1.93	15.0	-0.14	0.02
NU04	310.5	1640	0.44	0.02	21.2	0.87	0.01	0.01	22.7	0.89	0.29	2.32	13.4	0.46	0.05
NU04	313.5	1636	0.71	0.01	20.0	0.86	0.01	-0.26	24.0	1.26	0.12	2.07	14.4	0.00	0.05
NU04	316.5	1633	0.87	0.03	19.3	0.53	0.01	-0.22	23.8	1.20	0.32	2.15	14.1	0.08	0.05
NU04	319.5	1629						-0.46	24.9	1.19	0.43	2.21	13.8	0.17	0.05
NU04	322.5	1626	0.61	0.02	20.4	0.82	0.01	-0.15	23.5	1.09	0.25	2.12	14.2	0.34	0.05
NU04	325.5	1622	1.13	0.02	18.1	0.00	0.01	-0.54	25.3	1.18	0.21	2.04	14.6	0.25	0.05
NU04	328.5	1619	0.96	0.03	18.8	0.55	0.01	-0.67	25.9	1.23	0.12	2.03	14.6	0.13	0.01

NU04	331.5	1615	1.02	0.02	18.6	0.46	0.01	-0.48	25.0	1.34	0.25	2.06	14.5	0.07	0.02
NU04	334.5	1611	1.03	0.01	18.5	0.39	0.01	-0.97	27.4	1.35	0.18	2.13	14.2	-0.11	0.05
NU04	337.5	1608	0.74	0.03	19.9	0.58	0.00	-0.69	26.0	0.91	0.21	2.18	14.0	0.01	0.05
NU04	340.5	1604	0.89	0.01	19.1	0.36	0.01	-0.47	25.0	1.04	0.18	2.44	12.9	0.09	0.05
NU04	343.5	1601	1.07	0.01	18.4	0.52	0.01	-0.28	24.1	1.11	0.24	2.14	14.1	0.04	0.05
NU04	346.5	1597	0.89	0.01	19.2	0.62	0.01	-0.39	24.6	1.26	0.13	1.89	15.2	-0.01	0.01
NU04	349.5	1594	0.81	0.02	19.5	0.74	0.01	-0.48	25.0	1.07	0.13	2.13	14.2	0.21	0.05
NU04	352.5	1590	0.72	0.01	19.9	0.70	0.01	-0.40	24.6	1.31	0.38	2.29	13.5	0.19	0.00
NU04	355.5	1587	1.00	0.02	18.7	0.61	0.01	-0.49	25.1	0.92	0.13	2.56	12.4	0.23	0.05
NU04	358.5	1583	0.95	0.01	18.9	0.66	0.01	0.05	22.5	0.94	0.30	2.22	13.8	0.23	0.01
NU04	361.5	1580	0.66	0.01	20.2	0.86	0.01	-0.31	24.2	0.66	0.20	1.96	14.9	0.17	0.05
NU04	364.5	1576	1.00	0.02	18.7	0.63	0.01	-0.12	23.3	1.19	0.16	2.06	14.5	-0.04	0.05
NU04	367.5	1573	0.61	0.01	20.4	0.87	0.00	-0.24	23.9	1.25	0.14	2.09	14.4	-0.01	0.05
NU04	370.5	1569	0.88	0.01	19.2	0.57	0.01	-0.23	23.8	1.20	0.33	2.17	14.0	0.01	0.05
NU04	373.5	1566	0.52	0.02	20.8	0.65	0.01	-0.10	23.2	1.04	0.37	2.22	13.8	0.08	0.05
NU04	376.5	1562	0.80	0.01	19.6	0.61	0.01	-0.37	24.5	1.40	0.43	2.18	14.0	0.02	0.05
NU04	379.5	1559	1.19	0.01	17.8	0.70	0.00	0.03	22.6	0.98	0.31	2.17	14.0	0.19	0.05
NU04	382.5	1555	0.40	0.03	21.4	0.82	0.01	-0.79	26.5	1.55	0.09	2.09	14.3	0.18	0.05
NU04	385.5	1551	0.68	0.02	20.1	0.70	0.01	-0.54	25.3	1.64	0.23	2.15	14.1	0.01	0.05
NU04	388.5	1548	0.82	0.01	19.5	0.55	0.01	-0.45	24.9	0.96	0.29	2.04	14.6	0.17	0.01
NU04	391.5	1544	0.93	0.01	19.0	0.44	0.00	0.00	22.8	0.96	0.22	2.55	12.4	0.26	0.05
NU04	394.5	1541						-0.10	23.3	0.96	0.00	2.11	14.3	-0.09	0.05
NU04	397.5	1537	0.49	0.01	21.0	0.95	0.01	-0.04	22.9	1.07	0.08	2.10	14.3	0.19	0.05
NU04	400.5	1534	1.03	0.01	18.6	0.52	0.01	0.51	20.4	1.21	0.28	2.29	13.5	0.13	0.05
NU04	403.5	1530	0.86	0.01	19.3	0.64	0.00	-0.10	23.2	1.24	0.31	2.10	14.3	0.07	0.05
NU04	406.5	1527	0.80	0.02	19.6	0.63	0.01	0.05	22.5	1.08	0.22	2.07	14.4	-0.16	0.01
NU04	409.5	1523	0.73	0.01	19.9	0.95	0.01	0.22	21.7	1.02	0.18	2.28	13.6	0.50	0.01
NU04	412.5	1520	0.87	0.01	19.3	0.62	0.01	-0.70	26.1	1.36	0.14	2.09	14.3	-0.07	0.01
NU04	415.5	1516	0.56	0.02	20.7	0.70	0.01	0.10	22.3	0.92	0.21	2.26	13.6	0.21	0.01
NU04	418.5	1513	1.09	0.01	18.3	0.52	0.00	0.66	19.8	1.06	0.18	2.31	13.4	0.23	0.01
NU04	421.5	1509	0.56	0.01	20.6	0.90	0.01	-0.55	25.3	1.48	0.19	2.03	14.6	0.13	0.01
NU04	424.5	1506	0.81	0.01	19.5	0.87	0.01	-0.60	25.6	1.24	0.09	2.28	13.6	0.18	0.01
NU04	427.5	1502	0.47	0.01	21.1	0.64	0.01	-0.21	23.7	1.27	0.43	2.18	14.0	0.42	0.01
NU04	430.5	1499	0.82	0.01	19.5	0.70	0.01	-0.13	23.4	0.99	0.22	2.26	13.6	0.20	0.01
NU04	433.5	1495	0.93	0.01	19.0	0.59	0.01	-0.22	23.8	1.19	0.26	1.97	14.8	0.08	0.01
NU04	436.5	1491	0.77	0.02	19.7	0.79	0.01	-0.31	24.2	1.35	0.42	2.35	13.2	0.19	0.01
NU04	439.5	1488	0.52	0.01	20.8	0.66	0.01	-0.12	23.3	1.15	0.08	1.96	14.9	0.03	0.01
NU04	442.5	1484	0.85	0.01	19.4	0.83	0.01	-0.16	23.5	1.30	0.41	2.11	14.3	0.34	0.01
NU04	445.5	1481	0.79	0.01	19.6	0.76	0.01	-0.25	24.0	0.95	0.33	2.53	12.5	0.03	0.01
NU04	448.5	1477	0.86	0.01	19.3	0.20	0.01	-0.29	24.1	1.23	0.21	1.96	14.9	0.08	0.01

Chapter IV

NU04	451.5	1474	0.34	0.01	21.7	1.03	0.01				0.18	2.12	14.2	0.13	0.01
NU04	454.5	1470	0.73	0.01	19.9	0.80	0.01	-0.13	23.4	0.86	0.13	2.03	14.6	0.11	0.01
NU04	457.5	1467	1.14	0.01	18.1	0.32	0.01	-0.29	24.1	1.44	0.26	2.17	14.0	0.15	0.01
NU04	460.5	1463	0.97	0.01	18.8	0.61	0.01	0.05	22.5	0.34	0.14	2.00	14.7	0.12	0.01

Multiproxy environmental reconstruction Gulf of Taranto

TOC and lipid biomarkers											
Core [GeoB]	Depth [mm]	Year [AD]	TOC [%]	U ^K ₃₇	SST U ^K ₃₇ [°C]	c alkenones [μg/g]	TEX ₈₆	SST TEX ^H ₈₆ [°C]	c crenarchaeol [ng/g]	BIT	c sum <i>n</i> -C _{27,29,31} alkanes [μg/g]
10709-4	0	2006	1.28	0.61	16.74	0.278	0.53	19.6		0.17	0.81
10709-4	2.5	2003		0.62	17.19	2.257	0.53	19.5	0.261	0.14	1.05
10709-4	5	2000	1.42	0.57	15.65	0.242	0.53	19.8		0.14	1.37
10709-4	7.5	1997		0.54	14.66	0.330	0.54	20.4	0.240	0.15	0.81
10709-4	10	1994	1.17	0.56	15.37	0.600				0.14	0.92
10709-4	12.5	1991		0.55	15.08	0.202	0.52	19.2	0.237	0.15	1.08
10709-4	15	1988		0.54	14.86	0.392	0.53	19.6	0.259	0.15	1.14
10709-4	17.5	1985		0.58	16.07	0.669	0.51	18.7	0.227	0.16	0.84
10709-4	20	1982	1.21	0.58	15.96	0.272	0.52	19.3		0.18	1.07
10709-4	22.5	1980		0.56	15.36	0.503	0.54	20.0	0.249	0.15	1.05
10709-4	25	1977	0.99	0.56	15.45	0.558	0.52	19.1		0.12	0.81
10709-4	27.5	1974		0.57	15.80	0.484	0.53	19.7	0.232	0.16	0.97
10709-4	30	1971		0.59	16.18	0.952	0.52	19.4	0.272	0.16	1.06
10709-4	32.5	1968					0.54	20.5	0.225	0.15	0.92
10709-4	35	1965	1.14	0.65	18.01		0.54	20.1		0.17	0.94
10709-4	37.5	1962		0.63	17.61	1.700	0.52	19.4	0.201	0.17	0.88
10709-4	40	1959	1.12	0.64	17.64	1.208	0.53	19.6		0.18	0.78
10709-4	42.5	1956		0.63	17.63	0.830	0.55	20.9	0.220	0.17	1.08
10709-4	45	1953		0.62	17.05	0.310	0.53	19.9	0.197	0.18	0.85
10709-4	47.5	1950		0.59	16.27	0.224	0.54	20.3	0.208	0.18	0.96
10709-4	50	1947	1.12	0.58	16.11	0.175	0.53	19.8		0.19	0.71
10709-4	52.5	1944		0.56	15.49	0.291	0.54	20.1	0.219	0.16	0.84
10709-4	55	1941		0.61	16.92	0.485	0.54	20.3	0.243	0.18	0.94
10709-4	57.5	1938		0.54	14.65	0.235					0.88
10709-4	60	1935		0.63	17.35	0.267	0.51	18.9	0.189	0.19	1.05
10709-4	62.5	1932		0.57	15.82	0.164	0.52	19.4	0.190	0.20	0.93
10709-4	65	1930		0.57	15.67	0.143	0.54	20.1	0.163	0.20	0.81
10709-4	67.5	1927		0.62	17.18	0.147	0.52	19.2	0.163	0.21	0.79
10709-4	70	1924		0.58	16.12	0.146	0.54	20.4	0.157	0.21	0.62
10709-4	72.5	1921		0.58	15.98	0.158	0.54	20.4	0.161	0.21	0.61
10709-4	75	1918		0.59	16.27	0.161	0.53	19.5	0.154	0.22	0.62
10709-4	77.5	1915		0.53	14.60	0.111	0.52	19.4	0.176	0.21	0.61
10709-4	80	1912	1.04	0.58	16.09	0.220	0.52	19.0	0.168	0.22	0.93
10709-4	82.5	1909		0.55	14.98	0.147	0.54	20.1		0.23	0.56
10709-4	85	1906		0.56	15.31	0.145	0.53	19.7	0.162	0.22	0.70
10709-4	87.5	1903		0.58	15.91	0.128	0.54	20.1	0.171	0.21	0.60
10709-4	90	1900		0.59	16.20	0.182	0.55	20.7	0.155	0.23	0.64
10709-4	92.5	1897		0.60	16.68	0.166	0.54	20.5	0.154	0.23	0.59
10709-4	95	1894		0.59	16.33	0.172	0.54	20.5	0.144	0.23	0.68
10709-4	97.5	1891		0.60	16.46	0.103	0.53	19.6	0.137	0.24	0.80
10709-4	100	1888	0.96	0.63	17.63	0.155	0.53	19.5		0.28	1.21
10709-4	102.5	1885		0.59	16.31	0.164	0.54	20.1	0.138	0.25	1.13
10709-4	105	1882		0.59	16.17	0.118	0.54	20.2	0.139	0.24	0.87
10709-4	107.5	1880		0.58	16.00	0.110	0.54	20.1	0.132	0.24	1.06
10709-4	110	1877		0.59	16.21	0.156	0.54	20.4	0.126	0.25	0.61
10709-4	112.5	1874		0.61	16.90	0.139	0.53	19.8	0.128	0.25	0.65
10709-4	115	1871		0.59	16.18	0.136	0.54	20.4	0.126	0.25	0.89
10709-4	117.5	1868		0.60	16.60	0.093	0.53	20.0	0.145	0.25	0.80
10709-4	120	1865	0.91	0.60	16.53	0.149					0.81
10709-4	122.5	1862		0.59	16.22	0.144	0.54	20.1	0.121	0.26	0.92
10709-4	125	1859		0.59	16.28	0.075	0.53	19.6	0.117	0.26	0.72
10709-4	127.5	1856		0.61	16.81	0.083	0.54	20.6	0.112	0.26	0.98
10709-4	130	1853		0.59	16.29	0.085	0.54	20.1	0.117	0.26	0.98
10709-4	132.5	1850		0.59	16.38	0.091	0.55	20.6	0.116	0.26	0.86
10709-4	135	1847		0.59	16.24	0.072	0.54	20.3	0.113	0.27	0.83
10709-4	137.5	1844		0.58	15.95	0.106	0.54	20.2	0.109	0.27	0.94
10709-4	140	1841		0.59	16.25	0.113	0.55	21.0	0.110	0.27	0.65
10709-4	142.5	1838		0.63	17.34	0.094	0.56	21.5	0.103	0.28	0.69
10709-4	145	1835		0.59	16.16	0.071	0.55	20.8	0.113	0.27	0.77

Chapter IV

10709-4	147.5	1832		0.60	16.70	0.073	0.55	21.1	0.102	0.27	0.83
10709-4	150	1830		0.60	16.49	0.050	0.55	20.6	0.101	0.27	0.81
10709-4	152.5	1827		0.62	17.10	0.036	0.54	20.2	0.100	0.28	0.77
10709-4	155	1824		0.60	16.55	0.066	0.54	20.4	0.102	0.28	0.74
10709-4	157.5	1821		0.63	17.38	0.066	0.53	19.8	0.101	0.28	0.91
10709-4	160	1818					0.54	20.4	0.098	0.28	0.53
10709-4	162.5	1815					0.55	20.6	0.091	0.28	0.78
10709-4	165	1812		0.56	15.37	0.036	0.56	21.2	0.079	0.30	0.64
10709-4	167.5	1809		0.62	17.08	0.033	0.56	21.2	0.085	0.29	0.60
10709-4	170	1806		0.65	17.98	0.030	0.55	20.6	0.082	0.30	0.57
10709-4	172.5	1803		0.63	17.39	0.044	0.58	22.4	0.075	0.32	0.54
10709-4	175	1800					0.57	22.0	0.070	0.33	0.63
10709-4	177.5	1797					0.55	20.8	0.070	0.32	0.58
10709-4	180	1794					0.56	21.3	0.084	0.29	0.55
10709-4	182.5	1791		0.62	17.20	0.079	0.56	21.2	0.077	0.31	0.69
10709-4	185	1788		0.64	17.93	0.034	0.55	21.0	0.075	0.32	0.62
10709-4	187.5	1785		0.66	18.24	0.066	0.55	20.9	0.068	0.32	0.61
10709-4	190	1782		0.65	18.16	0.063	0.55	20.8	0.075	0.32	0.74
10709-4	192.5	1780		0.65	18.23	0.132	0.55	20.9	0.071	0.32	0.67
10709-4	195	1777		0.66	18.31	0.081	0.56	21.1	0.073	0.31	0.60
10709-4	197.5	1774		0.59	16.17	0.043	0.54	20.3	0.069	0.32	0.65
10709-4	200	1771	0.81	0.61	16.99	0.082	0.54	20.4		0.33	
10709-4	202.5	1768		0.63	17.62	0.063	0.55	20.9	0.076	0.30	0.58
10709-4	205	1765		0.62	17.13	0.068	0.55	21.0	0.075	0.31	0.57
10709-4	207.5	1762		0.64	17.87	0.104	0.54	20.6	0.066	0.31	0.59
10709-4	210	1759		0.61	16.95	0.077	0.55	20.8	0.073	0.30	0.93
10709-4	212.5	1756		0.62	17.18	0.066	0.55	20.9	0.078	0.30	0.49
10709-4	215	1753		0.61	16.75	0.052	0.54	20.3	0.076	0.31	0.67
10709-4	217.5	1750		0.58	16.04	0.065	0.55	20.7	0.078	0.30	0.75
10709-4	220	1747		0.61	16.98	0.077	0.56	21.2	0.074	0.31	0.68
10709-4	222.5	1744		0.61	16.82	0.055	0.56	21.2	0.074	0.34	0.75
10709-4	225	1741		0.59	16.30	0.064	0.53	19.7	0.074	0.31	0.56
10709-4	227.5	1738		0.59	16.24	0.062	0.53	20.0	0.072	0.31	0.71
10709-4	230	1735		0.59	16.32	0.061	0.54	20.3	0.072	0.32	0.62
10709-4	232.5	1732		0.60	16.68	0.067	0.56	21.3	0.074	0.31	0.66
10709-4	235	1730		0.56	15.37	0.051	0.55	20.9	0.071	0.31	0.63
10709-4	237.5	1727		0.60	16.44	0.062	0.56	21.2	0.071	0.31	0.59
10709-4	240	1724		0.58	15.98	0.044	0.55	21.0	0.071	0.32	0.67
10709-4	242.5	1721		0.59	16.23	0.058	0.56	21.6	0.074	0.31	0.71
10709-4	245	1718		0.59	16.28	0.055	0.57	21.9	0.073	0.31	0.59
10709-4	247.5	1715		0.58	16.07	0.054	0.54	20.4	0.071	0.31	0.58
10709-4	250	1712		0.59	16.26	0.073	0.54	20.5	0.070	0.31	0.83
10709-4	252.5	1709		0.61	16.90	0.072	0.55	20.9	0.070	0.32	0.69
10709-4	255	1706		0.58	15.92	0.074	0.56	21.1	0.089	0.31	0.74
10709-4	257.5	1703		0.57	15.71	0.055	0.54	20.5	0.087	0.31	0.59
10709-4	260	1700		0.56	15.52	0.035	0.56	21.3	0.091	0.30	0.62
10709-4	262.5	1697		0.62	17.20	0.056	0.56	21.4	0.093	0.29	0.55
10709-4	265	1694		0.57	15.74	0.073	0.54	20.5	0.095	0.29	0.59
10709-4	267.5	1691		0.59	16.32	0.064	0.55	21.1	0.092	0.30	0.47
10709-4	270	1688		0.56	15.55	0.079	0.56	21.6	0.091	0.30	0.65
10709-4	272.5	1685		0.58	15.96	0.073	0.56	21.5	0.093	0.30	0.64
10709-4	275	1682		0.58	15.90	0.056	0.55	21.1	0.108	0.27	0.50
10709-4	277.5	1680		0.56	15.54	0.048	0.57	21.8	0.102	0.28	0.56
10709-4	280	1677		0.57	15.79	0.067	0.55	21.0	0.096	0.29	0.54
10709-4	282.5	1674		0.56	15.55	0.086	0.56	21.2	0.094	0.28	0.58
10709-4	285	1671		0.59	16.38	0.110	0.56	21.5	0.092	0.29	0.52
10709-4	287.5	1668		0.59	16.29	0.050	0.55	20.9	0.097	0.29	0.55
10709-4	290	1665		0.58	15.95	0.085	0.54	20.2	0.093	0.29	0.77
10709-4	292.5	1662		0.59	16.41	0.062	0.56	21.1	0.093	0.28	0.54
10709-4	295	1659		0.59	16.24	0.081	0.55	20.8	0.102	0.28	0.48
10709-4	297.5	1656		0.58	16.14	0.076	0.55	20.9	0.098	0.29	0.57
10709-4	300	1653									
10709-4	302.5	1650		0.58	16.04	0.060	0.55	20.9	0.097	0.29	0.52

Multiproxy environmental reconstruction Gulf of Taranto

10709-4	305	1647	0.81	0.62	17.31	0.144						
10709-4	307.5	1644		0.57	15.84	0.048	0.55	20.7	0.097	0.29		0.49
10709-4	310	1641		0.60	16.48	0.054	0.55	20.6	0.100	0.29		
10709-4	312.5	1638		0.59	16.41	0.087	0.54	20.3	0.097	0.29		
10709-4	315	1635		0.58	16.11	0.073	0.54	20.5	0.088	0.30		0.65
10709-4	317.5	1632		0.61	16.93	0.057	0.56	21.2	0.082	0.30		0.52
10709-4	320	1630		0.58	16.00	0.063	0.54	20.2	0.086	0.30		0.77
10709-4	322.5	1627		0.59	16.42	0.057	0.53	19.8	0.090	0.30		0.59
10709-4	325	1624		0.60	16.61	0.062	0.54	20.4	0.091	0.30		0.58
10709-4	327.5	1621		0.60	16.65	0.047	0.54	20.2	0.089	0.30		0.84
10709-4	330	1618		0.60	16.48	0.077	0.53	19.9	0.087	0.30		0.69
10709-4	332.5	1615		0.59	16.39	0.080	0.55	20.6	0.091	0.29		0.50
10709-4	335	1612		0.61	16.92	0.094	0.54	20.2	0.083	0.31		0.46
10709-4	337.5	1609		0.60	16.51	0.082	0.55	20.8	0.092	0.30		0.43
10709-4	340	1606		0.59	16.44	0.079	0.53	19.9	0.081	0.32		0.45
10709-4	342.5	1603		0.59	16.22	0.075	0.54	20.5	0.081	0.32		0.52
10709-4	345	1600		0.59	16.32	0.085	0.54	20.0	0.080	0.31		0.50
10709-4	347.5	1597		0.59	16.33	0.073	0.55	20.7	0.095	0.29		0.54
10709-4	350	1594		0.59	16.19	0.109	0.53	20.0	0.103	0.28		0.91
10709-4	352.5	1591		0.61	16.99	0.133	0.54	20.3	0.111	0.27		0.57
10709-4	355	1588		0.62	17.09	0.102	0.53	19.6	0.124	0.25		0.58
10709-4	357.5	1585		0.63	17.54	0.104	0.54	20.2	0.125	0.25		0.84
10709-4	360	1582		0.61	17.01	0.073	0.54	20.1	0.117	0.26		0.31
10709-4	362.5	1580		0.59	16.15	0.105	0.53	19.8	0.101	0.27		0.46
10709-4	365	1577		0.64	17.81	0.136	0.54	20.3	0.091	0.29		0.47
10709-4	367.5	1574		0.63	17.40	0.036	0.54	20.4	0.080	0.30		0.46
10709-4	370	1571		0.61	16.88	0.074	0.55	20.8	0.074	0.31		0.61
10709-4	372.5	1568		0.62	17.21	0.074	0.55	20.6	0.072	0.31		0.73
10709-4	375	1565		0.60	16.62	0.089	0.55	20.6	0.073	0.32		0.56
10709-4	377.5	1562		0.55	15.16	0.095	0.54	20.2	0.074	0.31		0.42
10709-4	380	1559		0.59	16.15	0.064	0.54	20.5	0.084	0.31		0.88
10709-4	382.5	1556		0.60	16.67	0.048	0.54	20.5	0.078	0.30		0.70
10709-4	385	1553		0.58	16.06	0.079	0.53	19.8	0.075	0.30		0.62
10709-4	387.5	1550		0.59	16.37	0.069	0.54	20.5	0.080	0.30		0.76
10709-4	390	1547		0.60	16.56	0.058	0.54	20.5	0.074	0.31		0.69
10709-4	392.5	1544		0.59	16.26	0.090	0.54	20.4	0.078	0.29		0.95
10709-4	395	1541		0.64	17.72	0.067	0.54	20.3	0.078	0.31		0.59
10709-4	397.5	1538		0.58	15.85	0.071	0.55	20.8	0.077	0.30		0.60
10709-4	400	1535		0.61	16.93	0.071						0.91
10709-4	402.5	1532		0.58	16.04	0.083	0.55	20.7	0.079	0.30		0.40
10709-4	405	1530		0.61	16.84	0.043	0.54	20.5	0.082	0.29		0.86
10709-4	407.5	1527		0.59	16.39	0.105	0.55	20.7	0.080	0.28		0.59
10709-4	410	1524					0.55	20.7	0.082	0.28		
10709-4	412.5	1521		0.63	17.54	0.062	0.56	21.5	0.070	0.29		0.92
10709-4	415	1518		0.62	17.18	0.036	0.57	21.8	0.071	0.32		0.83
10709-4	417.5	1515		0.63	17.40	0.074	0.56	21.4	0.083	0.31		0.63
10709-4	420	1512	0.77	0.63	17.60	0.118	0.57	21.7	0.078	0.28		
10709-4	422.5	1509		0.60	16.49	0.046	0.58	22.4	0.073	0.31		0.71
10709-4	425	1506		0.62	17.16	0.046	0.58	22.6	0.072	0.31		0.49
10709-4	427.5	1503		0.60	16.55	0.073	0.56	21.5	0.071	0.32		0.71
10709-4	430	1500		0.65	17.95	0.041	0.56	21.4	0.072	0.31		0.60
10709-4	432.5	1497		0.63	17.34	0.084	0.57	21.8	0.073	0.30		0.70
10709-4	435	1494		0.64	17.65	0.067	0.56	21.2	0.070	0.30		0.70
10709-4	437.5	1491		0.63	17.57	0.070	0.57	22.1	0.069	0.31		0.61
10709-4	440	1488		0.69	19.41	0.075	0.58	22.6	0.076	0.28		0.52

CHAPTER V

Conclusions and Outlook

V.1. CONCLUSIONS

Lipid biomarker proxies used for the reconstruction of SSTs and the hydrological cycle are valuable tools, although their interpretation appears to be not straightforward due to their individual pitfalls introducing biases (CHAPTER I). In particular, this is true for their application in shelf systems, which provide sedimentary archives suitable for high-resolution paleoenvironmental reconstructions but where mechanisms influencing the environmental conditions are highly complex. The main focus of this thesis was to provide a calibration of marine and terrestrial lipid-derived proxies against the recent environmental conditions of the southern Italian shelf for future paleoclimatological investigations. The performed studies in this thesis aimed at a better understanding of how these proxies work in such a near-coastal environment. Inevitably, they highlight the importance of regional calibration studies prior an application to the past in order to constrain local factors that influence the proxies. Moreover, interpretations of paleoenvironmental conditions can benefit from an approach using multiple organic and inorganic proxies due to the different ecologies of source organisms. In the following section the major findings are summarized.

In this thesis, a detailed core top calibration combining the temperature proxies $U^{K'}_{37}$ and TEX_{86} was for the first time performed along the southern Italian shelf and Gulf of Taranto (CHAPTER II). Here, variations in the molecular temperature proxies could be assigned to differences in seasonal and/or spatial characteristics of the water column. The $U^{K'}_{37}$ -based temperatures reflected winter/spring SSTs in agreement with other studies demonstrating maximum haptophyte production during the colder season (e.g., Socal et al., 1999). The TEX_{86} -based temperatures for the nearshore sites also reflected winter SST. Most outstanding was a temperature increase based on TEX_{86} of $\sim 10^\circ\text{C}$ with distance to the coast (and increasing water depth), corresponding to summer SSTs at the most offshore sites. This resulted in a temperature offset between the $U^{K'}_{37}$ and TEX_{86} indices, which also been observed in other regions of the Mediterranean Sea, suggesting a general seasonal imprint of haptophyte and archaeal production (Menzel et al., 2006; Castañeda et al., 2010; Huguet et al., 2011). In the study area, this has been attributed to a shoreward increase of the impact of seasonal and spatial variability in nutrients and control of planktonic archaeal abundance by primary productivity, particle loading in surface waters and/or overprint by a cold-biased terrestrial TEX_{86} signal. BIT index values suggested a restricted delivery of soil OM to the Gulf of Taranto. Higher values appeared in the Gulf of Manfredonia in line with local river input and/or soil OM transported with Western Adriatic Current. This study emphasize that

regional calibrations are the key to understand SST proxy relations in near-coastal to marine transitions and sets the basis for paleoenvironmental reconstructions in the Gulf of Taranto. In the second study, the distribution of plant wax-derived *n*-alkanes in terrestrial and marine surface sediments was investigated for a modern calibration of $\delta D_{\text{plant-wax}}$ (CHAPTER III). The $\delta D_{\text{plant-wax}}$ has been shown to track changes in the terrestrial hydrological cycle (e.g., Sachse et al., 2004). Depicting the source areas of plant waxes and their delivery to the ocean are of major importance since remote regions can exhibit different signatures of vegetation and climate (e.g., Schefuß et al., 2003; Dahl et al., 2005; Seki et al., 2010). However, studies on the supply and transport of terrestrial OM are restricted to the northern and central Adriatic Sea suggesting a southward transport by the Western Adriatic Current (e.g., Tesi et al., 2007). The approach gave new insight in the provenance of long chain *n*-alkanes in the Gulf of Taranto by using their higher homologues abundance, $\delta^{13}\text{C}$ and δD composition. In the terrestrial samples a shift to more $\delta D_{\text{plant-wax}}$ values and higher ACL along a N-S transect followed the D enrichment of precipitation and increases in mean annual air temperature. We observed a stronger D enrichment in plant-waxes compared to precipitation and attributed this unusual relationship to an enhanced soil water evaporation and/or leaf water evapotranspiration from northern to southern Italy. Likewise, the $\delta^{13}\text{C}$ - δD signature of plant-waxes in sediments from the Gulf of Taranto allowed a correlation to local southern Italian sources. This study could show the absence of plant wax supply from northern Italian regions and, equally important, that $\delta D_{\text{plant-wax}}$ indeed can provide reasonable estimates for the precipitation-evaporation balance of southern Italy and therefore the central Mediterranean. Subsequently, the retrieved knowledge from the SST core top calibration has been applied to a reconstruction of environmental conditions in the Gulf of Taranto spanning the last 500 years. Here, the combination of temperature estimates based on $\text{U}^{\text{K}'}_{37}$ and TEX_{86} indices and the $\delta^{18}\text{O}$ of the planktonic foraminifer *G. ruber (white)* resulted in a complex picture of SST proxies and their source organisms. Most important, this showed that the proxy-derived SST variations do not reflect a simple annual mean SST relationship. In contrast, they reflect the temperature of the environment where (in time and space) the proxy-generating organism happened to be. This place is not motivated by temperature but by other factors such as climatic conditions, circulation changes and nutrient supply. Thus changes in the factors will result in a change in the SST proxy, even if the annual temperature cycle remains constant. These problems may be especially true for coastal settings where nutrients, food and light may be severely decoupled from “seasonal” or “annual” water temperature.

V.2. OUTLOOK – FUTURE PERSPECTIVES

This thesis contributed to a better understanding of lipid-derived proxies in near-coastal settings. However, the conducted studies also revealed open questions as well as the potential for further investigations on the recent and past environment.

V.2.1. Future work on the recent setting

- The lipid biomarker SST proxies were calibrated against the regional environment of the southern Italian shelf and Gulf of Taranto. However, the environmental factors (e.g., seasonal SST range, river runoff and vertical mixing introducing nutrients to the photic zone, circulation changes, productivity) vary between shelf regions due to morphological and climatological differences. Consequently, systematic core top studies on other shelf systems would provide a more comprehensive knowledge on lipid-derived SST proxies in near-coastal environments.
- The temperature offset between the $U^{K'}_{37}$ and TEX_{86} indices in our study area and the Mediterranean Sea (Menzel et al., 2006; Castañeda et al., 2010; Huguet et al., 2011) needs further investigation. In particular, since the production (depth and season) of planktonic crenarchaeota is not known for the Mediterranean Sea. To elucidate a seasonal difference in alkenone and GDGT production or transport would require extensive seasonal studies on particulate OM based on water column filters or sediment traps.
- The influence of GDGTs from sedimentary active archaea on the TEX_{86} signal in this region remains poorly understood. The strong temperature gradient observed in TEX_{86} may provide a suitable basis for further investigations applying simultaneous analysis of intact polar lipids (IPLs) and their hydrolyzed core lipids (Liu et al., 2011) along the near-coastal to open marine transects.
- Although the $\delta D_{\text{plant-wax}}$ in terrestrial and marine sediments proved to record the $\delta D_{\text{precipitation}}$, further studies on the predominant mechanism (soil water evaporation vs. evapotranspiration) should also focus on plant-based data by measuring the source water and leaf water along the climatic transect (Feakins and Sessions, 2010).
- The terrestrial supply inferred from long chain *n*-alkanes and the BIT index, as higher plant and soil OM indicators, could be verified with bulk OM parameters (C:N, $\delta^{13}\text{C}$ TOC) and more specific terrestrial biomarkers such as, lignin phenols

(angiosperm vs. gymnosperm; woody vs. non-woody) (Hedges and Mann, 1979; Goñi, 1997; Schmidt et al., 2010). Grain size analyses should be conducted and may provide more information on transport processes. To determine the sources and fate of the terrestrial OM, these studies should also include the NW Adriatic Sea.

V.2.2. Future work on sediment cores

- Due to the potential for paleoenvironmental studies on multidecadal resolution, future studies should encompass longer time scales and focus on time slices like the Roman Classical Period or Medieval Optimum.
- To exclude that the SST estimates are biased by differences in lateral transport, future work should include compound-specific ^{14}C -AMS dating on alkenones, GDGTs and planktonic foraminifera (Ohkouchi et al., 2002; Mollenhauer et al., 2008).
- Analyses on the Mg/Ca and ‘carbonate clumped isotopes’ (e.g., Gosh et al., 2007) of planktonic foraminifera would provide further SST estimates, which allow to extract the salinity effect on foraminiferal $\delta^{18}\text{O}$ and a complementary comparison to the lipid-derived SSTs.
- For future studies it would be interesting to compare the SST proxy relation at the ‘extreme ends’ of the core top calibration using a set of cores from the near-coastal to open marine environment in the Gulf of Taranto. Presumably, this would also allow us to estimate the amplitude/extension of circulation shifts.
- In order to study past variations in SST according to the hydro-climate conditions (e.g., wet vs. dry), the application of $\delta\text{D}_{\text{plant-wax}}$ would provide a powerful tool to link the marine and terrestrial environment. Additionally, the $\delta\text{D}_{\text{plant-wax}}$ and δD of algal lipids preserved in lake sediments (Sachse et al., 2004; Mügler et al., 2008) would enable us to reconstruct the water balance in the terrestrial environment.

V.3. REFERENCES

- Castañeda, I.S., Schefuß, E., Pätzold, J., Sinninghe Damsté, J.S., Weldeab, S., Schouten, S., 2010. Millennial-scale sea surface temperature changes in the eastern Mediterranean (Nile River Delta region) over the last 27,000 years. *Paleoceanography* 25, PA1208. Doi:10.1029/2009pa001740.
- Dahl, K.A., Oppo, D.W., Eglinton, T.I., Hughen, K.A., Curry, W.B., Sirocko, F., 2005. Terrigenous plant wax inputs to the Arabian Sea: Implications for the reconstruction of winds associated with the Indian Monsoon. *Geochim. Cosmochim. Acta* 69, 2547-2558.
- Feakins, S.J., Sessions, A.L., 2010. Controls on the D/H ratios of plant leaf waxes in an arid ecosystem. *Geochim. Cosmochim. Acta* 74, 2128-2141.
- Ghosh, P., Eiler, J., Campana, S.E., Feeney, R.F., 2007. Calibration of the carbonate 'clumped isotope' paleothermometer for otoliths. *Geochim. Cosmochim. Acta* 71, 2736-2744.
- Goñi, M.A., Ruttenger, K.C., Eglinton, T.I., 1997. Sources and contribution of terrigenous organic carbon to surface sediments in the Gulf of Mexico. *Nature* 389, 275-278.
- Hedges, J.I., Mann, D.C., 1979. The characterization of plant tissues by their lignin oxidation products. *Geochim. Cosmochim. Acta* 43, 1803-1807.
- Huguet, C., Martrat, B., Grimalt, J.O., Sinninghe Damsté, J.S., Schouten, S., 2011. Coherent millennial-scale patterns in UK'37; and TEXH86 temperature records during the penultimate interglacial-to-glacial cycle in the western Mediterranean. *Paleoceanography* 26, PA2218. Doi:10.1029/2010pa002048.
- Liu, X., Lipp, J.S., Hinrichs, K.-U., 2011. Distribution of intact and core GDGTs in marine sediments. *Org. Geochem.* 42, 368-375.
- Menzel, D., Hopmans, E.C., Schouten, S., Sinninghe Damsté, J.S., 2006. Membrane tetraether lipids of planktonic Crenarchaeota in Pliocene sapropels of the Eastern Mediterranean Sea. *Palaeogeogr., Palaeoclim., Palaeoecol.* 239, 1-15.
- Mollenhauer, G., Eglinton, T.I., Hopmans, E.C., Sinninghe Damsté, J.S., 2008. A radiocarbon-based assessment of the preservation characteristics of crenarchaeol and alkenones from continental margin sediments. *Org. Geochem.* 39, 1039-1045.
- Mügler, I., Sachse, D., Werner, M., Xu, B., Wu, G., Yao, T., Gleixner, G., 2008. Effect of lake evaporation on δD values of lacustrine n-alkanes: A comparison of Nam Co (Tibetan Plateau) and Holzmaar (Germany). *Org. Geochem.* 39, 711-729.
- Ohkouchi, N., Eglinton, T.I., Keigwin, L.D., Hayes, J.M., 2002. Spatial and temporal offsets between proxy records in a sediment drift. *Science* 298, 1224-1227.
- Sachse, D., Radke, J., Gleixner, G., 2004. Hydrogen isotope ratios of recent lacustrine sedimentary n-alkanes record modern climate variability. *Geochimica et Cosmochimica Acta* 68, 4877-4889.

- Schefuß, E., Ratmeyer, V., Stuut, J.B.W., Jansen, J., Sinninghe Damsté, J.S., 2003. Carbon isotope analyses of n-alkanes in dust from the lower atmosphere over the central eastern Atlantic. *Geochim. Cosmochim. Acta* 67, 1757-1767.
- Schmidt, F., Hinrichs, K.-U., Elvert, M., 2010. Sources, transport, and partitioning of organic matter at a highly dynamic continental margin. *Mar. Chem.* 118, 37-55.
- Seki, O., Nakatsuka, T., Shibata, H., Kawamura, K., 2010. A compound-specific n-alkane $\delta^{13}\text{C}$ and $\delta^2\text{D}$ approach for assessing source and delivery processes of terrestrial organic matter within a forested watershed in northern Japan. *Geochim. Cosmochim. Acta* 74, 599-613.
- Socal, G., Boldrin, A., Bianchi, F., Civitarese, G., De Lazzari, A., Rabitti, S., Totti, C., Turchetto, M.M., 1999. Nutrient, particulate matter and phytoplankton variability in the photic layer of the Otranto strait. *J. Mar. Syst.* 20, 381-398.
- Tesi, T., Miserocchi, S., Goñi, M.A., Langone, L., Boldrin, A., Turchetto, M., 2007. Organic matter origin and distribution in suspended particulate materials and surficial sediments from the western Adriatic Sea (Italy). *Estuar. Coast. Shelf Sci.* 73, 431-446.

DANKSAGUNG

Ich danke Prof. Dr. Kai-Uwe Hinrichs, dass er mir die Möglichkeit gegeben hat, diese Dissertation unter seiner hervorragenden wissenschaftlichen Expertise und Betreuung durchzuführen, für seine Förderung und das entgegengebrachte Vertrauen.

Für die Übernahme des Zweitgutachtens danke ich Prof. Dr. Gesine Mollenhauer, sowie für die Hilfe bei meinen ersten GDGT Analysen.

Mein großer Dank geht an Dr. Gerardus J.M. Versteegh für seine hervorragende wissenschaftliche Betreuung während der letzten Jahre. Für seinen Enthusiasmus, typisch niederländischen Humor, sein 'Ah, aber.....' und die Möglichkeit jederzeit spontane 2 Minuten Diskussionen auf den gesamten Vormittag auszuweiten.

Des Weiteren danke ich den Mitgliedern des MOCCHA Projektes für die Möglichkeit des wissenschaftlichen Austausches auf den zahlreichen Retreats der ESF: Prof. Dr. Stefano Bernasconi, Liang Chen, Prof. Dr. Gert de Lange, Marie-Louise Goudeau, Anna Lena Grauel, und PD Dr. Karin Zonneveld.

Darüber hinaus danke ich den folgenden Personen, die auf die eine oder andere Weise zur Entstehung dieser Dissertation beigetragen haben und mich auf diesem Weg begleitet haben:

- Dr. Marcus Elvert, Dr. Daniel Birgel und Dr. Julio Sepúlveda für die Einführung in die Organische Geochemie
- Xavi Prieto Mollar, sowie Jessica Schmal, Jenny Wendt und Raika Himmelsbach dafür, dass sie die Laborgeräte am Laufen halten und für unzählige SAP Bestellungen und Lösungsmittelnachschübe
- Birgit Schmincke für ihre Hilfe in administrative Angelegenheiten
- Enno Schefuß für die Bereitstellung der ASE sowie Ideen und Anregungen
- Kevin Becker, Carl Peters, Tim Kajs und Bernhard Viehweger für die Unterstützung bei Laborarbeiten
- momentane und ehemalige Room mates: Matthias Y. Kellermann, Jan Schröder, Rhong Zhu, Frauke Schmidt (Danke!), Simone Ziegenbalg, Miriam Sollich, Aimee

Gillespie und Julio Sepúlveda für die zahlreichen Hilfen und (un)wissenschaftlichen Kommentare

- Julius Lipp für die Einführung in die HPLC-Analytik
- allen weiteren aktuellen und ehemaligen Mitgliedern der AG Organische Geochemie und Geobiologie im Besonderen: Lars Hoffmann, Xiaolei Liu, Florence Schubotz, Marcos Yoshinaga und Lars Wörmer
- den Teilnehmern der RV POSEIDON (P339) 'CAPPUCCINO' Expedition, RV PELAGIA (64PE297) 'DOPPIO' Expedition und dem Land-Probennahmeteam
- der Deutschen Forschungsgemeinschaft und der European Scientific Foundation für die finanzielle Förderung dieser Arbeit im Rahmen des EuroMARC Projektes MOCCHA
- Bremen International Graduate School for Marine Sciences (GLOMAR) für die zahlreichen Kurse und Finanzierung von Konferenzteilnahmen
- meinen Eltern für die fortwährende Unterstützung.

Danke Marta, dass du jeden Tag für mich da bist, für deine Liebe und deine Geduld!

APPENDIX

Published manuscript I

Identification of polar lipid precursors of the ubiquitous branched GDGT orphan lipids in a peat bog in Northern Germany

Xiaolei Liu^{a,*}, Arne Leider^a, Aimee Gillespie^b, Jens Gröger^c, Gerard J.M. Versteegh^a,
and Kai-Uwe Hinrichs^{a,**}

Published in *Organic Geochemistry*

vol. 41, issue 7, page 653-660, doi:10.1016/j.orggeochem.2010.04.004

© 2010 Elsevier Ltd.

^a *Organic Geochemistry Group, MARUM Center for Marine Environmental Sciences & Dept. of Geosciences, University of Bremen, 28359 Bremen, Germany*

^b *Division of Geological and Planetary Sciences, California Institute of Technology, Pasadena, CA 91125, USA*

^c *Geochemistry and Hydrogeology Group, Dept. of Geosciences, University of Bremen, 28334 Bremen, Germany*

* *Correspondence to X.-L. Liu, Address: University of Bremen, Leobener Str./ MARUM, Room 2520, 28359 Bremen, Germany.*

** *Corresponding author.*

E-mail addresses: xliu@uni-bremen.de (X.-L. Liu), khinrichs@uni-bremen.de (K.-U. Hinrichs).

ABSTRACT

Two types of intact branched glycerol dialkyl glycerol tetraethers (GDGTs) were detected in peat bog samples from Bullenmoor, Northern Germany. Glucuronosyl and glucosyl branched GDGTs comprise on average ca. 4% of the microbial intact polar lipids in the anoxic, acidic peat layer ca. 20 cm below the surface of the bog, suggesting an important ecological role for the source microorganisms. No corresponding phospholipids were detected. Notably, glycosidic branched GDGTs are 5–10 times less abundant than their intact isoprenoid counterparts derived from Archaea, while branched GDGT core lipids exceed their isoprenoid analogues by about an order of magnitude. These contrasting relationships may reflect lower standing stocks of the biomass of producers of branched GDGTs, combined with higher population growth rates relative to soil Archaea. Search strategies for the microbial producers of these conspicuous orphan lipids should benefit from the discovery of their intact polar precursors.

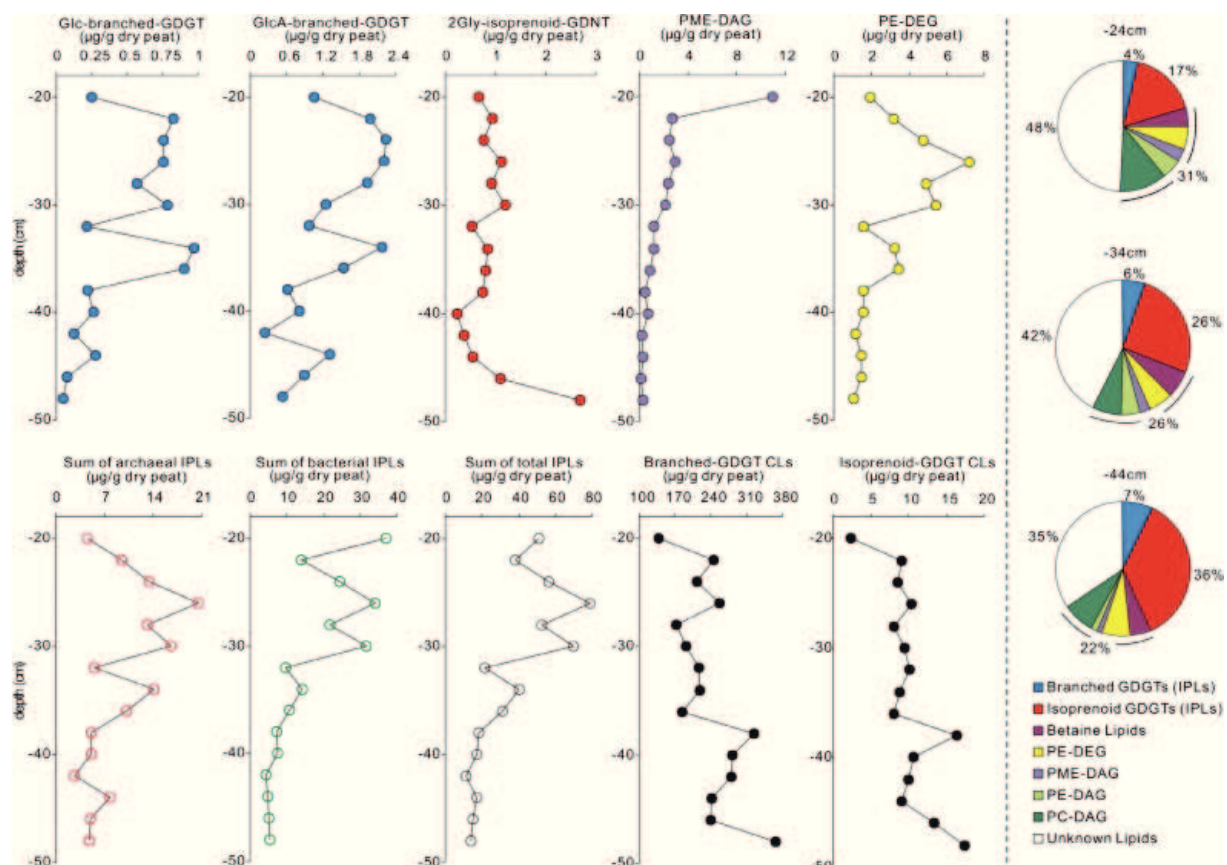


Figure A1. Depth profiles of concentrations of Glc-branched-GDGT, GlcA-branched-GDGT, 2Gly-isoprenoid-GDNT, PME-DAG, PE-DEG, sum of archaeal IPLs (all intact isoprenoid GDGTs), sum of bacterial IPLs (betaine lipids, PE-DEG, PME-DAG, PE-DAG and PC-DAG), sum of total IPLs, core lipids of branched and isoprenoidal GDGTs in Bullenmoor peat bog (since PE-DAG, PC-DAG and PE-DEG have the similar depth profile, only the depth profiles of PE-DEG and sum of bacterial IPLs are shown). Right: example pie charts showing relative abundance of all IPLs at depths of -24 cm, -34 cm and -44 cm

Manuscript II

Environmental changes observed by high-resolution XRF core scanning in Holocene (0-16 ka cal. BP) sediments from the Gulf of Taranto, Central Mediterranean

Marie-Louise S. Goudeau^{a,*,1} and Anna-Lena Grauel^{b,*,1}, Chiara Tessarolo^c, Arne Leider^{d,e},
Liang Chen^e, Stefano M. Bernasconi^b, Gerard J.M. Versteegh^{d,e}, Karin A.F. Zonneveld^e
and Gert J. de Lange^a

Submitted to *Geochemistry, Geophysics, Geosystems*
in January 2012

^a *Dept. of Geosciences, Utrecht University, Utrecht, The Netherlands*

^b *Geological Institute, ETH Zurich, 8092 Zurich, Switzerland*

^c *Milan-Bicocca University, 20123 Milan, Italy*

^d *MARUM Center for Marine Environmental Sciences University of Bremen, D-28334 Bremen, Germany*

^e *Dept. of Geosciences, University of Bremen, D-28334 Bremen, Germany*

** corresponding authors; ¹ equal contribution to this work*

E-mail addresses: MLSG: m.s.goudeau@uu.nl; ALG: anna.grauel@erdw.ethz.ch

Phone: +31 30 253 4991 (MLSG)

Fax: +31 30 253 5302 (MLSG)

Keywords

Sedimentology, geochemistry, XRF scan, paleoclimate, Mediterranean Sea, ocean circulation

ABSTRACT

An extensive, high resolution, sedimentological-geochemical survey was done using geoaoustics, XRF-scans, ICP-AES analyses, AMS ^{14}C -dating and grain size analyses of sediments in 11 cores from the Gallipoli area, the Gulf of Taranto, the southern Adriatic Sea and the central Ionian Sea spanning the last 16 ka cal. BP. The XRF-core scan Ca/Ti ratios along with AMS ^{14}C -dating were used to accurately correlate and date the cores. We focus the discussion on cores from the Gallipoli area where the sedimentation rates are relatively high and vary between ~ 0.92 and 0.58mm/yr . The observed variations are also reflected in the sediment composition and are related to changes in productivity, circulation in the Adriatic Sea and run-off. The Glacial termination is characterized by decreased productivity and increased run-off as part of the environmental change to warmer and wetter conditions in the Mediterranean region. Furthermore, the progressive change towards the modern circulation conditions in the southern Adriatic Sea plays an important role. Millennial-scale events are observed throughout the Mid- to Late-Holocene sediments, which we consider to be related to increased river run-off during 'wet' periods. This millennial-scale variability represents a combination of regional and global scale climate changes.

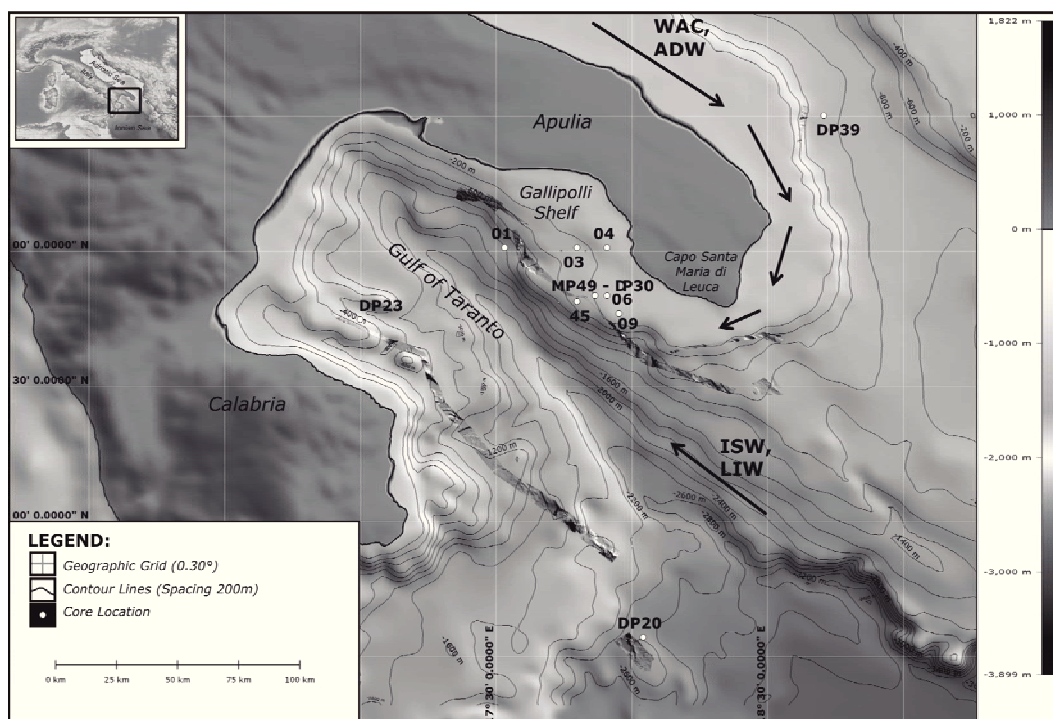


Figure A.2. Bathymetric map of the Gulf of Taranto together with the core locations and a scheme of the circulation and the major water masses pathways (WAC - Western Adriatic Current, ADW - Adriatic Deep Water, ISW - Ionian Surface Water, LIW - Levantine Intermediate Water).

**Erklärung gemäß § 6 Abs. 5 der Promotionsordnung der Universität Bremen
für die mathematischen, natur- und ingenieurwissenschaftlichen Fachbereiche**

Name: Arne Leider

Datum: 13.02.2012

Anschrift: Leipziger Str. 50a, 27356 Rotenburg

Hiermit versichere ich, dass ich die vorliegende Arbeit

1. ohne unerlaubte fremde Hilfe ausgeführt habe,
 2. keine anderen als die von mir angegebenen Quellen und Hilfsmittel benutzt habe und
 3. die den benutzten Werken wörtlich oder inhaltlich entnommenen Stellen als solche kenntlich gemacht habe.
-

Bremen, den 13.02.2012

Arne Leider